

The Pennsylvania State University

The Graduate School

College of Medicine

**CHARACTERIZATION OF UGTS ACTIVE AGAINST SUBEROYLANILIDE
HYDROXAMIC ACID (SAHA): VARIATIONS IN SAHA GLUCURONIDATION
ASSOCIATED WITH UGT GENETIC VARIANTS**

A Dissertation in

Genetics

by

Renee M. Balliet

© 2009 Renee M. Balliet

Submitted in Partial Fulfillment

of the Requirements

for the Degree of

Doctor of Philosophy

August 2009

The dissertation of Renee M. Balliet was reviewed and approved* by the following:

Philip Lazarus
Professor of Pharmacology
Associate Director of the Cancer Institute
Dissertation Adviser
Chair of Committee

Laura Carrel
Assistant Professor of Biochemistry and Molecular Biology

Lisa M. Shantz
Associate Professor of Cellular and Molecular Physiology

Christopher Herzog
Associate Professor of Pharmacology

Gavin Robertson
Co-Chair of Genetics Department

*Signatures are on file in the Graduate School.

ABSTRACT

Suberoylanilide Hydroxamic Acid (SAHA) is a histone deacetylase inhibitor used in the treatment of cutaneous T-cell lymphoma and in clinical trials for treatment of multiple other cancers. Variations in patient response and toxicities have been observed; however, no underlying cause has been identified for these differences. A mechanism that could be responsible for the observed differences is altered drug metabolism. A major mode of SAHA metabolism is by glucuronidation via the UDP-glucuronosyltransferase (UGT) family of enzymes.

The UGT superfamily of enzymes catalyzes the glucuronidation of a variety of endogenous compounds such as bilirubin and steroid hormones, as well as xenobiotics such as drugs and environmental carcinogens. These enzymes are located in the endoplasmic reticulum of cells and make xenobiotics and endogenous compounds more water soluble through their conjugation to glucuronic acid in a reaction with the hydrophilic co-substrate, UDPGA. This conjugation alters the biological properties of the compound to enhance its excretion in the urine or bile and typically converts substrates into products that are less pharmacologically active. These enzymes have been associated with altered drug metabolism and correlated with patient response and toxicity.

The primary goals of this thesis include: identification of the UGTs responsible for SAHA glucuronidation, characterization of the UGTs that are most active against SAHA, *in vitro* studies of UGT genotype/SAHA glucuronidation phenotype association, and characterization of the promoter region of the UGT1A10 gene. To identify and characterize the UGTs active against SAHA, homogenates from UGT-overexpressing HEK293 cell lines were used. The hepatic UGTs 2B17 and 1A9 and the extra-hepatic UGTs 1A8 and 1A10 exhibited the highest overall activity against SAHA as determined by V_{max}/K_M (16 ± 6.5 , 7.1 ± 2.2 , 33 ± 6.3 , and 24 ± 2.4 nL·min⁻¹·mg UGT protein⁻¹, respectively), with UGT2B17 exhibiting the lowest K_M (300 μ M) for SAHA of any UGT *in vitro*. While the UGT1A8p.Ala173Gly variant exhibited a 3-fold ($P < 0.005$) decrease in glucuronidation activity for SAHA as compared to wild-type UGT1A8, the UGT1A8p.Cys277Tyr variant exhibited no detectable glucuronidation activity; a similar

lack of detectable glucuronidation activity was observed for the UGT1A10p.Gly139Lys variant. To analyze the effects of the UGT2B17 gene deletion variant (UGT2B17*2) on SAHA glucuronidation phenotype, human liver microsomes (HLM) were analyzed for glucuronidation activity against SAHA as well as for UGT2B17 genotype. HLM from subjects homozygous for UGT2B17*2 exhibited a 45% ($P<0.01$) decrease in SAHA glucuronidation activity and a 75% ($P<0.002$) increase in K_M for SAHA as compared to the HLMs from subjects homozygous for the wild-type UGT2B17*1 allele. Further stratification of the HLM glucuronidation data by gender, identified a significant difference in SAHA glucuronidation between males and females, with females having significantly less glucuronidation. Characterization of the promoter of one of the most active glucuronidators of SAHA, UGT1A10, led to the identification of a novel deletion which was able to cause differential induction of luciferase reporter activity in colon derived cell lines. These data suggested that tissue specific regulation of UGTs may ultimately determine glucuronidation levels in specific tissues. Overall, these results suggest that several UGTs play important roles in the metabolism of SAHA and that females and UGT2B17-null males could potentially exhibit altered SAHA clearance rates and differences in overall response to the drug.

TABLE OF CONTENTS

List of Figures	ix
List of Tables	xii
List of Abbreviations	xiii
Acknowledgements	xv
Chapter 1: Literature Review	1
1.1 Introduction	1
1.1.1 Individualized Medicine and Genetic Variation	6
1.1.2 Cancer as a Complex Disease	4
1.2 HATs and HDACs	10
1.2.1 HATs	12
1.2.2 HDACs	13
1.2.3 HDAC Inhibitors	16
1.2.4 SAHA	19
1.2.5 SAHA Metabolism	24
1.3 UDP-glucuronosyltransferase	27
1.3.1 Gene Structure	29
1.3.2 Expression and Regulation	41
1.3.3 Endogenous Substrates	42
1.3.4 Exogenous Substrates	42
1.3.5 Genetic Variants	43
1.3.6 Pharmacogenetics and UGTs	45
Chapter 2: Identification and Characterization of UGTs against SAHA	51
2.1 Introduction	51
2.2 Materials and Methods	54
2.2.1 Generation of UGT-overexpressing cell lines	54
2.2.2 Preparation of cell homogenates	60
2.2.3 Glucuronidation Assays	61
2.2.4 SAHA-glucuronide confirmation	63
2.2.5 Kinetic analysis of interactions of UGTs with SAHA	64

2.3 Results	65
2.3.1 Characterization of UGT-overexpressing cell lines	65
2.3.2 Confirmation of SAHA-glucuronide formation	67
2.3.3 Screen of individual UGTs for activity against SAHA	71
2.3.4 Kinetic parameters for the glucuronidation of SAHA by individual UGT family members	75
2.4 Summary	79
Chapter 3: Characterization of the ability of variant UGTs to glucuronidate SAHA	81
3.1 Introduction	81
3.2 Materials and Methods	84
3.2.1 Generation of cell lines overexpressing UGT variants	84
3.2.2 Preparation of cell homogenates	86
3.2.3 Glucuronidation assays	87
3.2.4 Kinetic analysis of variant UGTs against SAHA	89
3.3 Results	90
3.3.1 Characterization of HEK293 cell lines overexpressing UGT variants	
3.3.2 Screen variant UGTs for activity against SAHA	90
3.3.3 Results of screening for glucuronidation of SAHA by UGT variants	96
3.4 Summary	99
Chapter 4: Characterization of SAHA glucuronidation by UGT in human tissue samples	103
4.1 Introduction	103
4.2 Materials and Methods	106
4.2.1 Human Liver Tissue	106
4.2.2 Preparation of Human Liver Microsomes	106
4.2.3 Isolation of DNA and RNA from tissue used to prepare HLM	107
4.2.4 Reverse transcription of RNA	109
4.2.5 Genotyping Assay for UGT2B17	109
4.2.5.1 Multiplex Real-Time PCR assay to determine UGT2B17 genotype	110
4.2.5.2 Copy Number Variation	111

4.2.6 Gender Identification Assay	112
4.2.7 Glucuronidation Assays for SAHA in HLM and Colon homogenates	106
4.2.8 Expression Assay for UGT2B17	113
4.3 Results	115
4.3.1 Analysis of UGT2B17 Genotype	115
4.3.2 UGT2B17 expression in HLM	120
4.3.3 UGT2B17 genotype/phenotype correlation in HLM	123
4.3.4 Confirmation of the gender of each HLM preparation and stratification of UGT2B17 expression and glucuronidation results by gender.	127
4.3.5 SAHA activity in colon homogenate	131
4.4 Summary	133
Chapter 5: UGT1A10 Promoter Study	138
5.1 Introduction	138
5.2 Materials and Methods	143
5.2.1 Human DNA used to screen for UGT1A10 polymorphisms	143
5.2.2 Amplification and Sequencing of the UGT1A10 promoter	143
5.2.3 Real-Time PCR genotype assay for novel UGT1A10 promoter deletion	144
5.2.4 Cloning of UGT1A10 promoter constructs into luciferase vector	145
5.2.5 Luciferase Assay for UGT1A10 constructs	148
5.2.6 Induction of Luciferase via UGT1A10 promoter	149
5.3 Results	151
5.3.1 Confirmation of Amplification and Sequencing of the UGT1A10 promoter	151
5.3.2 Genotypes observed for the UGT1A10 promoter	152
5.3.3 Effects of the UGT1A10 promoter region and its variants on gene expression	153
5.3.4 Effect of treatment with hypothesized inducers on UGT1A10 promoter driven luciferase activity	158
5.4 Summary	159
Chapter 6: General Discussion and Future Directions	163

Appendix A. Nucleotide Sugar Transporters	178
A.1 Introduction	178
A.2 Materials and Methods	182
A.2.1 Identification of SNPs	182
A.2.2 DNA Samples	182
A.2.3 Multiplex PCR assay	182
A.2.4 SNaPshot Assay for SNPs	185
A.3 Results	188
A.3.1 Identification of SNPs	188
A.3.2 Development of Multiplex PCR Assay to Analyze Nonsynonymous SNPs of the NSTs	186 6
A.3.3 Optimization of SNaPshot Assay for SNPs	193
A.4 Summary	198
REFERENCES	202

LIST OF FIGURES

Figure		Page
1.1	Schematic of the structure of histones in nucleosomes	11
1.2	Many functions of HDACs	15
1.3	Structure of trichostatin A and SAHA	21
1.4	SAHA inhibits HDAC activity by binding to the pocket of the catalytic site	21
1.5	Schematic of SAHA metabolism	25
1.6	Phylogenetic tree showing the relationships between the human UDP-glucuronosyltransferases (UGTs)	30
1.7	Genomic organization of the UGT1A locus and example of mRNA transcribed	31
1.8	The UGT2B family locus	32
1.9	Putative protein structure of UGT proteins	33
1.10	Comparison of the UGT1 locus in human, rat, and mouse	35
1.11	Expression patterns of UGTs in human tissue	37
1.12	Schematic representation of the UGT1 gene and the alternative splicing events taking place at the 5' and 3' ends of the locus	41
1.13	The effect of the mdr-1 SNP G2677T/A on the paclitaxel treatment outcome	46
2.1	Schematic diagram of the pcDNA3.1/V5-His-TOPO mammalian expression vector	57
2.2	Western blot analysis of UGT1A3 protein expression in the UGT1A3-overexpressing HEK293cell line	66
2.3	Western blot analysis of UGT2B15 protein expression in the UGT2B15 and UGT2B17-overexpressing HEK293 cell line	66
2.4	Optimization of the UGT activity assay with SAHA substrate using UGT1A7 cell homogenate	69
2.5	UPLC analyses of SAHA metabolites formed by UGTs in HLM	70

2.6	UPLC chromatograms from <i>in vitro</i> screening of UGT-overexpressing HEK293 cell lines for UGT activity against SAHA	73
2.7	Representative concentration dependence curves for SAHA glucuronide formation in homogenates of UGT-overexpressing cells	77
3.1	Western blot analysis of UGT1A7 star allele protein from HEK293 cell lines expressing UGT1A7	91
3.2	Western blot analysis of UGT2B15*2 protein from HEK293 cell lines expressing UGT2B15	91
3.3	UPLC chromatographs of cell homogenate of UGT1A8 star allele-overexpressing HEK293 cells assayed for activity against 4-MU	93
3.4	UPLC chromatographs of cell homogenate of UGT1A10 star allele-overexpressing HEK293 cells assayed for activity against 17-dihydroexemestane	94
3.5	UPLC chromatographs of cell homogenate of UGT1A7 star allele-overexpressing HEK293 cells assayed for activity against SAHA	94
3.6	UPLC chromatographs of cell homogenate of UGT1A8 star allele-overexpressing HEK293 cells assayed for activity against SAHA	95
3.7	UPLC chromatographs of cell homogenate of UGT1A10 star allele-overexpressing HEK293 cells assayed for activity against SAHA	95
3.8	Representative concentration dependence curves for SAHA glucuronide formation in homogenates of UGT variant-overexpressing cells	97
4.1	Diagram of microsome preparation	108
4.2	Gene structure and primer and probe locations for the UGT2B17 multiplex real-time PCR assay	110
4.3	UGT2B17 multiplex real-time PCR amplification plots	116
4.4	UGT2B17 multiplex real-time allelic discrimination plot	117
4.5	UGT2B17 copy number variation amplification plots	119
4.6	Variations of GAPDH expression in HLM sample set	121
4.7	UGT2B17 expression in human liver	123
4.8	SAHA-glucuronide formation versus UGT2B17 genotype in HLM	124
4.9	K_M for HLMs versus UGT2B17 genotype	125
4.10	UGT2B17 expression versus UGT2B17 genotype in human liver	126

4.11	Correlation between UGT2B17 glucuronidation rate for SAHA and UGT2B17 expression	127
4.12	Representative amplification plot from gender assay	128
4.13	HLM glucuronidation activity stratified by gender	130
4.14	HLM glucuronidation activity stratified by gender and UGT2B17 genotype	130
4.15	UGT2B17 expression in liver stratified by gender and UGT2B17 genotype	131
4.16	UPLC analyses of colon homogenate tested for the ability to glucuronidate SAHA	132
5.1	Deletion analysis of the <i>UGT1A8</i> , <i>-1A9</i> , and <i>-1A10</i> promoter in Caco-2 cells	139
5.2	Location of the prototypical aryl hydrocarbon/xenobiotic responsive element at the UGT1A locus	141
5.3	Basic Luciferase Vector	147
5.4	Deletion identification and schematic	152
5.5	Schematic of UGT1A10 Real-Time PCR assay design	153
5.6	Schematic of UGT1A10 promoter regions tested for effects on gene expression	155
5.7	UGT1A10 promoter driven luciferase activity in colon carcinoma cells, Caco-2	156
5.8	UGT1A10 promoter driven luciferase activity in lung carcinoma cells, A549	157
5.9	UGT1A10 promoter driven luciferase activity in lung carcinoma cells, H1299	157
A.1	Overview of SNaPshot procedure	186
A.2	Linkage Disequilibrium Plot of NST	189
A.3	Agarose gel of amplicons from PCR of NSTs	193
A.4	SNaPshot chromatograms of individually run NST SNP analysis	195
A.5	Chromatograms of multiplex SNaPshot analysis	197

LIST OF TABLES

Table		Page
1.1	List of HDACs by class	14
1.2	HDACi (Partial list)	17
1.3	Targets of SAHA in clinical trials	23
2.1	UGT over-expressing cell lines	55
2.2	Summary of SAHA glucuronidation formation of individual UGTs	72
2.3	Kinetic analysis of SAHA-glucuronide formation by UGTs using UGT-overexpressing cell homogenates	78
3.1	Kinetic analysis of SAHA-glucuronide formation by UGT1A variants	98
4.1	Summary of analysis used to identify the ideal control for normalization in HLMs	122
5.1	List of primers used for PCR amplifications of UGT1A10 wild-type and deletion promoter regions	148
A.1	Summary table of nonsynonymous NSTs	184
A.2	Summary table of probes used for NST variant analysis	187

LIST OF ABBREVIATIONS

(4-(2-hydroxyethyl)-1-piperazineethanesulfonic acid	HEPES
17 β -estradiol	E2
2-amino-1-methyl-6-phenylimidazo- [4,5-b]pyridine	PhiP
4-(methylnitrosamino)-1-(3-pyridyl)-1- butanone	NNK
4-(methylnitrosamino)-1-(3-pyridyl)-1-butanol	NNAL
4-methylumbelliferone	4-MU
7-Ethyl-10-hydroxy-camptothecin	SN-38
Acute myeloid leukemia	AML
adenoviral E1A-associated protein of 300kDa	p300
aryl hydrocarbons	Ah
benzo[a]pyrene	B[a]P
Base pair	bp
Bicinchoninic acid	BCA
Carbon dioxide	CO ₂
Coding DNA	cDNA
Copy number variation	CNV
cutaneous T-cell lymphoma	CTCL
Cyclic AMP response element-binding protein	CBP
Cytochrome P450	CYP
cytochrome P-450 monooxygenases	CYP450
Deoxyribonucleic acid	DNA
dibenzo[a, <i>l</i>]pyrene	DB[a, <i>l</i>]P
Dimethyl Sulfoxide	DMSO
dimethyl sulfoxide	DMSO
Dulbecco's Modified Eagle's Medium	DMEM
<i>Escherichia coli</i> β -glucuronidase	β -glucuronidase
Fetal Bovine Serum	FBS
Food and drug administration	FDA
Gastrointestinal	GI

Geneticin	G418
glutathione-S-transferases	GSTs
Glyceraldehyde 3-phosphate dehydrogenase	GAPDH
hepatocyte nuclear factors	HNF
hexamethylenebisacetamide	HMBA
histone acetyltransferases	HATs
Histone deacetylases	HDACs
Histone deacetylases	HDACs
Histone deacetylases inhibitors	HDACi
Human embryonic kidney fibroblast	HEK293
Human Liver Microsomes	HLM
Leukocyte Adhesion Deficiency II	LAD II
Magnesium Chloride	MgCl ₂
<i>N</i> '-nitrosornicotine	NNN
National Center for Biotechnology Information	NCBI
Nucleotide sugar transporters	NSTs
peptidylprolyl isomerase A	PPIA
Phosphate-Buffered Saline	PBS
polycyclic aromatic hydrocarbons	PAHs
Polymerase Chain Reaction	PCR
SAHA-glucuronide	SAHA-Gluc
sex-determining region Y gene	SRY
single nucleotide polymorphism	SNP
Site-directed mutagenesis	SDM
Suberoylanilide Hydroxamic Acid	SAHA
threshold cycle number	CT
Tris(hydroxymethyl)aminomethane	Tris
UDP-glucuronic acid	UDPGA
UDP-glucuronosyltransferase	UGT
Ultra Performance Liquid Chromatography	UPLC
xenobiotic responsive element	XRE

ACKNOWLEDGMENTS

First and foremost, I would like to thank my thesis advisor, Dr. Philip Lazarus, for all his guidance and support during my time as a graduate student. Phil is an amazing scientist and mentor and I owe much of my development as a scientist and as a critical thinker to him. In addition, I would like to acknowledge and thank all the past and present member of the Lazarus Lab. I would especially like to thank Dr. Ryan Dellinger for his patient mentorship, constant support, and understanding, even at 8 am in the morning. I would also like to thank Dr. Gang Chen for his valuable scientific insight and assistance with the SAHA project, Dr. Carla Gallagher for her assistance with genetic analyses, Dr. Diane McCloskey for editing my thesis, and everyone else who has helped me along the way. Without the scientific support and friendships I have made, this thesis would not have been possible.

I would also like to thank the members of my thesis committee, Drs Lisa Shantz, Laura Carrel, and Christopher Herzog for their time, patience and thoughtful suggestions during the development of my thesis. I would like to thank the members of Dr. Carrel's lab (Jill Stahl and Katie Schafer) for assistance with the SNaPShot assay. The members of the core facilities at Penn State College of Medicine including the Organic Synthesis Facility for the synthesis of SAHA, the Functional Genomics Core Facility for real-time PCR services, and the Molecular Genetics/DNA Sequencing Core for sequencing and SNaPShot services.

Last, and certainly not least, I would like to thank my wonderful family and friends. You have always been there for me no matter how stressful things got. Your support, patience, understanding, and love over the past few years have made this all possible; I truly could not have done this without you.

CHAPTER 1: Literature Review

1.1 INTRODUCTION

1.1.1 Individualized Medicine and Genetic Variation

The concept of individualized medicine is based on the understanding that many factors, including the genetic profile of the patient, personal habits of the patient, environmental factors, and the genetic profile of the disease itself, can influence the course of disease and how a patient will respond to a drug treatment. The goal of the personalized medicine approach is to determine as much as possible about the characteristics of the individual patient, both genetically and environmentally, and then, in that context, design unique drug treatments to maximize drug efficacy while minimizing toxicity. The multifaceted nature of human disease and response to treatment makes identification of all of the factors that influence how a patient will respond to a treatment very difficult. Most drugs target diseases which develop as a result of the combined actions of many gene products and environmental factors. In addition, personal habits such as diet and exercise can influence how individuals respond to drugs. Personal habits can be altered, however, the underlying genetic variations which contribute to differences cannot. Advances in technology have led to the ability to rapidly determine the genetic profiles of individuals and has made it possible to study genetic variations which may contribute to inter-individual differences in susceptibility to disease, course of disease, and response to treatment. Therefore, studies of genetic variation within genes known to be involved in disease processes or

drug metabolism are essential to the realization of the promise of individualized medicine.

Pharmacogenomics is an approach which examines how variations in the genome affect efficacy of and toxicity to drugs and therefore result in inter-individual differences in drug response. Results from pharmacogenomic studies may lead to the identification of biomarkers that can aid in determining which drug, amount, and regimen is optimal for a specific patient, and may also aid in drug development (1, 2). Understanding the characteristics of these genetic variants may also lead to better prediction of patient responses such as drug toxicity and adverse drug reactions. One pharmacogenomic methodology is to examine variations in the whole-genome and correlate these differences to patient response in order to identify associations between genetic variation and altered response to the drug. As defined by the NIH, a genome-wide association study (GWAS) involves rapidly scanning markers across the complete sets of DNA of many people to find genetic variations associated with a particular phenotype. The technologies to make this approach feasible to study populations have recently been made available. A few years ago, SNP genotyping platforms could only produce ~10,000 genotypes per individual; that number has increased 100-fold and platforms can now genotype 1 million SNPs per individual (3). This technology in combination with current SNP maps encompass about 85% of the genome (4) and have greatly enhanced the feasibility of performing GWAS. GWAS have been used for many complex phenotypes and diseases which are highly prevalent including Alzheimer's disease (5), prostate cancer risk (6), Parkinson's disease (7), schizophrenia (8), type 2 diabetes (9), and cancer risk (10-13). A specific example of a GWAS for a complex

phenotype is the autoimmune disease systemic lupus erythematosus [SLE; (14, 15)]. Although SLE has some identified genetic components (16, 17) and there are rare variants that are known to cause this disease (18-20), for the majority of cases a specific and direct genetic link is unclear. A GWAS examining SLE suggested that several genetic variants are associated with the development of this disease (15). In addition to identifying novel SLE susceptibility genes which can be further studied, some of the genes identified using this large scale screen were ones that had been shown previously to be associated with SLE, thus providing validity to the use of GWAS (15). This is one very specific example of how GWAS contribute to identifying genetic variants which correlate to a disease phenotype. GWAS are currently being employed for numerous complex phenotypes which do not have definitive underlying genetic associations. This type of approach of screening for genetic variants also can be applied to drug response phenotypes.

The study of pharmacogenomics is only in its infancy because the tools required to accomplish the screening tasks are just becoming widely available and therefore the literature is very limited. Drug response is a complex phenotype, therefore several genetic and environmental factors may be responsible for observed differences. For the topics that comprise the majority of this thesis, pharmacogenomic GWAS were not found in the literature. Currently, there are only a few reports of successful use of GWAS in relation to drug response (21-23) as well as one report of a study that is currently in the sample collecting stage (24). A good representative GWAS with respect to drug response phenotype and genetic variations is a study that looked at warfarin treatment. This study identified genes that modestly alter therapeutic warfarin dose (22)

and the results from this GWAS are consistent with previous findings (25-28). Another critical point that this pharmacogenomics paper emphasizes is that ample sample size is required in order to have enough power to detect genome-wide significance (22). This requirement is a major limitation to the feasibility of wide use of GWAS for understanding drug response phenotypes. Since pharmacogenomics requires a large population, this approach proves to be very difficult to use for drugs which are not widely prescribed or are in clinical trials with a limited population.

An alternative to examining the whole genome for variations correlated to drug response is to examine specific genes which have a connection to the drug. Such genes may include those that encode for proteins that the drug is targeting, genes which regulate the disease and which may be altered by the drug, or genes that encode proteins that interact with the drug during processes of transport or metabolism. The identification of such genes and subsequent genotyping studies can lead to elucidation of variants of these genes that can be analyzed for correlations to a drug response phenotype. This gene-specific approach to understanding genetic variation and altered drug response is known as pharmacogenetics. Specific examples of how pharmacogenetic studies have been utilized to aid in the development of personalized medicine are discussed in section 1.3.6.

1.1.2 Cancer as a Complex Disease

Together pharmacogenomics and pharmacogenetics are approaches that can be used to examine underlying genetic variations within patients that are responsible for inter-individual differences in drug response as well as to help to determine the best

drug choice based on genetic abnormalities of the disease. The most abundant and diverse of the complex diseases that are currently being examined through pharmacogenomic and pharmacogenetic approaches is cancer. Cancer is a disease in which cells proliferate in an uncontrolled manner, invade surrounding tissues, and in some cases, metastasize to distant sites. Different cancers vary greatly in many aspects, including the initiating cause (environmental factors, genetic predisposition), the affected region, the molecular events that lead to uncontrolled cell growth, and the extent to which the cancer will have an effect on the life-span of an individual. Despite an overwhelming number of studies to address these complexities, complete understanding of the many types of cancer that have been identified to date has not been achieved. This section will discuss a few selected aspects that have been identified to contribute to this set of diseases to illustrate the heterogeneous nature of cancer.

There are many factors that can increase a person's risk of developing cancer, such as exposure to exogenous compounds and the genetic make-up of an individual. A good example of a cancer for which exogenous compounds increase a person's risk is lung cancer, which is the leading cause of cancer death in the U.S, with more than 80% of lung cancer deaths attributable to smoking (29). Tobacco smoke contains over 60 known carcinogens (30) and millions of people smoke; however, only a fraction of smokers (~15%) will develop lung cancer in their lifetime (31). Surprisingly, these findings are adjusted for the quantity smoked, which suggest that the amount smoked only marginally contributes to the chances of developing cancer, suggesting that there are other factors involved. It has been shown that heritable traits can modify the effects

of environmental exposures, and multiple studies have shown a genetic component to lung cancer risk among smokers; however, currently, there is no definitive link between smoking and genetic make-up (32-35). Together, these studies illustrate some of the complexities that underlie the development of lung cancer and highlight the difficulty in predicting cancer susceptibility. These observations hold true for the vast majority of cancers.

There are some genetic variations that have strong links to the development of cancer. For example, germline mutations in BRCA1 and BRCA2 result in increased risk for breast and ovarian cancer; however, these genetic mutations alone are not enough to cause the cancers, and other factors, which are not fully understood, are also required (36-38). Another example of genetic variation that results in the predisposition for the development of cancers are germline mutations in the p53 gene that result in Li-Fraumeni syndrome which is characterized by the development of a wide range of primary cancers (39, 40). This syndrome highlights the fact that individuals with the same genetic mutation can develop cancer in different regions (40). In addition, individuals with known mutations do not have the same initiation and progression of the cancers or response to treatment suggesting that other factors are involved. It appears that multiple events are needed in order to develop neoplasms and additional changes are required for these cells to become malignant (41). These observations further illustrate the complexities that govern all aspects of cancer.

The molecular events that allow cells to proliferate uncontrollably without undergoing cell death, to migrate and colonize in other locations, and to survive in atypical cellular environments still remain elusive. Typically, one specific aspect is

studied; however, methods to study all the factors which may contribute to cancer will greatly aid in the understanding and treatment. Technological advances are assisting this goal with methods to assess proteomic, genomic, epigenomic, metabolomic, and transcriptomic, aspects that are contributing to cancer. These advances will aid in understanding the underlying complexities that result in the observed intra- and inter-individual differences associated with cancers and their treatment..

Cancer is among the leading cause of death worldwide and is the second leading cause of death in the United States (42). Information on harmful environmental exposures and better knowledge of how to reduce risk for cancer via proper diet and exercise along with regular visits to the doctor have assisted in reducing the number of cancer cases in developed countries (42). Despite progress towards reducing the number of cases, cancer still remains prevalent with an estimated 1.4 million new cases identified in 2008 for the United States alone (43).

Typical treatments for cancers include surgery, radiation and chemotherapy. Although these methods can increase a patient's life span, improving the quality of life for individuals with cancer has become increasingly important. For example, methods such as surgery and radiation not only target the cancerous regions, but also affect the healthy organs thereby leading to complications and harmful side effects. Many chemotherapeutic agents also have adverse side effects and vary in efficacy from patient to patient. Current trends in cancer drug development include targeting cancer cells specifically and identifying the underlying causes of inter-individual differences in response to treatment as a means to improving quality of life. One approach to identify the underlying causes of differences in response to treatment is to examine the genetic

makeup of an individual. More specifically, pharmacogenetics is an approach which correlates differences in drug response to the genetic makeup of individuals.

Pharmacogenetics can be used to assess genetic differences of a patient's cancerous cells or it can be used to understand differences in drug response based on the genetic makeup of an individual. Examining genetic differences between cancerous cells and normal cells, even in the same individual, can be very complex because cancer cells are very heterogeneous and often genetically unstable. Studying differences in the genetic makeup of an individual and comparing that to differing drug responses offers a more practical approach because a person's DNA is the same in the majority of his or her cells. More specifically, one could examine genetic differences related to the pathway the drug is targeting or the genetic variations in the genes which code for the enzymes involved in the drug's metabolism.

Drug metabolism is an important aspect to consider when assessing the overall effect of a drug because the ability of an individual to metabolize the drug will affect the overall concentration and exposure time that the active form of the drug spends in the body. Drug metabolism is broken down into two phases. Phase I enzyme activity typically leads to a more active polar metabolite. Phase II enzyme activity conjugates polar moieties to the drug and typically leads to drug inactivation and excretion. Many of the enzymes involved in drug metabolism have been shown to contain variant forms which have been shown to alter *in vitro* metabolism or drug efficacy and/or toxicity in patients.

Some chemotherapeutic agents have been examined to identify the enzymes involved in drug metabolism and how variants of the enzymes alter patient response;

however, many promising drugs have not been characterized. The goal of this thesis was to identify genetic alterations in the population which may contribute to differences in response to current chemotherapeutic agents. The chemotherapeutic agent chosen for examination was SAHA. This drug was chosen because it is a highly promising chemotherapeutic agent, which acts by inhibiting histone deacetylases, for the treatment of many types of cancer. Furthermore, the metabolites of SAHA have been identified and include products of a phase II drug metabolism pathway which utilizes enzymes that are known to have many variants which can lead to altered enzyme activity.

In this literature review, the enzymes involved in acetylation and why they are ideal targets for drug development will be described. Then the drugs which target this pathway will be discussed along with a further explanation of why SAHA was the most ideal drug of this class of compounds to examine for the studies described in this thesis. SAHA's use, toxicities, and drug metabolism will be examined. Finally, an in-depth background discussing the family of glucuronidation enzymes responsible for a significant level of SAHA metabolism will be given. Together, this information will provide a general basis of how SAHA works, demonstrate how response and toxicities vary in patients, and provide support for how genetic variants of UGTs may contribute to both response and efficacy of SAHA in patients.

1.2 HATs and HDACs

Histones are proteins around which DNA is wrapped and which are organized into nucleosomes [Figure 1.1, (44)]. Acetylation of histone proteins was identified in 1963 (45), however, the enzymes responsible for acetylation were not identified for over 30 years. As illustrated in Figure 1.1, the organization of the DNA around the histone is regulated by histone acetyltransferases (HATs) and histone deacetylases [HDACs; (46)]. HATs transfer acetyl moieties to the lysines of the amino-terminal tails of histones, which results in decondensation of the chromosome and allow transcription to occur. HDACs remove acetyl moieties from the lysines of the amino-terminal tails of histones which results in condensation of the chromosome and causes transcription to cease. By altering the conformation of DNA around histones, these enzymes regulate the ability of genes to be expressed (46, 47). In addition to histones, proteomic studies have identified acetylated lysine residues in a diverse array of proteins (48, 49). For example, a proteomic survey identified 388 acetylation sites in 195 proteins derived from HeLa cells and mouse liver mitochondria (48). Although HDACs and HATs were initially identified for their roles in transcriptional regulation via histone modifications, research has now shown that these enzymes regulate multiple genomic processes (ie. signaling, apoptosis, DNA repair) further supporting their importance in cellular function and regulation (50).

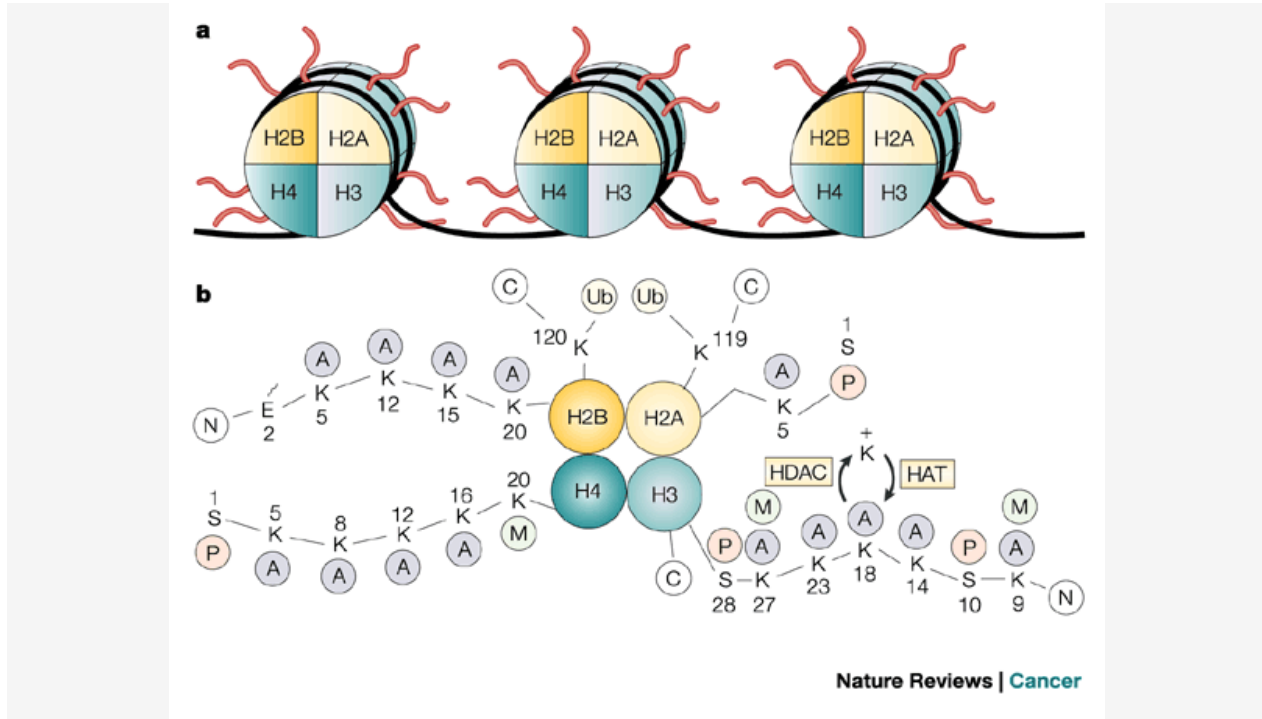


Figure 1.1: Schematic of the structure of histones in nucleosomes. **a** | The core proteins of nucleosomes are designated H2A (histone 2A), H2B (histone 2B), H3 (histone 3) and H4 (histone 4). Each histone is present in two copies, so the DNA (black) wraps around an octamer of histones the core nucleosome. **b** | The amino-terminal tails of core histones. Lysines (K) in the amino-terminal tails of histones H2A, H2B, H3 and H4 are potential acetylation/deacetylation sites for HATs and HDACs. Acetylation neutralizes the charge on lysines. A, acetyl; C, carboxyl terminus; E, glutamic acid; M, methyl; N, amino terminus; P, phosphate; S, serine; Ub, ubiquitin. [Reference from (44)].

Although HATs and HDACs are members of multiprotein complexes, making identification of their individual functions difficult, abnormal functions of these enzymes have been observed commonly in cancer cells and are a particular hallmark of leukemias and lymphomas. In addition to their direct role in histone acetylation, these enzymes regulate several diverse cellular processes [Figure 1.2; (51)]; however, no

studies have demonstrated a clear and direct mechanism for how HAT/HDACs affect cellular processes.

1.2.1 HATs

HATs are a family of enzymes that was first identified to acetylate core histones thus resulting in a conformational change of the histone/DNA complex which allowed for gene transcription via chromosome decondensation (52). As shown in Figure 1.1, the lysines (K) in the amino-terminal tails of the histone complexes are available for HATs to acetylate. The HAT family of enzymes is evolutionarily conserved and its members are classified based on their catalytic domains (52). These enzymes are typically found in complexes composed of multiple subunits (53). HATs have also been identified to acetylate a number of non-histone substrates including proteins known to regulate the cell cycle (54). This family of enzymes plays an important role in cell regulation, therefore disruptions or alterations in the normal activity of any of these enzymes may result in aberrant cellular function.

Genes encoding HATs have been shown to be amplified, translocated, and over expressed in malignancies (55). Cyclic AMP response element-binding protein (CBP) and adenoviral E1A-associated protein of 300kDa (p300) are two well-studied proteins that, among other functions, are responsible for histone acetylation, and defects in these genes have been linked to the development of cancers (56, 57). For example, Rubinstein-Taybi syndrome is caused by heterozygous germline mutation in the CBP gene, and individuals with this mutation are predisposed to tumors of neural crest origin in childhood (58, 59). In addition, somatic mutations of both CBP and p300 have been

associated with leukemia and lymphoma; specifically, a translocation of the CBP gene t(8,16) (p11,p13) was shown to be associated with the M4/M5 subtype of acute myeloid leukemia (AML) (60). A translocation that results in a fusion protein of p300 and monocytic leukemia zinc-finger protein also results in a sub-class of AML (61, 62). The association between alteration in HATs and cancer supports the examination of acetylation as it relates to the development and treatment of cancer.

1.2.2 HDACs

As HATs are responsible for the addition of an acetyl group, HDACs facilitate the removal of the charge-neutralizing acetyl group from histone lysine tails, thus resulting in chromosomal condensation and repression of gene transcription (44). HDACs are divided into four classes according to phylogenetic analyses and sequence homology to yeast prototypes [Table 1.1; (50, 63, 64)]. HDACs function in various subcellular compartments, in multisubunit complexes, and individual HDACs are not redundant in their biological activity (50, 65). Similar to HATs, HDACs are also key enzymes involved in gene regulation and protein regulation throughout the cell; although their exact roles and functions in these processes are not completely understood.

Class	Enzymes
I	HDAC1, HDAC2, HDAC3, HDAC8
Ila	HDAC4, HDAC5, HDAC7, HDAC9
Ilb	HDAC6, HDAC10
III	SIRT 1,2,3,4,5,6,7
IV	HDAC11

HDAC: Histone deacetylases; SIRT: Sirtuin

Table 1.1: List of HDACs by class.

Studies have identified a variety of carcinomas, tumors, and cancers that have overexpression of specific HDACs (Table 1.1). For example, prostate, gastric, colon, and breast carcinomas overexpress HDAC1 (66-70), gastric, colorectal, and cervical cancers overexpress HDAC2 (62, 67, 71-73), while HDAC3 is overexpressed in colon tumors and HDAC6 is overexpressed in breast cancer tissue (62, 67, 74). In addition to overexpression, alterations in HDAC transport are also linked to cancer as in the case of acute promyelocytic leukemia (75, 76). Furthermore, studies have found that histone H4 hypoacetylation is a hallmark of many cancers (77), supporting the negative consequences of over expression of HDACs. However, it has yet to be fully understood how overexpression of HDACs and hypoacetylation directly affect the development of cancerous cells.

Studies support that the acetylation status of a cell is crucial and that aberrant acetylation is linked to cancer. Since HDACs have been shown to be over expressed in cancer, and hypoacetylation of H4 is a hallmark of many cancers, this pathway has been a target for drug development. The HDAC family of enzymes has been identified as a promising target to reverse aberrant epigenetic states associated with cancer via

regulation of levels of histone and non-histone protein acetylation and gene expression (70, 78, 79).

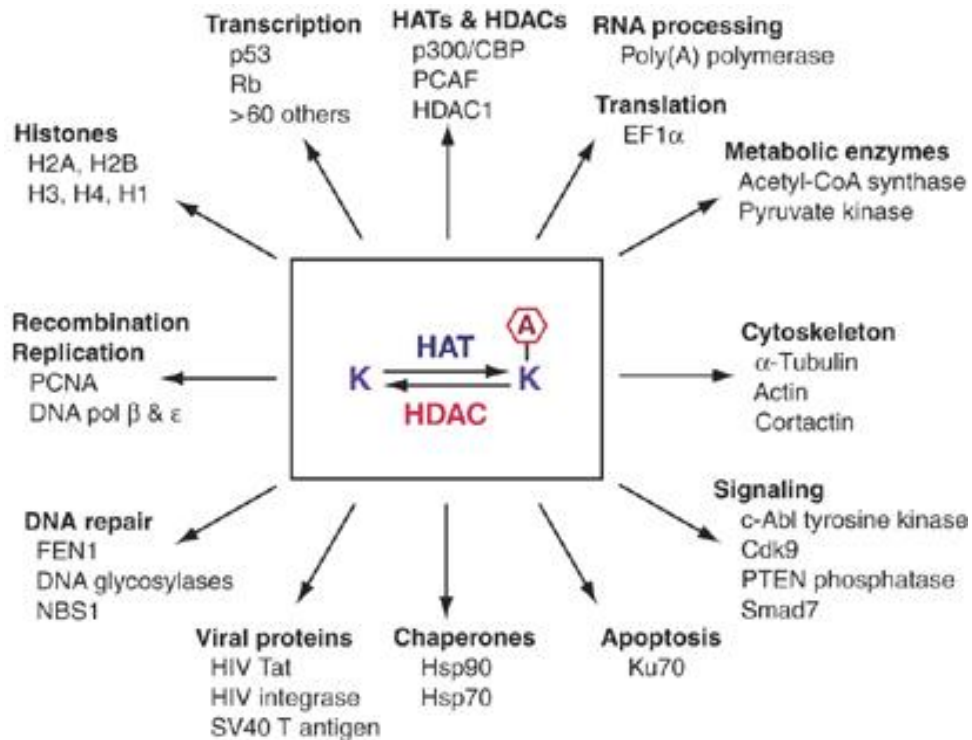


Figure 1.2: Many functions of HDACs. Schematic illustration of the prevalence of reversible lysine (K) acetylation in diverse cellular processes. The hexagon with the letter A refers to acetylation. For each process, only representative proteins are listed. In particular, acetylation of acetyl-CoA synthase is a key regulatory mechanism conserved from bacteria to humans (Starai *et al.*, 2002; Hallows *et al.*, 2006; Schwer *et al.*, 2006). Cdk9, cyclin-dependent kinase 9; FEN1, *Flap endonuclease 1*; NBS1, *Mijmegen breakage syndrome protein 1*; PCNA, *proliferating cell nuclear antigen*; PTEN, *phosphatase and tensin homolog*; Rb, *retinoblastoma suppressor protein*. [Reference from (51)].

1.2.3 HDAC Inhibitors

As HDACs are important regulators of transcription, cell cycle regulation and are overexpressed in both hematological and solid malignancies; they are an ideal target for cancer therapies. Natural inhibitors of HDACs, including trichostatin A (*Streptomyces platensis*) and sulforaphane (found within cruciferous vegetables), have been studied for their anticancer abilities; in addition, compounds have been synthesized to optimize anti-HDAC activity. The first synthetic compound identified as a HDAC inhibitor (HDACi) was sodium butyrate (80). Since then, several classes of inhibitors have been developed to target HDACs.

HDACis are divided into several groups, based on chemical structure, which include aliphatic acids, cyclic peptides, benzamides, and hydroxamic acid derivatives [Table 1.2; (78)]. Aliphatic acids such as butyrate, phenylbutyrate, and valproic acid are relatively weak inhibitors of HDACs (78, 79, 81, 82). Conversely, cyclic peptides like depsipeptide are potent inhibitors of HDACs and are structurally complex (78). Of all the classes of HDACis, the hydroxamic acid derivatives are the most potent pan-HDAC isoform inhibitors (83).

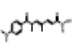
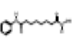
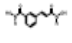
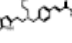
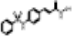
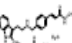


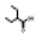
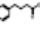

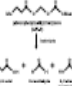
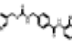
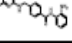
Class	Compound	Structure	HDAC Target (Potency)	Effects on Transformed Cells	Stage of Development (Reference)
Hydroxamates	TSA		Class I and II (nmol/L)	TD; GA; A; AI; AE	N/C
	SAHA, Zolinza, vorinostat		Class I and II (μmol/L)	TD; GA; AI; AE; MF; AU; S; PP; ROS-CD	Merck Food and Drug Administration approved for CTCL (4)
	CBHA		N/A (μmol/L)	GA; A; AI; AE	Merck (4)
	LAQ-824		Class I and II (nmol/L)	GA; A; AI	Novartis phase I (discontinued)
	PDX-101		Class I and II (μmol/L)	GA; A	TopoTarget phase II (57)
	LBH-589		Class I and II (nmol/L)	GA; A; ROS-CD	Novartis phase I (51)
	ITF2357		Class I and II (nmol/L)	GA; A; AI	Italfarmaco phase I (56)
Cyclic peptide	PCI-24781 Depsipeptide (FK-228)	NA 	Class I and II (NA) Class I (nmol/L)	N/A TD; GA; A; AI; AE; MF; ROS-CD	Pharmacyclics phase I Gloucester Pharmaceuticals phase IIb for CTCL and PTCL (63) phases I and II
Aliphatic Acids	Valproic Acid		Class I and IIa (mmol/L)	TD; GA; A; S	Abbot phase II
	Phenyl butyrate		Class I and IIa (mmol/L)	TD; GA; A; AI; AE	Phase II
	Butyrate		Class I and IIa (mmol/L)	TD; GA; A; AI; AE	Phase II
	AN-9		N/A (μmol/L)	TD; GA; A	Titan Pharmaceuticals phase II
Benzamides	MS-275		HDAC1, HDAC2, HDAC3 (μmol/L)	TD; GA; A; AI; AE; ROS-CD	Schering AG phase II (51)
	MGCD0103		Class I (μmol/L)	TD; GA; A	Methylgene phase II (60)

Table 1.2: HDACi (Partial list). Abbreviations: GA, growth arrest; TD, terminal differentiation; A, apoptosis; AI, cell death by activating intrinsic apoptotic pathway; AE, cell death by activating extrinsic apoptotic pathway; MF, mitotic failure; AU, autophagic cell death; S, senescence; PP, polyploidy; ROS-CD, reactive oxygen species–facilitated cell death; N/A, not available; CBHA, M-carboxycinnamic acid bishydroxamate; CTCL, cutaneous T-cell lymphoma; CTCL, peripheral T-cell lymphoma. [Reference from (78)].

The original hydroxamic acid HDACis were derived from hybrid polar compounds like hexamethylenebisacetamide (HMBA). This group of HDACis was initially studied based on the observation that dimethyl sulfoxide (DMSO) caused growth arrest and terminal differentiation of leukemia cells, leading to further investigation of compounds of similar structure (65). First generation hybrid polar compounds, like HMBA, were found to induce differentiation of a variety of transformed cells (84-87); however, when administered to patients, they led to toxicities including severe thrombocytopenia (88). Based on these original studies, a second generation of hybrid polar compounds were synthesized and tested with promising results for applications in cancer treatment (85).

Several hydroxamic acid derivatives and their analogues have been synthesized and tested both *in vitro* and *in vivo* for efficacy and potency as possible chemotherapeutic agents. These compounds contain a zinc-chelating moiety, a linker, and an external motif for surface recognition (89). Several of these hydroxamates, including, SAHA, PDX-101, and LVH-589, are being tested in clinical trials both alone and in combination with other drugs (78).

HDACis are among the most promising new anticancer agents because of their ability to induce growth arrest, differentiation, and apoptotic cell death (90-92). HDACis have lower toxicities than previous treatments, are effective in μM doses, and can target a variety of cancers. However, how these drugs work is still not understood. Studies have examined the expression of genes in transformed cells affected by HDACis and found that 2-10% are altered, with a similar number of genes down-regulated and up-regulated (93-96). For example, HDACis cause the selective upregulation of tumor suppressor genes in malignant tumor cells (90-92, 97-99) but there are no good

explanations for this observation. In addition to not fully understanding how these HDACis work, it is also unclear why tumor cells are sensitive to these inhibitors and normal cells are relatively resistant. One possible explanation is that normal cells can compensate for the inhibition of one or more pathways whereas, cancer cells are comprised of multiple defects and cannot compensate for the pathways HDACis are affecting (78). Of the current HDACi compounds, SAHA has thus far been the most efficacious in the treatment of cancer and is FDA approved (100) and therefore will be the focus of our pharmacogenetic analysis.

1.2.4 SAHA

Trischostatin A is a naturally occurring product of *Streptomyces platensis* and *Streptomyces sioyaensis* that is structurally related to SAHA [Figure 1.3; (101, 102)]. SAHA contains a hydrophobic phenyl ring, a six-carbon hydrophobic methylene spacer, two polar sites, and a terminal hydroxamic acid group. The hydroxamic acid moiety of SAHA has a high affinity for biometals which confers value to biomedicine due to its ability to interact with biological compounds [ie. the biometal Zn(II) is present in enzymes and SAHA's hydroxamic acid moiety can interact with this metal resulting in altered enzyme function (103)]. SAHA was first synthesized and described in 1996 as part of a screen of hybrid polar compounds which were tested for their ability to induce differentiation of transformed cells (85). That study demonstrated that SAHA was more potent than HMBA as an inducer of murine erythroleukemia cell erythroid differentiation (85). Derivatives and analogs of SAHA have been tested as potential chemotherapeutic

agents; however, none have been identified to have equivalent overall benefits when compared to SAHA.

After identification of SAHA as a HDACi (104), further investigation found that it inhibits HDACs by a direct interaction with the HDAC catalytic site; more specifically, SAHA inserts its aliphatic chain into the pocket of the enzyme interacting with the Zn²⁺ ion [Figure 1.4; (105-107)]. All of the effects of inhibiting HDACs are not known, but SAHA has been shown to induce cell cycle arrest and terminal cell differentiation in transformed cells, cause cell death and block angiogenesis (44, 79, 82, 108). *In vitro* studies have helped to elucidate the mechanisms by which SAHA affects cancer cells (109-111). For example, the lymphoblastic cell line, CEM, showed a total of 2,205 (22.1%) expressed genes to be altered by SAHA, with a similar number being up-regulated and repressed (96). SAHA's inhibition of HDACs is relatively rapidly reversible which may provide normal cells with compensatory abilities that protect them from cell death (65). Although underlying mechanisms of action remained elusive, when administered to rats or mice induced to develop cancers, SAHA treatment resulted in suppressed tumor growth with little or no toxicity (110, 112, 113). Tests in both *in vitro* and *in vivo* animal cancer models supported SAHA's role as a chemotherapeutic agent.

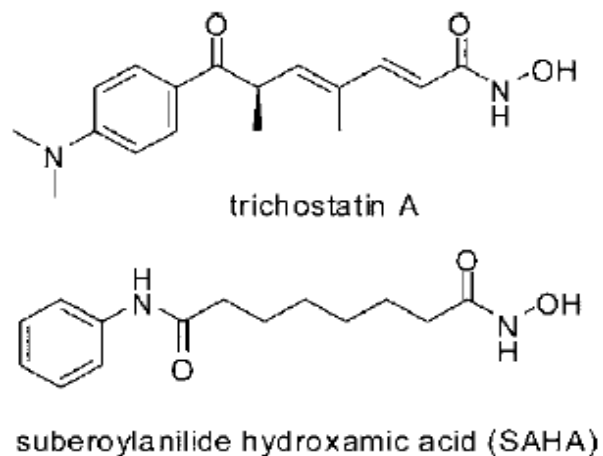


Figure 1.3: Structure of trichostatin A and SAHA. [Reference from (101)].

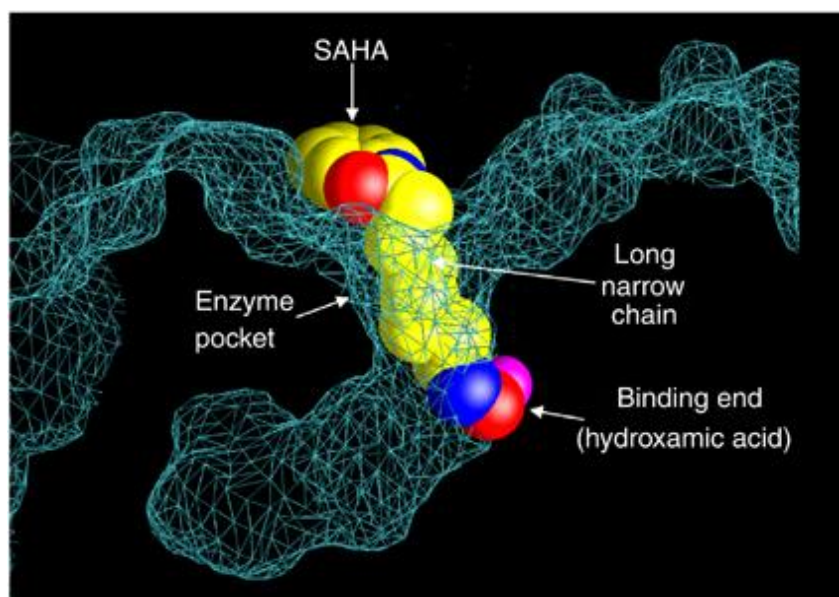


Figure 1.4: SAHA inhibits HDAC activity by binding to the pocket of the catalytic site. The hydroxamic acid moiety of SAHA binds to a zinc atom (pink), allowing the rest of the molecule to lie along the surface of the HDLP protein. [Reference from (44)].

The first clinical trial of SAHA as a chemotherapeutic agent found that it was well tolerated and had antitumor activity against solid and hematological tumors (55, 114). Further clinical studies, which focused on cutaneous T-cell lymphoma (CTCL), found additional promising results and in 2006, the Food and Drug Administration (FDA) approved SAHA for the treatment of CTCL (100, 115, 116). Although SAHA is in its initial phase as an FDA approved chemotherapeutic agent, many clinical trials are testing its use against a variety of cancers [Table 1.3; (117)].

SAHA was initially administered to patients intravenously; however, to make treatment easier, an oral dosage was designed with equal efficacy (55, 114, 118, 119). Current clinical trials administer SAHA orally at a range of 200-400 mg depending on patient response. Although SAHA is known for being well-tolerated and having minimal toxicity, some patients still exhibit adverse effects (55, 100, 114, 118, 119). The most common adverse events include diarrhea, fatigue, nausea, and anorexia, with some patients having intolerable responses (100). Studies have looked at affects of both varying dosages of SAHA and food intake in conjunction with SAHA as a means to understand differences in patient response; however, no clinically relevant information has been obtained (120).

SAHA Target	Combination*
Advanced solid tumors	Yes
Nasopharyngeal carcinoma or Nasal type natural killer	Yes
Renal Cell	Yes
Transforming myelodysplastic syndromes, Myeloproliferative disorders	Yes
Unresectable solid tumors or Lymphoma and Hepatic Dysfunction	No
Prostatectomy patients	Yes
HER2-Negative primary operable breast cancer	Yes
Glioblastoma multiforme	Yes
Mantle Cell lymphoma or refractory diffuse large B-cell lymphoma	Yes
Blood stem cell transplant patients	Yes
Non-Small cell lung cancer (stage I-III)	No
Neoadjuvant treatment for ductal carcinoma in situ of the breast	No
Ovarian cancer	Yes
Locally advanced or metastatic solid tumors	Yes
Colorectal Cancer	Yes
Metastatic or unresectable epithelial solid tumors	Yes
Advanced malignant pleural mesothelioma	No
Malignant gliomas	Yes
Breast cancer	No
Advanced upper gastrointestinal cancer	Yes
Small Cell lung cancer	Yes
Non-hodgkin Lymphoma	Yes
Pancreatic cancer	Yes
Patients with brain metastases	Yes
Acute Leukemia	Yes

Table 1.3: Targets of SAHA in clinical trials. Partial list of the National Cancer Institute’s information on clinical trials for SAHA. *Combination column is to highlight that the majority of trials are in combination with other drugs (117).

1.2.5 SAHA Metabolism

When administered to patients, SAHA is the active compound that inhibits HDACs and is also metabolized into one of two inactive compounds. The pathways through which SAHA can be metabolized are via hydrolysis followed by beta-oxidation to produce 4-anilino-4-oxobutanoic acid or via glucuronidation to produce SAHA-glucuronide [Figure 1.5; (55, 114)]. The rate of SAHA metabolism will contribute to the amount of active drug present *in vivo*. In serum from patients treated with SAHA, SAHA-glucuronide and 4-anilino-4-oxobutanoic acid were on average 3- to 4- and 10- to 13-fold higher, respectively, than that of the parent compound (120). However, these relative levels may be skewed due to the differences in the apparent terminal half-life of each compound. For example, the SAHA-glucuronide was shown to have a half-life of ~1.8 hours, which is similar to that of SAHA, but a much longer half-life was observed (~6 to 9 hours) for 4-anilino-4-oxobutanoic acid (7). This suggests that the overall contribution of glucuronidation to SAHA metabolism may be underestimated, since SAHA-glucuronide is cleared from the system more rapidly, and that it is a significant process that warrants further investigation.

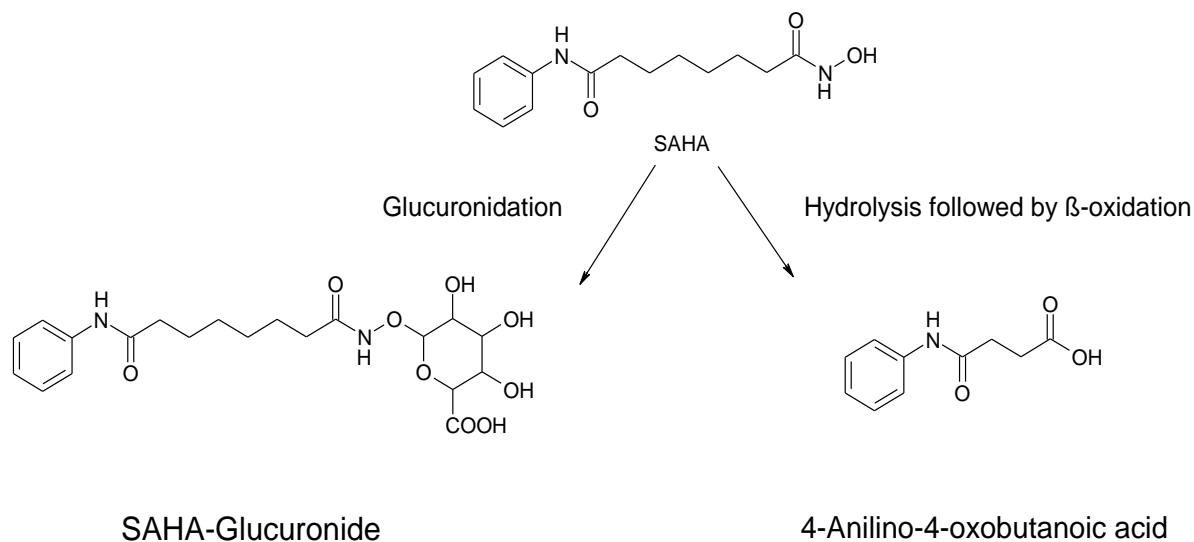


Figure 1.5: Schematic of SAHA metabolism.

While metabolites of SAHA are known, the pathways by which SAHA is metabolized have not been well-characterized. Glucuronidation appears to be contributing to a significant portion of SAHA metabolism and studies of other drugs have identified enzyme variants which lead to altered glucuronide formation and patient response. For example, it was recently demonstrated, *in vitro*, that the UGT2B7p.His268Tyr variant was associated with decreased liver microsomal glucuronidation activity against major active metabolites of Tamoxifen (121). *In vivo* data demonstrate that the UGT1A6*2 variant causes more rapid glucuronidation of salicylic acid than wild-type UGT1A6, supporting the importance of altered abilities of enzyme variants to metabolize drugs (122). Perhaps the most important support for the need to understand drug metabolism is the link between the UGT1A1*28 allele and

increased toxicity to Irinotecan (123-125), which prompted the FDA to recommend genetic screening for the UGT1A1*28 allele in patients who may be considered for treatment with this agent (126). As glucuronidation has been shown to be an important mode of metabolism for SAHA, identification of the individual UGTs responsible for this process will lay the foundation to understand how variants of these enzymes may affect overall SAHA metabolism. Characterization of both wild-type and variant UGTs may aid in better understanding differences in patient response and toxicity to SAHA.

1.3 UDP-GLUCURONOSYLTRANSFERASE

The UGT superfamily of enzymes catalyzes the glucuronidation of a variety of endogenous compounds such as bilirubin and steroid hormones, as well as xenobiotics such as drugs and environmental carcinogens (127-129). These enzymes are located in the endoplasmic reticulum of cells and make xenobiotics and endogenous compounds more water soluble through their conjugation to glucuronic acid in a reaction with the hydrophilic co-substrate, UDPGA. This conjugation alters the biological properties of the compound to enhance its excretion in the urine or bile and typically converts substrates into products that are less pharmacologically active (129-131).

Three main families of UGTs have been identified which are classified, based upon structural and amino acid sequence homology, into several families and subfamilies each containing several UGT genes. The UGT 1A family gene complex has been localized to chromosome 2 in humans. This unique gene complex consists of 13 UGT family 1A-specific exons (127, 132) that are highly conserved between species, with the same gene structure observed in both humans (127) and rodents (133). These independent exon 1s share a common set of exons 2-5 and result in functional proteins. The UGT2B family members are derived from independent genes located on chromosome 4. There are at least six members of the human UGT2B enzyme family that have been hypothesized to have evolved by whole gene duplication and conversion, since these genes show no evidence of shared exons but are all clustered on chromosome 4 in humans (134, 135). UGT1As and UGT2Bs mRNA are expressed in various tissues throughout the body and are predominately expressed in liver, kidney and gastrointestinal (GI) track (136).

The UGT2A enzymes were originally found to be expressed in olfactory tissues, and studies which looked at the ability of UGTs to glucuronidate exogenous substrates did not typically screen this UGT family of enzymes (137). However, recent studies have identified the UGT2A enzymes to be expressed in other tissues and have tested these enzymes for activity against substrates which could be relevant to those areas (138-141). The UGT2A1 enzyme is expressed in lung and trachea (138-140) and is active against odorants, steroid hormones (estradiol, testosterone and epitestosterone), and some drugs (137, 142, 143). Substrates for UGT2A2 include, estradiol, testosterone and epitestosterone (142, 143). While UGTs 2A1 and 2A2 are extra-hepatic, UGT2A3 was recently identified to be expressed in liver, GI tract and kidney, and has been shown to glucuronidate bile acids [chenodeoxycholic acid, deoxycholic acid, hyodeoxycholic acid, and ursodeoxycholic acid; (141)]. The work presented in this thesis was conducted prior to the aforementioned studies in which the UGT2A enzymes were found to be expressed in tissues which potentially could contribute to the glucuronidation of the substrate of interest. Therefore, this thesis concentrates on the UGT1A and UGT2B family of enzymes; however, this does not mean the UGT2As are not important, it only supports that the UGT field is rapidly expanding.

The UGT families of enzymes are important to study with respect to cancer due to their roles in detoxification and elimination of carcinogens. In addition, UGTs also play an important role in the metabolism of chemotherapeutic agents which could affect patient response to treatment. Therefore, understanding UGT expression patterns, their modes of regulation, and identifying functional polymorphic variants are important to elucidating the multiple roles of UGTs in cancer.

1.3.1 Gene Structure

The UGT family 1A gene complex has been localized to chromosome 2q37 and spans more than 200 kb (144). This unique gene complex consists of 13 UGT family 1A-specific exons (69,70) that are highly conserved between species, with the same gene structure observed in both humans (127) and rodents (133). Based on the high homology of UGTs, this locus is hypothesized to have evolved as a result of gene duplication (134, 145). Figure 1.6 illustrates the homology among the many human UGTs and highlights UGT1A gene clustering; for example, UGTs 1A5, 1A3 and 1A4 are clustered together. The naming of the UGTs is based on the first exon and the numbering of these exons is based on the order in which they were found and not on similarity of structure or function. These independent exon 1A regions are responsible for the wide range of substrate specificity demonstrated by the UGT1A family of enzymes while the common region coded by exons 2-5 is involved in UDPGA binding (129). As illustrated in Figure 1.7, the nine functional proteins coded for on this locus differ only in their amino-terminus as a result of joining the independent exon 1 regions to a shared carboxy-terminus encoded by exons 2-5 (127, 146, 147). Transcripts are produced by exon sharing, combining the first exon with the common exons 2-5 and not by alternative RNA splicing (145, 148).

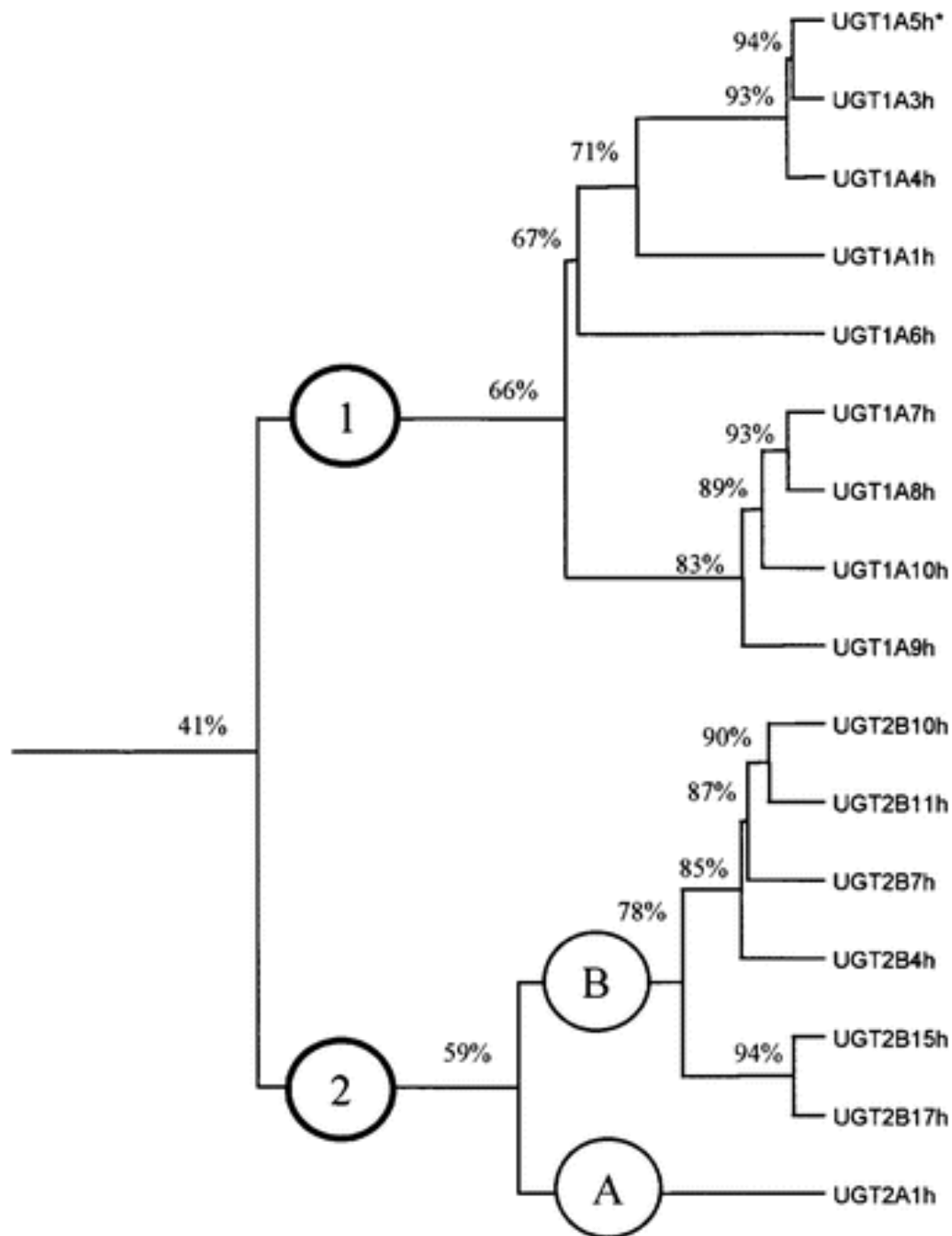


Figure 1.6: Phylogenetic tree showing the relationships between the human UDP-glucuronosyltransferases (UGTs). The median percentage identity of amino acid sequences between UGTs split by a node is shown. (*Asterisk*) Indicates the gene product has not been identified. [Reference from (145)]

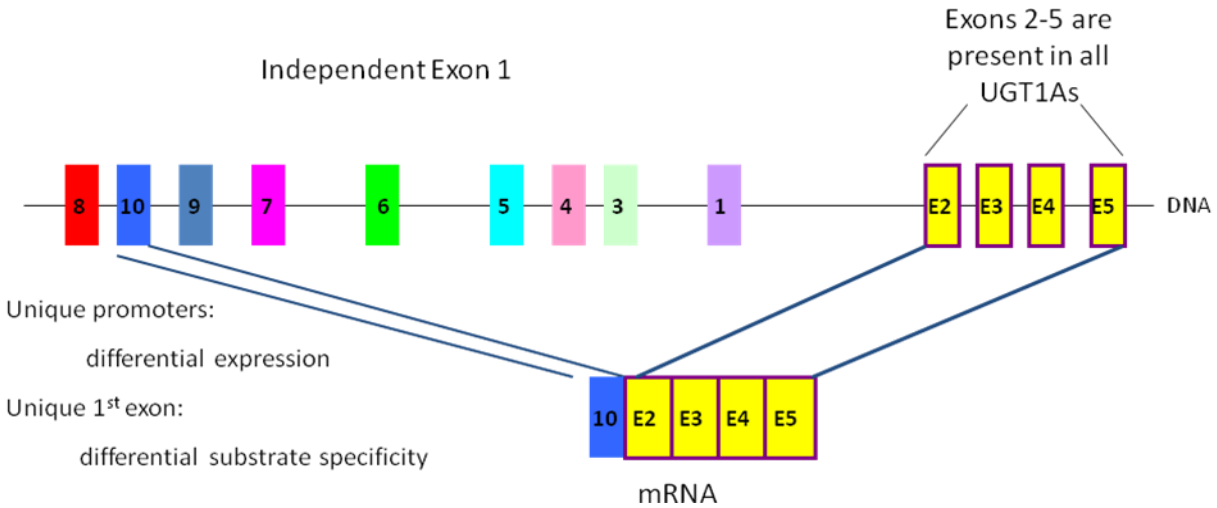


Figure 1.7: Genomic organization of the UGT1A locus and example of mRNA transcribed. The top diagram illustrates the UGT1A locus located on 2q37 spanning 200 kb. This figure highlights the independent exons 1 that are spliced to the common exons 2-5 using UGT1A10 as an example of the mRNA that would have been transcribed and processed (bottom). These independent exons 1 give each UGT differential expression and substrate specificity. This figure is not drawn to scale; the independent exon 1 accounts for half of the mRNA

Whereas the UGT1As share a common region consisting of exons 2-5, the UGT2B family is composed of gene clusters located on 4q13 (149). The UGT2B family likely evolved by whole gene duplication and conversion since these genes show no evidence of shared exons but are clustered on a single chromosome in humans (135). There are at least 6 protein coding genes in the UGT2B family and several pseudogenes have been identified (Figure 1.8).

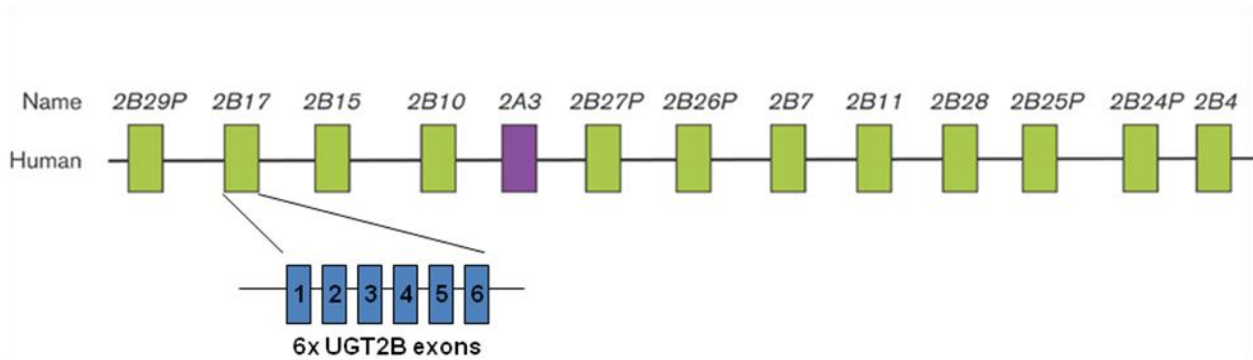


Figure 1.8: The UGT2B family locus. Each gene, consisting of six exons, is represented by a colored rectangle. Pseudogene names end in the label P. The genes are not drawn to scale. The human UGT2B genes extend over approximately 1.45 Mb. The figure is derived from Builds 35.1 of the human genome. [Reference from (134)].

All UGT genes code for proteins that are ~ 530 amino acids in length. These proteins contain similar regions, including a substrate binding site, a glucuronic acid binding site, and a hydrophobic transmembrane region, which are illustrated in Figure 1.9. Due to their location in membranes, UGTs have not been stably purified (150). Therefore determination of their exact catalytic mechanism(s) remains elusive. Although highly homologous to one another, each UGT has a unique profile for glucuronidation and efficiency for substrates.

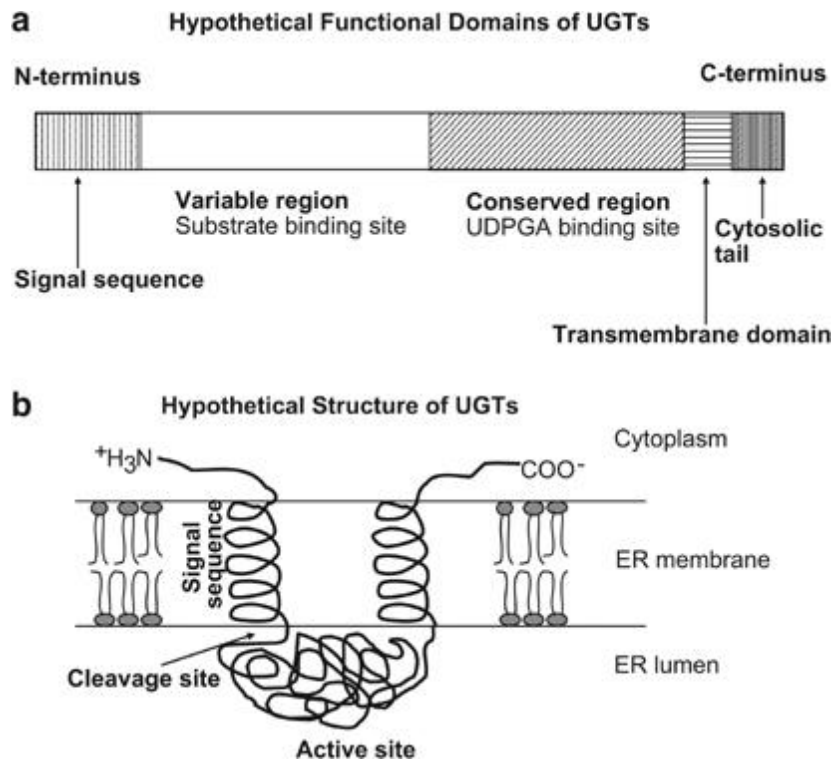


Figure 1.9: Putative protein structure of UGT proteins. (a) Functional domains are depicted in a linearized protein. (b) The UGT protein is depicted as it is presumed to be located within the endoplasmic reticulum membrane. [Reference from (146)].

UGTs are found in many species including mice and rats which would be convenient model organisms in which to study *in vivo* glucuronidation of xenobiotic substrates. However, as illustrated in Figure 1.10, mice, rats, and humans produce different UGTs that vary in homology between species and exhibit large differences in substrate specificity, thus making relative comparison of glucuronidation between species difficult. For example, when comparing hepatic glucuronidation of mycophenolic acid (the active metabolite of the immunosuppressant prodrug, mycophenolate mofetil), UGT1A9 is the predominant UGT responsible in human liver microsomes (HLM) whereas Ugt1a1 and 1a7 are the principle metabolizers in rat liver microsomes. Such

a difference in the specificity of glucuronidation is also observed in between the extra-hepatic UGTs 1a8 and 1a10 in rat as compared to human UGTs 1A8 and 1A10 (151, 152).

Recently, chimeric mouse lines that contain human hepatocytes have been generated and characterized, and these humanized chimeric mice may be useful as an animal model for drug development and characterization (153). However, no studies have as yet characterized the glucuronidation of xenobiotics in this system. In addition, transgenic mice containing the entire UGT1A locus have been developed (154). These mice have been shown to exhibit similar tissue-specific UGT1A expression to that of humans (154). However, these mice only contain the UGT1A locus and don't have all the UGT2Bs that are found in humans and which play important roles in xenobiotic metabolism. Together, these data suggest that animal models like chimeric and transgenic mice may be useful to provide a general understanding on the glucuronidation of xenobiotic compounds, but the overall relevance to humans is limited.

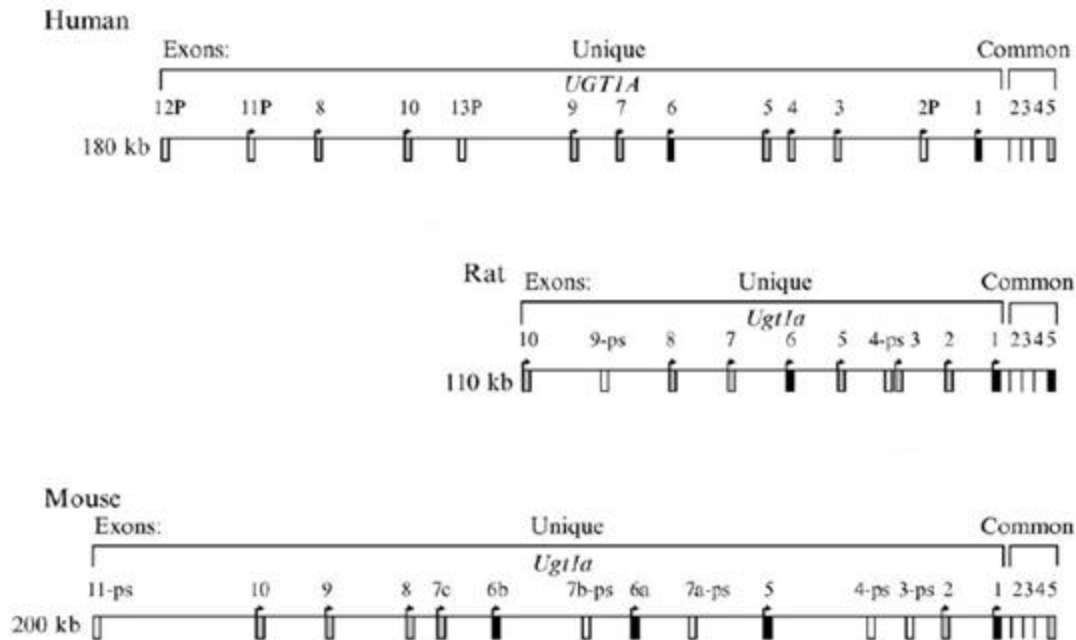


Figure 1.10: Comparison of the UGT1 locus in human, rat, and mouse. Relative positions of the unique first exons at the UGT1 complex locus in human (144), rat (133), and mouse (155). Illustration represents relative positions. Human, rat, and mouse loci are located on chromosomes 2, 9, and 1, respectively. [Reference from (155)].

1.3.2 Expression and Regulation

Each UGT has a unique promoter region which contributes to the expression pattern of the individual enzyme. Despite high homology with one another, each enzyme found on the UGT1A locus is regulated in a unique, strict, tissue-specific pattern (129, 156). Assessment of expression using antibodies against individual UGTs is made difficult due to the high homology of these enzymes and thus cross-reactivity of many antibodies raised against the UGTs.

As determined by real-time polymerase chain reaction [PCR; (Figure 1.11)], UGTs are expressed in a tissue-specific manner. All UGTs, except UGTs 1A8 and 1A10

and possibly 1A5 and 1A7, are expressed in the liver, the major site of metabolism and detoxification of compounds to be cleared from the body. Hepatic enzymes are typically thought to have the greatest effect on overall glucuronidation of substrates. Although the liver is identified as the most important region for drug metabolism, studies have shown that the gastrointestinal tract (GI) also plays an important role (157-159). The GI tract absorbs nutrients and is a barrier to unwanted chemicals, and UGT expression has been identified in the mucosal epithelia layer of these tissues (160). Other areas where UGTs are expressed include the lung, the tissues of the aerodigestive tract [tongue, esophagus, tonsil, floor of the mouth, larynx; (161)] which are frequently exposed to air pollutants, and tissues which are exposed to high levels of hormones [breast, prostate, ovary, colon; (136, 162)]. Consideration of the tissue sites of expression of individual UGTs provides insight into their endogenous functions and possibly aids in identifying which specific UGTs are important for metabolizing exogenous compounds.

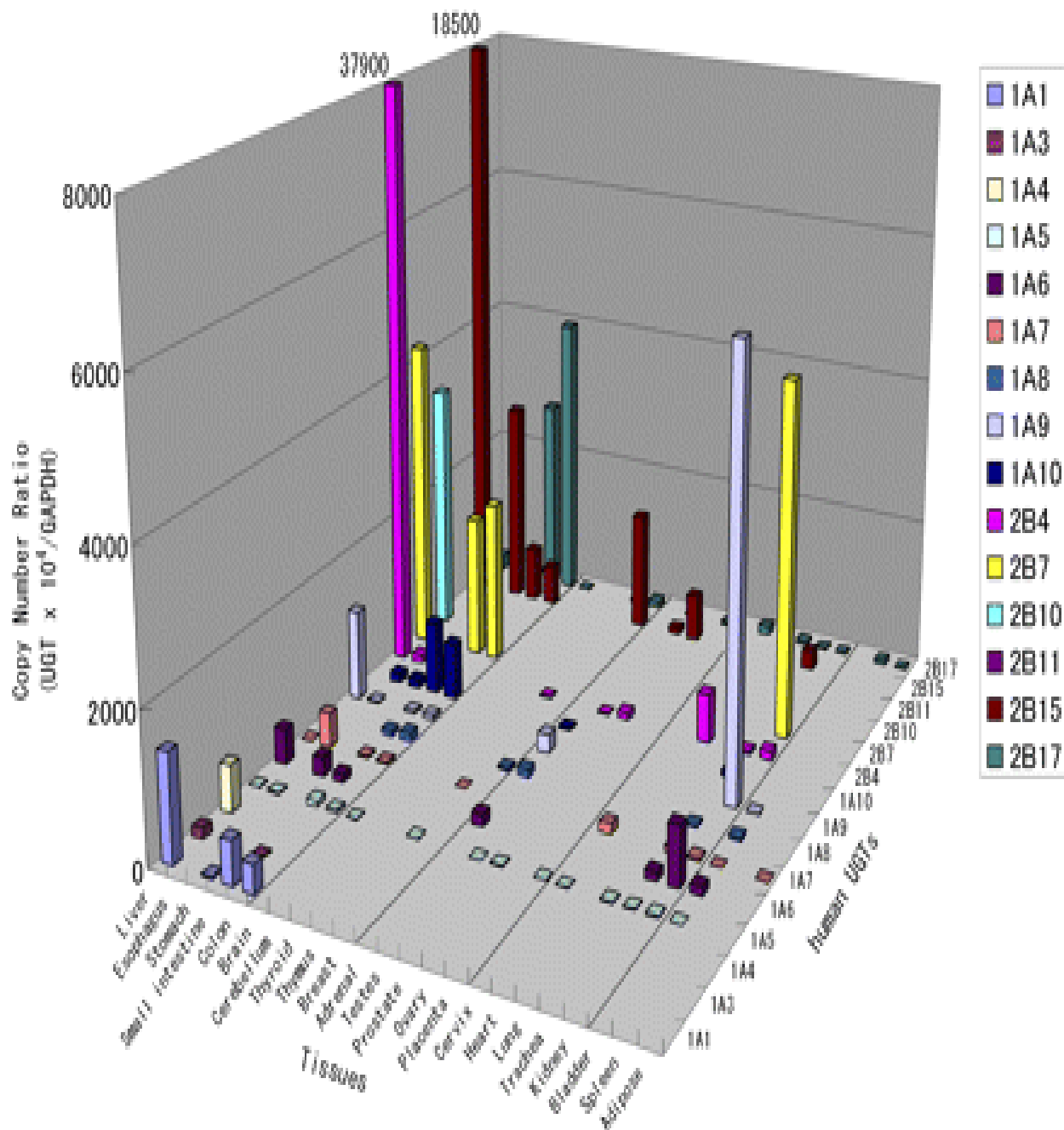


Figure 1.11: Expression patterns of UGTs in human tissue. Using twenty-three types of human tissues, RNA was isolated and synthesized to cDNA. cDNAs were diluted 6 times with sterilized water, and 5 μ l of each sample was subjected to real-time PCR. The units of the y-axis represent the UGT copy number $\times 10^4$ normalized to GAPDH, and the 37,900 and 18,500 values are included as off-scale data of UGT2B4 and UGT2B15, respectively. Each data point represents the mean value ($n = 3-4$), and error bars were omitted for clearer viewing. All of the data were reconfirmed by repeated examination. [Reference from (136)].

When assessing the overall role of UGTs in metabolism, it is also important to consider how the expression of these enzymes are regulated. Figure 1.11 illustrates that expression levels of UGTs vary within a given tissue. Studies examining transcription factors that regulate UGT expression have identified key regulatory elements. All UGT genes have been identified to contain putative hepatocyte nuclear factor 1 (HNF1)-binding sites (163, 164). Although the name suggests regulation of hepatic genes, HNFs are also expressed in kidney, pancreas, stomach, intestine, and colon and have been shown to regulate both hepatic and exclusively extra-hepatic UGTs (156, 165). The intestine-specific transcription factor, caudal-related homeodomain protein 2 (Cdx2), which cooperates with HNF1 α , has been shown to regulate UGTs 1A8, 1A9, and 1A10 in Caco-2 cells, and studies identified the region 400 bp upstream of the ATG translational start-site to be important for transcription factor-binding and regulation (156, 165). Specific transcription factors and response elements have been shown to contribute to UGT expression, with most of those studies being conducted for UGT1A1 (166, 167).

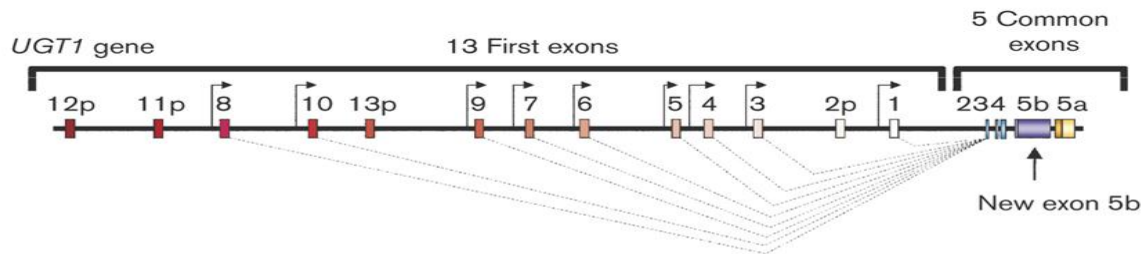
In addition to transcriptional regulation, UGT catalysis has recently been shown to require phosphorylation (160, 168-170). UGT1A1 was the first UGT suggested to be regulated by phosphorylation in order to achieve optimal glucuronidation activity (169). Further studies identified UGTs 1A7 and 1A10 as also requiring phosphorylation to reach maximal glucuronidation activity (160, 168, 170). There are many levels at which UGTs may be regulated and further investigation of the elements involved as well as their variants may aid in our understanding of the variations of UGT expression.

Inter-individual differences of UGT mRNA expression have been observed in tissue specimens from the same site (171). A possible source for inter-individual differences may be exposure to inducers of UGTs. Studies have identified that some UGTs can be induced by aryl hydrocarbons (Ah) via the xenobiotic responsive element (XRE) (172), and by phenobarbital via the phenobarbital responsive enhancer (173). Endogenous substrates have also been shown to induce expression of UGTs. For example, examination of LNCaP cells after treatment with androgens demonstrated a decrease in expression of UGTs 2B10 and 2B17 and an increase in expression of UGT2B11, a pattern that was mirrored by glucuronidation activity profiles for each enzyme (174). Estrogen has also been shown to up-regulate UGTs 1A10 and 2B15 expression as shown in estrogen receptor-positive breast cancer cells (175, 176).

Recent studies have identified a novel mechanism of regulation where UGT1A enzymes are alternatively spliced to generate several mRNA isoforms [Figure 1.12 (177, 178)]. Initially, UGT1A1 was found to have an alternatively spliced mRNA (variant, v2) that results in a protein containing a unique 10-residue sequence [isoform, i2 (178)]. Subsequent studies identified a similar process for all UGT1A genes, producing a total of three alternatively splice mRNAs, v1 (containing exon 5a), v2 (containing exon 5b), and _v3 (containing exon 5a and 5b) resulting in two proteins, i1 and i2 (the latter translated from _v2 or _v3 which are identical) [Figure 1.12; (178)]. For example, UGT1A10 mRNA could be UGT1A10_v1, UGT1A10_v2, or UGT1A10_v3 translating protein UGT1A10_i1 or UGT1A10_i2, respectively. Consistent with all UGTs, these isoforms are widely distributed in human tissue (177) and current studies are underway by members of the Lazarus laboratory to examine tissue and individual differences in

expression. Due to the recent identification of these splice variants, the differential regulation of their expression has not yet been explored; however, further studies examining the underlying mechanisms of expression would greatly enhance our understanding of the role of these isoforms.

(a) 5' Alternative splicing events (alternative exon 1)



(b) 3' New alternative splicing events (alternative exon 5)

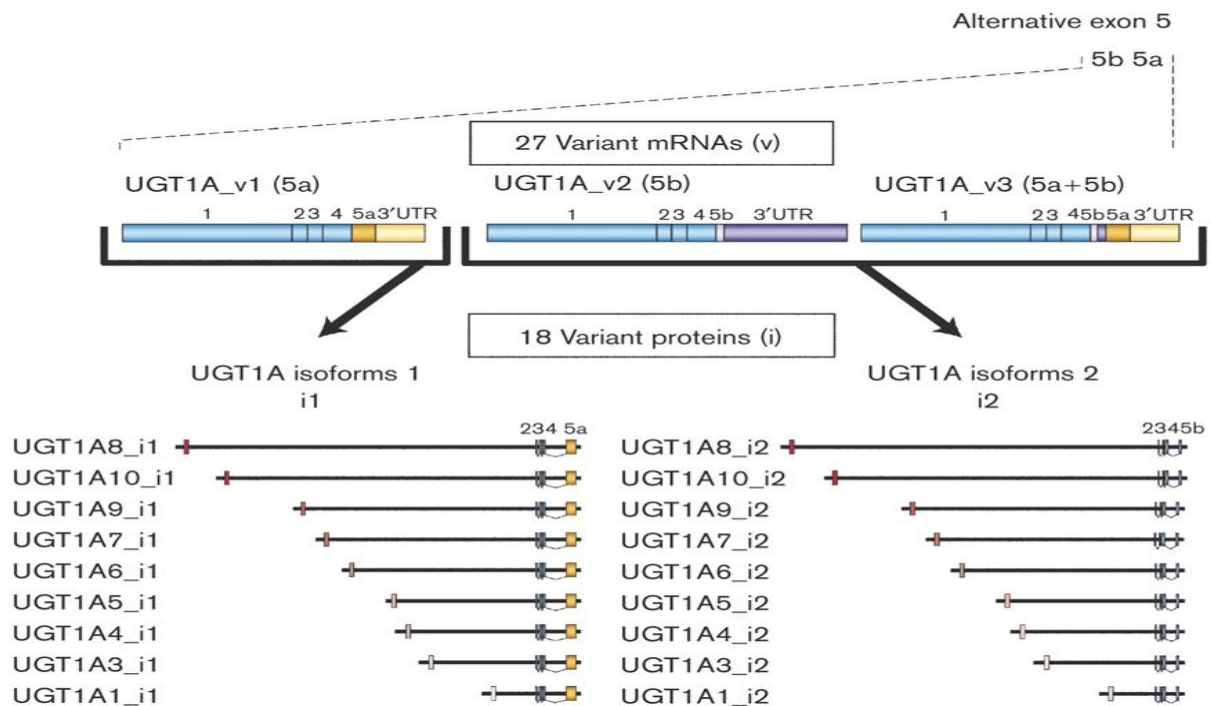


Figure 1.12: Schematic representation of the UGT1 gene and the alternative splicing events taking place at the 5' and 3' ends of the locus. (a) The originally described genomic structure of UGT1 locus which includes 17 exons: 13 first exons and four common exons (2–5). This UGT1 locus was more recently identified to encode one additional exon (referred to as the new exon 5b) and it was shown that the common region comprises five shared exons instead of four. This newly identified UGT1A gene products (mRNAs) are referred to as variants, or v, whereas new proteins are named isoforms, or UGT1A_i. The previously described 'classical' UGT1As are named UGT1A_i1 and the newly described UGT1A proteins are referred to as UGT1A_i2. (b) Exon 5a and the new exon 5b are alternatively spliced, generating variant UGT1A mRNAs: v1 (containing 5a), v2 (5b) and v3 (5a+5b). The proteins translated from v3 are identical to those encoded by the UGT1A_v2 mRNAs, as they have identical open reading frames. These data suggest the existence of nine additional UGT1A_i2 proteins, increasing to 18 the number of proteins encoded by UGT1. [Reference from (177)].

1.3.3 Endogenous Substrates

The endogenous role of UGTs is to transfer glucuronic acid to polar substrates for excretion from the body through bile and urine. Glucuronic acid is transferred to a functional group –OH, –NH₂, –COOH, –SH or C-C (147) which typically results in the inactivation of the substrate; however, increased activity of the glucuronide conjugate has been observed in some cases [eg: the bile acid, lithocholic acid-3-O-glucuronide (179)]. Endogenous metabolic substrates that undergo glucuronidation include bilirubin, steroids, and bile acids. Variations in the ability to metabolize these endogenous compounds have been observed in humans. For example, the presence of excess bilirubin (hyperbilirubinemia) leads to a visible jaundiced appearance (180) and ranges from barely noticeable symptoms to lethality (181). The activities of UGTs against endogenous substrates are consistent with their expression patterns. For example, UGT1A10 is the predominant enzyme which inactivates estrone, 17β-estradiol (E₂), and its hydroxylated derivatives (160, 182), and is found in breast, ovaries, and uterus (183).

1.3.4 Exogenous Substrates

The ability to detoxify environmental pollutants is essential to reduce a person's susceptibility to the development of cancers. Many compounds are known to be carcinogenic, like those found in tobacco smoke, which primarily affects the lung. Extensive studies have noted the important role of glucuronidation in excretion of these carcinogens (128, 130, 161, 184-188). The most abundant and mutagenic tobacco carcinogens are the polycyclic aromatic hydrocarbons (PAHs) including benzo[a]pyrene (B[a]P) and dibenzo[a,h]pyrene (DB[a,h]P), and *N*-nitrosamines including

4-(methylnitrosamino)-1-(3-pyridyl)-1- butanone (NNK) and *N'*-nitrosonornicotine (NNN). Several UGTs have been shown to be involved in the glucuronidation and detoxification of the major procarcinogenic metabolites of many of these compounds, including the major procarcinogenic metabolite of NNK, 4-(methylnitrosamino)-1-(3-pyridyl)-1-butanol [NNAL; (128, 186, 187, 189)]. Other highly mutagenic carcinogens present in tobacco smoke and in the environment which are glucuronidated by the UGTs include heterocyclic amines such as 2-amino-1-methyl-6-phen-ylimidazo- [4,5-b]pyridine (PhiP) and its procarcinogenic metabolite, *N*-hydroxy (OH)-PhiP (190, 191). Therefore, glucuronidation plays an extremely important role in the elimination of a variety of toxic exogenous compounds, especially those found in tobacco smoke.

In addition to the glucuronidation of carcinogens, which could ultimately reduce the risk of developing cancers, UGTs also metabolize drugs such as those used as chemotherapeutic agents. As glucuronidation typically results in inactivation and excretion of substrates, an individual's ability to properly glucuronidate a chemotherapeutic drug can alter the overall exposure to the active substrate. Studies have shown that the metabolism of chemotherapeutic compounds is important for overall drug efficacy and/or patient response (123, 192, 193). Examples of altered drug response due to variations in glucuronidation are examined in section 1.3.6.

1.3.5 Genetic Variants

Genetic polymorphisms within the UGT1A locus are very common and many of these variants are found in linkage disequilibrium with each other and exhibit different allele prevalences in different populations (194, 195). A considerable number of

prevalent functional polymorphisms have been identified previously in several UGT genes, including 1A1, 1A3, 1A4, 1A6, 1A7, 1A8, 1A10, 2B4, 2B7, 2B15 and 2B17 (188, 196-205), with several of these implicated as determinants of cancer risk or response to chemotherapy. The best examples of how UGT variants affect different aspects of glucuronidation are the extensively-studied UGT1A1 variants. The promoter region UGT1A1 'TATA' box polymorphism is commonly associated with Gilbert's Syndrome which is characterized by increased levels of bilirubin due to decreased glucuronidation. The UGT1A1*28 variant, which is characterized by the presence of an additional TA repeat in the TATA sequence of the *UGT1A1* promoter, [(TA)₇TAA, instead of (TA)₆TAA)], is associated with reduced function in the UGT1A1 transcriptional promoter which results in decreased expression (198) and has been implicated in increased risk for breast cancer (201) and with decreased formation of the glucuronide conjugate of the important procarcinogenic B[a]P metabolite, BaP-7,8-diol(-)(206). This single variant of one UGT affects both endogenous and exogenous glucuronidation and has been linked to a number of detrimental effects.

Many other UGT variants have been linked to alterations in glucuronidation of specific substrates and risk for cancers. UGT1A7-specific genetic variants are associated with reduced UGT1A7 metabolic function (201), are linked to increased risk for hepatocellular carcinoma (207), and have been shown to be strongly linked to increased risk for orolaryngeal cancer (208). The UGT1A10 codon 139 polymorphism, resulting in a non-conservative Glu>Lys amino acid change, has been linked to decreased risk for orolaryngeal cancer (203) and has been shown to result in decreased glucuronidation against several PAHs as compared to the wild-type enzyme (185). Two

studies have identified a deletion of the UGT2B17 gene locus (UGT2B17*2), that has an allelic prevalence of 30% in Caucasians (205, 209) which has been linked to decreased formation of the *N*-glucuronide conjugate of NNAL, the major carcinogenic metabolite of NNK. This variant has also been linked to altered glucuronidation rates of several compounds (187) and increased risk for lung cancer (210, 211). Previous studies have identified two nonsynonymous genetic variants of UGT1A8 which have been linked to altered activity against metabolites of B[a]P (202) as well as other substrates (202, 212). It is interesting to note that not all variants lead to decreased glucuronidation and that a given variant may react differently with each substrate. For example, the UGT2B7p.His268Tyr variant was recently associated with decreased liver microsomal glucuronidation activity against major active tamoxifen metabolites (121); however, this same variant was shown to have no effect or exhibit increased activity against other substrates [eg. morphine; (213)].

1.3.6 Pharmacogenetics and UGTs

Polymorphisms in drug metabolizing enzymes have been shown to alter drug efficacy and/or toxicity leading to inter-individual differences in drug response (192, 214). An individual's genotype can alter drug response through many pathways. Mutations in the genes which encode for enzymes that transport drugs like the drug-efflux pump, P-glycoprotein, are correlated with significantly lower rates of clearance of the ovarian chemotherapeutic agent, paclitaxel, resulting in improved patient response (the patients had complete response and were relapse-free for at least 1 year) [Figure 1.13, (215, 216)]. In addition to drug transport, variants in phase I and phase II drug

metabolizing enzymes have been shown to alter drug efficacy and/or toxicity also leading to inter-individual differences in drug response.

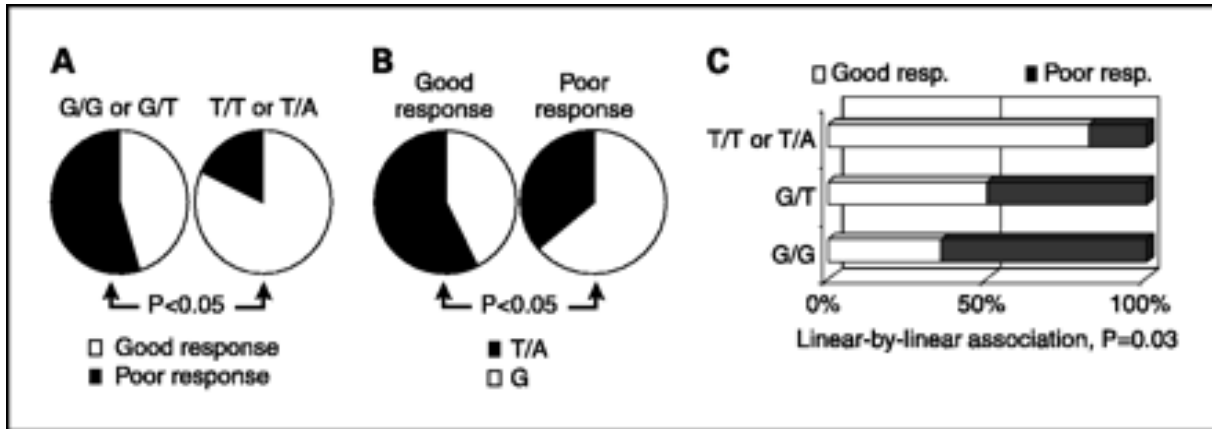


Figure 1.13: The effect of the *mdr-1* SNP G2677T/A on paclitaxel treatment outcome. A, treatment outcome, good response (*white*) and poor response (*black*), was evaluated for homozygously mutated individuals (T/T or T/A) and compared with the response of the individuals having G/G or G/T at position 2677. Patients who were homozygously mutated were significantly more likely to respond to paclitaxel treatment than patients carrying the other genotypes (Fisher's exact test, $P = 0.04$; relative risk, 1.81; 95% confidence interval for the relative risk: $1.17 < \text{relative risk} < 2.79$). B, the nucleotide frequencies (2 x homozygous + heterozygous) in the two treatment groups were also compared using an exact test. A significantly higher frequency of T or A at position 2677 was found in the group of patients that had responded well to treatment compared with those who responded poorly (Fisher's exact test, $P = 0.03$; relative risk, 1.59; 95% confidence interval for the relative risk: $1.03 < \text{relative risk} < 2.45$). C, the dose response effect of the allele variants on the success and failure of paclitaxel treatment was tested using the χ^2 test for linear-by-linear association and was found to be significant (χ^2 test for linear-by-linear association, $P = 0.03$). [Reference from (215)].

As mentioned previously, drug metabolism is an important aspect to consider when assessing the overall effect of a drug because the ability of an individual to metabolize the drug will affect the amount of active drug and the amount of time that it can act in the body. Drug metabolism is broken down into two phases: phase I typically leads to an active more polar metabolite and phase II typically leads to the conjugation of a compound to the drug that results in inactivation and excretion of the drug; however, there are exceptions to these generalizations. Phase I drug metabolizing enzymes convert functional groups through reactions causing dehydrogenation/hydrogenation, oxidation, hydrolysis, reduction, or monooxygenation (217). The most abundant and well studied phase I enzymes are the cytochrome P-450 monooxygenase (CYP450) family of enzymes which oxidize approximately 78% of the hepatically cleared top 200 drugs prescribed in the US (218). Genetic variants of CYP450s that result in aberrant expression or altered enzyme activity have been suggested to be clinically relevant in altering metabolism and effects of chemotherapeutic agents including flutamide, tegafur, cyclophosphamide, paclitaxel, and tamoxifen (219).

Phase II drug metabolizing enzyme reactions include sulphation, glutathione-conjugation, and glucuronidation of functional groups. Sulphation occurs when one of the sulfotransferases catalyzes the transfer of a sulphate-moiety to a nucleophilic group of the substrate therefore increasing the water solubility of the substrate. Variants of members of the sulfotransferase family of enzymes have been associated with shorter patient survival after treatment with the chemotherapeutic agent, tamoxifen (220-222). Similarly, patient survival was assessed for platinum-based treatments in association

with genotypes of glutathione-S-transferases (GSTs), which are the enzymes responsible for conjugating glutathione to substrates and which typically results in detoxification (223). Cancer patients were genotyped for GSTs and overall survival was assessed after treatment with platinum-based compounds for breast, ovarian, colorectal or lung cancer. These studies yielded conflicting results as to the role of GSTs in patient survival (221). However, a correlation between GST variants and decreased response and increased toxicities to anthracycline-based agents in the treatment of acute myeloid leukaemia have been observed consistently (221, 224-227).

Glucuronidation and the enzymes responsible for this process were discussed in the above sections (1.3.1- 1.3.5) and these phase II enzymes have been shown to play important roles in pharmacogenetics. The best example of UGTs and pharmacogenetics is a variant of the UGT1A1 enzyme which has clear and direct clinical impact. The UGT1A1*28 allele is associated with decreased UGT1A1 expression (206, 228), and in human liver microsomes [HLM; (206, 229)] this decrease in expression has been correlated with decreased glucuronidation of 7-ethyl-10-hydroxy-camptothecin (SN-38), the major active metabolite of Irinotecan (230). Similarly, these *in vitro* correlations were also observed in the levels of urinary SN-38-glucuronide in patients treated with Irinotecan (123, 124, 193, 229). These decreases in excretion have been linked to increased Irinotecan toxicity in patients (123-125) prompting the FDA to approve genetic screening for the UGT1A1*28 allele in patients who may be considered for treatment with this agent (126). The UGT1A1*28 variant and its role in patient drug response exemplify the importance of understanding the genetic differences in patients in order to improve treatment.

Additional studies continue to examine the roles of the UGT family of enzymes and how variants in these enzymes may alter drug response and toxicity. A UGT2B7 promoter variant was associated with reduced glucuronidation of morphine in patients with sickle cell disease (231); however, another study that looked at this same variant and morphine treatment in cancer patients did not find a correlation (232). Due to the complexity of studying patients, important foundational information can be gained from identifying affects of UGT variants *in vitro* and then applying this information to more complex *in vivo* situations, and this approach has been initiated for several drugs. The anesthetic, propofol, is directly glucuronidated as its major route of elimination (233). In liver, the primary site of detoxification, UGT1A9 has been identified as the only UGT to glucuronidate propofol (234) and variants of this enzyme have been associated with decreased glucuronidation *in vitro* (204). Variants of UGT2B7 were recently associated with decreased liver microsomal glucuronidation activity against major active metabolites of tamoxifen which may be linked to altered patient response to tamoxifen (121, 235). Overall, continued characterization of the UGTs responsible for metabolism of drugs may aid in a better understanding of differences in patient response and toxicity.

In this literature review, SAHA's role as a very promising drug for the treatment of many cancers was discussed. It was also shown that differences in patient responses (and toxicities) vary, therefore requiring SAHA doses to be altered. Since drug metabolism may contribute to these differences, the metabolism of SAHA was examined and two main pathways were identified, with the glucuronidation pathway playing a major role in SAHA metabolism. The UGT family of enzymes, known to

glucuronidate substrates, was discussed and it was emphasized how variants of these enzymes can have altered abilities to glucuronidate substrates. Together, this information led to the hypothesis that genetic alterations in the UGTs responsible for SAHA glucuronidation may alter the drug's efficacy and/or toxicity. Addressing this hypothesis will lead to the identification of the specific UGTs responsible for SAHA glucuronidation and how variants of these UGTs affect SAHA glucuronidation. This information will aid in understanding possible genetic differences in patients, which can lead to differences in SAHA response. Furthermore, this information will enhance the field of pharmacogenetics by characterizing genetic variants and correlating them with altered drug metabolism.

CHAPTER 2: Identification and Characterization of UGTs active against SAHA

2.1 INTRODUCTION

There are many factors that can affect how effective a drug will be and these factors will vary for each patient. Using current drugs, physicians try to optimize treatment by administering a dose of drug which will be effective and not harmful to the patients; however, individuals vary with respect to drug absorption, distribution, metabolism, and elimination and therefore optimal drug dosage has been based on trial and error. Traditional methods to identify drug-specific effects and side effects are based on pharmacokinetics and pharmacodynamics (236). However, in order to more completely understand the dose/effect relationship as well as to understand differences in patient responses to a drug, a clear understanding of pharmacogenetics is essential (237, 238).

As mentioned previously, SAHA is used in the treatment of cutaneous T-cell lymphoma and is used in clinical trials for the treatment of a variety of other cancers including breast, lung, and colon cancer (100, 239). SAHA is a promising chemotherapeutic agent but has side effects that include anemia, dehydration, fatigue and gastrointestinal (GI) disturbances (240). Although differences in patient response to SAHA have been observed (100, 114, 120, 240), the mechanisms underlying the variability of responses remain obscure. Studies have been conducted to assess the optimal drug delivery method (orally versus intravenously) and how food might influence the overall pharmacokinetics; however, no significant findings have resulted (114, 120).

Drug metabolism pathways were previously discussed as a source of individual differences. SAHA is known to be glucuronidated through reactions, catalyzed by UGT enzymes, in which a glucuronic acid moiety is transferred to SAHA and which results in inactivation and excretion of the drug. Furthermore the UGT family of enzymes has been shown to include variants which lead to enzymes that have altered abilities to glucuronidate drugs. These data support the need to characterize the SAHA glucuronidation pathway to see if UGT variants can alter SAHA glucuronidation and ultimately alter patient response.

There are two main approaches that one can take to assess the role of UGTs in glucuronidation of SAHA. One method includes starting with samples such as urine and blood from patients treated with SAHA and using these samples to detect metabolite formation, to screen for UGT genotype, and then to assess these data to determine whether correlations exist between UGT genotype and metabolite formation. This approach, which is directly relevant to patient samples, is not quite feasible at the current time. First, this approach would require that all genetic variants of the UGTs be screened in patient samples and screening UGTs for genetic variants is very complex due to the high homology shared among all UGTs. UGT genotyping assays are not currently offered with commercially available DNA/mRNA array chips or other large scale assays. Similarly, genotyping techniques like restriction fragment length polymorphism and real-time PCR SNP assays are difficult, if not impossible, to design because making specific primers and probes for a UGT SNP may not be feasible due to the sequence homology shared by all UGTs. Furthermore, to perform correlation studies, a large population will be required to obtain the power to detect any effect from

genetic variations, especially low prevalence SNPs, and, as SAHA is a relatively new drug, large patient samples cannot be obtained at this time.

An alternative approach to assess SAHA glucuronide formation is to use *in vitro* assays. These systems can be altered and designed to assess each individual UGT for glucuronidation activity for SAHA. One of the most widely used *in vitro* systems for UGTs is the human embryonic kidney fibroblast (HEK)293 cell line, a cell line that does not express endogenous UGTs (241, 242) and which can be transfected with individual overexpressing UGTs. By first assessing each individual UGT for its ability to glucuronidate SAHA, only those UGTs that exhibit activity should then be assessed for how variants of these enzymes affect SAHA glucuronidation. This approach provides valuable information, such as identifying the individual UGTs responsible for SAHA glucuronidation, which cannot be determined *in vivo*. Although there are limitations to this method, it provides a feasible way to identify the UGTs responsible for SAHA glucuronidation. Therefore, the goal of this study was to identify the specific UGTs which are responsible for SAHA glucuronidation. This information can be used to further analyze variants *in vitro* or genotype patients based on the UGTs which glucuronidate SAHA *in vivo*. Overall, this information will provide the necessary foundation to further characterize the SAHA glucuronidation pathway.

2.2 MATERIALS AND METHODS

2.2.1 Generation of UGT-overexpressing cell lines

The human embryonic kidney fibroblast (HEK)293 cell line, a cell line that does not express endogenous UGTs (241, 242) (purchased from American Type Culture Collection), was used to generate UGT-overexpressing cell lines. All UGT cell lines that have been previously made and characterized are listed in Table 2.1. In order for a complete analysis of all the UGT1A and UGT2B enzymes (except UGT2B28 which wild-type has not been successfully amplified), two new wild-type UGT-overexpressing cell lines, UGT1A3 and UGT2B15, were generated for the experiments outlined in this study; all other cell lines used have been described previously (Table 2.1). Wild-type UGT1A3 and UGT2B15 cDNA was synthesized by standard reverse transcription using total RNA from normal human liver specimens. Total RNA was isolated from adjacent normal liver tissue as described previously (128). cDNA was generated using the SuperScript™ First-Strand Synthesis System for RT-PCR (Invitrogen) by following the manufacturer's protocol. Briefly, 2 μ L (~50 ng) of total RNA was mixed with 10 mM dNTP mix, 0.5 μ g/ μ L Oligo(dT)₁₂₋₁₈ in a total volume of 10 μ L and incubated for 5 min at 65°C then quickly placed on ice for 1 min. A mix containing 1x (final concentration) RT buffer, 25 mM MgCl₂, 0.1 M DTT, and 40 units RNaseOUT recombinant RNase inhibitor was added to each reaction and incubated at 42°C for 2 min. Following the 2 min incubation, 50 units of SuperScript II RT was added to each tube and the tubes were incubated at 42°C for 50 min followed by incubation at 70°C for 15 min to terminate the reaction. The original RNA was removed by adding 2 units of RNase H to each reaction and incubating for 20 min at 37°C. All cDNA was stored at -20°C.

UGT	Reference first described
1A1	King CD, Green MD, Rios GR, Coffman BL, Owens IS, Bishop WP, Tephly TR. The glucuronidation of exogenous and endogenous compounds by stably expressed rat and human UDP-glucuronosyltransferase 1.1. <i>Arch Biochem Biophys</i> 1996;332:92-100
1A3	Sun, D., Sharma, A. K., Dellinger, R. W., Blevins-Primeau, A. S., Balliet, R. M., Chen, G., Boyiri, T., Amin, S., and Lazarus, P. Glucuronidation of active tamoxifen metabolites by the human UDP glucuronosyltransferases. <i>Drug Metab Dispos</i> , 35: 2006-2014, 2007.
1A4	Sun, D., Chen, G., Dellinger, R. W., Duncan, K., Fang, J. L., and Lazarus, P. Characterization of tamoxifen and 4-hydroxytamoxifen glucuronidation by human UGT1A4 variants. <i>Breast Cancer Res</i> , 8: R50, 2006.
1A5	Balliet RM, Chen G, Gallagher CJ, Dellinger RW, Sun D, Lazarus P. Characterization of UGTs Active against SAHA and Association between SAHA Glucuronidation Activity Phenotype with UGT Genotype. <i>Cancer Res</i> 2009
1A6	Ebner T , Burchell B. Substrate specificities of two stably expressed human liver UDP-glucuronosyltransferases of the UGT1 gene family. <i>Drug Metab Dispos</i> 1993;21:50-5
1A7	Zheng Z, Fang JL, Lazarus P. Glucuronidation: an important mechanism for detoxification of benzo[a]pyrene metabolites in aerodigestive tract tissues. <i>Drug Metab Dispos</i> 2002;30:397-403
1A8	Sun, D., Sharma, A. K., Dellinger, R. W., Blevins-Primeau, A. S., Balliet, R. M., Chen, G., Boyiri, T., Amin, S., and Lazarus, P. Glucuronidation of active tamoxifen metabolites by the human UDP glucuronosyltransferases. <i>Drug Metab Dispos</i> , 35: 2006-2014, 2007.
1A9	Dellinger, R. W., Chen, G., Blevins-Primeau, A. S., Krzeminski, J., Amin, S., and Lazarus, P. Glucuronidation of PhIP and N-OH-PhIP by UDP-glucuronosyltransferase 1A10. <i>Carcinogenesis</i> , 28: 2412-2418, 2007.
1A10	Dellinger, R. W., Fang, J. L., Chen, G., Weinberg, R., and Lazarus, P. Importance of UDP-glucuronosyltransferase 1A10 (UGT1A10) in the detoxification of polycyclic aromatic hydrocarbons: decreased glucuronidative activity of the UGT1A10139Lys isoform. <i>Drug Metab Dispos</i> , 34: 943-949, 2006.
2B4	Ren, Q., Murphy, S. E., Zheng, Z., and Lazarus, P. O-Glucuronidation of the lung carcinogen 4-(methylnitrosamino)-1- (3-pyridyl)-1-butanol (NNAL) by human UDP-glucuronosyltransferases 2B7 and 1A9. <i>Drug Metab Dispos</i> , 28: 1352-1360, 2000.
2B7	Coffman BL, Rios GR, King CD, Tephly TR. Human UGT2B7 catalyzes morphine glucuronidation. <i>Drug Metab Dispos</i> 1997;25:1-4
2B10	Chen G, Dellinger RW, Sun D, Spratt TE, Lazarus P. Glucuronidation of tobacco-specific nitrosamines by UGT2B10. <i>Drug Metab Dispos</i> 2008;36:824-30
2B11	Dellinger, R. W., Chen, G., Blevins-Primeau, A. S., Krzeminski, J., Amin, S., and Lazarus, P. Glucuronidation of PhIP and N-OH-PhIP by UDP-glucuronosyltransferase 1A10. <i>Carcinogenesis</i> , 28: 2412-2418, 2007.
2B15	Sun, D., Sharma, A. K., Dellinger, R. W., Blevins-Primeau, A. S., Balliet, R. M., Chen, G., Boyiri, T., Amin, S., and Lazarus, P. Glucuronidation of active tamoxifen metabolites by the human UDP glucuronosyltransferases. <i>Drug Metab Dispos</i> , 35: 2006-2014, 2007.
2B17	Dellinger, R. W., Chen, G., Blevins-Primeau, A. S., Krzeminski, J., Amin, S., and Lazarus, P. Glucuronidation of PhIP and N-OH-PhIP by UDP-glucuronosyltransferase 1A10. <i>Carcinogenesis</i> , 28: 2412-2418, 2007.

Table 2.1: UGT over-expressing cell lines.

The synthesized cDNA (2 μ L) was utilized for PCR amplification of the UGT1A3 and UGT2B15 coding regions. The sense and antisense primers used for PCR amplification of UGT1A3 were UGT1A3S (sense, 5'-AAAGCAAATGTAGCAGGCAC-3') and UGT1A3AS (antisense, 5'-GGAAATGACTAGGGAATGGTTC-3'), corresponding to nucleotides -61 to -42 and +1635 to +1656, respectively, relative to the UGT1A3 translation start site. The sense and antisense primers used for PCR amplification of UGT2B15 were UGT2B15S (sense, 5'-TTCGGCACGAGTAAGACCAG-3') and UGT2B15AS (antisense, 5'-AGGAGGAGTCCCATCTTTCA-3'), corresponding to nucleotides -21 to -2 and +1622 to +1641, respectively, relative to the UGT2B15 translation start site. PCR amplification for both UGT 1A3 and 2B15 was performed in a GeneAmp 9700 thermocycler (Applied Biosystems, Foster City, CA) as follows: 1 cycle at 94°C for 2 min, 35 cycles at 94°C for 30 s, 55°C for 30 s, and 68°C for 4 min, followed by a final cycle of 7 min at 68°C. Reactions contained 1X *Pfx* amplification buffer, 50 mM MgSO₄, 15 mM dNTP mix, 20 μ M sense primer, 20 μ M antisense primer, and 2.5 units Platinum *Pfx* DNA polymerase (Invitrogen) in a final volume of 50 μ L. Due to the high homology between UGT1A3 and UGT1A4, the PCR product of UGT1A3 amplification was digested with the restriction enzyme *Xba*I before gel extraction to remove co-amplified UGT1A4 PCR product. Following electrophoresis in a 1% agarose gel, the specific PCR products of UGT1A3 (1662 base pairs) and UGT2B15 (1662 base pairs) were purified using the QIAEX II gel extraction kit and subsequently subcloned into the pcDNA3.1/V5-His-TOPO mammalian expression vector (Figure 2.1).

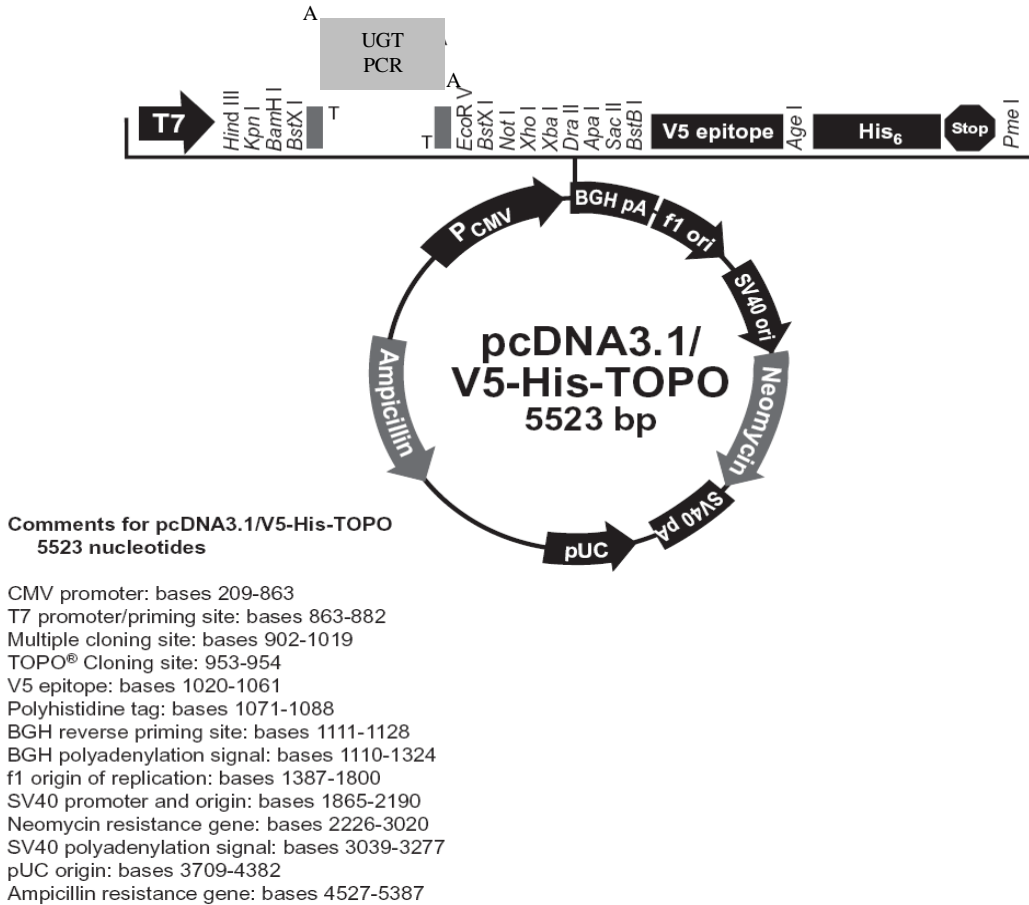


Figure 2.1: Schematic diagram of the pcDNA3.1/V5-His-TOPO mammalian expression vector. Diagram of the expression vector used for UGT-overexpression; the UGT PCR product is highlighted in the gray box. [Reference from Invitrogen].

The addition of 3' A-overhangs was necessary for cloning into the vector and these were generated by incubating purified DNA with 1 unit *Taq* polymerase (Eppendorf), 10 mM dNTP mix, and 1X buffer for 10 min at 72°C. This was followed immediately by ligation into the expression vector using the pcDNA3.1/V5-His-TOPO TA expression kit (Invitrogen). The TOPO cloning ligation reaction contained 4 µL of fresh PCR product with 3' A-overhang, 1.2 mM salt solution, and 10 ng pcDNA3.1/V5-His-TOPO plasmid and was incubated on ice for 30 min. The TOPO cloning reaction (2 µL)

was then incubated with 50 μ L of One Shot TOP10 chemically competent cells (Invitrogen) and incubated on ice for 30 min followed by heat-shock for 30 s at 42°C with immediate subsequent transfer of the reaction to ice. Cells were plated on ampicillin-resistant agarose plates, grown overnight, and individual colonies were picked for further analysis. Confirmation of cDNA insertion and orientation was performed by restriction enzyme digestion. UGT1A3 and UGT2B15 wild-type sequences were confirmed by dideoxy sequencing of the entire PCR-amplified UGT1A3 or UGT2B15 cDNA product using two vector primers (T7 and BGH; Integrated DNA Technologies, Inc., Coralville, IA), and a UGT1A3 internal antisense primer (UGT1A3intAS; 5'-TTCGCAAGATTCGATG-3', corresponding to nucleotides +1028 to +1046 relative to the UGT1A3 translation start site) or a UGT2B15 internal sense primer (2B15intS; 5'-GATAGCATTCCCTGCTG -3', corresponding to nucleotides +1482 to +1497 relative to the UGT2B15 translation start site).

UGT1A3- and UGT2B15- overexpressing HEK293 cell lines were generated by standard electroporation techniques in a GenePulser Xcell (Bio-Rad, Hercules, CA) using 10 μ g of pcDNA3.1/V5-His-TOPO/UGT plasmid DNA with 5×10^6 HEK293 cells (in 0.5 mL) in serum-free DMEM media, with electroporation at 250 V and 1000 μ F. After transfection, HEK293 cells were grown in 5% CO₂ to 80% confluence in DMEM media supplemented with 4.5 mM glucose, 10 mM HEPES, 10% fetal bovine serum, 100 U/mL penicillin, 100 μ g/mL streptomycin, and G-418 (700 μ g/mL medium) for the selection of G-418-resistant cells. Selection medium was changed every 2 to 3 days. Pooled UGT 1A3- and 2B15- overexpressing cells were selected and tested for UGT expression via

Western blotting analysis (described below). All UGT-overexpressing cell lines were maintained in G-418 selection DMEM media as described above.

Levels of UGT expression in UGT-overexpressing cell lines were determined as described previously (184). Specifically, levels of UGT1A3 expression in the cell line was measured by Western blot analysis using the anti-UGT1A antibody at 1:5000 dilution as per the manufacturer's instructions (BD Bioscience) and was quantified relative to a UGT1A standard of known concentration. The UGT1A antibody was in whole-serum prepared from a rabbit that had been immunized with a peptide specific to all UGT1As. The β -actin housekeeping protein was used for standardization of UGT protein levels and was assayed using a 1:5000 dilution of anti- β -actin antibody (Sigma). Secondary antibodies were supplied with the Dura ECL kit (anti-rabbit and anti-mouse) and were used at 1:3000 dilutions. All proteins were detected by chemiluminescence using the SuperSignal West Dura Extended Duration Substrate (Pierce Biotechnology). UGT1A protein levels were quantified against a known amount of human UGT1A protein (100 ng – 400 ng, supplied in the Western blotting kit provided by Gentest) by densitometric analysis of X-ray film exposures (5 s to 5 min exposures) of Western blots using a GS-800 densitometer with Quantity One software (Bio-Rad, Hercules, CA). Quantification was made relative to the levels of β -actin observed in each lane (also quantified by densitometric analysis of Western blots as described above). X-ray film bands were always below densitometer saturation levels. Relative UGT1A protein levels are reported as the mean of three independent Western blot experiments, with Western blot analysis performed using the same UGT1A-containing cell homogenates used for activity assays.

Protein levels of UGT2B15 in the UGT2B15-overexpressing cell line were determined as described previously by Dr. Ryan Dellinger (184). Western blot analysis of UGT2B15 was conducted using a synthesized affinity-purified chicken anti-UGT2B antibody. This antibody targeted the peptide CKWDQFYSEVLGRPTTL, which is common to all human UGT2B family members (Pocono Rabbit Farm, Canadensis, PA). The UGT2B Antibody was used at a 1:5000 dilution to detect all of the UGT2Bs which were quantified against 200 to 250 ng of a human UGT2B protein standard (supplied in the Western blotting kit provided by Gentest) by densitometric analysis of X-ray film exposures (1 s - 2 min) of the Western blots using a GS-800 densitometer with Quantity One software (Bio-Rad). All cell homogenate protein levels were normalized to the levels of β -actin observed in each lane (quantified by densitometric analysis of Western blots as described above). X-ray film bands were always below densitometer saturation. Densitometric results were always consistent irrespective of the exposure time. Western blot and subsequent densitometric analyses were performed in triplicate on three separate occasions, by using the same UGT-containing cell homogenates used for activity assays, with relative UGT protein levels expressed as the mean of these experiments.

2.2.2 Preparation of cell homogenates

Homogenates for each individual UGT were prepared as follows. Cells were grown, as described in section 2.2.1, on 100 mm plates to 80% confluence (~25 plates) before the preparation of cell homogenates. Cells were collected from the plate by repeatedly pipetting 10 mL of Phosphate-Buffered Saline (PBS) over cells. Cells were

then collected in a 50 mL conical tube, centrifuged at 700 g for 5 min followed by aspiration of the supernatant. Pelleted cells were then resuspended in PBS, centrifuged and supernatant removed to ensure that there was no residual media in pelleted cells. After the final centrifugation and removal of supernatant, pelleted cells were resuspended in Tris-buffered saline (25 mM Tris base, 138 mM NaCl₂, and 2.7 mM KCl, pH 7.4) and subjected to three rounds of freeze-thaw before gentle homogenization using a dounce homogenizer. Cell homogenates were stored at -80°C. Total homogenate protein concentrations were measured using the BCA protein assay (Pierce). Total RNA was extracted using the RNeasy Mini kit from Qiagen as per manufacturer's protocol and used to further confirm expression of the correct UGT mRNA.

2.2.3 Glucuronidation Assays

Human liver microsomes (described in section 4.2.2) were tested and used to optimize the SAHA glucuronidation assay. HLMs (40 µg of total protein) were initially incubated with alamethicin (50 µg/mg protein) for 15 min in an ice bath to permeabilize membranes. UGT activity was determined in a standardized assay mix containing 50 mM Tris buffer (pH 7.5), 10 mM MgCl₂, 4 mM UDPGA and 65 µM to 8 mM of substrate, and the assay mix was incubated 1 h at 37°C. Reactions were terminated by the addition of cold acetonitrile adding the same volume as the initial reaction (40 µL). Reactions were then centrifuged at 13,000 g for 10 min at 4°C and supernatants were collected. Reactions containing 1mM or more SAHA were diluted 5-fold with 50/50

water and acetonitrile. Glucuronidation product formation was then assessed using Ultra Performance Liquid Chromatography (UPLC) as described below.

The ability of cell homogenates from human UGT-overexpressing cell lines to glucuronidate SAHA was determined in a manner similar to that described previously (184, 186, 243). Cell homogenate (40 or 400 μg protein) was initially incubated with alamethicin (50 $\mu\text{g}/\text{mg}$ protein) for 15 min in an ice bath to permeabilize membranes. UGT activity was determined in a standard assay mix containing 50 mM Tris buffer (pH 7.5), 10 mM MgCl_2 , 4 mM UDPGA and 65 μM to 8 mM of substrate, and the assay mix was incubated 1 h at 37°C. Reaction mixes were terminated by the addition of cold acetonitrile adding the same volume as the initial reaction (40 μL). Reactions were then centrifuged at 13,000 g for 10 min at 4°C and supernatants were collected. Reactions containing 1 mM or more SAHA were diluted 5-fold with 50/50 water/ acetonitrile. Glucuronidation product formation was then assessed using UPLC as described below.

Glucuronidation assays (1-10 μL) were analyzed for SAHA-glucuronide by UPLC on a Waters ACQUITY UPLC™ System (Milford, MA) equipped with an automatic injector and a UV detector operated at 244 nm. UPLC separation was accomplished using a BEH 1.7 μm C18 column (2.1 mm x 100 mm, Waters) with gradient elution as follows: starting with 5.6% buffer B (100% acetonitrile) and 94.4% buffer A (10 mM ammonium acetate, pH 5.0 and 10% acetonitrile) the flow rate was maintained at 0.3 mL/min; a subsequent linear gradient to 72% buffer B over 3 min was then performed. The amount of SAHA glucuronide formed was calculated based on the ratio of the areas under the curves for the peaks representing the glucuronide versus that representing SAHA. As controls, glucuronidation assays were performed using HLM as a positive

control for glucuronidation activity, and untransfected HEK293 cell homogenate protein as a negative control for glucuronidation activity.

2.2.4 SAHA-glucuronide confirmation

SAHA-glucuronide was initially confirmed by sensitivity to *Escherichia coli* β -glucuronidase [β -glucuronidase; (Sigma Chemical Co., St. Louis, MO)] treatment as previously described (128, 186, 244). Briefly, activity assay mixes were treated with 1000 U of β -glucuronidase at 37°C for 16 h and then analyzed by UPLC for cleavage of the SAHA-glucuronide.

In addition to β -glucuronidase sensitivity, the SAHA-glucuronide metabolite was confirmed via mass spectrometry by Dr. Gang Chen of the Lazarus lab. Triple-quadrupole tandem mass spectrometric detection was performed on an ACQUITY[®] SQD (Waters Corp. Milford, MA, USA) with an electrospray ionization (ESI) interface. For separation, an UPLC system consisting of a binary gradient pump, an auto sampler (4°C), and a column oven (35°C) were used. A 100 × 2.1 mm i.d. Acquity UPLC Beth C18 column with 1.7 μ m particles (Waters) was used for separation of the SAHA-glucuronide. A 0.2 μ m prefilter was installed before the column. Eluents were (A) 90% 10mM NH₄AC pH5.0 and 10% CAN, and (B) 100% CAN. The flow-rate was 0.3 mL/min. Sample volumes of 10 μ L were injected. Gradient conditions were as follows: 0–1.5 min, 20% B; 1.5–2.5 min, linear gradient to 72% B; 2.5–5 min, 72% B; 5-7min isocratic 20% B.

The mass spectrometer operated in positive mode was set up to scan the daughter ion of m/z 441.4. The following optimized mass spectrometry parameters were

employed: capillary voltage 0.57 kV, cone voltage 30 V, collision energy 15 V source temperature 450°C and desolvation temperature 140°C. Nitrogen was used as the desolvation and cone gas with a flow rate of 760 L/h. Argon was used as the collision gas at a flow rate of 0.1 mL/min. Data acquisition and analysis were performed using the MassLynx™ NT 4.1 software with QuanLynx™ program (Waters Corp., Milford, MA, USA).

2.2.5 Kinetic analysis of interactions of UGTs with SAHA

All UGT cell lines (Table 2.1) were initially screened using 400 µg total protein in 40 µL reactions incubated with 8 mM SAHA. To determine V_{max} and K_M values, UGT activity was determined as described in section 2.2.3, using at least 6 concentrations of SAHA ranging from 65 µM to 8 mM. V_{max} and K_M values were determined from Michaelis-Menton plots of UGT activity versus SAHA concentration. Kinetic constants were determined using Prism Version 5 software (GraphPad Software, San Diego, CA, USA). All experiments were performed in triplicate for kinetic analysis of UGT-overexpressing cell homogenates and were independent assays.

2.3 RESULTS

2.3.1 Characterization of UGT-overexpressing cell lines

In order to screen all the UGT1As and UGT2Bs (except UGT2B28) to determine if they are able to glucuronidate SAHA, it was first necessary to make UGT1A3 and UGT2B15 expressing HEK293 cell lines. These two UGTs were the only wild-type cell lines missing from our lab's UGT cell line set. To confirm correct amplification and insertion of UGT amplicons into the pcDNA3.1/V5-His-TOPO/ vector, the cloned UGT1A3 and 2B15 inserts were sequenced, were compared with sequences deposited in GenBank, and were confirmed to be 100% homologous to the wild-type UGT1A3 (gi:40849853) and UGT2B15 (gi:5881245) sequences. After transfection into HEK293 cells and selection by G418, RNA was isolated from these cell lines and correct transcription was confirmed by sequencing. UGT protein levels in each cell line were measured by Western Blot. Figure 2.2 and 2.3 are representative of blots used for quantification of UGT1A3 and UGT2B15 proteins, respectively. From 3 independent Western blots and densitometric measurements, the amount of UGT1A3 expression in the cell homogenate was determined to be 31 ng UGT1A3/ μg total cell homogenate protein and UGT2B15 expression was determined to be 15.5 ng UGT1A3/ μg total cell homogenate protein.

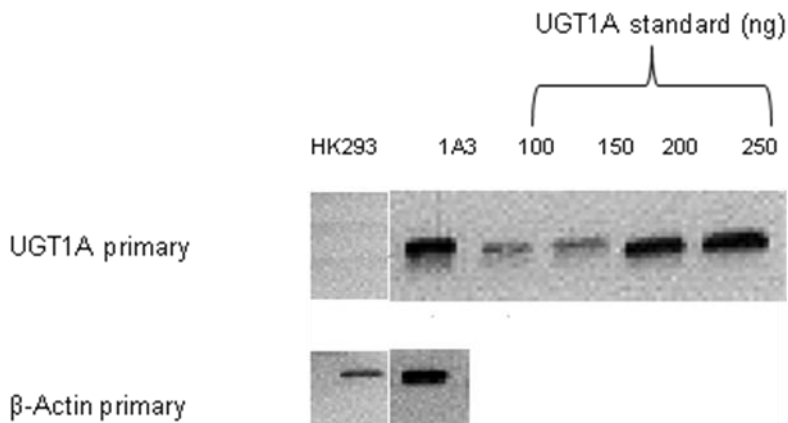


Figure 2.2: Western blot analysis of UGT1A3 protein expression in the UGT1A3-overexpressing HEK293 cell line. Cell homogenate (20 μ g total protein) was loaded. The amount of UGT1A3 expression was normalized against the levels of β -Actin and was quantified by densitometry as described in Materials and Methods (section 2.2.1). Protein from homogenates of untransfected HEK293 cells was used as a negative control. Product size is 50 kDa.

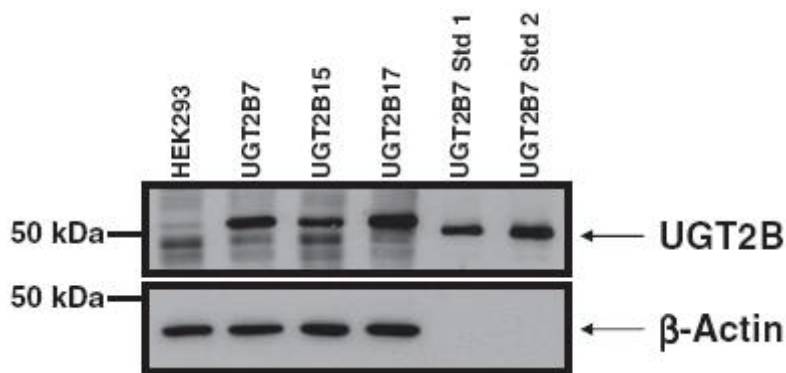


Figure 2.3: Western blot analysis of UGT2B15 protein expression in the UGT2B15 and UGT2B17-overexpressing HEK293 cell line. UGT 2B7, 2B15, and 2B17 protein levels were quantified by comparison to known amounts of UGT2B7 protein standard (from Gentest) with quantification standardized to the levels of β -actin observed in each lane. UGT2B7 Std 1, 200 ng of UGT2B7 protein; UGT2B7 Std 2, 250 ng of UGT2B7 protein. Twenty micrograms of homogenate protein was loaded in each lane for UGT 2B7-, 2B15-, and 2B17-overexpressing cells. The negative control HEK293 (20 μ g of homogenate protein) lane shows no UGT2B expression in the parental HEK293 cells. [Reference from (245)].

2.3.2 Confirmation of SAHA-glucuronide formation

Although the SAHA-glucuronide has been identified in the serum and urine of patients treated with SAHA, it has yet to be determined which UGT enzyme(s) is/are responsible for this activity (246). To determine which UGTs glucuronidate SAHA, an activity assay followed by UPLC analysis of the products was optimized using UGT1A7 cell homogenate and human liver microsomes (Figure 2.4). The chromatogram of the UGT1A7 cell homogenate incubated with co-substrate, UDPGA which is required for glucuronidation (Figure 2.4A) shows the UDPGA peak and cell homogenate background peaks. UDPGA is the co-substrate required for glucuronidation; this compound is transferred by the UGT enzymes to the substrates being glucuronidated which typically results in inactivation and excretion. This co-substrate needs to be in excess amounts for glucuronidation to occur in the *in vitro* system.

Figure 2.4B is the UPLC chromatogram of SAHA dissolved in DMSO and diluted with 50/50 water/acetonitrile and demonstrates a retention time of 2.85 min for unmetabolized SAHA. Figure 2.4C is the UPLC chromatogram of UGT1A7 homogenate that has undergone incubation with both the UGT co-substrate, UDPGA, and the substrate, SAHA to detect the presence of UGT glucuronidation activity. The un-conjugated SAHA peak was again observed at the retention time of 2.85 min and a peak postulated to be the SAHA glucuronide was observed with a retention time of 2.59 min. To confirm that the peak at 2.59 min was the SAHA-glucuronide further analysis was conducted.

The peak that was postulated to be the SAHA glucuronide was initially tested for sensitivity to β -glucuronidase, which is an enzyme that cleaves the glucuronic acid from

its substrates. The product peak that had been observed in the chromatogram of the complete UGT assay mix at 2.59 min and proposed to be SAHA glucuronide was now absent from the chromatogram (Figure 2.4D). These results are similar to those observed previously for other glucuronides (235) and strongly suggest that the peak at 2.59 min is SAHA-glucuronide.

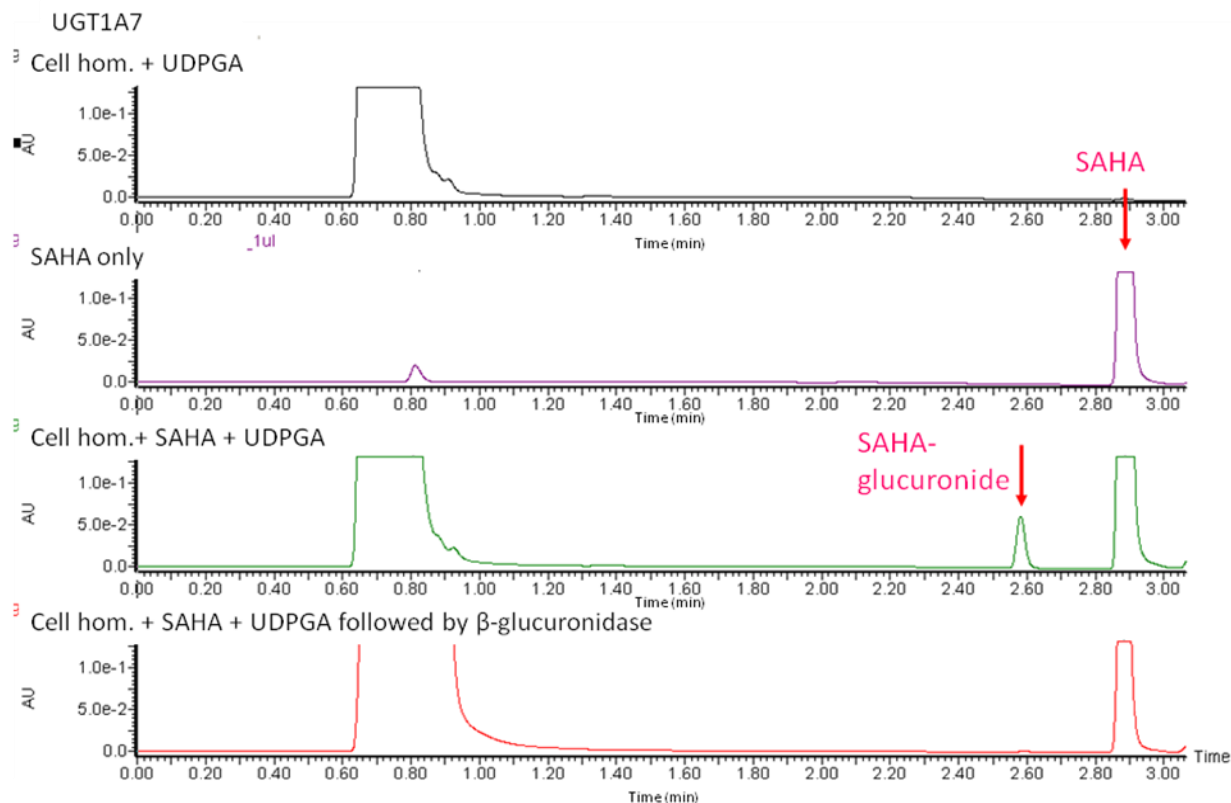


Figure 2.4: Optimization of the UGT activity assay with SAHA substrate using UGT1A7 cell homogenate. Representative UPLC traces of glucuronidation assays using 8000 μ M SAHA, performed as previously described in the Materials and Methods (2.2.3), are shown for incubations containing, (A) UGT1A7-overexpressing cell homogenates (40 μ g protein) and UDPGA; (B) SAHA dissolved in DMSO and diluted with 50/50 water:acetonitrile; (C) UGT1A7-overexpressing cell homogenates (40 μ g protein) incubated with co-substrate, UDPGA and substrate, SAHA ; and (D), products of UGT1A7 activity assay followed by incubation with β -glucuronidase.

To further confirm that the observed peak at 2.59 min is SAHA glucuronide, HLM and mass spectrometry were used. UGT activity assays, similar to those used for UGT1A7 cell homogenates, were performed using SAHA substrate and HLM as the protein source. The results indicated formation of SAHA glucuronide by HLM as indicated by the peak at 2.59 min (Figure 2.5A) which is absent following treatment with β -glucuronidase (Figure 2.5 A and B). The mass spectrum for the postulated SAHA-O-

glucuronide observed at 2.59 min in the UPLC chromatogram ($[M+H]^+$ of 441 for protonated molecules) showed a clear daughter ion at m/z 265 corresponding to the $[M+H]^+$ of SAHA (Figure 2.5C), a pattern that was identical to the previously published ion spectra for SAHA-glucuronide (247).

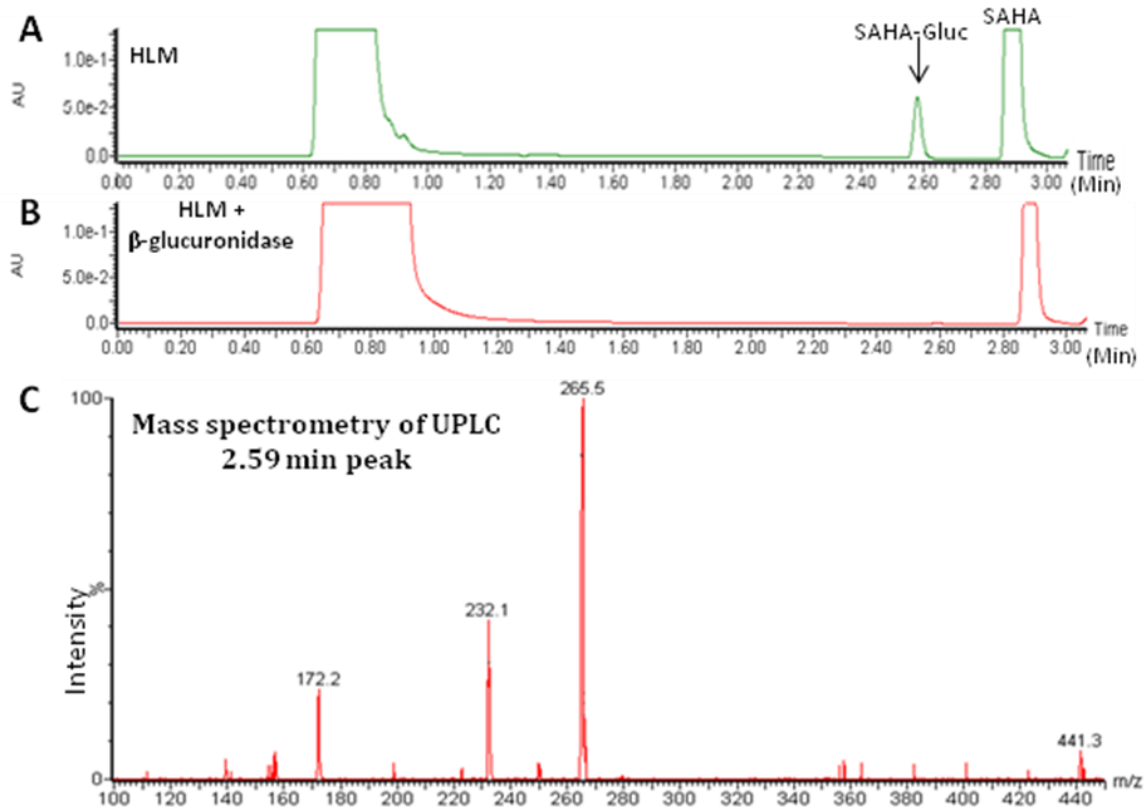


Figure 2.5: UPLC analyses of SAHA metabolites formed by UGTs in HLM. Representative UPLC traces of glucuronidation assays using 200 μ M SAHA, performed as previously described in the Materials and Methods (2.2.3), are shown for incubations containing, (A) HLM (20 μ g protein); or (B), HLM incubated with β -glucuronidase. Representative tandem MS/MS trace of the putative SAHA-glucuronide peak from HLM glucuronidation activity assays is shown in panel C.

2.3.3 Screen of individual UGTs for activity against SAHA

To identify UGTs that are able to glucuronidate SAHA, an initial screen using cell lines overexpressing wild-type UGTs 1A1, 1A3, 1A4, 1A5, 1A6, 1A7, 1A8, 1A9, 1A10, 2B4, 2B7, 2B10, 2B11, 2B15 and 2B17 was performed with 400 µg total cell homogenate protein and 8 mM SAHA (the highest concentration at which SAHA could be dissolved in DMSO without precipitating out of the solution). UPLC analysis of glucuronidation assays for each of the UGTs tested indicated a peak for unconjugated SAHA at a retention time of 3 min and, for those UGTs which exhibited glucuronidation of SAHA, a peak for SAHA glucuronide at a retention time of 2.62 min (Figure 2.6). Of the UGTs tested, UGT 1A3, 1A7, 1A8, 1A9, 1A10 and 2B17 each exhibited high levels of glucuronidation against SAHA, while UGTs 1A1, 1A4, 1A6 and 2B7 exhibited relatively less glucuronidation of SAHA. No detectable glucuronidation activity of SAHA was observed in our *in vitro* glucuronidation assays for UGTs 1A5, 2B4, 2B10, 2B11, or 2B15. Table 2.2 summarizes the results from the initial screen.

UGT	Activity*	UGT	Activity*
1A1	+	2B4	-
1A3	+++	2B7	++
1A4	+	2B10	-
1A5	-	2B11	-
1A6	+	2B15	-
1A7	+++	2B17	+++
1A8	+++		
1A9	+++		
1A10	+++		

* (+++) high glucuronidation activity, K_M and V_{max} values could be determined; (++) glucuronidation activity detected, $K_M > 8$ mM; (+) glucuronidation activity detected, but kinetic values could not be ascertained; (-) glucuronidation activity not detected.

Table 2.2: Summary of SAHA glucuronidation formation of individual UGTs.

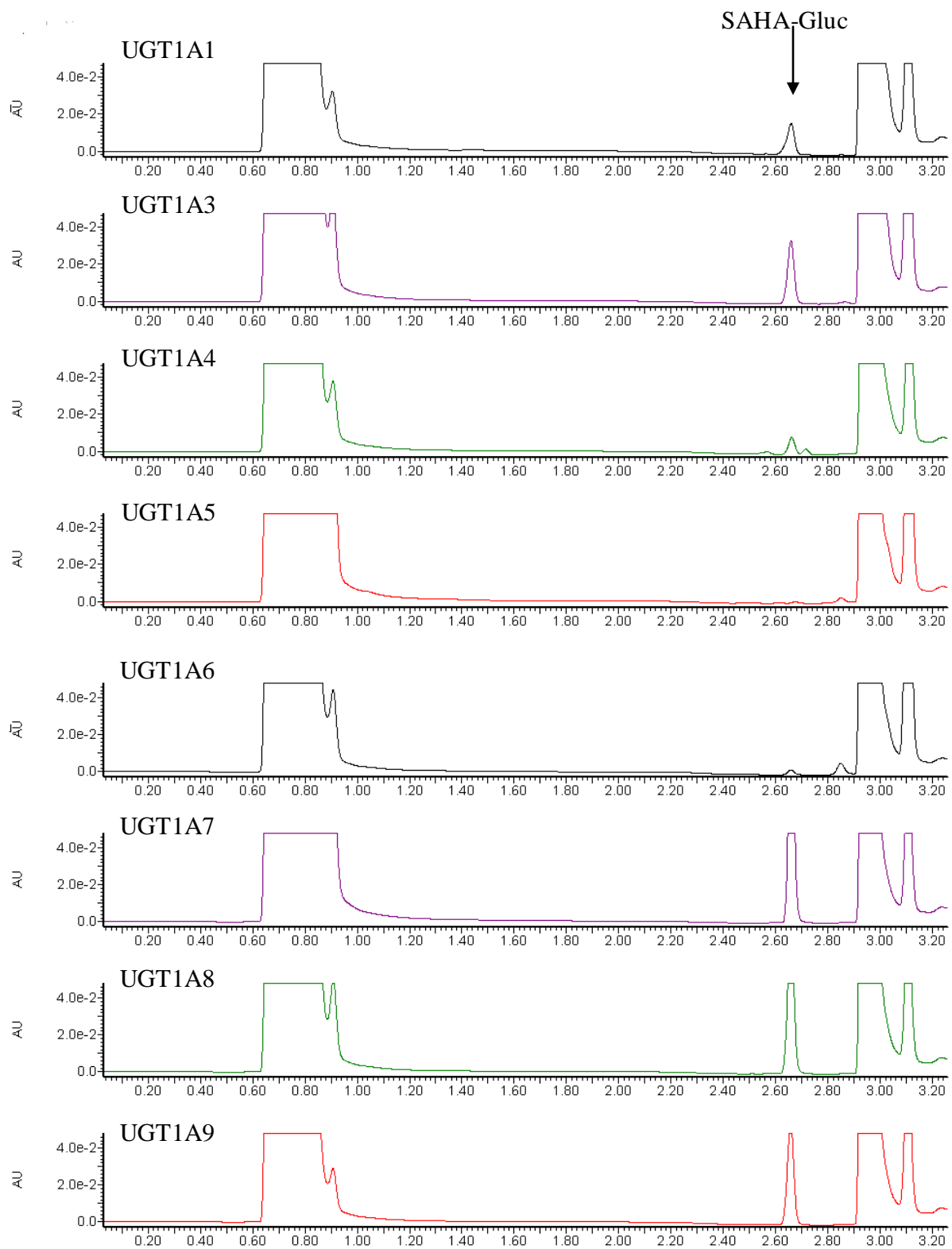


Figure 2.6: UPLC chromatograms from *in vitro* screening of UGT-overexpressing HEK2993 cell lines for UGT activity against SAHA. Each glucuronidation assay (40 μ L) contained 400 μ g total protein and was incubated for 1 h and assessed by UPLC.

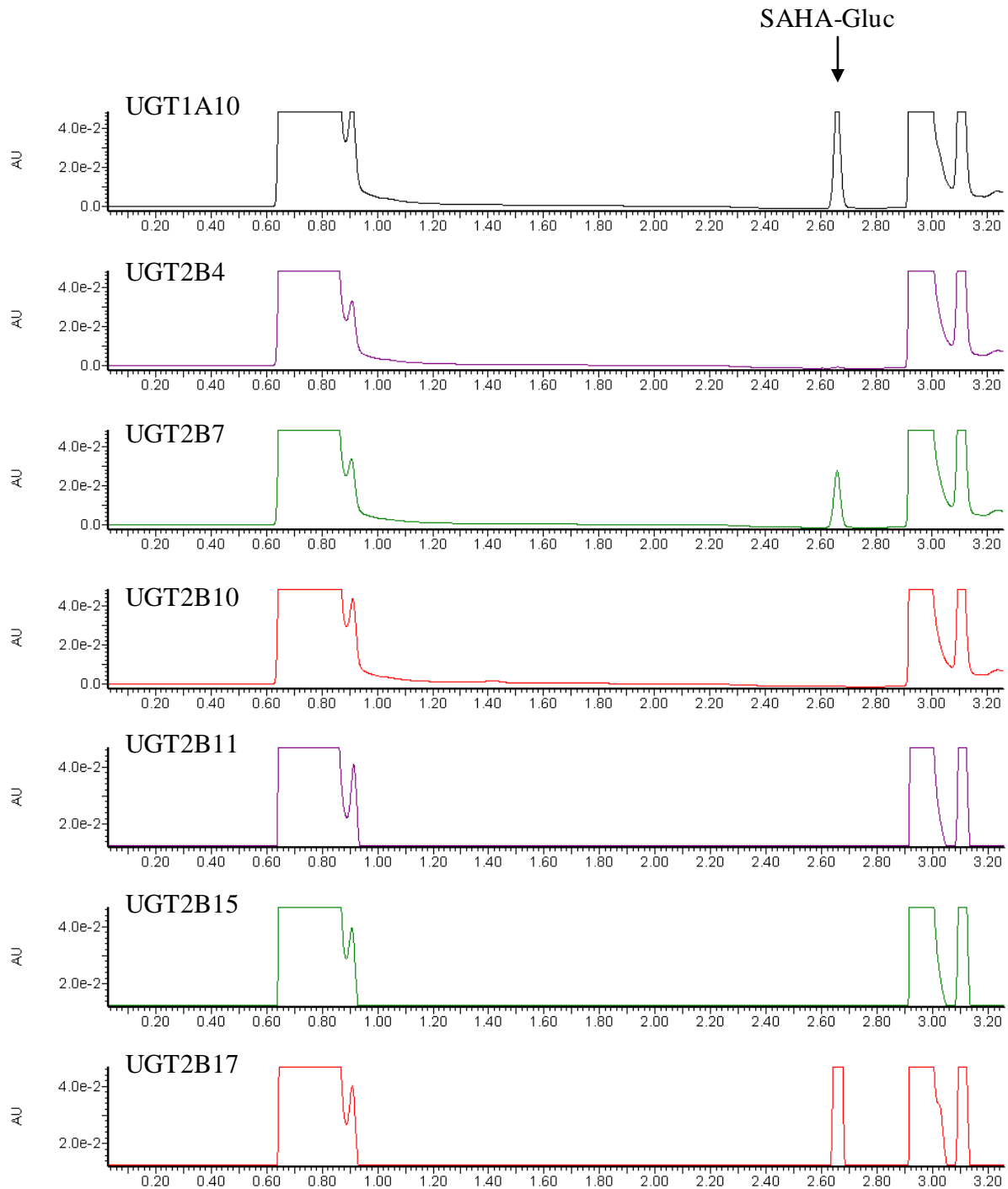


Figure 2.6 (continued): UPLC chromatograms from *in vitro* screening of UGT-overexpressing HEK293 cell lines for UGT activity against SAHA. Each glucuronidation assay (40 μ L) contained 400 μ g total protein and was incubated for 1 h and assessed by UPLC.

2.3.4 Kinetic parameters for the glucuronidation of SAHA by individual UGT family members

To identify which UGTs were most active against SAHA, kinetic analysis was performed. Although UGT 1A1, 1A4, 1A6 and 2B7 each exhibited detectable levels of glucuronidation against SAHA (Figure 2.6), the K_M for each was above 8 mM, which was the highest concentration of SAHA that could be used therefore an accurate K_M could not be measured. UGT 1A3, 1A7, 1A8, 1A9, 1A10 and 2B17 each exhibited levels of glucuronidation of SAHA for which kinetic parameters could be determined and a representative kinetic analysis plot for each UGT is shown in Figure 2.7. Each cell line's stock homogenate was tested in triplicate as independent experiments for glucuronidation activity.

Direct comparison of the kinetic parameters for the individual UGTs analyzed required that activity results from the same quantity of UGT protein be analyzed for each determination. Therefore, Western analysis was performed on homogenates of each HEK293 UGT-overexpressing cell line tested and the UGT activities were then normalized to account for observed differences in amounts of UGT expression. Since the same standard of UGT protein was used to determine the quantity for each UGT cell homogenate, it is possible to adjust protein values to compare activity. Furthermore, we can use this UGT adjusted V_{max} to compare to K_M (V_{max}/K_M) and yield a value which represents overall enzyme efficiency. Traditionally, K_{cat} , which includes factoring in the enzyme molecular weight, would be calculated to assess overall enzyme efficiency; however, our method adjusted only by quantity of UGT. Both K_{cat} and V_{max}/K_M showed the same patterns for enzyme efficiency for the UGTs that were examined. As shown in

Table 2.3, UGT2B17, UGT1A8 and 1A10 were considerably more active against SAHA than any other UGT family members as determined by values of V_{max}/K_M . UGT2B17 exhibited the lowest K_M of all the UGTs screened, which at 300 μ M, was 3-fold lower than that of UGT1A10 which exhibits the next lowest K_M value of 1mM.

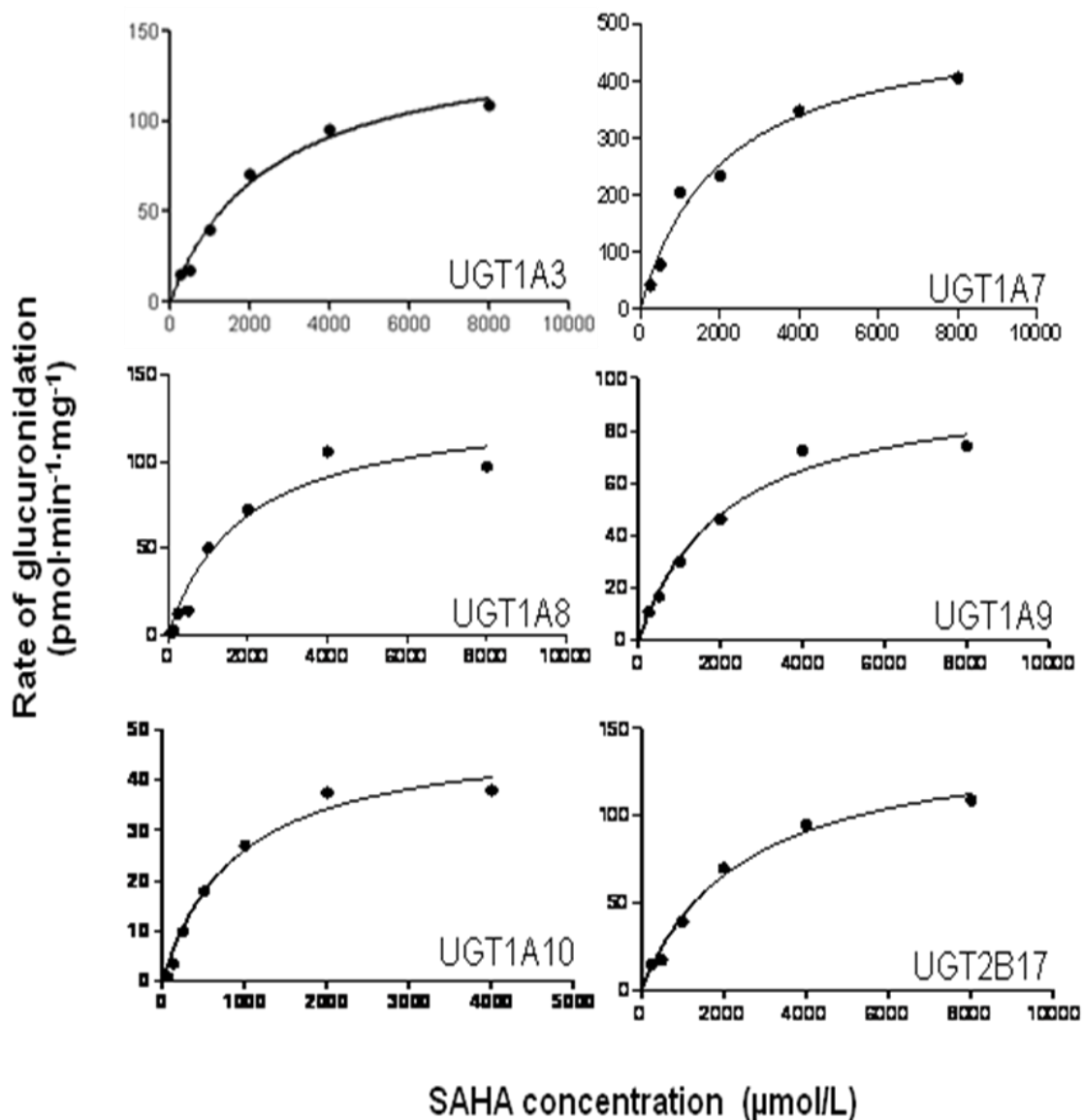


Figure 2.7: Representative concentration dependence curves for SAHA glucuronide formation in homogenates of UGT-overexpressing cells. Incubations to determine the concentration dependence of SAHA glucuronide formation were performed for 1 h at 37°C using 400 μg total protein. Shown are representative plots from the three replicate assays performed for each UGT as described in section 2.2.5.

UGT	K_M (mM)	V_{max} ($\mu\text{mol}\cdot\text{min}^{-1}\cdot\mu\text{g}^{-1}$) ^b	V_{max}/K_M ($\text{nL}\cdot\text{min}^{-1}\cdot\mu\text{g}^{-1}$) ^b
UGT1A3	3.4 ± 0.8	6.0 ± 1.8	1.7 ± 0.2
UGT1A7	2.7 ± 0.6	10 ± 0.4	3.9 ± 0.6
UGT1A8	1.9 ± 0.1	62 ± 7.6	33 ± 6.3
UGT1A9	1.6 ± 0.5	11 ± 1.3	7.1 ± 2.2
UGT1A10	1.0 ± 0.1	24 ± 2.7	24 ± 2.4
UGT2B17	0.3 ± 0.1	3.7 ± 0.7	16 ± 6.5

^a All reactions were performed using 40 μg of UGT-overexpressing cell homogenate and incubated for 1 h at 37°C. Kinetic data are reported as mean \pm standard deviation for three independent experiments.

^b V_{max} values are adjusted per μg of the corresponding UGT protein as determined by Western blot analysis.

Table 2.3: Kinetic analysis of SAHA-glucuronide formation by UGTs using UGT-overexpressing cell homogenates.^a

2.4 SUMMARY

Pharmacokinetic studies have identified two inactive metabolites, SAHA-glucuronide and 4-anilino-4-oxobutanoic acid, in patients treated with SAHA, [Figure 1.5; (55, 246)] and it has been hypothesized that UGT genotype is important to patient response (119). The present study is the first to identify and to characterize the enzymes responsible for the glucuronidation of SAHA, while the details of how SAHA is metabolized to 4-anilino-4-oxobutanoic acid have not yet been elucidated. The current results demonstrate that several UGTs, including 1A1, 1A3, 1A4, 1A6, 1A7, 1A8, 1A9, 1A10, 2B7, and 2B17 exhibit glucuronidation activity against SAHA.

UGT1A8 and UGT1A10, which are expressed exclusively in extra-hepatic tissues, were the best overall glucuronidators of SAHA in our *in vitro* system. *In vivo*, these enzymes may play important roles in tissues which are targets of SAHA, such as lung, breast, colon, small intestine, and tissues of the aerodigestive tract (136, 161, 185, 248). Of the hepatic UGTs, UGT2B17 was identified as the major hepatic enzyme involved in the glucuronidation of SAHA. The K_M exhibited by UGT2B17 against SAHA was 5- and 11-fold lower than those observed for the other active hepatic UGTs, 1A9 and 1A3, respectively.

Our goal was to identify individual UGTs that had the ability to glucuronidate SAHA and this required a system in which only one UGT was expressed. However, there are limitations to this assay design. Since activity is assessed *in vitro* many of the enzymes which transport the drugs and co-substrate into the ER lumen are not present, thus requiring holes to be made in the membrane which could confound the overall

glucuronidation process. Studying UGT activity in humans, tissues, and most cell lines would not result in the identification of the specific UGTs which glucuronidate SAHA due to the multiple UGTs which are expressed simultaneously. Therefore, the assay used in this section is ideal for the particular goal of examining the glucuronidation abilities of individual UGTs.

This study has enhanced the understanding of the enzymes involved in the metabolism of SAHA; however, more characterization of the glucuronidation pathway could possibly help identify inter-individual differences resulting from UGT variants. Each of the UGTs that have now been demonstrated to be most active for glucuronidation of SAHA including UGT 1A8, 1A10, and 2B17, are known to have variants that alter the ability of the enzyme to glucuronidate other substrates (202, 203, 205, 209). These variants could also affect SAHA glucuronidation and should be characterized. In addition, while this study used recombinant individual UGTs to identify the specific enzymes involved in the glucuronidation of SAHA, further studies using *in vitro* systems such as hepatocytes or human tissue, which contain multiple UGTs, would better simulate *in vivo* conditions and further our understanding of SAHA metabolism.

Chapter 3: Characterization of the ability of variant UGTs to glucuronidate SAHA

3.1 INTRODUCTION

Cancer is a complex disease that varies among individuals and even cancers that develop in the same primary site may differ at the molecular level from individual to individual. The complexities of cancer make this disease ideal for development of individualized medicine. Methods for development of individualized treatment include examining the tumor microenvironment and/or examining the genetic make-up of an individual. Although individualized medicine is in its early stages, some results that demonstrate promise in the field have already been achieved. Expression microarrays have been used to classify breast cancer at the molecular level and this has aided the assessment of clinical outcomes and determination of optimal treatments for individual breast cancers (249-251). This same approach could be integrated with chemotherapeutic agents that are currently used in the clinic as well as with those that are currently being developed.

Chemotherapeutic agents have a narrow therapeutic index in which the drug is effective and the dosage is not toxic (238). Identifying an appropriate dose with optimal chemotherapeutic effects is challenging considering the many ways in which individuals differ (i.e. diet, exercise, gender, weight) that may affect drug response.

Pharmacogenetics is an approach which correlates differences in drug response to the genotypes of individuals. This approach was based on the observation that antimalarial drugs caused hemolysis in patients from families that have glucose-6-phosphate

dehydrogenase deficiency (238, 252). With advances in technology and extensive information on genetic variations in the population readily available, consideration of an individual's genotype when making decisions about the treatment of a disease is flourishing. There are many pathways involved in drug action for which it has been demonstrated that an individual's genotype can alter drug response. For example, a G2677T/A single nucleotide polymorphism (SNP) in ABCB1 (also known as mdr-1), which encodes a P-glycoprotein drug-efflux pump, is correlated with a significantly lower rate of clearance of paclitaxel and better response in ovarian cancer patients (patients had complete responses and were relapse-free for at least 1 year) [Figure 1.13, (215, 216)]. In addition to effects on drug transport, variants of drug metabolizing enzymes have been shown to alter drug efficiency and/or toxicity thus leading to inter-individual differences in drug response.

Drug metabolism is broken down into two phases: phase I typically leads to an active more polar metabolite and Phase II typically leads to the conjugation of a compound that results in the inactivation and excretion of the drug; however, there are exceptions to these generalizations. Alterations in enzymes that metabolize a drug can alter the pharmacokinetics that influence the concentration of drug that reaches its target (253). The CYP450 family of enzymes is a family of phase I enzymes that oxidize approximately 78% of the top 200 drugs prescribed in the US that are cleared hepatically (218). Genetic variants of CYP450s, that result in aberrant expression or altered enzyme activity, have been suggested to be clinically relevant in alterations of metabolism of chemotherapeutic agents including flutamide, tegafur, cyclophosphamide, paclitaxel, and tamoxifen (219). Although these phase I enzymes

are relevant to altered drug metabolism and possibly to patient response, it has yet to be recommended by the FDA that genetic screening be conducted before administration of these drugs. In addition, a phase II enzyme variant of UGT1A1 has had a clear and direct clinical impact. The UGT1A1*28 allele, which is associated with decreased UGT1A1 expression (228), has been linked to decreased glucuronidation of SN-38, the major active metabolite of Irinotecan, both in HLM and in the urine of patients treated with Irinotecan (123, 124, 193, 229). The resulting decreases in excretion have been linked to increased Irinotecan toxicity in patients (123-125) prompting the FDA to approve genetic screening for the UGT1A1*28 allele in patients who may be considered for treatment with this agent (126). Other current studies focus on the UGT family of enzymes and understanding how variants of these enzymes may alter drug toxicity. For example, the UGT2B7p.His268Tyr variant was recently associated with decreased liver microsomal glucuronidation activity against major active tamoxifen metabolites which may be linked to altered patient response to tamoxifen (121). Characterization of the UGTs responsible for metabolism of drugs may aid in better understanding differences in patient response and toxicity.

Although variation in patient response to SAHA has been observed, no studies have yet looked for genetic variants in the enzymes of the SAHA metabolic pathway. UGT 1A7, 1A8, 1A10, and 2B17, now identified as the most active UGTs against SAHA, all have variants with prevalence greater than 2%. The goal of the study presented in this section was to further analyze SAHA metabolism by determining whether genetic variants of the major SAHA-glucuronidating enzymes could potentially contribute to altered metabolism of SAHA *in vitro*.

3.2 MATERIALS AND METHODS

3.2.1 Generation of cell lines overexpressing UGT variants

For the present study, 3 new variant UGT1A7 HEK293 cell lines were generated and a UGT2B15 variant was also generated (although not necessary for analysis with SAHA). The UGT1A7 coding region was originally amplified from laryngeal RNA, reverse-transcribed to cDNA and ligated into pcDNA3.1/V5-His-TOPO/UGT plasmid (184). The QuickChange SDM kit (Stratagene, La Jolla, CA) was used to performed site-directed mutagenesis (SDM) for the UGT1A7*2 and UGT1A7*4 alleles (encoding UGT1A7p.[Asn129Lys + Arg131Lys] and UGT1A7p.Trp208Arg variants, respectively) using a previously-synthesized wild-type UGT1A7 clone (184). The UGT1A7*3 allele (encoding the UGT1A7p.[Asn129Lys + Arg131Lys + Trp208Arg] variant) was made using the newly-synthesized UGT1A7*2 clone as template. Primer set UGT1A7-129/131S (sense, 5'-GCAGGAGTTTGTTTAATGACCGAAAATTAGTAGAATACTTAAAGG-3') and UGT1A7-129/131AS (antisense, 5'-CCTTTAAGTATTCTACTAATTTTCGGTCATTAAACAAACTCCTGC-3'), corresponding to nucleotides +371 to +422 relative to the UGT1A7 translation start site, were used to generate constructs that encode for the amino acid changes at UGT1A7 codons 129 (Asn>Lys) and 131 (Arg>Lys). Primer set UGT1A7-208S (5'-CATGACTTTCAAGGAGAGAGTACCGGAACCACATCATGCACTTG-3') and UGT1A7-208AS (5'-CAAGTGCATGATGTGGTTCCGTACTCTCTCCTTGAAAGTCATG-3'), corresponding to nucleotides +607 to +652 relative to the UGT1A7 translation start site,

were used to generate constructs that encode for the amino acid change at codon 208 (Trp>Arg). Similarly, SDM was used to generate cDNA for UGT2B15*2 (encoding for UGT2B15p.Asp085Tyr) from wild-type UGT2B15 (previously described in section 2.2.1) using primers UGT2B15-85S (sense, 5'-TACATCTTTAACTAAAAATGATTTGGAAGATTCTCTTCTG-3') and UGT2B15-85AS (antisense, 5'-CAGAAGAGAATCTTCCAAATCATTTTTAGTTAAAGATGTA-3') with both primers corresponding to nucleotides +234 to +273 relative to the UGT2B15 translation start site. The underlined base for each primer indicates the base-pair change.

SDM PCR amplification was performed as follows: 1 cycle of 95°C for 4 min, 25 cycles of 95°C for 30 s, 55°C for 1 min, and 68°C for 16 min, and then a final cycle of 68°C for 7 min. All constructs were confirmed by dideoxy sequencing of the entire coding region of each vector using the T7 and BGH vector primers (Integrated DNA Technologies). Each newly generated UGT-expressing construct was compared with the sequence described in GenBank, and was confirmed to be 100% homologous to its respective allele.

Each construct was used to generate individual UGT-overexpressing HEK293 cell lines by standard electroporation techniques in a GenePulser Xcell (Bio-Rad, Hercules, CA). The standard protocol used 10 µg of pcDNA3.1/V5-His-TOPO/UGT plasmid DNA with 5×10^6 HEK293 cells in 0.5 mL serum-free DMEM medium, with electroporation at 250 V and 1000 µF. After transfection, HEK293 cells were grown to 80% confluence in a 5% CO₂ atmosphere in DMEM medium supplemented with 4.5 mM glucose, 10 mM HEPES, 10% fetal bovine serum, 100 U/mL penicillin, 100 µg/mL streptomycin, and G-418 (700 µg/mL medium) for the selection of G-418-resistant cells,

with selection medium changed every 2 to 3 days. G-418-resistant cell lines were selected and analyzed for UGT expression via Western blotting analysis as described in section 2.2.1. Levels of UGT2B15 were measured by Dr. Dellinger of the Lazarus lab. All other cell lines overexpressing UGT1A and UGT2B variants analyzed in this study have been described previously (section 2.2.1). Cells from each UGT-overexpressing cell line were grown in DMEM to 80% confluence, as described above, prior to preparation of cell homogenates.

3.2.2 Preparation of cell homogenates

Homogenates for each individual UGT variant were prepared as follows. Cells were grown, as described in section 3.2.1, in 100 mm plates to 80% confluence (~25 plates) before the preparation of cell homogenates. Cells were collected from the plate with 10 mL of PBS, centrifuged, the supernatant removed, the cell pellet resuspended in PBS, centrifuged and the supernatant removed to ensure no residual media in pelleted cells. After final centrifugation and removal of supernatant, pelleted cells were resuspended in Tris-buffered saline (25 mM Tris base, 138 mM NaCl₂, and 2.7 mM KCl, pH 7.4) and subjected to three rounds of freeze-thaw before gentle homogenization. Cell homogenates were stored at -80°C. Total homogenate protein concentrations were measured using the BCA protein assay. To confirm sequence of overexpressing mRNA, total RNA was extracted using the RNeasy Mini kit from Qiagen as per manufacturer's protocols.

3.2.3 Glucuronidation Assays

Glucuronidation activities of cell homogenates from human UGT-overexpressing cell lines toward SAHA were determined similarly to those described previously (184, 186, 243). Cell homogenate (40 or 400 μg protein) was initially incubated with alamethicin (50 $\mu\text{g}/\text{mg}$ protein) for 15 min in an ice bath to permeabilize the membranes. Incubations (40 μL) were subsequently performed at 37°C for 1 h in reaction buffer of 50 mM Tris (pH 7.5), 10 mM MgCl_2 , 4 mM UDPGA and 65 μM to 8 mM of substrate. Reactions were terminated by the addition of cold acetonitrile, adding the same volume as the initial reaction mix (40 μL). Reaction mixes were then centrifuged at 13,000 g for 10 min at 4°C and supernatants were collected. Reactions containing 1 mM or more SAHA were diluted 5-fold with 50/50 water/ acetonitrile. Glucuronidation product formation was then assessed using UPLC as described previously.

Glucuronidation assays (1-10 μL) were analyzed for SAHA glucuronide by UPLC on a Waters ACQUITY UPLC™ System (Milford, MA) equipped with an automatic injector and a UV detector operated at 244 nm. UPLC was performed using a BEH 1.7 μm C18 column (2.1 mm x 100 mm, Waters) with gradient elution as follows: starting with 5.6% buffer B (100% acetonitrile) and 94.4% buffer A (10 mM ammonium acetate, pH 5.0) and 10% acetonitrile) the flow rate was maintained at 0.3 mL/min; a subsequent linear gradient to 72% buffer B over 3 min was then performed. The amount of glucuronide formed was calculated based on the ratio of the glucuronide versus SAHA. As controls, glucuronidation assays were performed using HLM as a positive control for glucuronidation activity, and untransfected HEK293 cell homogenate protein as a negative control for glucuronidation activity.

To confirm general activity of variant UGTs that did not exhibit activity against SAHA, activity assays were tested against known substrates; this work was done by Dr. Dongxiao Sun of the Lazarus lab. Glucuronidation activities of cell homogenates from UGT1A8 and UGT1A10 variant overexpressing cell lines were determined similarly to those described previously (184, 186, 243). Cell homogenate (200 μ g protein) was initially incubated with alamethicin (50 μ g/mg protein) for 15 min in an ice bath to permeabilize membranes. UGT activity was determined in a standard assay mix containing 50 mM Tris buffer (pH 7.5), 10 mM $MgCl_2$, 4 mM UDPGA and substrate (75 μ M of 4-methylumbelliferone (4-MU) for UGT1A8* and 75 μ M of 17-dihydroexemestane for UGT1A10*), and the assay mix was incubated 1 h at 37°C. Reactions were terminated by the addition of cold acetonitrile adding the same volume as the initial reaction (40 μ L). Reactions were then centrifuged at 13,000 g for 10 min at 4°C and supernatants were collected. Glucuronidation product formation was then assessed using UPLC as described below.

Glucuronidation assays (5 μ L) were analyzed for 4-MU and 17-dihydroexemestane glucuronide by UPLC on a Waters ACQUITY UPLC™ System (Milford, MA) equipped with an automatic injector and a UV detector operated at 254 nm for 17-dihydroexemestane or 316 nm for 4-MU. UPLC for 17-dihydroexemestane was performed using a BEH 1.7 μ m C18 column (2.1 mm x 50 mm, Waters) with gradient elution as follows: starting with 19% buffer B (100% acetonitrile) and 81% buffer A (5 mM ammonium acetate, pH 5.0) the flow rate was maintained at 0.3 mL/min; a subsequent linear gradient to 75% buffer B over 4 min was then performed. UPLC for 4-MU was performed using a BEH 1.7 μ m C18 column (2.1 mm x 50 mm, Waters) with

gradient elution as follows: starting with 2% buffer B (100% acetonitrile) and 98% buffer A (5 mM ammonium acetate, pH 5.0) the flow rate was maintained at 0.3 mL/min; a subsequent linear gradient to 70% buffer B over 8 min was then performed. As controls for both 17-dihydroexemestane and 4-MU, glucuronidation assays were performed using HLM as a positive control for glucuronidation activity, and untransfected HEK293 cell homogenate protein as a negative control for glucuronidation activity.

3.2.4 Kinetic analysis of variant UGTs against SAHA

Variant cell lines of the most active UGTs were initially screened using 400 µg total protein in 40 µL reactions and were incubated with 8 mM SAHA. To determine V_{\max} and K_M values for the variant UGTs, UGT activity was determined as described in section 2.2.3, using at least 6 concentrations of SAHA ranging from 65 µM to 8 mM. V_{\max} and K_M values were determined from Michaelis-Menton plots of UGT activity versus SAHA concentration. Kinetic constants were determined using Prism Version 5 software (GraphPad Software, San Diego, CA, USA). All experiments were performed in triplicate for kinetic analysis of UGT-overexpressing cell homogenates and were independent assays.

3.3 RESULTS

3.3.1 Characterization of HEK293 cell lines overexpressing UGT variants

To confirm correct amplification and insertion of cDNA into the pcDNA3.1/V5-His-TOPO/ vector, the sequence of the cloned inserts from each variant of UGT1A7 and 2B15 were compared with the sequences described in GenBank and were confirmed to be 100% homologous to each variant allele UGT1A7*2 (gi:12002128), UGT1A7*3 (gi:12002130), UGT1A7*4 (gi:12002132) and UGT2B15*2 (gi:5881245) sequence. After transfection of each expression plasmid into HEK293 cells and selection of G418 resistant cells, RNA was isolated from each cell line to ultimately confirm correct transcription of the UGT. UGT protein levels in each cell line were measured by Western Blot. Shown in Figures 3.1 and 3.2 are representative blots used for quantification of the expression of the variant UGT1A7 and UGT2B15 proteins.

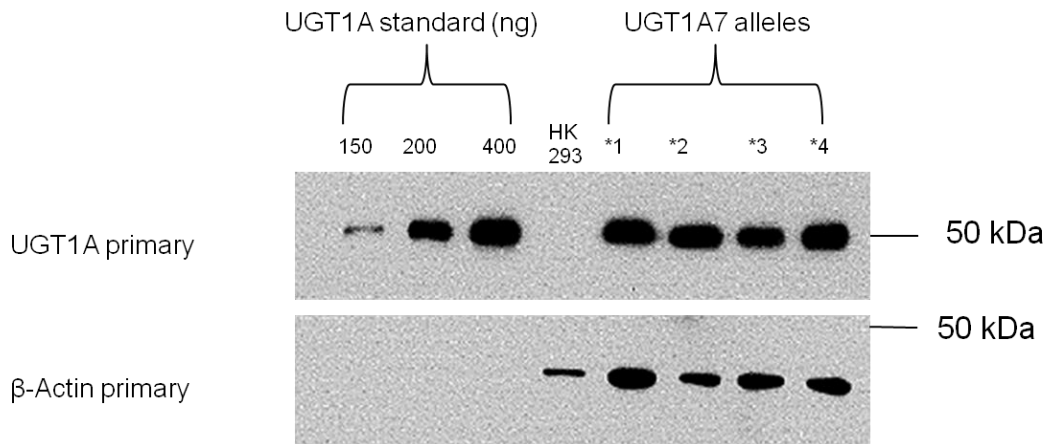


Figure 3.1: Western blot analysis of UGT1A7 star allele protein from HEK293 cell lines expressing UGT1A7*. 20 μ g of cell homogenate protein was used for each sample. The amount of UGT1A7* expression was normalized to the levels of β -Actin and was quantified by densitometry as described in materials and methods (section 3.2.1). Untransfected HEK293 cell protein was used as a negative control.

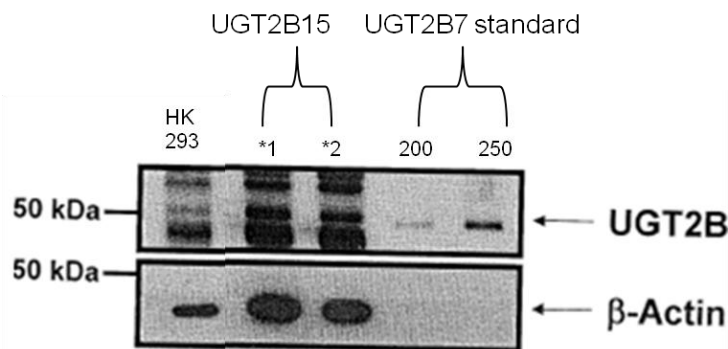


Figure 3.2: Western blot analysis of UGT2B15*2 protein from HEK293 cell lines expressing UGT2B15. UGTs2B15*1 and 2B15*2 protein levels were quantified using known amounts of UGT2B7 protein standard (from Gentest) with quantities normalized to the levels of β -actin observed in each lane as described in materials and methods (section 3.2.1). UGT2B7 Std 1, 200 ng of UGT2B7 protein; UGT2B7 Std 2, 250 ng of UGT2B7 protein. Twenty micrograms of cell homogenate protein was loaded in each lane for the determination of UGT 2B15*1 and 2B15*2 levels. The lane containing the negative control parental HEK293 homogenate (20 μ g of homogenate protein) shows no UGT2B expression. [Reference from (245)].

3.3.2 Results of screening for glucuronidation of SAHA by UGT variants

Kinetic analyses of nonsynonymous variants of UGTs, 1A7, 1A8 and 1A10, the most active UGTs against SAHA, were performed to address potential inter-individual differences in glucuronidation rates (Table 3.1). UGT1A7 has three common (>2% prevalence in Caucasians, African Americans and Asians) amino acid changing polymorphisms including: UGT1A7p.[Asn129Lys + Arg131Lys] (encoded by the UGT1A7*2 allele), UGT1A7p.[Asn129Lys + Arg131Lys + Trp208Arg] (encoded by the UGT1A7*3 allele), and UGT1A7p.Trp208Arg (encoded by the UGT1A7*4 allele) (201). There are two nonsynonymous polymorphisms of the UGT1A8 allele, UGT1A8p.Ala173Gly (encoded by UGT1A8*2) and UGT1A8p.Cys277Tyr (encoded by UGT1A8*3) and a single nonsynonymous polymorphism that produces the UGT1A10p.Glu139Lys protein [encoded by UGT1A10*2; (202, 203)]. There are no known common nonsynonymous variants for UGT2B17. An initial screen, to assess SAHA glucuronidation ability, using HEK293 cell lines overexpressing variant alleles for UGT1A7*2, UGT1A7*3, UGT1A7*4, UGT1A8*2, UGT1A8*3 and UGT1A10*2 was performed. For each activity assay, 400 µg total cell homogenate protein was tested with 8 mM SAHA (the highest concentration at which SAHA could be dissolved in DMSO).

Neither UGT1A8*3 nor UGT1A10*2 exhibited activity towards SAHA (Figure 3.6 and 3.7, respectively). However, both the UGT1A8*3 and UGT1A10*2 variants exhibited detectable levels of activity against 4-MU (Figure 3.3) or 17-dihydroexemestane (Figure 3.4), respectively, indicating that the UGT1A8 and UGT1A10 variant cell homogenates used for these glucuronidation assays contained active UGT enzymes. All other variants

exhibited some level of activity toward SAHA and were further characterized. The chromatograms for this initial screen are illustrated in Figures 3.5 - 3.7.

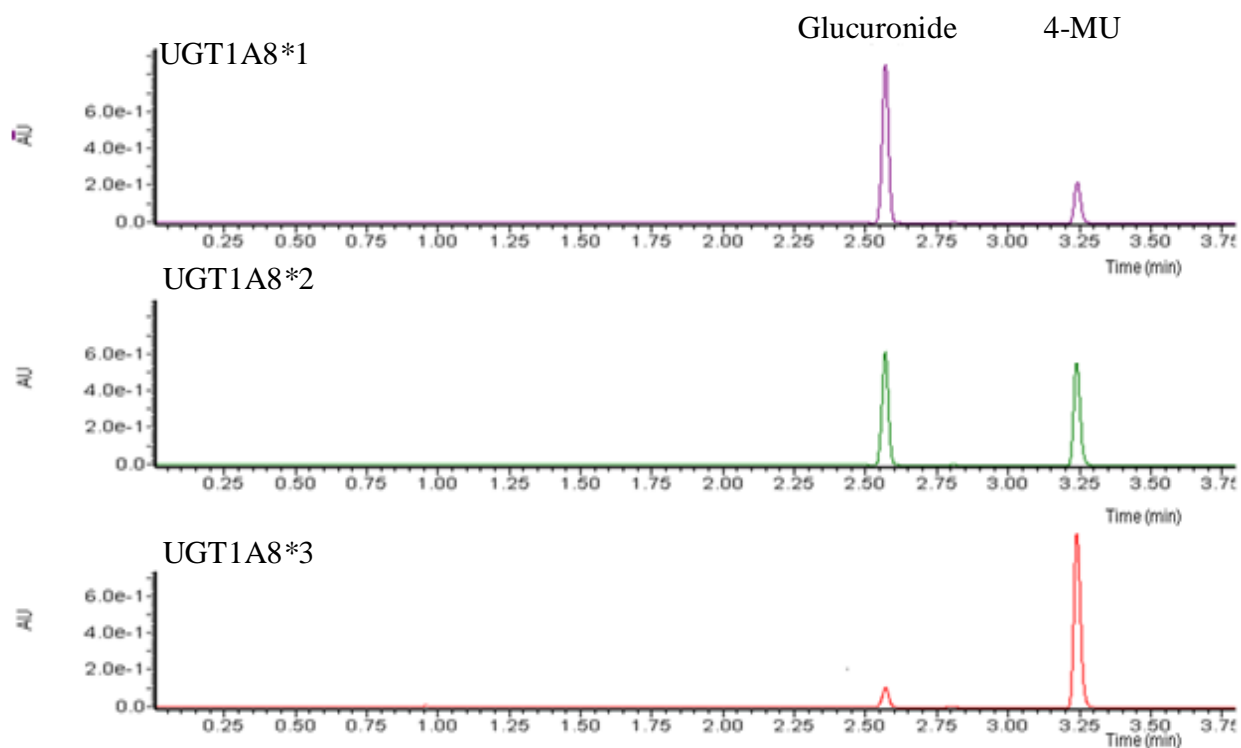


Figure 3.3: UPLC chromatographs of cell homogenate of UGT1A8 star allele-overexpressing HEK293 cells assayed for activity against 4-MU.

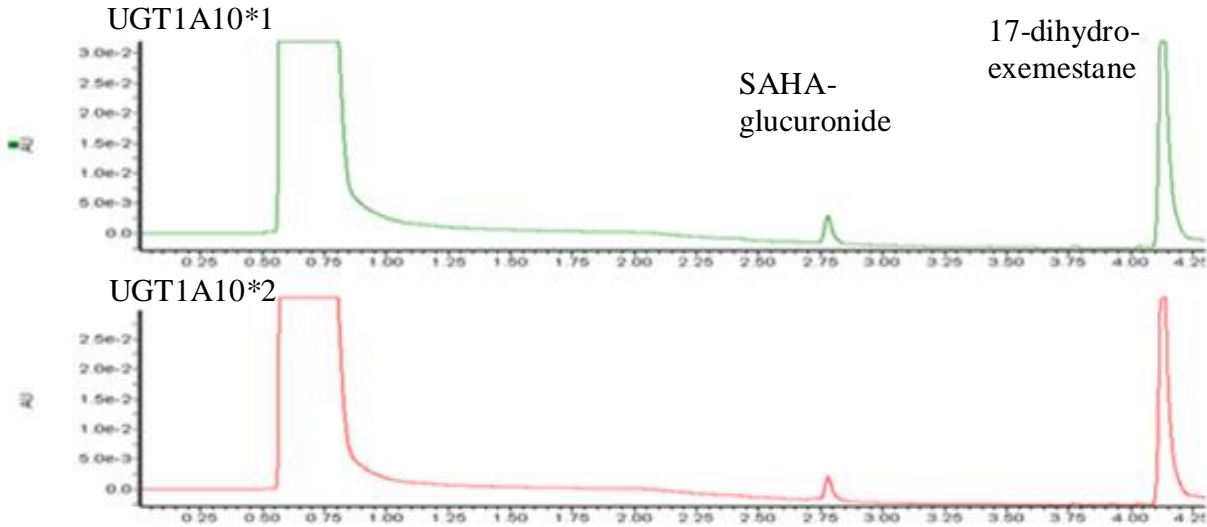


Figure 3.4: UPLC chromatographs of cell homogenate of UGT1A10 star allele-overexpressing HEK293 cells assayed for activity against 17-dihydroexemestane.

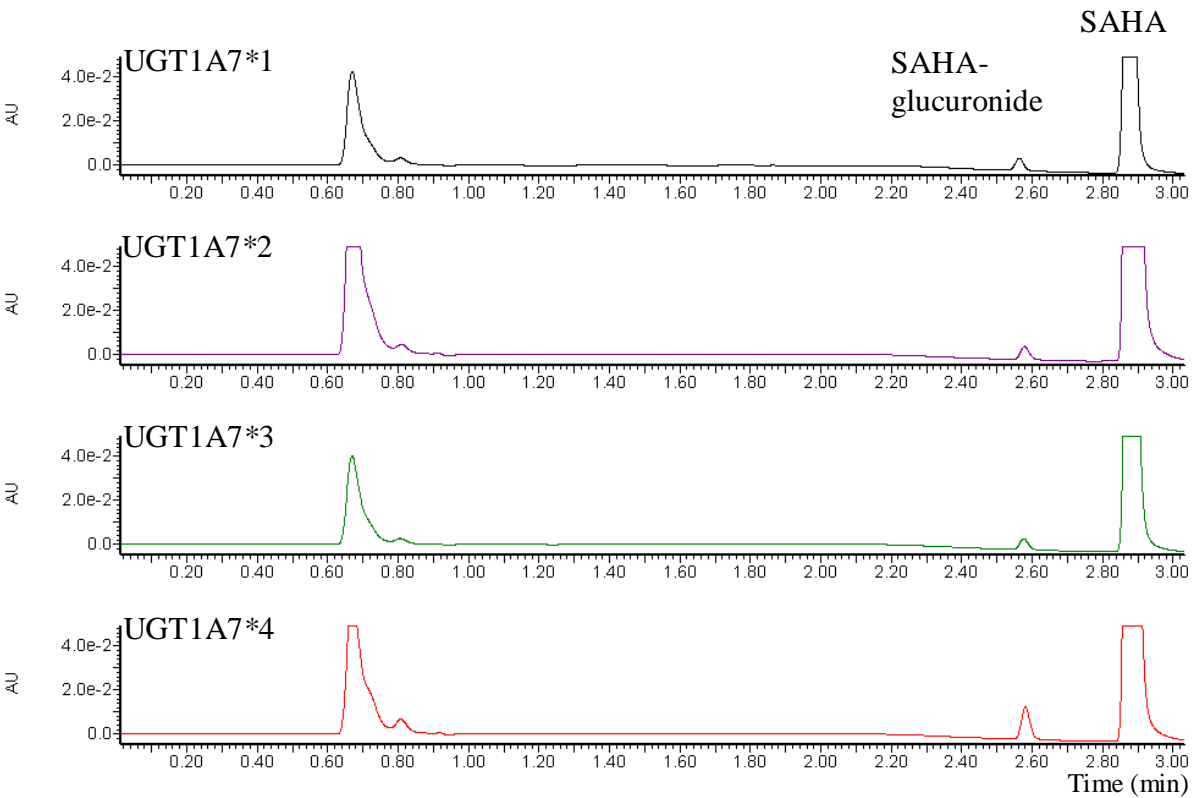


Figure 3.5: UPLC chromatographs of cell homogenate of UGT1A7 star allele-overexpressing HEK293 cells assayed for activity against SAHA.

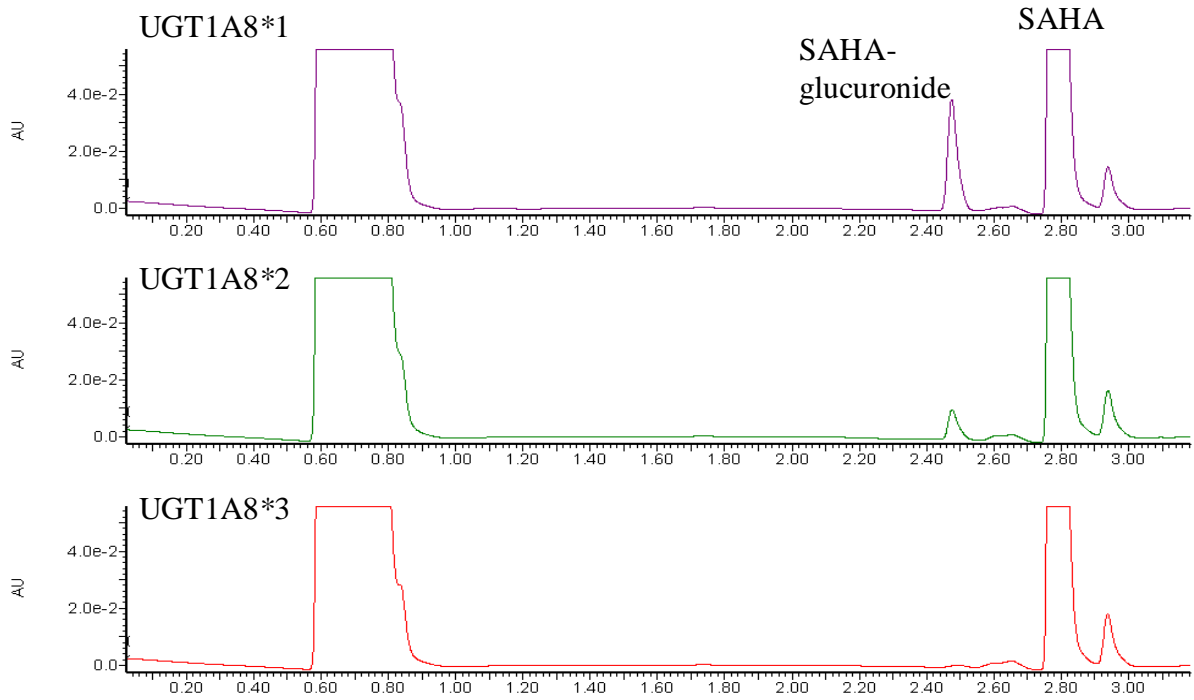


Figure 3.6: UPLC chromatographs of cell homogenate of UGT1A8 star allele-overexpressing HEK293 cells assayed for activity against SAHA.

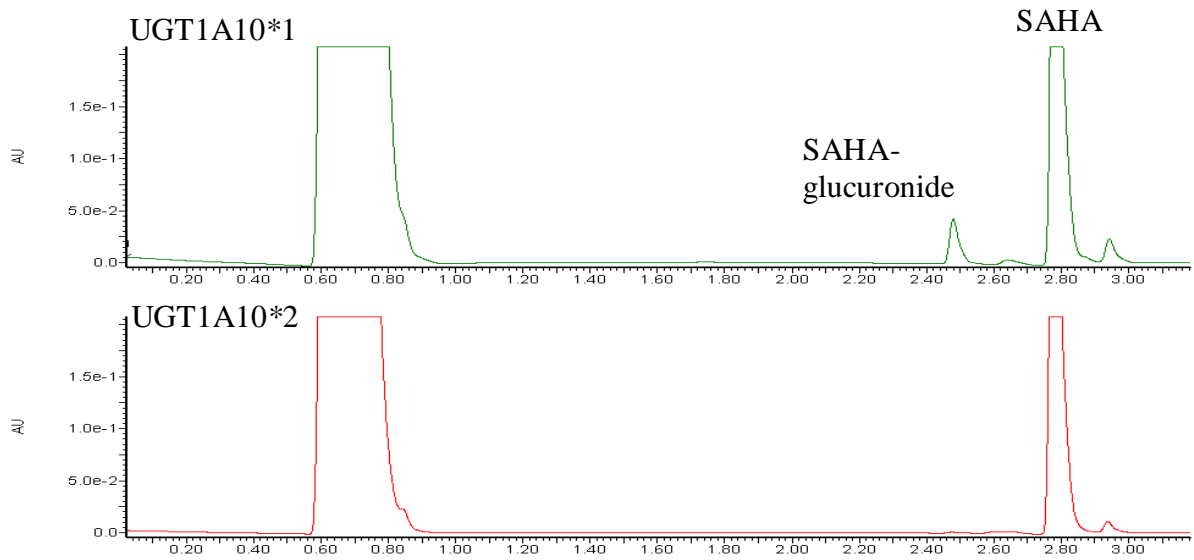


Figure 3.7: UPLC chromatographs of cell homogenate of UGT1A10 star allele-overexpressing HEK293 cells assayed for activity against SAHA.

3.3.3 Rate of SAHA glucuronidation by individual UGT family members

Kinetic parameters for the glucuronidation of SAHA by UGT variants were determined from Michaelis-Menton plots of UGT activity (as determined by UPLC as described) versus SAHA concentration. Representative plots for each UGT variant analyzed are shown in Figure 3.8. Normalization of the UGTs to one another to allow for direct comparisons of V_{max} and to K_M values was based on UGT expression in the individual UGT-overexpressing cell homogenates as determined by Western blot analysis as described previously (245). As shown in Table 3.1, the UGT1A8*2 variant exhibited a 3-fold ($P < 0.005$) decrease in glucuronidation activity as compared to UGT1A8 wild-type; no detectable glucuronidation activity was observed for the UGT1A8*3 variant using up to 8 mM SAHA. Similarly, no glucuronidation activity against SAHA was observed for the UGT1A10*2 variant. No significant difference in glucuronidation activity was observed against SAHA for any of the UGT1A7 variants.

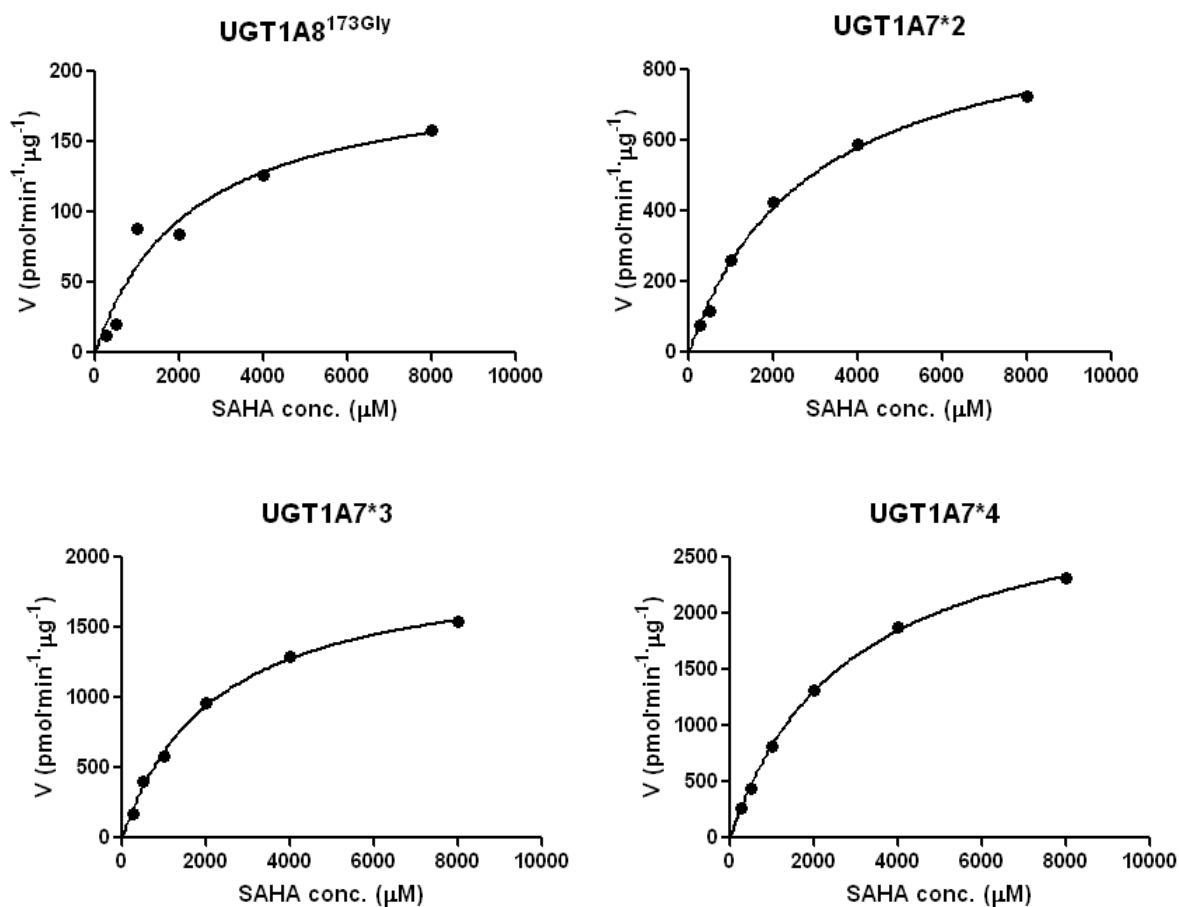


Figure 3.8: Representative concentration dependence curves for SAHA glucuronide formation in homogenates of UGT variant-overexpressing cells. UGT activity assays were carried out using 400 μg total protein. Incubation was for 1h at 37°C followed by UPLC analysis of reaction mixes. Shown are representative plots from the three replicates assays performed for each UGT as described in section 3.3.3.

UGT allele	amino acid change	K_M (mM)	V_{max} ($\mu\text{mol}\cdot\text{min}^{-1}\cdot\mu\text{g}^{-1}$) ^b	V_{max}/K_M ($\text{nL}\cdot\text{min}^{-1}\cdot\mu\text{g}^{-1}$) ^b	Allele frequency (Caucasian)
UGT1A7*1		2.7 ± 0.6	10 ± 0.4	3.9 ± 0.6	0.358
UGT1A7*2	[Asn129Lys]+[Arg131Lys]	2.5 ± 0.3	12 ± 2.5	5.0 ± 1.6	0.264
UGT1A7*3	[Asn129Lys]+[Arg131Lys]+[Trp208Arg]	2.3 ± 0.3	15 ± 4.0	6.7 ± 2.0	0.361
UGT1A7*4	Trp208Arg	2.2 ± 0.5	12 ± 4.4	5.4 ± 1.9	0.017
UGT1A8*1		1.9 ± 0.1	62 ± 7.6	33 ± 6.3	0.83
UGT1A8*2	Ala173Gly	3.0 ± 0.7	34 ± 2.6	12 ± 2.2	0.15
UGT1A8*3	Cys277Tyr		no detectable activity		0.02
UGT1A10*1		1.0 ± 0.1	24 ± 2.7	24 ± 2.4	0.99
UGT1A10*2	Gly139Lys		no detectable activity		0.01

^a All reactions were performed using 40 μg of HEK293 UGT-overexpressing cell homogenate and incubated for 1 h at 37°C. Kinetic data are reported as mean \pm standard deviation for three independent experiments.

^b V_{max} values are adjusted per μg of the corresponding UGT protein as determined by Western blot analysis.

Table 3.1: Kinetic analysis of SAHA-glucuronide formation by UGT1A variants.^a

3.4 SUMMARY

Variation in patient response to SAHA has been observed clinically (100, 120, 240). Recent studies indicate that resistance to HDAC inhibitors such as SAHA may be multifactorial (254), and that a pharmacogenetic mechanism may be responsible for the differences in overall response to SAHA treatment (119, 254). This study is the first to characterize variants of enzymes involved in the SAHA glucuronidation pathway with regard to their abilities to glucuronidate SAHA. The previous section (2.3.3) detailed the identification of UGTs 1A7, 1A8, 1A10, and 2B17, all of which have variants with prevalence greater than 2%, as the UGTs most active in glucuronidation of SAHA. The results presented here demonstrated that UGT variants significantly exhibit alterations in SAHA glucuronidation as compared to the wild-type enzymes.

UGT2B17 was identified previously as the most active hepatic UGT with SAHA as the substrate (section 2.3.3). Two separate studies identified a deletion of the UGT2B17 gene locus (UGT2B17*2), that has an allelic prevalence of 30% in Caucasians (205, 209). This variant has been linked to altered rates of glucuronidation of several compounds (187) and increased risk for cancer (210, 211); however, this has been debated (255-257). This prevalent variant of the most active hepatic UGT could not be assessed under our current *in vitro* system; however, studies using human tissue or clinical data could assess whether this whole-gene deletion affects SAHA metabolism.

The extra-hepatic UGT1A8 and UGT1A10 were overall the most active against SAHA. Previous studies have identified two nonsynonymous genetic variants of

UGT1A8, UGT1A8*2 (encoding UGT1A8p.Ala173Gly) and UGT1A8*3 (encoding UGT1A8p.Cys277Tyr), which have been linked to altered glucuronidation activity (202). The UGT1A8p.Ala173Gly variant exhibited a 3-fold significant lower overall *in vitro* glucuronidating activity against SAHA as determined by V_{max}/K_m compared with wild-type UGT1A8. This effect on SAHA glucuronidation is consistent with the fact that the Ala>Gly amino acid substitution at UGT1A8 codon 173 is a conservative nonpolar amino acid change and with data from previous *in vitro* metabolic studies that support UGT1A8p.Ala173Gly has activity against substrate (202, 212). The UGT1A8p.Cys277Tyr variant was shown to be inactive against SAHA in *in vitro* experiments using homogenates from cell lines overexpressing this variant. However, the homogenate for this variant did exhibit minimal activity against other substrates which supports that the homogenate is functional. The Cys277Tyr may play an important role in enzyme activity because almost all UGT1As have a cysteine located in this region (un-published data by Dr. Ryan Dellinger). This cysteine at amino acid 277 could possibly be involved in a disulfide bridge formation to another cysteine. The formation of a dimeric cystine amino acid could also be critical for secondary structure or catalysis (258). Unpublished studies by the Lazarus lab have shown that UGT1A9^{183Gly} variant exhibited no dimerization compared to wild-type UGT1A9, suggesting that the wild-type cysteine at codon 183 is central to UGT1A9 homodimerization. A similar scenario can be occurring with the UGT1A8p.Cys277Tyr variant. While the prevalence of UGT1A8*3 is relatively low in the population [$<3\%$ in Caucasians; (202, 203)], its presence could potentially have high penetrance in terms of metabolism of SAHA in tissues that are targets of the drug and where UGT1A8 is highly

expressed. The 3-fold reduction in glucuronidation of SAHA caused by the UGT1A8*2 allele, which is more common with ~28% prevalence in Caucasians (202), could impact larger segments of the population.

UGT1A10, the second most active UGT for SAHA glucuronidation, has a genetic variant that results in an amino acid change at position 139 (Glu>Lys) [encoded by the UGT1A10*2; 4% prevalence in blacks (203)]. The UGT1A10*2 variant has been linked to decreased glucuronidation activity and increased cancer risk (185, 203). The UGT1A10p.Gly139Lys variant, while active against other substrates, was shown to be inactive against SAHA *in vitro*. This result suggests that the nonconservative amino change of Glu to Lys at codon 139 renders UGT1A10 less active. Similarly to UGT1A8*3, the prevalence of UGT1A10*2 allele is relatively low in the population [<3% in Caucasians; (202, 203)]; its presence could potentially have high penetrance in terms of metabolism of SAHA in tissues that are targets of the drug and where UGT1A8 is highly expressed.

UGT1A7, the third most active UGT for SAHA glucuronidation, has 3 genetic variants, UGT1A7*2 (encoding UGT1A7p.[Asn129Lys + Arg131Lys]), UGT1A7*3 (encoding UGT1A7p.[Asn129Lys + Arg131Lys + Trp208Arg]), and UGT1A7*4 (encoding UGT1A7p.Trp208Arg); of which UGT1A7*2 and UGT1A7*3 have been linked to altered activity *in vitro* (201). However, these variants did not exhibit altered glucuronidation activity with SAHA substrate. These UGT1A7 variants have both conserved and nonconserved changes and have been shown to have altered activity for other substrate which suggest that these regions are important but not for SAHA activity.

One limitation to this study is that only the most active wild-type UGT's variants were tested for reduced activity. It could be possible, that the allele's we originally tested were not the most active form of the UGT. To address this possibility, we could screen all known UGT alleles using our *in vitro* system. Another possibility is to first observe how the current data accounts for SAHA-glucuronide formation correlated to UGT genotype in patients. If altered SAHA-glucuronide formation is observed and the originally identified variants do not account for this difference, this would support screening the other UGT alleles that were not originally assessed.

These data from our *in vitro* system suggest that there will be variations in glucuronidation of SAHA in individuals carrying variant alleles of the most active SAHA glucuronidating UGTs. Although this study has provided essential information, there are limits to *in vitro* analysis and further studies will be required to better understand the role of UGTs as they pertain to SAHA glucuronidation. One question that needs to be addressed is how the UGTs co-expressed in tissues affect SAHA glucuronidation to better assess whether some of these UGTs will be able to compensate for the reduced SAHA glucuronidation of variant UGTs. Another issue is whether UGTs in extra-hepatic tissues, where SAHA is being targeted, are able to glucuronidate the drug. These analyses could be addressed using primary cells or tissues to perform glucuronidation assays. Ultimately, studies using data from patients treated with SAHA will provide the best analysis. However, the studies presented in this section provide the necessary foundation to continue the study of SAHA glucuronidation and its relationship to patient response to the drug in the clinic.

Chapter 4: Characterization of SAHA glucuronidation by UGT in human tissue samples

4.1 INTRODUCTION

The liver is the major site of drug metabolism (259, 260) and contains many phase I, phase II, and phase III enzymes which aid in the metabolism of xenobiotics (261, 262). As the liver is an important location of drug metabolism, understanding how drugs interact with the enzymes of this organ would aid in predicting how the drugs would be metabolized in humans. Traditionally, animal models were used to assess drug metabolism; however, animals do not possess all enzymes found in humans and therefore those models have limitations (147, 263). An optimal system for studying metabolism would include human enzymes. One method to examine drug metabolism is to use recombinant human enzymes, with the advantage of being able to examine individual enzymes. However, to simulate *in vivo* conditions more accurately, all enzymes that are present in human systems should be examined. Primary human hepatocytes provide a good *in vitro* model of liver metabolism; however, primary hepatocytes are difficult to obtain, tricky to prepare and store, can only be used for a short duration, and results are hard to reproduce (264, 265). An alternative to primary human hepatocytes is microsomes prepared from human tissue. This method can be used to examine *in vitro* drug metabolism without sacrificing enzymes found in humans, and it is a method for which specimens are easier to obtain and results are reproducible. Microsomes, which are derived from membrane bound vesicles in the cell,

like the endoplasmic reticulum, are prepared from human tissue by differential centrifugation (266, 267). Since many phase I and II enzymes are located in the membrane of the endoplasmic reticulum, they are also present in a functional state in the microsomes. Once microsomes are prepared, they are easily stored in aliquots at -80°C for many future analyses.

The studies detailed in chapters 2 and 3 have identified the affects of UGTs and their variants on SAHA metabolism; however, these experiments were conducted using recombinant UGT enzymes in cell lines which do not endogenously express UGTs. These findings showed that the hepatic UGTs 2B17 and to a lesser extent, 1A9 and 1A3 (5- and 11-fold lower, respectively), individually, were able to actively glucuronidate SAHA. However, in addition, it is important to assess SAHA glucuronidation under conditions where multiple UGTs are present and which are more relative to *in vivo* conditions. For this reason, specimens from humans were used to assess glucuronidation of SAHA activity. Human liver tissue, specifically HLM, is ideal to use to further extend the studies of SAHA glucuronidation by UGTs because it is a system that contains all of the UGTs present for *in vivo* hepatic clearance. Along with the hepatic UGTs, UGTs 1A8 and 1A10 were identified as the two UGTs to most actively glucuronidate SAHA, but these enzymes are expressed exclusively extra-hepatically. Since SAHA is being used as a chemotherapeutic agent targeting cancers of the lung, breast, colon, small intestine, and tissues of the aerodigestive tract (136, 161, 185, 248), these extra-hepatic enzymes could potentially be most important in metabolism of the drugs in target tissue where these enzymes are expressed. To test SAHA glucuronidation in such a target tissue, colon tissue was chosen as a representative

because it has high expression of the extra-hepatic UGTs 1A8 and 1A10 (136, 183).

Together, these studies aim to enhance the understanding of the role UGTs play in

SAHA metabolism.

4.2 MATERIALS AND METHODS

4.2.1 Human Tissue

The normal human liver tissue specimens used for these studies have been described previously (186). Briefly, normal human liver tissue specimens were provided by the Tissue Procurement Facility at the H. Lee Moffitt Cancer Center from individuals (n=100) undergoing surgery for resection of hepatocellular carcinoma. All individuals were Caucasian with 60 males and 40 females included. Tissue samples were quick-frozen at -80°C within 2 h after surgery. Colon tissue was obtained from the Penn State College of Medicine Tissue Bank and homogenate was prepared as previously described for cell line homogenates.

4.2.2 Preparation of Human Liver Microsomes

Human liver microsomes were prepared through differential centrifugation as previously described (267). Due to limited individual tissue specimens, all microsomes were prepared by Andrea Primeau of the Lazarus lab. Tissue (0.5 mg) was suspended in 1.5 mL homogenizing buffer (50 M Tris, pH 7.5, 1.15% KCl, 1 mM disodium EDTA) and homogenized on ice using an electric homogenizer. As illustrated in Figure 4.1, microsomes were prepared from homogenates by centrifugation at 10,000 g for 15 min at 4°C followed by ultracentrifugation of the supernatant at 100,000 g for 1 h at 4°C to pellet the microsomal fraction. The pellet was then resuspended in Tris-buffered saline and stored in aliquots of 10-20 mg microsomal protein/mL at -80 °C. Microsomal protein concentrations were measured using the bicinchoninic acid protein assay.

4.2.3 Isolation of DNA and RNA from tissue used to prepare HLM

During the differential centrifugation process to prepare HLMs, fractions were saved for isolation of RNA and DNA. Total RNA for all samples (n=100) was extracted by Andrea Primeau using the RNeasy Mini kit from Qiagen as per manufacturer's protocols. DNA extractions for all samples (n=100) were carried out by Dr. Gang Chen using phenol/chloroform extraction. Briefly, the "low speed pellet" containing the nuclear fraction (see Figure 4.1) was suspended in 1.2 mL digestion buffer (100 mM NaCl₂, 10 mM Tris-Cl, pH 8, 25 mM EDTA, pH8, 0.5% sodium dodecyl sulfate, and 0.1 mg/mL proteinase K)/100 mg tissue and incubated with shaking at 50°C for 18 h. Samples were then extracted with an equal volume of phenol/chloroform/isoamyl alcohol mixture (25/24/1) and centrifuged for 10 min at 1,700 g in a swinging bucket rotor. Supernatant was collected and ½ volume of 7.5 M ammonium acetate and 2x original volume of 100% ethanol were added and then centrifuged for 2 min at 1,700 g. Supernatant was removed and rinsed with 70% ethanol and after complete removal of ethanol, DNA was resuspended in water and stored in -20°C.

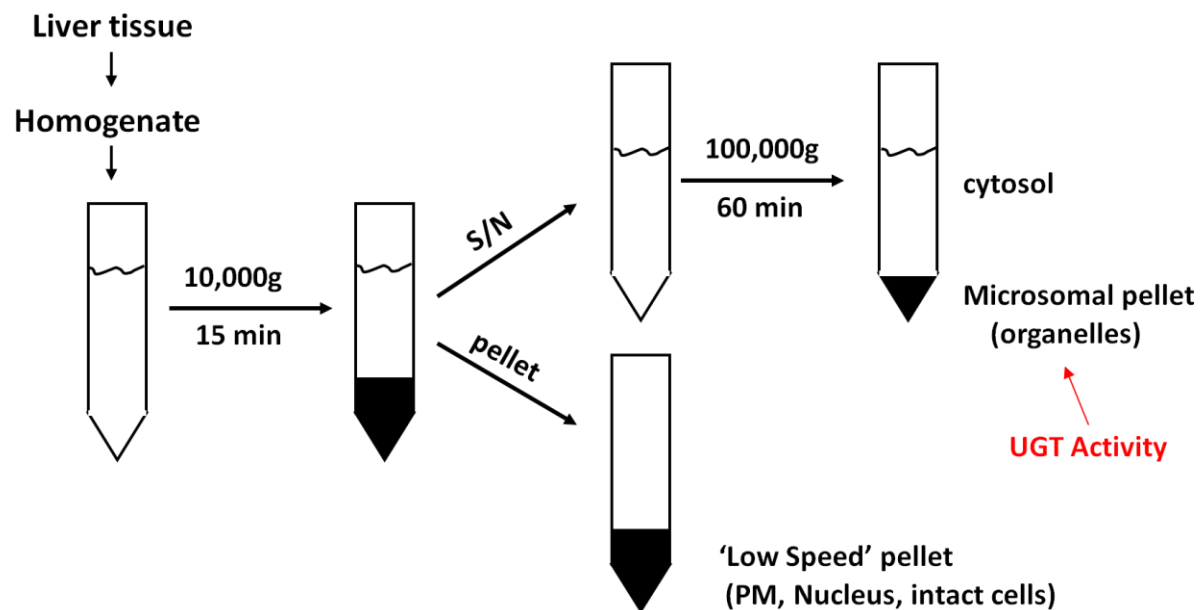


Figure 4.1: Diagram of microsome preparation. Liver tissue (0.5 mg) was suspended in 1.5 mL homogenizing buffer and homogenized using an electric homogenizer followed by centrifugation at 10,000 g for 15 min at 4°C then ultracentrifugation of the supernatant at 100,000 g for 1 h at 4°C with the pellet containing the microsomal fraction.

4.2.4 Reverse transcription of RNA

Total RNA (5 µg) isolated from each of the normal liver tissue samples examined in this analysis was reverse-transcribed in a final volume of 20 µL containing 1× RT-PCR buffer, 0.5 mM of each deoxynucleotide triphosphate, 40 units of recombinant RNase inhibitor, 200 units of SuperScript II reverse transcriptase, and 1 µL of oligo (dT)₁₂₋₁₈ (500 µg/mL). Samples were incubated at 42°C for 60 min and reverse transcriptase was inactivated by heating at 65°C for 5 min followed by cooling to 4°C.

4.2.5 Genotyping Assay for UGT2B17

A whole-gene deletion of UGT2B17 is prevalent in populations. Two previously published data from our lab determined the UGT2B17 genotype of the individuals from whom each liver tissue sample was excised (187, 256). For the initial genotyping of UGT2B17 in the Lazarus lab, a PCR method was used as described previously (187). However, a high-throughput method was necessary to screen larger numbers of samples; therefore, a multiplex real-time PCR assay was developed as previously described (256). In addition to these two previously describe methods, the present study required a novel method to test for copy number variation (CNV) in UGT2B17. The following sections will highlight the multiplex real-time PCR assay (256) and the novel method to test for CNV for UGT2B17. By highlighting and discussing results of the previously published multiplex real-time PCR assay for UGT2B17 it will allow for direct comparison and validation of the newly developed UGT2B17 CNV assay.

4.2.5.1 Multiplex Real-Time PCR assay to determine UGT2B17 genotype

The method for HLM genotyping for UGT2B17 has been described previously (256). Briefly, a multiplex real-time PCR using primers and probes specific for either the UGT2B17 intact allele or the UGT2B17-null allele were designed. Figure 4.2 illustrates where the primers and probes for this assay bind to genomic DNA. Reactions (20 μ L) were performed in 384-well plates using the ABI 7900 HT Sequence Detection System, with incubations performed at 50°C for 2 min; 95°C for 15 min; and 40 cycles of 94°C for 1 min, 60°C for 1 min 30 s. Reactions included QuantiTect Multiplex PCR Mater Mix (1 X final concentration; Qiagen), 0.4 μ M each primer, 0.2 μ M for each probe and 20-100 ng of DNA. Genotypes were assigned by the automatic calling feature of the allelic discrimination option in SDS 2.2.2 software (Applied Biosystems).

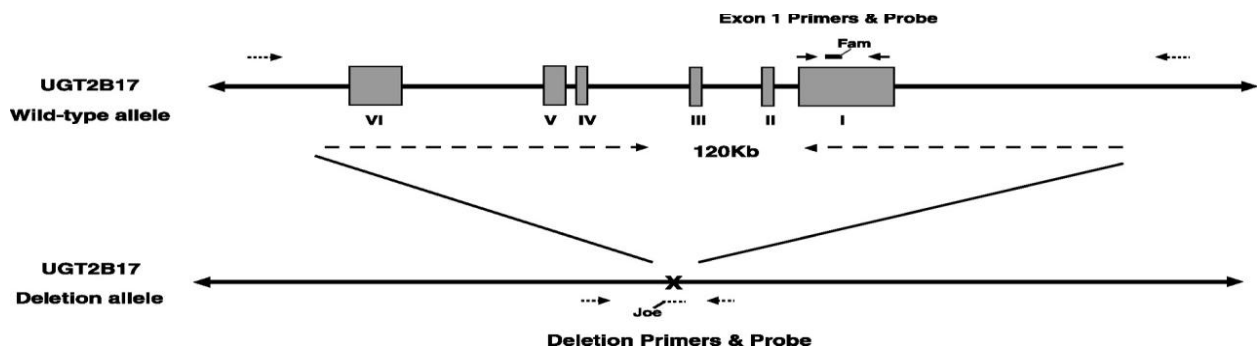


Figure 4.2: Gene structure and primer and probe locations for the UGT2B17 multiplex real-time PCR assay. I to VI, exons of the *UGT2B17* gene on the wild-type allele. The deletion allele is shown below the wild-type allele, indicating that the 120 kb are deleted including the entire *UGT2B17* gene. Dashed arrows, primers that will amplify the deletion allele; dashed line (with fluorescent label Joe), deletion probe. Solid arrows, primers that will amplify exon 1 of *UGT2B17* from the wild-type allele; solid line (with fluorescent label Fam), deletion probe. [Reference from (256)].

4.2.5.2 Copy Number Variation

When initial assays to screen for UGT2B17 genotype were developed in our lab, information on possible CNV in the UGT2B17 region was not known. However, during the course of this thesis, new data in the field suggested that the region in which UGT2B17 is located could contain CNV (268). To determine the copy number of UGT2B17 in genomic DNA from liver specimens, a real-time PCR assay was developed. UGT2B17 specific primers and probe were designed for use with genomic DNA; the sense and antisense primers used for amplification of UGT2B17 were UGT2B17S (sense, 5'- GGAGTATCTTTATGGCATTCTCTGTATG -3') and UGT2B17AS (antisense, 5'- CTGCAGGTTATCATCCAGGAGAG -3'), and a 6-Fam-labeled probe (sense, 5'-TTGAATGTCAGCCTGCCT:mgbnfq-3'), all located within the intron between exons 5 and 6 of UGT2B17. This primer/probe set was multiplexed with the internal control gene TaqMan RNaseP(VIC) (ABI), which has been shown to have two alleles (269). Reactions (10 μ L) were done in 384-well plates using the ABI 7900 HT Sequence Detection System, with incubations done at 50°C for 2 min, 95°C for 10 min; and 40 cycles of 95° C for 15 s, 60°C for 1min. Reactions included TaqMan Universal PCR master mix (1x final concentration; ABI), 0.2 μ M of UGT2B17 primer/probe, 1x RNaseP primer/probe assay, and 20 ng of DNA. Negative controls were run and threshold cycle number (CT) values were determined by SDS 2.2.2 software (ABI). Copy number was determined by $\Delta CT = CT_{UGT2B17} - CT_{RNaseP}$.

4.2.6 Gender Identification Assay

To verify the gender of our samples, a high-throughput multiplex real-time PCR assay with allelic discrimination was used. A primer/probe set specific for males, sex-determining region Y gene (SRY) (ABI, Hs00243216_s1) was multiplexed with TaqMan RNase P(VIC) control gene. Reactions (10 μ L) were done in 384-well plates using the ABI 7900 HT Sequence Detection System, with incubations done at 50°C for 2 min, 95°C for 10 min; and 40 cycles of 95° C for 15 s, 60°C for 1min. Reactions included TaqMan Universal PCR master mix (1x final concentration; ABI), 1x for each primer/probe assay, and 50 ng of DNA. Negative controls were run and detection of SRY was determined by SDS 2.2.2 software (ABI).

4.2.7 Glucuronidation Assays for SAHA in HLM and Colon homogenates

Colon homogenates (n=2) were screened for glucuronidation of SAHA using 2000 μ M SAHA. HLMs (n=100) were screened for ability to glucuronidate SAHA using 200 μ M SAHA, a concentration similar to the K_M for SAHA of the most active hepatic UGT, UGT2B17. Kinetic analysis of HLMs (n=26) used a range of SAHA concentrations between 65 and 8000 μ M. HLM (20 μ g of total protein) or colon homogenate (200 μ g of total protein) was initially incubated with alamethicin (50 μ g/mg protein) for 15 min on ice to permeabilize membranes. Incubations (20 μ L) were subsequently performed for 1 h at 37°C in 50 mM Tris buffer (pH 7.5), 10 mM $MgCl_2$, 4 mM UDPGA and 200 μ M substrate. Reactions were terminated by the addition of cold acetonitrile adding the

same volume as the initial reaction (20 μ L). Reactions were then centrifuged at 13,000 g for 10 min at 4°C and supernatants were collected and analyzed by UPLC.

Glucuronidation assays (2 μ L) were analyzed for SAHA glucuronide by UPLC on a Waters ACQUITY UPLC System (Milford, MA) equipped with an automatic injector and a UV detector operated at 244 nm. UPLC was performed using a BEH 1.7 μ m C18 column (2.1 mm x 100 mm, Waters) with gradient elution as follows: starting with 5.6% buffer B (100% acetonitrile) and 94.4% buffer A (10 mM ammonium acetate, pH 5.0 and 10% acetonitrile) the flow rate was maintained at 0.3 mL/min; a subsequent linear gradient to 72% buffer B over 3 min was then performed. The amount of glucuronide formed was calculated based on the ratio of the area under the curve for the peak representing the SAHA glucuronide to that representing unmetabolized SAHA. As controls, glucuronidation assays were performed using HLM as a positive control for glucuronidation activity, and untransfected HEK293 cell homogenate protein as a negative control for glucuronidation activity.

4.2.8 Expression Assay for UGT2B17

To analyze UGT2B17 expression levels in liver specimens, real-time PCR was performed using the TaqMan Gene Expression Assay kit from Applied Biosystems (Foster City, CA). UGT2B17 expression in liver specimens was measured in two independent experiments each using a different housekeeping gene control for normalization of the results. For the first set of expression assays, TaqMan assay ID: Hs00854486_sH was used for UGT2B17 and ID Hs99999905_m1 for glyceraldehyde 3-phosphate dehydrogenase (GAPDH), the housekeeping gene control. For the second

set of experiments, Dr. Gallagher used TaqMan assay ID: Hs00854486_sH for UGT2B17 and Hs99999904_m1 for peptidylprolyl isomerase A (cyclophilin A; PPIA) as the housekeeping gene control. In addition, the TaqMan Human endogenous control plate (ABI) was used to identify the ideal internal control gene in HLM samples (n=6) as per manufacturer's protocol (this plate was run by Dr. Carla Gallagher).

Real-time PCR assays were performed in a volume of 10 μ L containing equal amounts of cDNA (20 ng) from each liver specimen. GAPDH or PPIA was used for normalization of gene expression. PCR assays were carried out in 384-well thin-well PCR plates covered with optically clear sealing film (Applied Biosystems). Amplification, detection, and data analyses were performed using the ABI 7900HT sequence detection system and SDS 2.2.2 software using standard settings provided by ABI (Applied Biosystems). Results were expressed using the comparative threshold method following the recommendations of the manufacturer (Applied Biosystems). The CT value for UGT2B17 was normalized against either GAPDH or PPIA and calculated as $\Delta CT = CT_{UGT2B17} - CT_{GAPDH \text{ or } PPIA}$. Relative UGT2B17 mRNA expression was expressed as $UGT2B17 \text{ mRNA} = 2^{(-\Delta CT)}$.

4.3 RESULTS

4.3.1 Analysis of UGT2B17 Genotype

In the present study, two methods were developed to genotype genomic DNA that was purified from the same liver specimens used for HLM SAHA glucuronidation assays for the UGT2B17 deletion polymorphism. Both methods required real-time PCR and yielded the same results for UGT2B17 genotype (256). The first method was designed to specifically detect the presence of intact UGT2B17 or deletion of the whole UGT2B17 gene. Examples of amplification plots from this method show that when only wild-type alleles (*1/*1) are present, the fluorescent label Fam is detected, when only deletion containing alleles (*2/*2) are present, the fluorescent labeled Joe is detected, and when both alleles (*1/*2) are present the fluorescent labels Fam and Joe are both detected (Figure 4.3). An example of the automatic allelic discrimination used to determine UGT2B17 genotype in the 100 HLMs is illustrated in Figure 4.4. These results show the clear clustering of the UGT2B17*1/*1 (n = 58), UGT2B17*1/*2 (n = 29), and UGT2B17*2/*2 (n = 13) alleles.

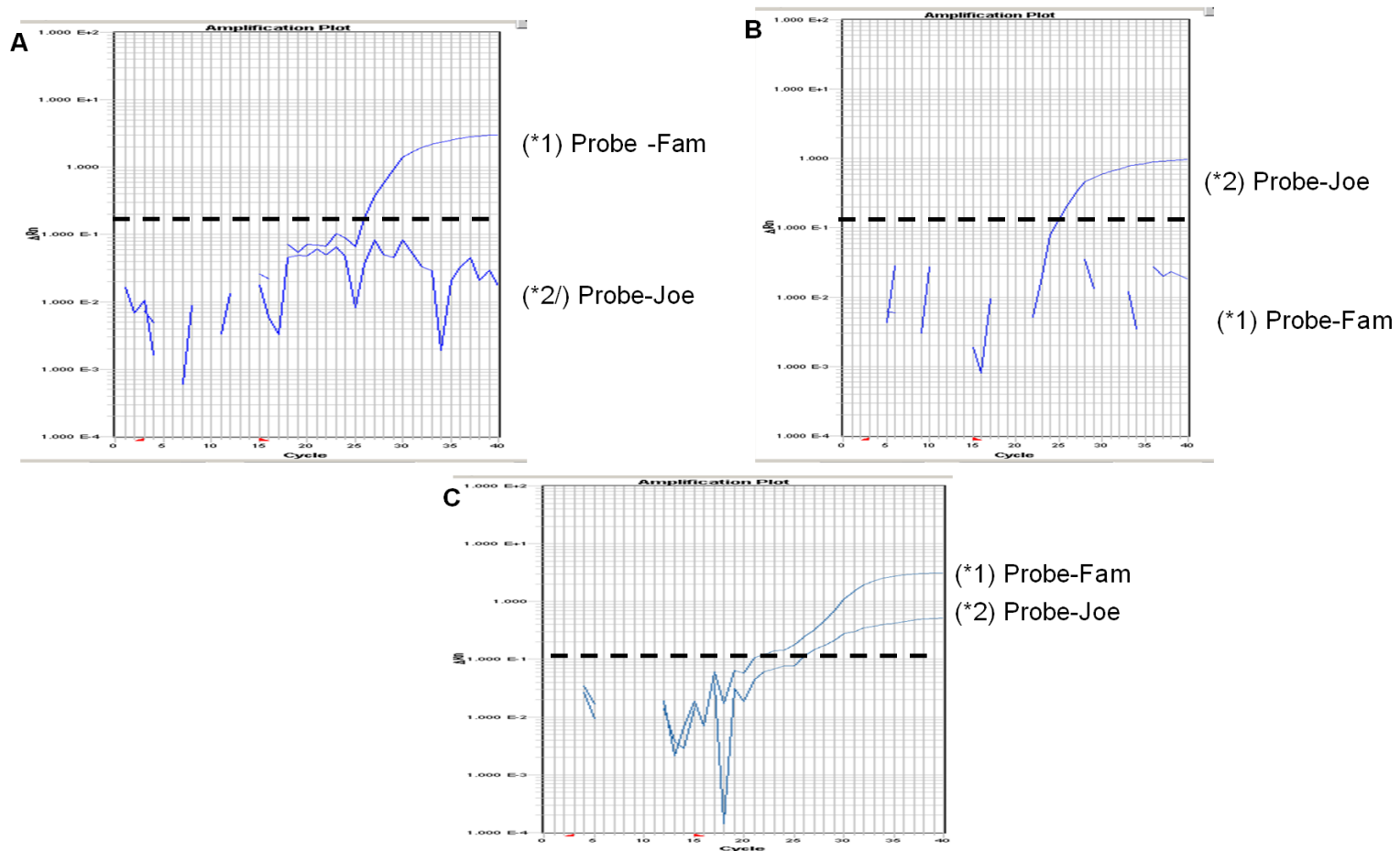


Figure 4.3: UGT2B17 multiplex real-time PCR amplification plots. (A) Amplification plot for UGT2B17 homozygous wild-type sample (*1/*1) with fluorescent label Fam detected, (B) Amplification plot for UGT2B17 homozygous deletion sample (*2/*2) with fluorescent label Joe detected, (C) Amplification plot for UGT2B17 heterozygous sample (*1/*2) with both fluorescent labels detected. Dashed line on amplification plot represents point at which amplification (curve) is above background noise indicating that the allele is present.

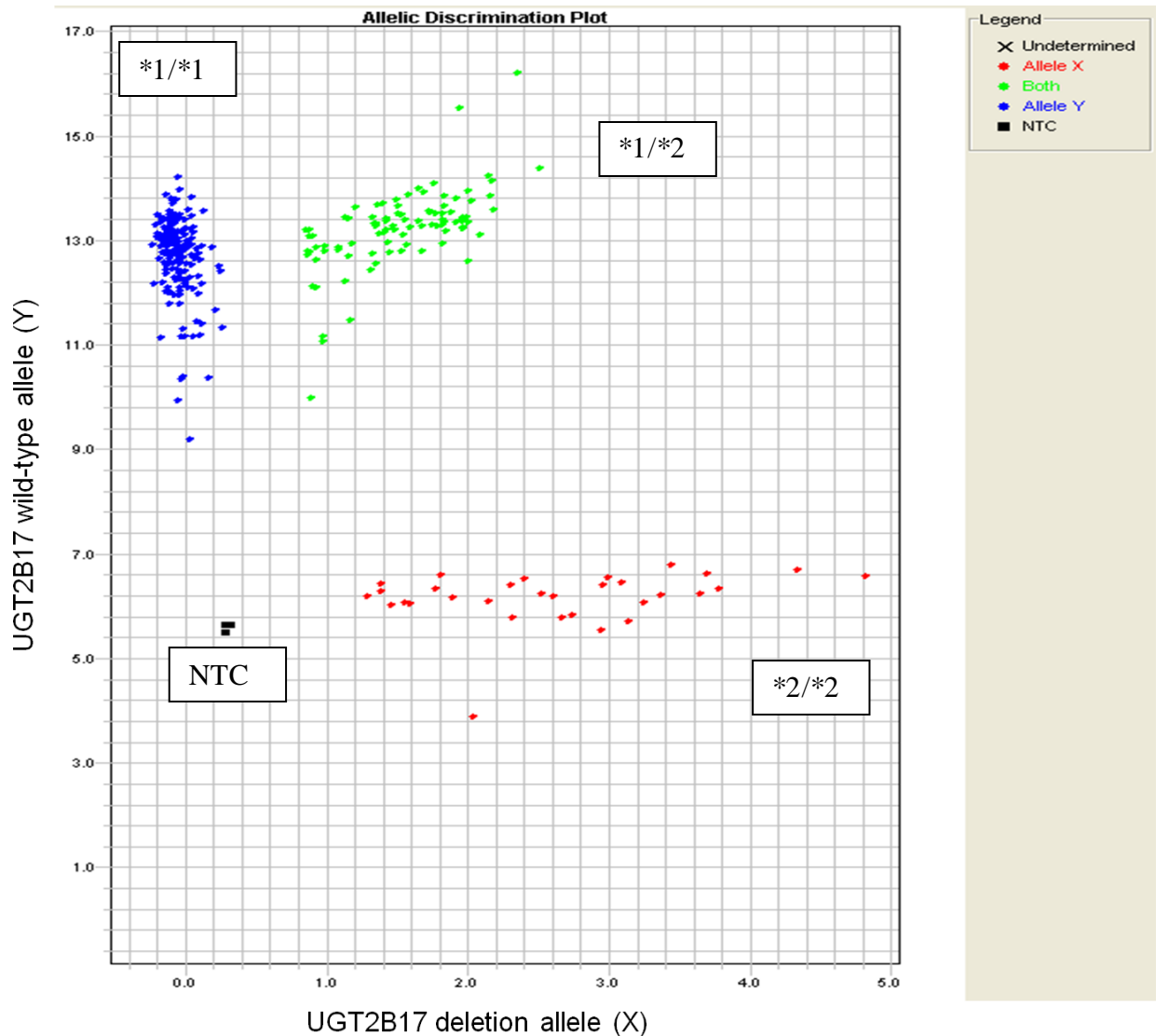


Figure 4.4: UGT2B17 multiplex real-time allelic discrimination plot. The plot of the automatic calling feature of the allelic discrimination program was used for genotyping. The y-axis represents the UGT2B17 (*1) the x-axis represents the UGT2B17 (*2) and the middle grouping is the UGT2B17 (*1/*2); non-template controls (NTC) were water.

During the course of genotyping samples for the UGT2B17 deletion, it was determined that copy number variation occurred in the UGT2B17 region but the specific number of alleles present were not determined (268, 270). The real-time PCR method previously described could only detect if the wild-type UGT2B17 allele or the UGT2B17-null allele was present, but it could not determine the number of wild-type alleles. With

this limitation, a second method was designed to detect only the presence of the intact UGT2B17 allele and compare the copy number to a known two-allele standard, RNaseP. This method was specifically designed to determine how many intact UGT2B17 alleles are present in each specimen using the genomic DNA. Similar methods have been used to identify the number of alleles of CYP2D6, which was found to vary from 0 to 3 alleles (269). Data from the present study indicates that the UGT2B17 copy number varied from 0 to 2 alleles in samples that were screened (n=100). Figure 4.5 shows a representative amplification plot for each copy number of UGT2B17 observed in tested samples. These results were consistent with the genotype determined previously for these samples. In addition, the presence of 0, 1, or 2 UGT2B17 allele(s) in the population was confirmed by others (271).

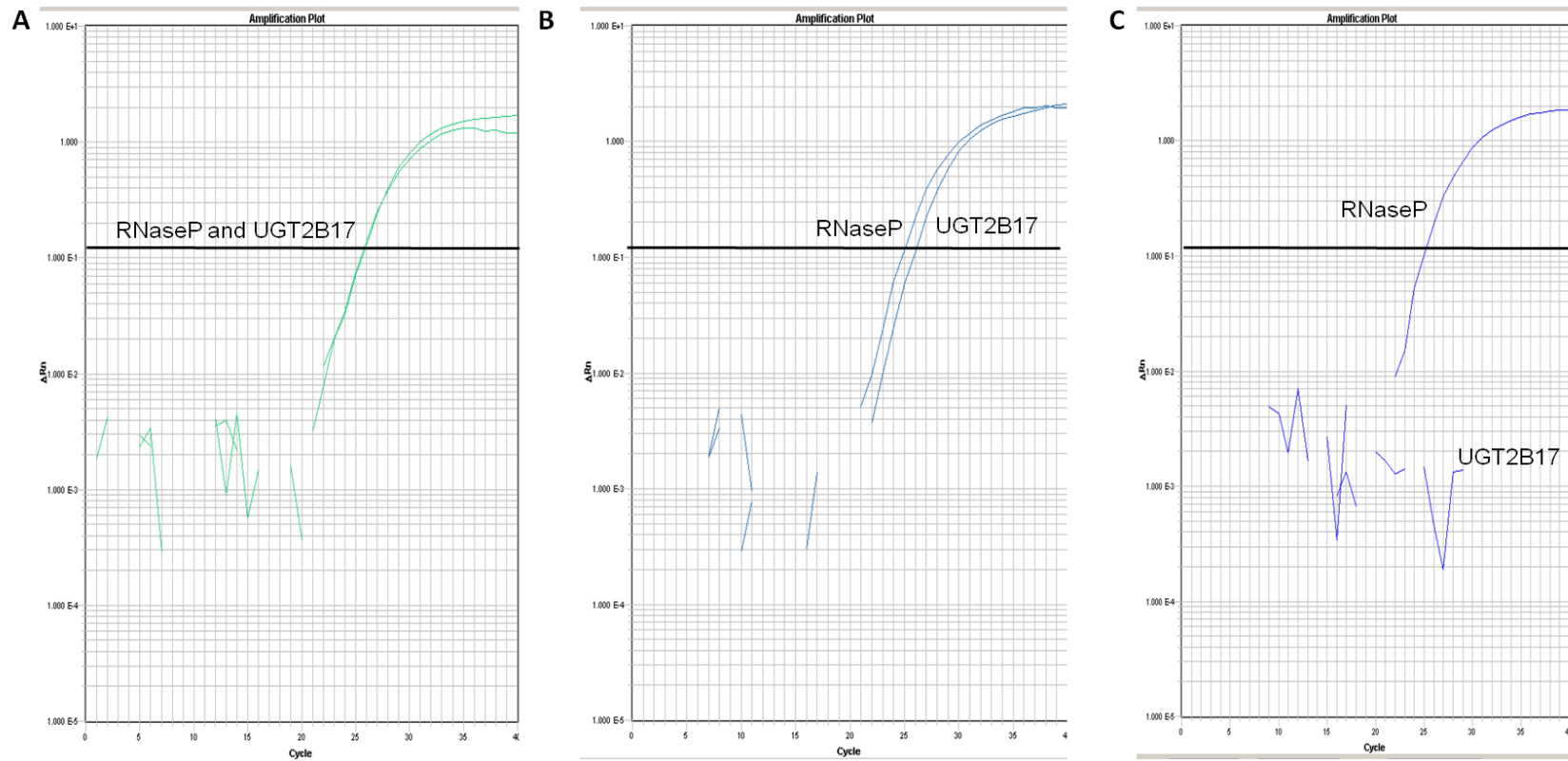


Figure 4.5: UGT2B17 copy number variation amplification plots. Real-time PCR amplification plots for UGT2B17 *1 allele with RNaseP as internal control gene. (A) Plot of UGT2B17 two allele sample, (B) Plot of UGT2B17 one allele sample, (C) Plot of UGT2B17 null sample.

4.3.2 UGT2B17 expression in HLM

To extend the analysis of correlations between UGT2B17 genotype and SAHA glucuronidation in HLM, expression of UGT2B17 was examined. Initially, the GAPDH gene was used as an internal control to which UGT2B17 expression in HLM was normalized. However, during the analysis, it was determined that the expression of GAPDH varied widely in the samples despite the use of the same amount of cDNA for each analysis (Figure 4.6). To choose a more appropriate control for normalization, the TaqMan Human endogenous control plate was used to identify the ideal internal control and a summary of the screen is presented in Table 4.1. Based on those results, PPIAA was identified as the ideal control gene for expression studies in HLM and was therefore used to assay the HLM samples for UGT2B17 expression. A graph depicting UGT2B17 expression levels in the 87 HLM which have at least one allele present is shown in Figure 4.7. UGT2B17 expression ranged from 0 to 1.5 fold relative to PPIA with a mean value of 0.3418 relative UGT2B17 expression.

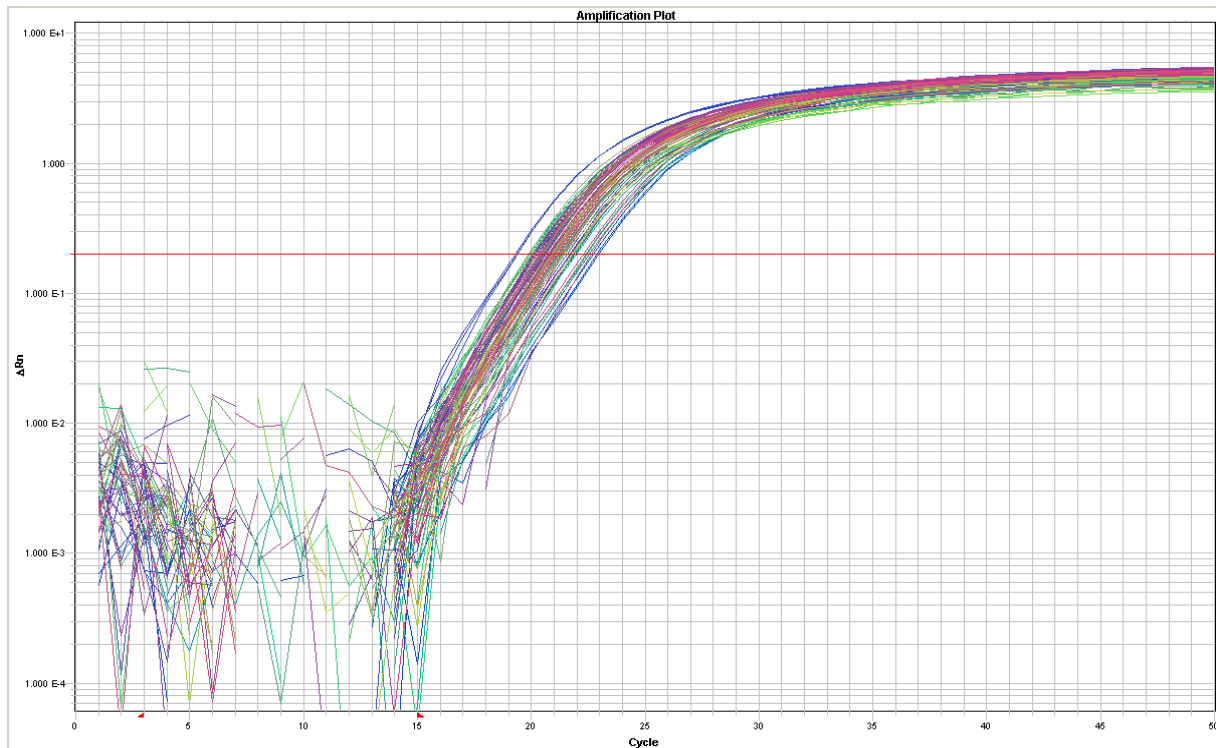


Figure 4.6: Variations of GAPDH expression in HLM sample set. This plot of real-time PCR analysis of GAPDH expression in multiple HLM samples demonstrates large inter-individual variations in expression of this gene which had been chosen as an internal control to use for normalization of UGT2B17 expression from sample to sample.

Detector	CT range
PP1A	1.1
GUSB	1.45
RPL30	1.46
GADD45A	1.5
MRPL19	1.5
POP4	1.5
RPL37A	1.5
MT-ATP6	1.6
B2M	1.7
RPS17	1.7
HPRT1	2.2
EIF2B1	2.5
PSMC4	2.5
UBC	2.5
PGK1	2.7
CDKN1B	3
PES1	3
RPLP0	3
TBP	3
ELF1	3.5
YWHAZ	3.5
GAPDH	3.7
HMBS	4
IPO8	4
TFRC	4
ACTB	5
CASC3	6
PUM1	6
ABL1	7
CDKN1A	7
POLR2A	10

Table 4.1: Summary of analysis used to identify the ideal control for normalization in HLMs. The TaqMan human endogenous control plate was used for real-time PCR analysis of 6 liver cDNA samples. Each sample was run in duplicate and results from duplications were consistent. Results show that 21 of the 32 potential control genes have CT ranges that are lower than that of GAPDH and indicate that PPIA is a much better choice for a normalization control in these liver samples.

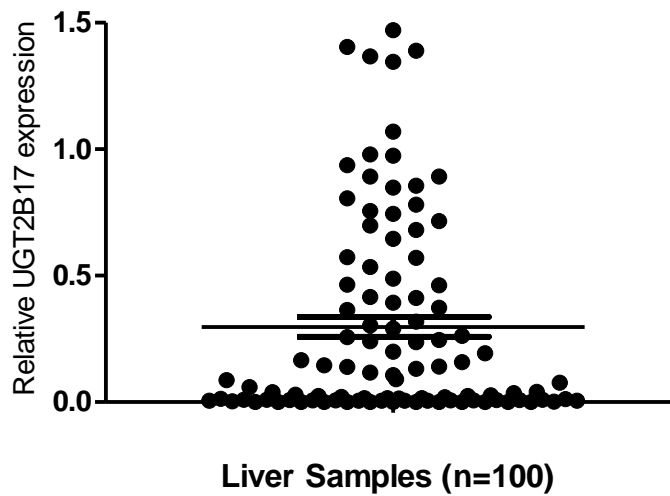


Figure 4.7: UGT2B17 expression in human liver. UGT2B17 expression was determined relative to PPIA by real-time PCR as described in the Materials and Methods. Dots represent individual samples, the thin line represents the mean and the darker bars represent the standard error.

4.3.3 UGT2B17 genotype/phenotype correlation in HLM

Data from recent studies have demonstrated the occurrence of a prevalent polymorphic deletion of the entire UGT2B17 gene (205, 209) that was associated with a reduced rate of glucuronidation activity in human liver microsomes (187). To examine the effect of the UGT2B17 whole-gene deletion on SAHA glucuronidation in human liver, HLM were prepared from normal liver tissue from 100 independent subjects. These HLM preparations were assayed for the formation of SAHA glucuronide in the presence of 200 μM SAHA (the apparent K_M of SAHA for UGT2B17 *in vitro*) and the results were then correlated with UGT2B17 genotype. As shown in Figure 4.8, a 45% ($P = 0.01$) decrease in SAHA-glucuronide formation was observed in HLM from subjects with the UGT2B17 (*2/*2) genotype as compared to HLM with at least one intact UGT2B17 allele. The levels of SAHA-glucuronide formation observed in HLM from

subjects with one or two intact UGT2B17 alleles were not significantly different from one another.

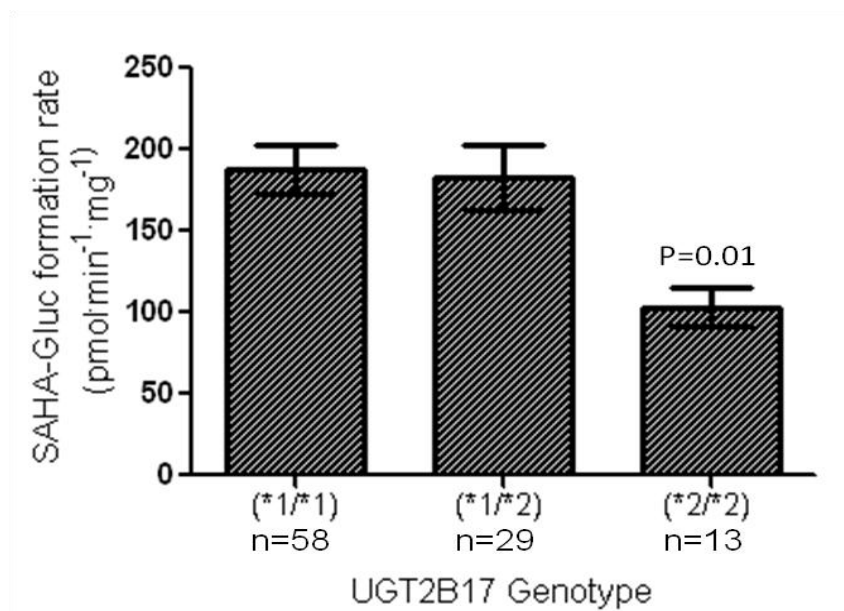


Figure 4.8: SAHA-glucuronide formation versus UGT2B17 genotype in HLM.

Glucuronidation activity assays were performed on HLM prepared from the liver specimens whose genotypes were determined in Figure 4.4 using 200 μ M SAHA, and SAHA metabolites were separated by UPLC as described in the Materials and Methods. Comparative analysis was performed using HLM from subjects with the UGT2B17 (*1/*1) genotype as the referent, with the p-value shown for HLM from subjects with the UGT2B17 (*2/*2) genotype; error bars represent standard error.

To determine whether the association observed between UGT2B17 genotype and HLM glucuronidation of SAHA was also manifested as a change in kinetic parameters, kinetic analysis was performed for all 13 of the HLM specimens from subjects exhibiting the UGT2B17 (*2/*2) genotype, and 13 randomly-chosen HLMs from subjects exhibiting the wild-type UGT2B17 (*1/*1) genotype. The reduction in SAHA glucuronidation in HLM from UGT2B17 (*2/*2) subjects was reflected in a significant (p-

value = 0.0018) 75% increase in the apparent K_M for SAHA of 2.1 mM compared to the K_M for UGT2B17 (*1/*1) of 1.2 mM (Figure 4.9). No change in V_{Max} was observed in HLMs from subgroups having different UGT2B17 genotypes.

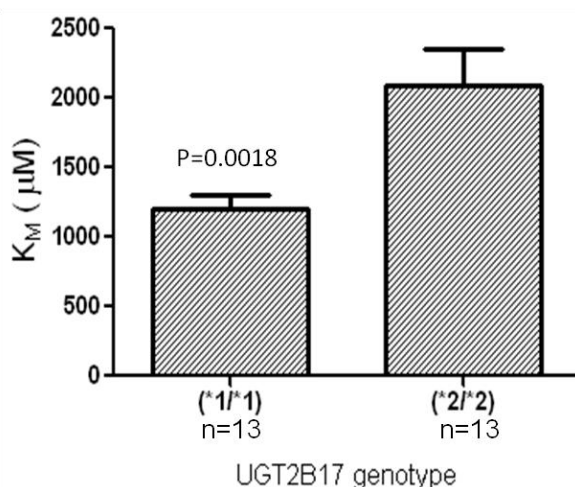


Figure 4.9: Apparent K_M for SAHA versus UGT2B17 genotype. Glucuronidation activity assays and kinetic analyses were performed for the thirteen HLM samples that exhibited the UGT2B17(*1/*1) genotype, and for thirteen randomly-chosen HLM from subjects with the UGT2B17(*2/*2) genotype. Glucuronidation assays were performed using 65-8000 μM SAHA, and SAHA metabolites were separated by UPLC, and K_M for SAHA was determined as described in the Materials and Methods.

Similar to the decrease of SAHA-glucuronide formation of the UGT2B17(*2/*2) genotype observed in HLM, a significant ($p < 0.001$) decrease in UGT2B17 expression also was observed in HLM from subjects with the UGT2B17 (*2/*2) genotype as compared to subjects with at least one intact UGT2B17 allele. There was no significant difference in UGT2B17 expression in HLM from subjects with one versus two intact

UGT2B17 alleles (Figure 4.10). A significant ($R^2=0.30$, $P\text{-value}<0.0001$) correlation was observed between SAHA-glucuronide formation in HLM and UGT2B17 expression in the same HLM (Figure 4.11).

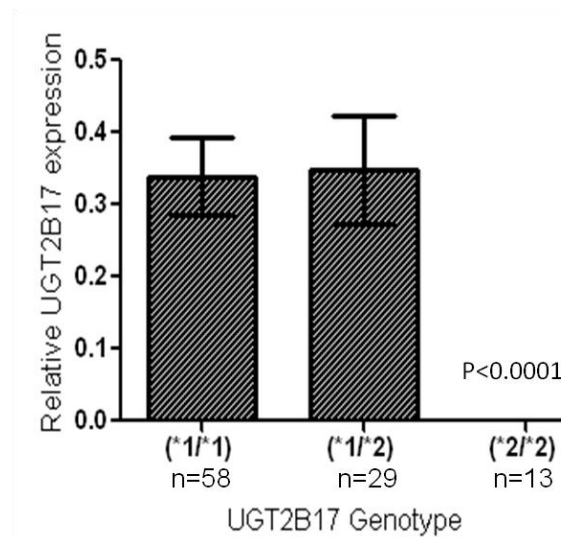


Figure 4.10: UGT2B17 expression versus UGT2B17 genotype in human liver. UGT2B17 expression was determined relative to PPIA as the 'housekeeping' gene by real-time PCR as described in the Materials and Methods. Comparative analysis was performed using the UGT2B17 (*1/*1) genotype group as the referent, with the p-value shown for the UGT2B17 (*2/*2) genotype group; error bars represent standard error.

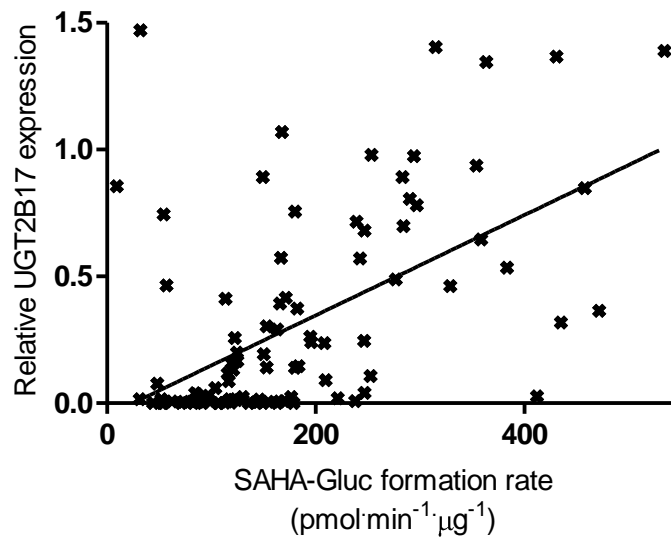


Figure 4.11: Correlation between UGT2B17 glucuronidation rate for SAHA and UGT2B17 expression. Correlation between SAHA glucuronide formation and UGT2B17 expression in the same HLM. The correlation coefficient (r^2) and the p-value (determined by linear regression) are shown.

4.3.4 Confirmation of the gender of each HLM preparation and stratification of UGT2B17 expression and glucuronidation results by gender.

The major role of endogenous UGT2B17 in the body is to metabolize androgens, and studies have indicated that UGT2B17 is regulated by androgen receptors (272, 273). To further understand the role of UGT2B17 genotype in glucuronidation activity of human liver microsomes, the data was stratified by gender. Although data existed on the gender of individuals from whom liver tissue was extracted, it was important to confirm the reported data. Therefore a real-time PCR assay was developed to determine gender and was based on detection of the male SRY gene and the endogenous control gene, RNaseP. A representative amplification plot for a male and a female are shown in Figure 4.12. DNA from HLM preparations (n=100) was assayed to

determine the gender of the donor and the results were compared to the patient reported genders for which two samples had conflicting data. Based on our assay, the gender of the HLM donors (n=100) consisted of 60 males and 40 female.

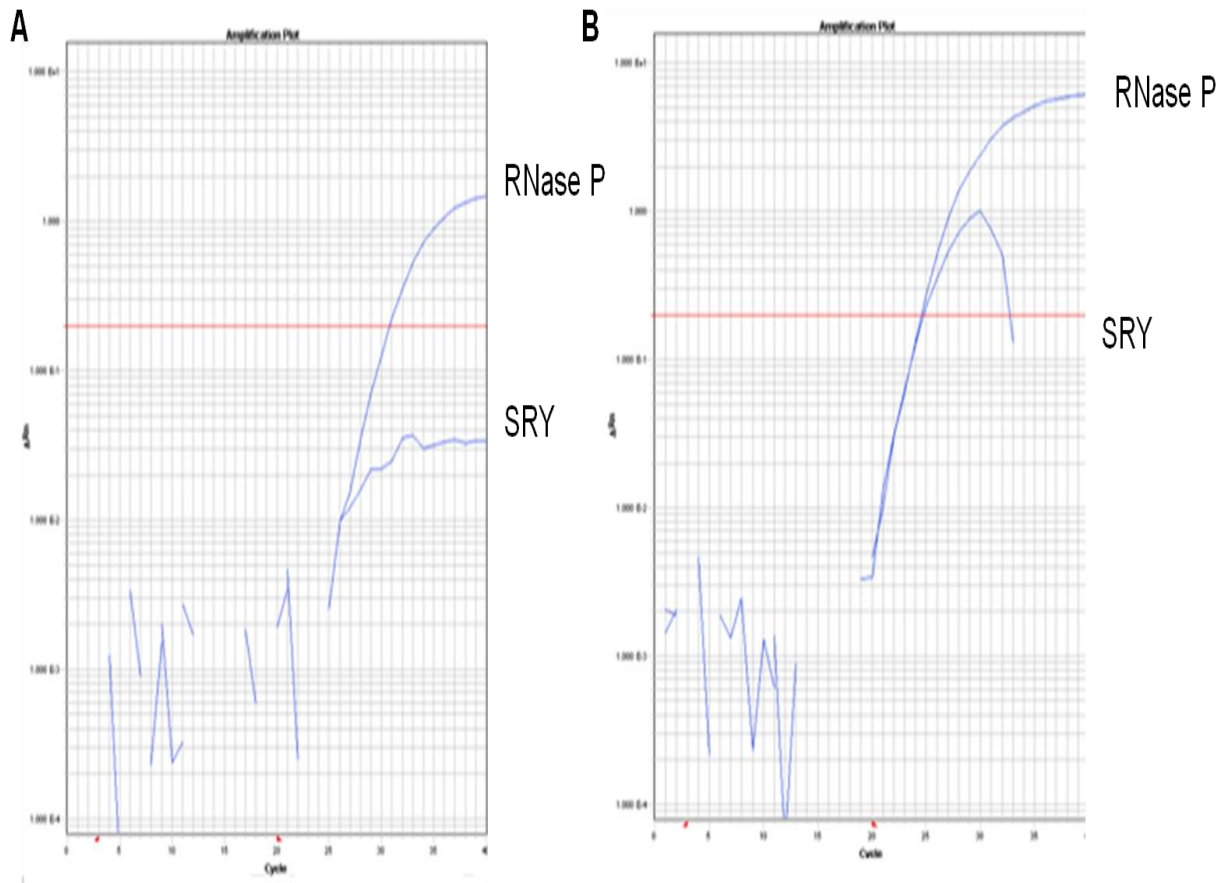


Figure 4.12: Representative amplification plot from gender assay. Shown are amplification plots representative of those obtained from the assay of (A) an HLM preparation from a female and (B) an HLM preparation from a male. The SRY gene is amplified only in males (B) and is not detectable above background in females (A).

The gender identification information was used to further the analysis of SAHA glucuronidation in HLMs. When stratified by gender, it was observed that HLMs from males and females glucuronidate SAHA at significantly different rates (Mann-Whitney test, P-value= 0.0067), with HLM from females exhibiting 45% less glucuronidation activity than males (Figure 4.13). When SAHA glucuronidation activity for SAHA was further stratified by UGT2B17 genotype and gender, the significant reduction in SAHA glucuronidation initially observed with the UGT2B17(*2/*2) genotype was now only seen in males (Figure 4.14). The UGT2B17 genotype and gender differences observed for the ability of HLM to glucuronidate SAHA was mirrored in the expression pattern of UGT2B17 (Figure 4.15). A significant decrease (Mann-Whitney test, P-value = 0.004) in mRNA expression of UGT2B17 was observed between samples extracted from males HLM versus females.

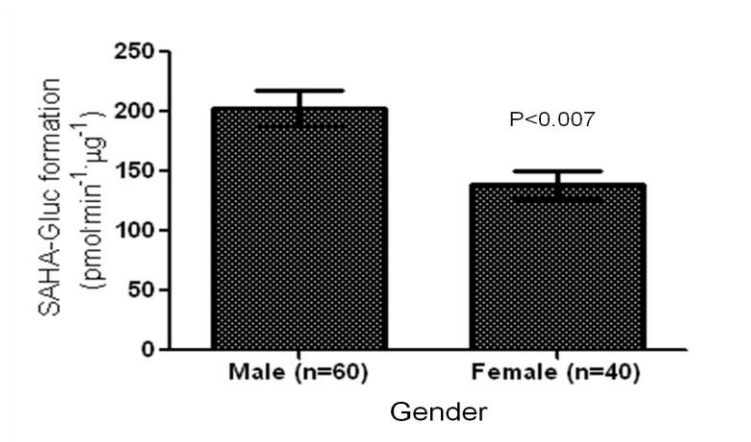


Figure 4.13: HLM glucuronidation activity stratified by gender. A significant difference in HLM glucuronidation of SAHA was observed between males and females. Glucuronidation activity and gender are described in the Materials and Methods; error bars represent standard error.

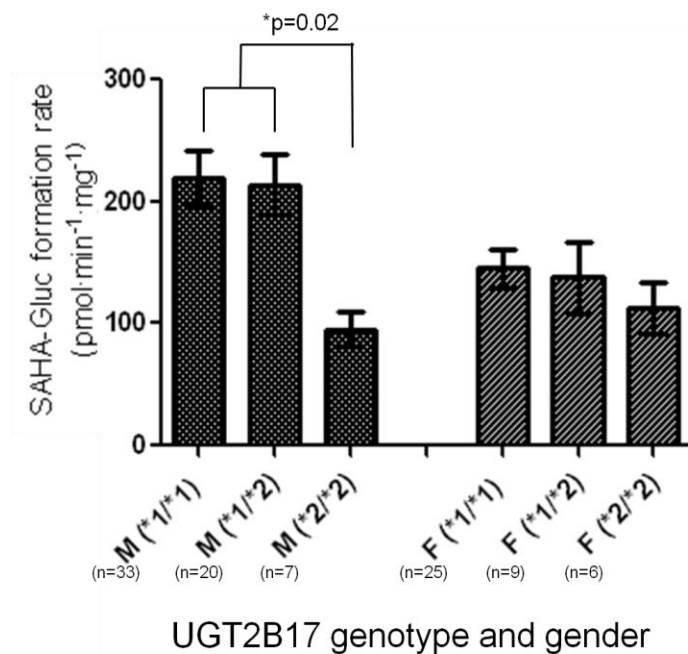


Figure 4.14: HLM glucuronidation activity stratified by gender and UGT2B17 genotype. Male's (M) with UGT2B17 *2/*2 alleles have a significant reduction in glucuronidation of SAHA as compared to males either *1/*1 or *1/*2 (*p=0.02). Glucuronidation activity, gender, and genotype assays are described in the Materials and Methods; error bars represent standard error.

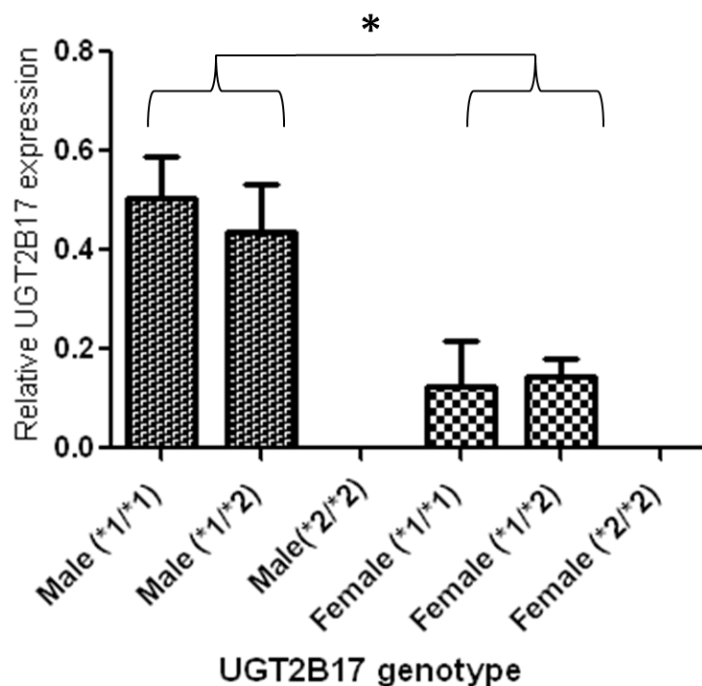


Figure 4.15: UGT2B17 expression in liver stratified by gender and UGT2B17 genotype. UGT2B17 expression was determined relative to PPIA as the 'housekeeping' gene by real-time PCR as described in the Materials and Methods. Comparative analysis was performed using male UGT2B17 (*1/*1 and *2/*2) genotype group as the referent, with the p-value shown for the female UGT2B17 (*1/*1 and *2/*2) genotype groups (p=0.004); error bars represent standard error.

4.3.5 SAHA activity in colon homogenate

Data detailed in previous sections identified two UGTs, UGT1A8 and UGT1A10, to be most active for SAHA glucuronidation and variants of these enzymes were shown to have altered abilities to glucuronidate SAHA. These UGTs, along with UGT1A7, are expressed exclusively extra-hepatically and could potentially have great importance in tissues including lung, breast, colon, small intestine, and tissues of the aerodigestive tract (136, 161, 185, 248) where these enzymes are expressed and to which SAHA is being targeted as a chemotherapeutic agent. To test the validity of the hypothesis that

metabolism of SAHA is important in such a target tissue, colon tissue was used because it has high expression of extra-hepatic UGTs (136, 183). Results show that a significant amount of SAHA glucuronide is formed in colon homogenate (Figure 4.16).

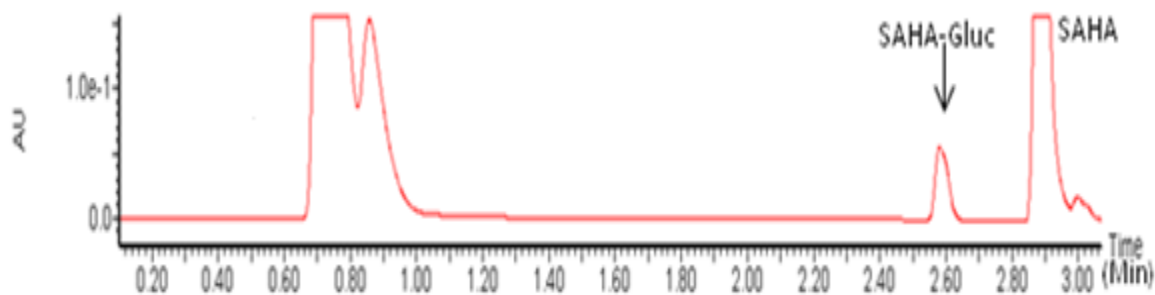


Figure 4.16: UPLC analyses of colon homogenate tested for the ability to glucuronidate SAHA. UPLC trace of a representative glucuronidation assay using colon homogenate (200 μg total protein) and 2000 μM SAHA, performed as previously described in the Materials and Methods.

4.4 SUMMARY

Liver is a major site for drug metabolism and therefore the UGTs expressed in hepatic tissue could strongly affect the overall patient response to SAHA. The study detailed in section 3.3.3 (Table 2.3) demonstrated that UGT1A3, UGT1A9, and UGT2B17 are hepatic UGT enzymes involved in the glucuronidation of SAHA. These studies identified that the K_M exhibited by UGT2B17 for SAHA was 5-fold and 11-fold lower than the K_M s observed for UGTs 1A9 and 1A3, respectively, the other active hepatic UGTs indicating that UGT2B17 has the best overall affinity for SAHA. In addition, UGT2B17 exhibited a 2.3-fold and 9.4-fold higher V_{max}/K_M as compared to UGTs 1A9 and 1A3, respectively, indicating that UGT2B17 has the best overall efficiency for the glucuronidation of SAHA. To determine those kinetic values, each UGT was examined separately *in vitro*.

The studies reported in chapter 3 examined variant UGTs and their abilities to glucuronidate SAHA *in vitro*; however, to fully assess the role of variants, especially one in which the gene is deleted, a system is required which closely resembles the *in vivo* conditions where multiple UGTs are expressed. To further characterize the hepatically expressed UGTs, hepatocytes or liver tissue would be an optimal system to examine SAHA glucuronidation and we chose to further our analysis using HLM because of their availability and reproducibility.

UGT2B17 has the best overall efficiency for glucuronidation of SAHA, which of the hepatic UGTs, is known to have a whole-gene deletion with an allelic prevalence of ~30% in Caucasians and ~75% in Asians (205, 209, 274). In order to examine the affect

of this UGT2B17 deletion on glucuronidation, we first needed to examine the HLMs to determine the UGT2B17 genotype. Of the 100 samples tested, we identified 13 as UGT2B17 (*2/*2) specimens. Based on a comparison of the levels of SAHA-glucuronide formation in HLM from UGT2B17-deleted subjects [exhibiting the UGT2B17 (*2/*2) genotype] versus HLM from subjects wild-type for UGT2B17, we observed a ~45% ($P = 0.01$) decrease in SAHA-glucuronide formation in HLMs of the UGT2B17(*2/*2) genotypes, which suggests that 45% of HLM glucuronidation activity can be attributed to UGT2B17.

We then examined the kinetic parameters of SAHA glucuronidation in HLM from subjects with UGT2B17 (*1/*1) genotype versus UGT2B17 (*2/*2) genotype. We found that the apparent K_M for SAHA is significantly increased (75%, $p = 0.0018$) in HLM from [UGT2B17 (*2/*2); ($K_M=2.1$ mM)] subjects as compared to HLM from [UGT2B17 (*1/*1); ($K_M=1.2$ mM)] subjects. These results support both the HEK293 cell homogenate data which showed that UGT2B17 had the best overall enzyme affinity for SAHA (Table 2.3) and results indicating that UGT2B17 is responsible for ~45% of the glucuronidation in HLM (Figure 4.8). Furthermore, the observed kinetics of the hepatic UGTs from the HEK293 cell homogenate system were predictive of the kinetics for HLM glucuronidation of SAHA. Using the HEK293 cell homogenate system, the K_M s for SAHA for UGT2B17, UGT1A9, and UGT1A3 were 0.3 mM, 1.6 mM, and 3.4 mM, respectively. Using the HLM system, the apparent K_M for SAHA was determined to be higher for UGT2B17(*2/*2) samples (2.1 mM) where UGT2B17 is deleted on both alleles, than that for UGT2B17(*1/*1) samples (1.2 mM) which have two copies of the intact UGT2B17 gene. When UGT2B17 is not present, HLMs have an apparent K_M

similar to the K_M s of UGTs 1A9 and 1A3; however, when UGT2B17 is expressed in HLM, the apparent K_M is decreased to a value more representative of the K_M of UGT2B17. Together, results from the current analyses further suggest that UGT2B17 is a major hepatic enzyme involved in the glucuronidation of SAHA and, that there is a high degree of integrity of the HEK293 cell line system for prediction of the more complex kinetics of systems where multiple UGTs are expressed.

Perhaps the most important finding with respect to pharmacogenetics is the significant decrease in SAHA-glucuronide formation observed in HLM from subjects with the UGT2B17-null genotype. The 45% decrease in SAHA-glucuronide formation observed in HLM from subjects who are UGT2B17-null was similar to the 50% decrease in glucuronidation activity observed in HLM from subjects homozygous for the UGT1A1*28 allele against SN-38, the major metabolite of Irinotecan (125). Irinotecan-treated patients with this UGT1A1 genotype exhibit higher SN-38 levels (230) and significant toxicity (123). Therefore, the similar alteration in glucuronidation activity for SAHA observed in HLM from subjects with the UGT2B17-null genotype suggests that a similarly significant impact on overall levels of circulating SAHA and subsequent toxicity or overall patient response could be observed in patients treated with SAHA whom are UGT2B17-null.

Previous studies have shown that *in vitro* UGT2B17 was down-regulated by androgens in prostate cell lines and UGT2B17 expression was not induced in the presence of 17 β -estradiol in MCF7 cells (174, 175). Furthermore, an increased risk for lung cancer was observed only in females with the UGT2B17 (*2/*2) genotype. To further our characterization of SAHA glucuronidation *in vitro*, we tested the hypothesis

that there may be differences in glucuronidation between males and females. We determined, by real-time PCR, the gender of the subjects from which each HLM preparation was made. With these data, we stratified our SAHA glucuronidation data by gender and observed a 45% ($p < 0.007$) reduction in SAHA glucuronidation in females compared to males independent of UGT genotype (Figure 4.13). This data is the first to show, using human specimens, that a difference in glucuronidation exists between males and females. Furthermore, when we stratified our data by gender and UGT2B17 genotype; the originally observed UGT2B17(*2/*2) decrease in glucuronidation (Figure 4.8) was now only seen in males (Figure 4.14). This data suggests that UGT2B17 is the enzyme that is differentially expressed in males and female. To test this observation, we then examined UGT2B17 mRNA expression in HLM specimens. We found that females, regardless of UGT2B17 genotype, had significantly less ($p = 0.004$) UGT2B17 mRNA expression compared to males with at least one intact UGT2B17 allele (*1/*1 or *2/*2); (Figure 4.15). This expression data provides further support for the important role that UGT2B17 has in glucuronidation of SAHA in HLM. The most clinically relevant result is that these data suggest gender differences in glucuronidation which may not only affect SAHA metabolism, but also may affect a vast array of drugs and carcinogens in which glucuronidation is predominantly carried out by UGT2B17. This study has provided a strong foundation which supports further investigation of gender differences with respect to regulation of UGTs and overall glucuronidation.

Another interesting observation was that no difference in SAHA-glucuronide formation was observed in HLMs from subjects with either one or two intact copies of the UGT2B17 gene. This corresponded with the fact that no difference in UGT2B17

mRNA expression was observed in the same liver specimens as determined by real-time PCR. This suggests that UGT2B17 is regulated at the transcriptional level and that the amount of UGT2B17 mRNA to protein is consistent as determined by activity. These results and the observed gender difference in expression strongly support further investigation of UGT2B17 regulation mechanisms.

Together, the data presented in this section suggest that the presence of genetic variation in active UGTs, especially UGT2B17, is associated with alterations in SAHA metabolism. Furthermore, potential differences in response to SAHA based on gender warrant further investigation. Patient data should be examined to determine whether these differences observed in our *in vitro* model are potentially associated with observed differences in overall SAHA toxicity or patient response to SAHA.

CHAPTER 5: UGT1A10 Promoter Study

5.1 INTRODUCTION

The data presented in the previous section indicates that mechanisms which control UGT2B17 expression are not yet fully understood and that hormonal regulation may be involved. Mechanisms for regulation of expression and activity of the various UGTs are of interest because they are expressed at different levels throughout the body. Interestingly, although most UGTs are expressed in the liver, UGTs 1A7, 1A8, and 1A10 are expressed exclusively extra-hepatically. Previous studies have analyzed the elements involved in regulation of expression of these extra-hepatic UGTs and have identified regions that are crucial for expression (156, 165, 275, 276). For example, Figure 5.1 shows the results of a study which identified the regions necessary for expression of UGTs 1A8, 1A9, and 1A10 using a luciferase assay system. This study demonstrated that the first 140 bp upstream of the ATG translational start site are required for maximum induction using UGT1A8 and UGT1A9 and that the first 400 bp upstream of the UGT1A10 ATG translational start site is required for maximum induction of luciferase activity (165). UGT1A10 is of particular interest because it is important for SAHA metabolism, and it is also involved in metabolism of carcinogens in various target tissues.

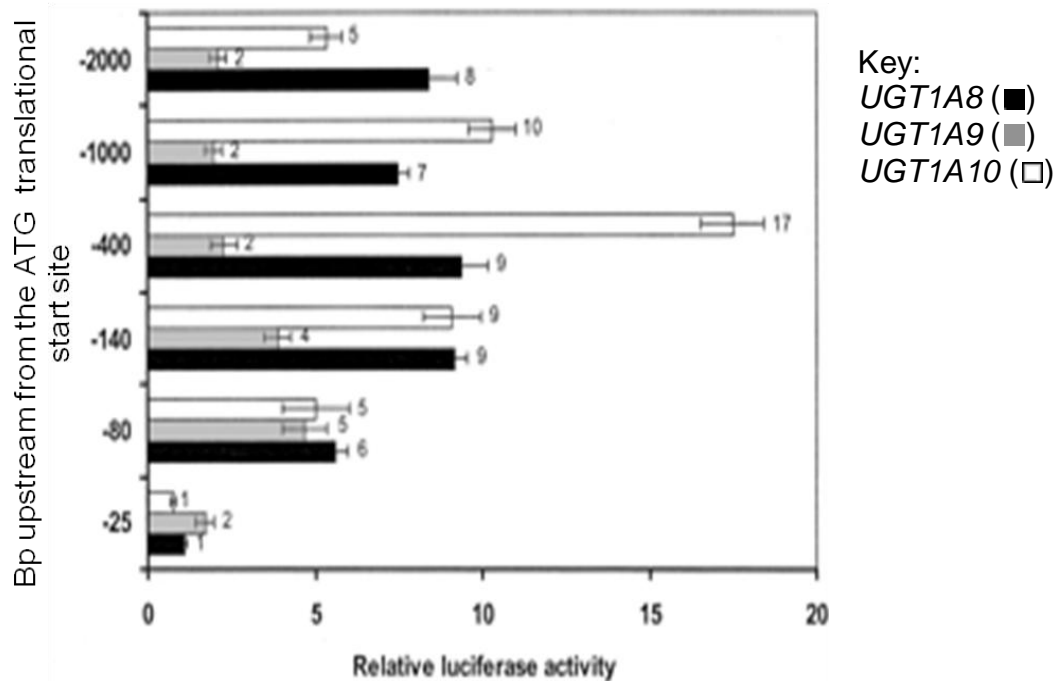


Figure 5.1: Deletion analysis of the *UGT1A8*, *-1A9*, and *-1A10* promoter in Caco-2 cells. Deletion constructs (0.5 μ g) containing varying lengths of the *UGT1A8* (■), *UGT1A9* (■), and *UGT1A10* (□) promoters were transfected into Caco-2 cells with 0.025 μ g of the pRL-null vector as an internal control of transfection efficiency. Cells were harvested 48 h after transfection and were assayed for firefly and *R. reniformis* luciferase activities. Relative luciferase activities are expressed as a fold induction over the promoterless pGL3-basic vector (set at a value of 1). The results shown are a representative experiment of three individual experiments performed in triplicate (\pm S.D.). [Reference from (165)].

UGT1A10 glucuronidates a variety of carcinogens including those found in tobacco smoke such as hydroxy derivatives of benzo[a]pyrene (161, 243) and PhIP and its major metabolite, *N*-hydroxy-PhIP (184). Two SNPs in the coding region of the UGT1A10 enzyme were previously identified, with the codon 139 Glu>Lys SNP shown to result in altered UGT1A10 activity *in vitro* (184, 185) and to be associated with altered risk for orolaryngeal carcinoma (203). Consistent with its role in metabolizing carcinogens, UGT1A10 has been detected in a variety of tissues commonly exposed to

carcinogens including those within the gastrointestinal tract (132, 183), the aerodigestive tract (161), and in lung (185).

Of interest in tissues susceptible to tobacco-induced cancers, is the induced expression of the UGT1As by aryl hydrocarbons (Ah) via the xenobiotic responsive element [XRE; (172, 277, 278)]. Computer searches for location of XRE in UGT1A genes have identified a conserved prototypical region (gcgtg) within 2 kb of the translational start site in all UGT1As, except UGT1A8; however, the efficacy of these sites is not fully known [Figure 5.2; (279)]. Studies have shown that UGT1A1 is inducible at a XRE region (-3381/-3299) with Ah receptor ligands including 2,3,7,8-tetrachlorodibenzo-p-dioxin, B-naphthoflavone, and B[a]P metabolites (278) and a similar induction by Ah's was observed for UGT1A6 (279). The ability of UGTs to be induced is crucial in response to harmful compounds since any impairment in detoxification mechanisms could increase susceptibility to various cancers.

Human			
UGT1A1	(-594)	CTCATGGCGCGTGCTCGTGTG	(-574)
UGT1A1	(-6542)	ACAGTTTTGCGTGGCCCTTTG	(-6522)
UGT1A2	(-176)	GAGGCACAGCGTGGGGTGGAC	(-156)
UGT1A2	(-546)	ATTCATGAGCGTGAATGTGGA	(-526)
UGT1A3	(-40)	CAGGCACAGCGTGGGGTGGAC	(-20)
UGT1A3	(-1393)	GCCATCCTGCGTGTGCTGCCC	(-1373)
UGT1A3	(-1604)	ACTACCAGGCGTGTCCACCC	(-1584)
UGT1A4	(-48)	CAGGCACAGCGTGGGGTGGAC	(-28)
UGT1A4	(-214)	CAAGATAGGCGTGATTGGTCT	(-194)
UGT1A5	(-1105)	TCTCATGGGCGTGAGACCATT	(-1085)
UGT1A5	(-4382)	ACATGGTAGCGTGTGCCTGTA	(-4362)
UGT1A6	(-1511)	AGGAACTCGCGTCCAGCCAG	(-1491)
UGT1A7	(-545)	GCATGGCAGCGTGCCTGTA	(-525)
UGT1A9	(-687)	TTCCCACTGCGTGCATGTAT	(-667)
UGT1A10	(-263)	CACTTGCAGCGTGCTCTCCCT	(-243)

Figure 5.2: Location of the prototypical aryl hydrocarbon/xenobiotic responsive element at the UGT1A locus. The XRE, gcgtg, is a conserved consensus sequence in UGT1 genes. Ah bind the Ah-receptor, which interacts with the XRE elements upstream of responsive genes to elicit an increase in mRNA synthesis. Computer searches identified the sequences shown. [Reference from (127)].

In addition to its role in carcinogen metabolism, UGT1A10 also has been identified as a major glucuronidator of estrogens and their hydroxylated metabolites (160, 182). Consistent with this role, UGT1A10 is expressed in breast (162, 176) and endometrium (280). Recently, studies have determined that UGT1A10 is regulated by estrogen in the MCF7 estrogen receptor-positive cell line (176). Since UGT1A10 is responsible for estrogen glucuronidation and is also regulated by estrogen, we similarly hypothesize that, aromatic hydrocarbons that are glucuronidated by UGT1A10 can also regulate this enzyme via XRE elements. The goals of the present study were, (1) to screen the UGT1A10 promoter region for polymorphisms and determine their potential effect on UGT1A10 expression and (2) to test the ability of Ah to induce UGT1A10 expression through interactions with XREs in the promoter region of the UGT1A10 gene.

5.2 MATERIALS AND METHODS

5.2.1 Human DNA used to screen for UGT1A10 polymorphisms

To screen the UGT1A10 promoter region for polymorphisms, genomic DNA purified from 97 normal human liver specimens excised during surgery for removal of hepatocellular carcinoma was utilized as previously described (186). UGT1A10 promoter polymorphic prevalence was examined in healthy Caucasians (n=156) and African Americans (n=133) as previously described (281-283).

5.2.2 Amplification and Sequencing of the UGT1A10 promoter

The 2000 bp upstream of the UGT1A10 ATG translational start site were amplified by PCR using a sense primer (UGT1A10S; 5'-TAGCTCTTCTTGTTACATTGATCCC-3', corresponding to nucleotides -2006 to -1982 relative to the UGT1A10 translation start site) and an antisense primer (UGT1A10AS; 5'-CGGTTCTGATCTTCCAGAGTG-3', corresponding to nucleotides +243 to +263 relative to the UGT1A10 translation start site). PCR amplifications were performed in a 50 µL reaction volume containing 50-100 ng of purified genomic DNA in 1X Taq buffer with 0.4mM of each deoxynucleotide trisphosphate, 20 pmol of both sense and antisense and 1.25 U of Taq DNA polymerase. The reaction mixtures underwent the following incubations in a MyCycler (BioRad, Hercules, CA): one cycle of 95°C for 2 min, 41 cycles of 95°C for 30 sec, 64°C for 30 sec, and 72°C for 3 min, and a final extension cycle of 72°C for 10 min. PCR amplicons were run on 0.8% agarose gels that were subsequently stained with ethidium bromide and examined over ultraviolet light using a

computerized photo imaging system (Alphamager 2000, Alpha Innotech Corp. San Leandro, Ca). The expected band size was 2269 bp. Samples were purified from the gel using QIAquick Spin (Qiagen, CA) and sequenced on an ABI 377 DNA Sequencer (Applied Biosystems, Foster City, CA). Sequences were analyzed for polymorphisms using BLAST (National Center for Biotechnology Information; NCBI), with 100% of all nucleotides covered for all amplicons.

5.2.3 Real-Time PCR genotype assay for novel UGT1A10 promoter deletion

Multiplex allelic discrimination assays were performed to assess the prevalence of the UGT1A10 promoter polymorphism. Identification of the wild-type UGT1A10 promoter included sense (5'-TCCTGAATAATATCCTGAAGAGG-3') and antisense (5'-CATGCTTTGCCTTTGACG-3') primers (corresponding to -1153 to -1131 and -899 to -882, respectively, relative to the UGT1A10 translation start site) and a probe (5'-FAM-AGATCTGGGATACATGTA-MGB-3', corresponding to -1096 to -1079 relative to the UGT1A10 translation start site) specific for the wild-type allele. Identification of the UGT1A10 promoter deletion variant included sense (5'-TTGATCTCTGTTGATTTAAAGTCTG-3') and antisense (5'-GCAGTAGACACACACATAAA-3') primers (corresponding to -281 to -257 and +33 to +52, respectively, relative to the UGT1A10 deletion variant translation start site) and a probe (5'-VIC-TTGGTAAATATTCCTCAGCA-MGB-3', corresponding to -203 to -185 relative to the UGT1A10 deletion variant translation start site) specific for the UGT1A10 deletion variant. Reactions included all wild-type and deletion primers and probes. Reactions (25 µL) were performed in 96-well plates using the ABI 7900 HT Sequence

Detection System, with reaction conditions of an initial cycle of 50°C for 2 min and 95°C for 15 min, and 50 cycles of 94°C for 30 sec, 55 for 30 sec, and 60°C for 1 min.

Reactions included QuantiTect Multiplex PCR Master Mix (1x final concentration), 0.4 µM of each primer, 0.2 µM of each probe, and 20 ng of genomic DNA. Negative controls (no DNA template) were run on every plate and genotypes were assigned by the automatic calling feature of the allelic discrimination option in SDS 2.2.2 software (Applied Biosystems, Foster City, CA).

5.2.4 Cloning of UGT1A10 promoter constructs into luciferase vector

UGT1A10 promoter regions containing 186, 441, or 2204 bp upstream of the ATG translational start site were cloned into the pGL3-Basic vector which contains the sequence for the firefly luciferase reporter enzyme (Figure 5.3). UGT1A10 promoter regions were amplified to include restriction sites for direct insertion into the vector. PCR amplifications were performed in 50 µL reactions containing 100 ng of purified genomic DNA in 1X Pfu DNA polymerase reaction buffer with 0.4mM of each deoxynucleotide trisphosphates, 20 pmol of both sense and antisense primers, and 2.5 U of PfuTurbo DNA Polymerase. The following cycling conditions were used to amplify samples: one cycle of 95°C for 2 min, 41 cycles of 95°C for 30 sec, 65°C for 30 sec, and 72°C for 3 min, and a final extension cycle of 72°C for 10 min. Genomic DNA from an individual who exhibited a homozygous wild-type UGT1A10 promoter was used to amplify 186 bp, 441 bp, and 2204 bp of wild-type UGT1A10 5' flanking region beginning at -5 bp upstream of the UGT1A10 translation start site. Genomic DNA from an individual who exhibited a homozygous UGT1A10 deletion variant promoter was used to amplify 441

and 2204 of UGT1A10 5' deletion promoter flanking region beginning at -5 bp upstream of the UGT1A10 translation start site. The primers used for PCR amplifications of UGT1A10 wild-type and deletion promoter regions were designed with the addition of restriction enzyme sites at their 5' proximal ends for vector insertion in the correct orientation and are listed in Table 5.1. The 186 bp and 441 bp PCR-amplified UGT1A10 promoter fragments (wild-type and/or variant promoters) were inserted into the KpnI and MluI restriction enzyme sites of the pGL3-Basic vector. Due to the presence of a KpnI site within the 2204 bp PCR fragment, the 2204 bp PCR fragments for both the wild-type and variant UGT1A10 promoters were inserted into the MluI and XmaI restriction enzyme sites of the pGL3-Basic vector. All PCR fragments were inserted into their corresponding restriction enzyme-digested pGL3-Basic vectors by ligation with T4 DNA ligase. UGT1A10 plasmid-containing One-shot bacterial colonies were selected by ampicillin resistance after transformation and were analyzed by restriction fragment length polymorphism analysis to ensure the presence of an insert. All vectors containing inserts were purified using the Hi-speed plasmid maxi kit (Qiagen) and sequenced in full to confirm the construct.

The -1271C>G variant was generated with the QuickChange SDM kit by site-directed mutagenesis using the 2204 bp wild-type UGT1A10 promoter-containing vector as template. Primers used were 5'-TTCCTTCATTTCAACGTTGGTGAATCTGATG-3' (sense) and 5'-CATCAGATTCACCAACGTTGAAATGAAGGAA-3' (antisense), and reactions were carried out as previously described (185).

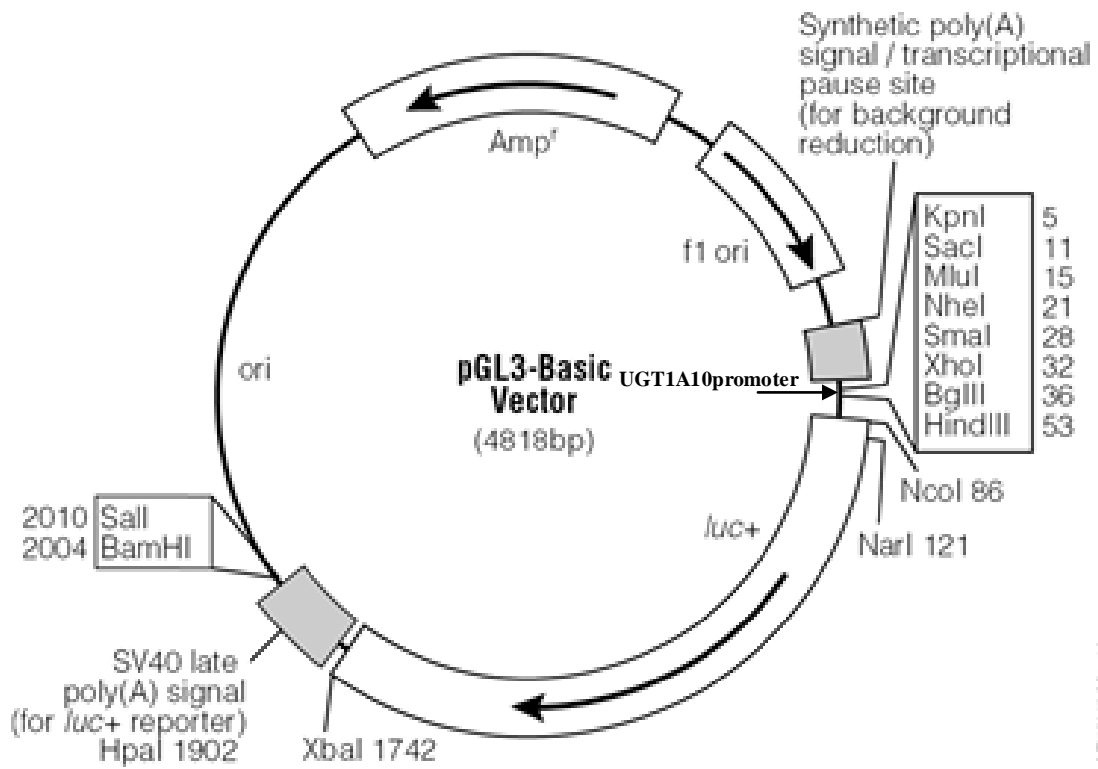


Figure 5.3: Basic Luciferase Vector. Vector used for construction of all UGT1A10 promoter containing vectors. UGT1A10 promoter insertion is highlighted in figure; promoters were inserted in proper orientation relative to the ATG translational start site. [Reference from Promega].

Primer name	Restriction Site	Primer sequence (5' – 3')	Primer location
WT186S	KpnI	5'-AGTAGGTACCTCAGCAAATGATACT-3'	-190 to -176 ^a
WT186AS	MluI	5'-AGCCACGCGTGAAGTGCAGCCCGAGCC-3'	-21 to -5 ^a
WT441S	KpnI	5'-CTGTGGTACCCCTGGAACATGAGATGCC-3'	-445 to -428 ^a
WT441AS	MluI	5'-AGCCACGCGTGAAGTGCAGCCCGAGCC-3'	-21 to -5 ^a
WT2204S	MluI	5'-AGCCACGCGTGTATTAGGTTTGCTTGGT-3'	-2208 to -2187 ^a
WT2204AS	XmaI	5'-TATACCCGGGGAAGTGCAGCCCGAGCC-3'	-21 to -5 ^a
Del441S	KpnI	5'-GCGGGCGGTACCTAAAGTCTCCCACTA-3'	-445 to -431 ^b
Del441AS	MluI	5'-AGCCACGCGTGAAGTGCAGCCCGAGCC-3'	-21 to -5 ^b
DEL 2204S	MluI	5'-CGGCCACGCGTGAATGCTTGTG-3'	-2208 to -2198 ^b
DEL 2204AS	XmaI	5'-TATACCCGGGGAAGTGCAGCCCGAGCC-3'	-21 to -5 ^b

^a Relative to the UGT1A10 wild-type translation start site

^b Relative to the UGT1A10 deletion variant translation start site

Table 5.1: List of primers used for PCR amplifications of UGT1A10 wild-type and deletion promoter regions. Primers were designed with the addition of restriction enzyme sites at their 5' proximal ends for vector insertion in the correct orientation.

5.2.5 Luciferase Assay for UGT1A10 constructs

Cells for luciferase assays were maintained as follows: Caco-2 cells were cultured in MEM with 1 mM MEM non-essential amino acids, 0.1 mM sodium pyruvate, 10% fetal bovine serum, and 100 U/ml penicillin-streptomycin. A549 and H1299 cells were cultured in RPMI-1640 with 10% fetal bovine serum and 100 U/ml penicillin-streptomycin. For luciferase assays, cells were plated in 6-well plates and grown in 5% CO₂ to 80-90% confluence. Co-transfection of 3.95 µg of the UGT1A10 promoter-containing pGL3-Basic constructs and 0.05 µg of the pRL-TK plasmid was performed using Lipofectamine 2000 as recommended by the manufacturer (Invitrogen). The Dual-Luciferase reporter assay system (Promega) was utilized for all luciferase assays. Luciferase and renilla

luminescence, corresponding to the pGL3-Basic and pRL-TK plasmids, respectively, were determined using the Synergy HT multi-detection microplate reader (BIO-TEK, Vermont). All assays were performed in triplicate as independent experiments.

5.2.6 Induction of Luciferase via UGT1A10 promoter.

Induction of luciferase expression from UGT1A10-luciferase promoter constructs were tested in Caco-2, H1299, A549 and MCF7 cells. Caco-2, H1299 and A549 cell lines were maintained and transfected as described in the previous section (section 5.2.5). After removal of transfection mixture (6 h), cells were rinsed with phosphate-buffered saline and treated with either media, media plus DMSO (same volume as volume of induction agents used in treatment of cells) or treatment media. Treatment media included metabolites of B[a]P which have been described previously to induce UGT1A1 expression (278). Metabolites 1-OH-B[a]P, 7-OH-B[a]P, or 9-OH-B[a]P (0.01 - 50 μ M) were incubated with the colon or lung cell lines (4 - 48 h) and then analyzed using the Dual-Luciferase reporter assay system, as described above, for luciferase activity via induction of the UGT1A10 promoter.

As a positive control for induction of luciferase activity from the UGT1A10-luciferase promoter construct, cell assay conditions previously described to induce endogenous UGT1A10 mRNA in MCF7 cells were used (162). MCF7 cells were cultured in DMEM supplemented with 10% fetal bovine serum and 100 U/ml penicillin-streptomycin (maintenance media) at 37°C and 5% CO₂. Two days prior to transfection and treatment, cells were harvested by trypsination, centrifuged at 700 g for 5 min, resuspended and washed twice in phosphate-buffered saline and then plated at 3×10^5

cells/dish in phenol red-free DMEM supplemented with 10% charcoal-stripped bovine calf serum (treatment media) to remove estrogens from the culture medium. Cells were then transfected as previously described and treatment media with E₂ (0.001 – 2 nM) was placed on cells for 4 – 24 h prior to running luciferase assays. For dose-response and time course studies of E₂-induction of luciferase expression from the UGT1A10 luciferase promoter, MCF7 cells were treated with vehicle (0.1% ETOH) or various doses of E₂ for up to 24 h in treatment media; cells were then harvested and analyzed for luciferase activity using the Dual-Luciferase reporter assay. Estrogen receptor luciferase reporter vector (Panomics, Fremont, CA) was used as a positive control.

5.3 RESULTS

5.3.1 Confirmation of the Amplification and Sequencing of the UGT1A10 promoter

Previous studies have identified several SNPs within the UGT1A10 coding region, all of which were of low prevalence (<5%) in both Caucasians and African Americans (281). To identify polymorphisms in the promoter and 5' untranslated region (UTR) of the UGT1A10 gene, PCR was used to amplify a 2269 bp product corresponding to bp -2006 to +263 of the UGT1A10 gene relative to the translational start site using high-quality genomic DNA purified from normal liver specimens from 97 independent subjects. In 4 of the 97 subjects, two amplicons were observed, the expected 2269 base pair fragment, and a smaller fragment of approximately 600 bp (Figure 5.4A). Sequence analysis indicated that while the larger 2269 bp amplicon corresponded to the wild-type UGT1A10 promoter, the smaller fragment corresponded to a UGT1A10 promoter that exhibited a deletion of the region -190 to -1856 relative to the UGT1A10 translational start site (Figure 5.4B). Out of the 97 samples amplified, 3 were heterozygous and one was homozygous for this deletion polymorphism (allelic prevalence = 2.6%). In addition to the promoter deletion polymorphism, sequence analysis of the 2269 bp UGT1A10 promoter amplicon from 47 subjects resulted in the identification of a single polymorphism (C>G) located -1271 bp upstream of the UGT1A10 ATG translational start site which corresponds to rs2741032 in the NCBI's Entrez SNP database.

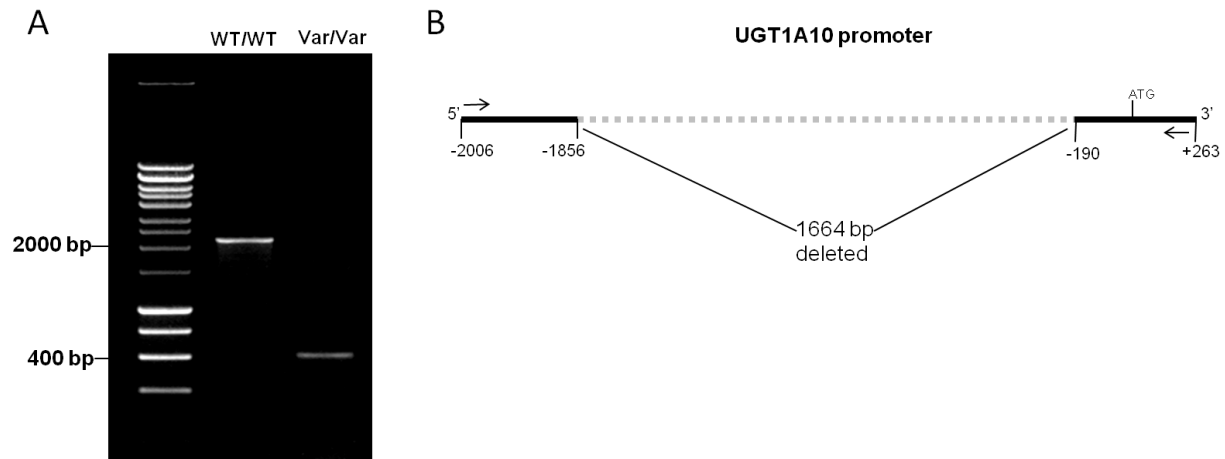


Figure 5.4: Deletion identification and schematic. (A) Agarose gel (0.8%) containing PCR-amplified products using genomic DNA from subjects exhibiting a homozygous wild-type (WT/WT) or homozygous variant (Var/Var) genotypes for the UGT1A10 promoter deletion polymorphism. (B) Schematic representation of the UGT1A10 promoter deletion polymorphism. Arrows indicate sense (UGT1A10S) and antisense (UGT1A10AS) primers used for PCR amplification of the UGT1A10 promoter.

5.3.2 Genotypes observed for the UGT1A10 promoter

To better assess the prevalence of the deletion in the UGT1A10 promoter region among different racial groups, a multiplex real-time PCR assay was designed as illustrated in Figure 5.5 and genotypes were assigned by the automatic calling feature of the allelic discrimination option in SDS 2.2.2 software (Applied Biosystems, Foster City, CA). In addition to the liver samples from 97 Caucasian hepatocellular carcinoma patients analyzed in the initial screen, additional samples from 156 healthy Caucasian and 133 healthy African American controls were analyzed for the deletion genotype. Of the additional 156 Caucasians examined, 7 were heterozygous for the UGT1A10 deletion (no additional Caucasian subjects homozygous for the deletion were identified). Of the 133 African Americans examined, 13 were heterozygous and 1 was homozygous for the deletion. The resulting allelic frequencies of the deletion polymorphism in these

control populations were 2.2% in Caucasians and 5.6% in African Americans. The allelic frequencies followed Hardy-Weinberg equilibrium for both populations.

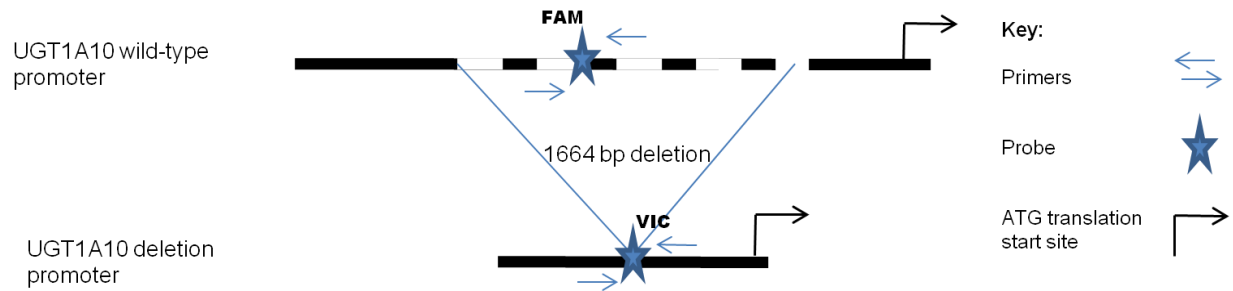


Figure 5.5: Schematic of UGT1A10 Real-Time PCR assay design. Top figure is the UGT1A10 wild-type promoter and the bottom figure is the promoter with a 1664 bp deletion. Primers and probes are illustrated with the wild-type primer probe set in the deleted region and the deletion detecting probe spanning the deletion site and primers on either side.

5.3.3 Effects of the UGT1A10 promoter region and its variants on gene expression

The constructs consist of the regions directly upstream the UGT1A10 ATG translational including three different size fragments: 141 bps, 441, bps, and 2204 bps. We amplified these fragments from either an individual that was homozygous UGT1A10 wild-type or homozygous for the novel UGT1A10 promoter deletion. Wild-type UGT1A10 promoter constructs consisted of 186 bp (referred to as WT186), 441 bp (referred to as WT441), and 2204 bp (referred to as WT2204) of 5' flanking UGT1A10 5' UTR (Figure 5.6A). To confirm our constructs and experimental design we initially tested these wild-type UGT1A10 constructs in Caco-2 cells (Figure 5.7). In Caco-2 cells, these wild-type constructs of various sizes exhibited the same UGT1A10-promoter luciferase induction as previously described (165) with 400 bp exhibiting maximal

expression and 2000 bp showing a decrease in expression which is suggestive of a repressor element in the region between 400-2000 bp upstream of the ATG translational start site.

Once the initial wild-type constructs and Caco-2 assay conditions were confirmed to be working, we then made UGT1A10 promoter variant constructs to see if any differences were observed. A 2204 bp UGT1A10 5' UTR construct containing the C>G transversion at bp -1271 (referred to as 2204^G) was constructed. In addition, two constructs containing 441 bps and 2204 bps were amplified from an individual homozygous for the UGT1A10-promoter deletion (Figure 5.6B) and are referred to as DEL441 and DEL2204, respectively. These constructs were then used to determine if either the 1664 bp deletion or the C>G SNP located in the UGT1A10 promoter could affect gene expression.

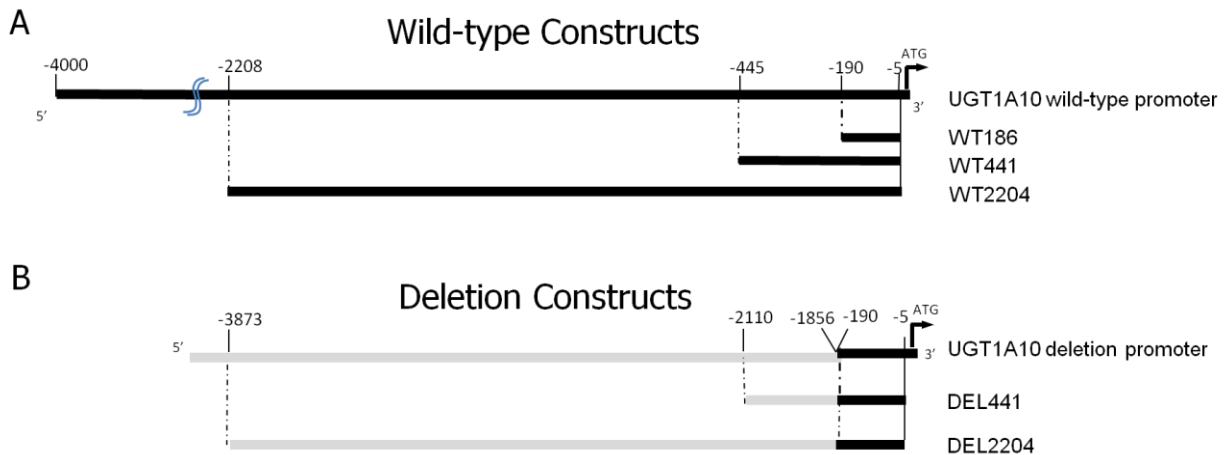


Figure 5.6: Schematic of UGT1A10 promoter regions tested for effects on gene expression. (A) Schematic representation of the PCR amplification strategy used for the UGT1A10 promoter luciferase assays. Top constructs illustrate the PCR-amplified fragments containing either 186 bp, 441 bp, or 2,204 bp of wild-type (WT) UGT1A10 promoter. The bottom constructs illustrate the PCR-amplified fragments containing either 441 bp or 2204 bp of deletion (DEL) variant UGT1A10 promoter. The grey lines indicate the promoter region located directly upstream of the UGT1A10 deletion; UGT1A10 deletion-containing luciferase vectors were constructed so that the UGT1A10 deletion and wild-type promoters were the same size.

Each construct was co-transfected with pRL-TK as an internal control for transfection efficiency, and then cells were harvested and assayed for luciferase activity as a measure of luciferase expression. All Luciferase assays were run in at least three independent experiments. As shown in Figure 5.7, both deletion containing constructs (DEL441 and DEL2204) exhibit a 3-fold increase in luciferase expression in Caco-2 cells. This result is consistent with the hypothesis of a repressor element in the regions between -400 and -2000 bp relative the UGT1A10 translational start site observed in our preliminary assays and by others (165). To see if this pattern was consistent in cell lines derived from other areas where UGT1A10 is expressed, we examined the lung cell lines A549 and H1299. Figures 5.8 and 5.9 are illustrations of UGT1A10 promoter region induced luciferase expression in two lung cell lines, A549 and H1299,

respectively. UGT1A10-induced luciferase activity did not vary significantly between wild-type and promoter deletion constructs for either of the lung cell lines tested. This data indicates that there are different regulation mechanism in Caco-2 cells compared to A549 cells and H1299 cells.

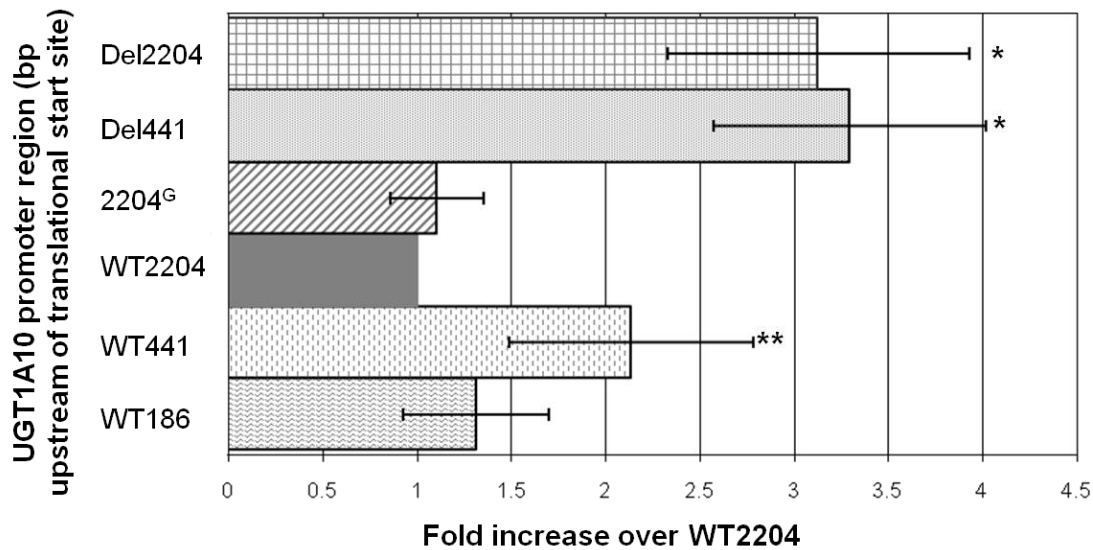


Figure 5.7: UGT1A10 promoter driven luciferase activity in colon carcinoma cells, Caco-2. Luciferase expression driven from UGT1A10 promoter region constructs in Caco-2 cells. Individual samples were normalized to renilla luciferase expression and then the triplicate averages were adjusted to WT2204 and represent expression relative to the activity from the WT2204 construct. Bars indicate standard deviation. *, P = 0.009; **, P = 0.048, a significant increase in luciferase activity was observed when compared with the WT2204-overexpressing cell line.

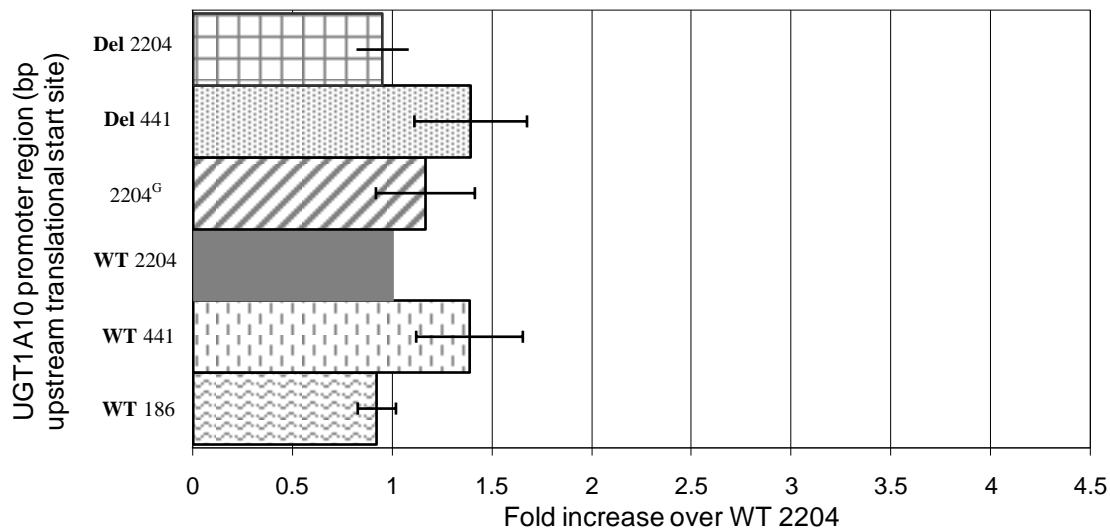


Figure 5.8: UGT1A10 promoter driven luciferase activity in lung carcinoma cells, A549. Luciferase expression driven from UGT1A10 promoter region constructs in A549 cells. Individual samples were normalized to renilla luciferase expression and then the triplicate averages were adjusted to WT2204 and represent expression relative to the activity from the WT2204 construct. Bars represent standard deviation.

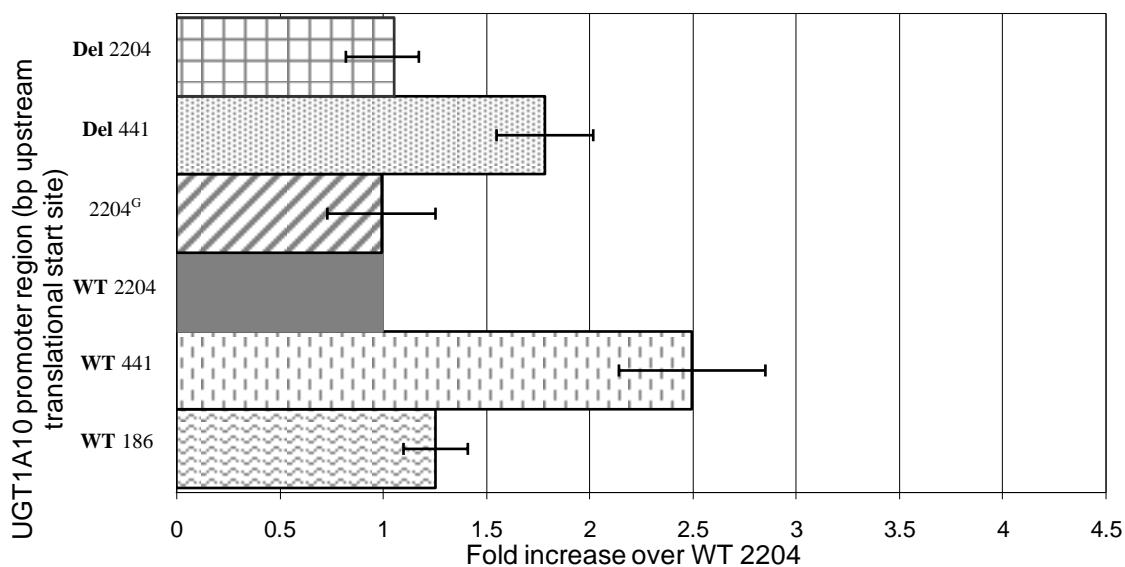


Figure 5.9: UGT1A10 promoter driven luciferase activity in lung carcinoma cells, H1299. Luciferase expression driven from UGT1A10 promoter region constructs in H1299 cells. Individual samples were normalized to renilla luciferase expression and then the triplicate averages were adjusted to WT2204 and represent expression relative to the activity from the WT2204 construct. Bars represent standard deviation.

5.3.4 Effect of treatment with hypothesized inducers on UGT1A10 promoter driven luciferase activity

UGT1A10 promoter region luciferase reporter constructs, WT2204 and DEL2204, were tested in Caco-2, H1299, or A549 cells for induction of luciferase activity by B[a]P metabolites, 1-OH-B[a]P, 7-OH-B[a]P, or 9-OH-B[a]P. Treatment with vehicle only (DMSO) was used as a control. Experiments were carried out to optimize both carcinogen concentrations and times of treatment; however, no induction of either construct was observed under any conditions listed in any of the cell lines. This lack of induction from Ah treatment prompted further investigation of these constructs. We then tested these same constructs and a known estrogen induced luciferase reporter construct in an MCF7 cell line system that has been described previously to induce endogenous UGT1A10 in the presence of 17 β -estradiol [E₂; (176)]. Although our constructs represented only a small region of the 5' UTR, the 2000 bp region contained 10 hypothetical estrogen receptor binding domains as determined by a transcription element search system. Although the estrogen receptor luciferase reporter positive control was induced in our system, no induction of the UGT1A10 promoter constructs was observed. These data suggest that the promoter constructs designed for this assay do not carry the necessary regions for induction of the UGT1A10 promoter region by E₂. Since induction of endogenous UGT1A10 has never been tested with B[a]P metabolites, it is difficult to assess whether induction occurs or if our constructs do not contain the necessary region.

5.4 SUMMARY

We sought to further characterize the UGT1A10 promoter. We first screened for polymorphisms in the promoter region of UGT1A10 which may lead to altered expression of this important extra-hepatic enzyme. Although HapMap, a database which contains known genetic variants was available, is designed for SNP analysis, it is not optimal for directly detecting large deletions or low-prevalence SNPs (284, 285). For this reason we sequenced 2000 bp upstream of the UGT1A10 ATG translational start site in DNA from 42 normal human liver specimens which resulted in the identification of a novel deletion polymorphism in the UGT1A10 promoter region. We next examined the prevalence of this novel deletion in two different populations. Due to the large genetic variability among racial groups, we decided to examine two self-identified groups, whites and blacks. Based on real-time PCR genotyping for the UGT1A10 promoter deletion, an allelic prevalence of 2.2% was found for whites whereas blacks had an allelic prevalence of 5.6%. If this deletion is identified to be relevant to UGT1A10 expression, this difference in prevalence between populations may ultimately explain differences, in susceptibility to cancers, such as orolaryngeal carcinoma which has been associated with UGT1A10 (203).

An *in vitro* assay was used to examine the potential effect of the deletion polymorphism on expression of UGT1A10. Since UGT1A10 is expressed extra-hepatically, three cell lines derived from two organs in humans, lung and colon, where UGT1A10 is known to be endogenously expressed, were used. The Caco-2 cells

derived from colon carcinoma, were initially tested to compare the current assay system to those previously described (156, 165). Using similarly sized promoter regions, the same vector, and the same cell line (Caco-2) enabled a direct comparison of results. The current data were consistent with the pattern observed previously, with maximal relative expression resulting from a 400 bp region upstream of the UGT1A10 translational start site, and a decreased expression resulting from the larger 2000 bp upstream region. These data support the presence of a repressor element within the -440 to -2000 bp region upstream of the UGT1A10 translational start site. Upon transfection of the deletion containing luciferase reporter constructs into the Caco-2 cell line, an increase in luciferase expression was observed with these deletion-containing constructs, again supporting the presence of a repressor element located in the region corresponding to that deleted in the deletion genotype. Interestingly, the two lung cell lines tested did not exhibit this pattern of UGT1A10 promoter induced luciferase activity. One possible explanation for this difference in expression is the necessity for the UGT1A10 promoter luciferase constructs to be induced. Previous studies have shown that in MCF7 cells, E2 treatment is required for maximal mRNA expression of UGT1A10 (176). Other studies have showed that UGT1A1 is inducible by carcinogens and that UGT1A10 contained a hypothetical XRE binding site (172, 277, 278). Together, these data led to the hypothesis that the lack of UGT1A10 induced luciferase activity in lung cells could be explained by the fact that inducing substrates were not present in the media. To test this hypothesis, we treated the colon and lung cells with aryl hydrocarbons such as metabolites of B[a]P. No induction was observed with any of the B[a]P metabolites in any of the cell lines. No studies prior to this have examined

induction of UGT1A10 by carcinogens; therefore, we could not conclude if our system and/or the constructs were functioning properly. To further characterize the inducibility of the UGT1A10 promoter luciferase constructs, we tested induction of the constructs to see if they can be induced by E₂ in a MCF7 cell system that has been previously shown to induce endogenous UGT1A10 (176). Our MCF7 system did not show any induction of the UGT1A10 promoter containing constructs in this previously-characterized system; however, our estrogen receptor luciferase reporter positive control did exhibit response to treatment suggesting that the UGT1A10 luciferase constructs do not contain the necessary elements for induction.

Many factors could contribute to the lack of induction of the UGT1A10 luciferase reporter constructs. Possibilities include that the promoter regions chosen do not contain the elements required for induction, the cell lines used do not express the required transcription factors, or UGT1A10 is not induced by Ahs via XRE elements. Further studies could include examination of larger regions of the 5'UTR or an assessment of endogenous UGT1A10 expression in cells treated with B[a]P metabolites. Endogenous expression is ideal to examine induction because it may be affected by the methylation of the promoter or other factors for which a vector construct could not adequately substitute for the natural environment. However, with regard to our goal of characterizing the promoter deletion, examination of endogenous UGT1A10 may not be feasible because the homozygous UGT1A10 promoter deletion may not be found in cell lines.

Overall, these studies examined the promoter region of UGT1A10 and identified a novel deletion that has a prevalence of 2.2% and 5.6% in whites and blacks,

respectively. This variant may play a role in the regulation of UGT1A10 and the ability for it to be induced, which may ultimately affect the glucuronidation of carcinogens by this enzyme. Therefore studies should continue to examine induction of the UGT1A10 promoter.

Chapter 6: General Discussion and Future Directions

Cancer is a devastating disease and current chemotherapeutic agents used in the treatment of cancer do not prove efficacious for every patient and often have harmful side effects. One way to improve patient treatment and outcomes would be to understand the underlying differences among individuals. By understanding the differences that lead to altered drug response it will be possible to choose a treatment course designed for maximal efficacy in an individual. One aspect by which individuals may vary is in their ability to metabolize drugs (192, 214). Pharmacogenetics is the study of genetic variants which lead to altered drug response and many of the enzymes involved in drug metabolism are highly polymorphic (194, 195). The main objective of the work presented in this dissertation was to characterize the glucuronidation pathway of SAHA, a highly promising chemotherapeutic agent. The specific aims were to identify the UGTs responsible for glucuronidation and to determine whether variants of these enzymes have an altered ability to glucuronidate SAHA. The methodologies used and information gained from the presented work provides a basis for characterization of many other glucuronidated drugs as well.

The studies presented in this dissertation are the first to characterize the glucuronidation pathway of SAHA metabolism. The identification of the specific UGTs responsible for SAHA glucuronidation (1A1, 1A3, 1A4, 1A6, 1A7, 1A8, 1A9, 1A10, 2B7, and 2B17) and the characterization of these enzymes will contribute to the overall understanding of SAHA metabolism. Although the liver is the major site of drug metabolism, we identified, through kinetic analysis, that the extra-hepatic UGTs 1A8

and 1A10 exhibit the best overall efficacy for the glucuronidation of SAHA. Since these UGTs are not expressed in the liver, we propose that they may be important in glucuronidation of SAHA in target tissues such as breast, lung and colon. Based on this hypothesis, we prepared colon microsomes, tested for SAHA glucuronidation, and were able to show that this process occurs in a SAHA target tissue, colon, where UGTs 1A8 and 1A10 are expressed. This evidence suggests that in addition to UGTs expressed in liver, the extra-hepatic UGTs could be important in the glucuronidation of drugs in target tissue and contribute to overall glucuronidation capacity.

Furthermore, the identification of a decreased rate of glucuronidation of SAHA by variants of the most active UGTs, including 1A8 and 1A10, may provide a source for understanding observed differences in patient response and toxicity. As discussed previously, these two extra-hepatic UGTs may be crucial in metabolizing SAHA in target tissue. Hypothetically, a colon cancer patient homozygous for the UGT1A10*2 allele, which codes for the UGT1A10 enzyme that was shown not to glucuronidate SAHA, may respond better to treatment with SAHA since target tissue exposure to the active form of SAHA will be greater compared to someone who has the wild-type allele and will metabolize SAHA more rapidly. On the other hand, the extra-hepatic UGTs could be contributing to overall glucuronidation and individuals with these variants could have increase toxicity. Although these possibilities have not been studied in patients, these scenarios can now be examined based on the data presented in this dissertation. This would require the patients to be genotyped for the UGT1A8 and UGT1A10 variants and physicians to detail overall response to SAHA treatment, examine toxicity and tumor

response, and then assess whether there are any correlations of these data with UGT genotype.

UGT2B17 was identified as the primary glucuronidator in liver as determined by kinetics in the *in vitro* HEK293 cell line system. We were able to further assess UGT2B17's role in liver by examining glucuronidation in HLMs from homozygous UGT2B17*2 individuals who have a whole gene deletion of UGT2B17. HLMs provide a system where other UGTs are present and can compensate for the loss of UGT2B17. Kinetic analysis allowed us to determine that UGT2B17 accounts for 45% of overall glucuronidation in HLM. Presumably, UGTs 1A9 and 1A3, which were identified in the *in vitro* HEK293 cell line system to glucuronidate SAHA, account for the rest of the glucuronidation observed in UGT2B17-null HLMs. The apparent K_M was lower (1.2 mM) in HLM from UGT2B17*1/*1 compared to when UGT2B17 was not present in HLMs (2.1 mM). These data suggest that individuals homozygous for the UGT2B17*2 allele could potentially metabolize SAHA at a significantly slower rate compared to individuals with at least one UGT2B17*1 allele. This could result in different exposure to the active form of SAHA, which could influence response and toxicities, and therefore should be examined in patients.

In order to determine if a genotype/phenotype correlation in response to a drug exists, a large population size is required, especially for low-prevalence polymorphisms. SAHA is currently FDA-approved to treat cutaneous T-cell lymphoma, which is classified as a rare disease by the NIH with a total of about 16,000 to 20,000 cases in the US (286). As a rare disease with a small sample size, it would be reasonable to question the practicality of further examining altered SAHA response in patients based

on genetic differences. However, current clinical trials suggest that SAHA, primarily used in combination with other chemotherapeutic agents, is beneficial for many other types of cancers. SAHA is being tested as a treatment for small cell lung cancer, breast cancer, ovarian cancer, colorectal cancer, pancreatic cancer, brain metastases, other leukemias and advanced solid tumors (117). These cancers affect a large segment of the population where altered response to SAHA due to genetic differences can be observed. For example, the NCI estimates about 150,000 new colon/rectal cancer cases for this year (287), and UGT2B17*2 has a 30% allele frequency, which would mean that 15,000 people who could potentially be given SAHA do not contain the gene which is responsible for 45% of SAHA glucuronidation in liver.

The data presented in this thesis supports that pharmacogenetic factors may affect SAHA response, as it relates to UGT genotype, and should be considered when administering SAHA to patients. To test this hypothesis, the next step would be to collect, for further analysis, urine and blood samples from patients treated with SAHA. We have identified key UGTs and their variants which may lead to altered SAHA response. Based on this information, UGT genotypes of patients can be determined and can then be correlated to the amount of SAHA-glucuronide produced in urine and blood. The CNV real-time PCR assay for the UGT2B17 variant developed during this thesis work could readily be used for genotype analysis. Similar real-time PCR assays can be used for the other UGT variants and methods for screening SAHA and its glucuronide metabolite in urine and blood have been developed and optimized (247). Together, determination of UGT genotype and the measurement of *in vivo* SAHA glucuronide formation by an individual can provide further information about the role of UGT genetic

variants and their effect on metabolism. Furthermore, patient response and toxicity to SAHA and UGT genotype can be correlated to see if individuals prescribed SAHA should be tested for UGT variants before starting treatment.

Also interesting is the finding that there is a gender difference observed in the abilities of HLMs to glucuronidate SAHA. In general, women and men have many physical differences such as height and weight which can influence the required dose of a drug. However, this study suggests that there may be gender differences in the overall metabolism of SAHA even after adjusting for these variables. Furthermore, any drug which is predominantly glucuronidated by UGT2B17 may result in differences in response and toxicity based on the gender of a patient. This information is very valuable because all women, regardless of size or diet, may metabolize SAHA, or other substrates predominantly glucuronidated by UGT2B17, at lower levels than men and physicians should be monitoring for this factor.

SAHA is a hydroxamic acid derivative and has a similar chemical structure to other compounds of this class. Currently, several hydroxamic acid derivatives are in clinical trials (65, 117), and these compounds may be metabolized by mechanisms similar to SAHA. For example, the HDACi Valproic acid, a hydroxamic acid derivative, has been shown to be glucuronidated. UGTs active against Valproic acid have been identified and variants of these enzymes have been characterized and used in clinical analyses to assess altered patient response. No significant correlations have been found to date (288, 289); however, a major limitation to these studies is that only the UGTs 1A1, 1A6, 1A9, 2B7, and 2B15 have been screened for ability to glucuronidate Valproic acid. This incomplete characterization of all UGTs could be the reason that the

studies did not observe any significant clinical differences in patient response and toxicity to Valproic acid based on UGT genotype. A complete characterization of all the UGTs responsible for Valproic acid glucuronidation would be required to properly assess effects of variant UGTs on *in vivo* glucuronidation. Due to the incomplete analysis of Valproic acid, the only hydroxamic acid derivative HDACi other than SAHA to be screened for glucuronidation by UGTs, a comparison between HDACi compounds and the UGTs responsible for glucuronidation cannot be made. Furthermore, prediction of the exact UGTs that would glucuronidate any hydroxamic acid derivative would be inaccurate because subtle changes in UGT enzyme composition have been shown to alter overall glucuronidation of substrates (185, 186, 235, 290). However, the Valproic acid studies illustrate the necessity to fully characterize all the UGTs, similarly to the characterization of SAHA glucuronidation, to eliminate the possibility that the uncharacterized UGTs could be playing a major role in glucuronidation.

To fully characterize the glucuronidation of a substrate and to identify the individual UGTs that have activity, an *in vitro* system is necessary; however, the accuracy of *in vitro* glucuronidation systems have been debated (291-295). Initial studies to assess the ability of individual UGTs to glucuronidate substrates used insect derived baculosomes, which are the microsomal fraction of insect cells that were transfected with UGT-expressing vectors. However, insect cells do not utilize the same post-translational processing as humans and it could be argued that the proteins produced in this system are not comparable to the human forms, but this has never been examined. To eliminate the potential problem resulting from differences in post-translational processing which may occur in insect cells, recent studies have used the

HEK293 cell line, a human cell line which does not endogenously express UGTs, to overexpress UGTs and to characterize their glucuronidation activities (241, 242). For glucuronidation to occur, substrates must reach the internal active sites of the UGT enzymes which are located within the ER membrane. Human cells, *in vivo*, have enzymes which transport substrates, and the co-substrate UDPGA, to the UGT active site; however, *in vitro* these enzymes are not active. Therefore, *in vitro* systems must use detergents to make the membrane which surrounds the UGT enzyme permeable. Alamethicin is currently the most well-characterized and most widely used detergent for glucuronidation assays (296) and unpublished data by Dr. Dongxio Sun of the Lazarus lab supports that alamethicin is a more efficient detergent than the previously used Triton X-100. Although these *in vitro* systems for studying glucuronidation have limitations, they are currently the best models to study glucuronidation by individual UGTs.

In the present studies, *in vitro* assays of HEK293 cell lines were initially used to identify the most active individual UGTs. These results were then confirmed and extended through assays using HLMs where multiple UGTs are expressed. The K_M values determined in the HEK293 cell assays for the hepatic UGTs 1A3, 1A9, and 2B17 (3.4 mM, 1.6 mM, and 0.3 mM, respectively) were mirrored when comparing the apparent K_M in HLMs. When UGT2B17 was present in HLMs, the apparent K_M was lower (1.2 mM), and more representative of the K_M determined for UGT2B17 (0.3 mM). However, when UGT2B17 was not present in HLMs, the apparent K_M was higher (2.1 mM) which is similar to the K_M of UGT1A9 (1.6 mM) and UGT1A3 (3.4 mM). These

results substantiate the validity of the use of the individual UGT HEK293 *in vitro* assay system to determine relative UGT kinetics.

The SAHA kinetic data from the *in vitro* systems used in this study are consistent; however, their physiological relevance has yet to be supported. The K_M and V_{max} for each UGT have been determined using a cell homogenate system and K_M values of the hepatic UGTs were further substantiated by the HLM data. All the determined K_M concentrations were well above the amount of SAHA given to patients; however, the kinetic data can be used to assess the general contribution of each UGT. The slope of the individual UGT kinetic plots is representative of the V_{max} over K_M . Therefore, since this slope includes SAHA concentrations which could be physiologically relevant, the V_{max}/K_M value can be used to compare overall enzyme efficiency for SAHA which should translate to the general significance of each UGT *in vivo* assuming similar overall expression. However, it is known that UGTs vary in expression and as studies continue to examine their expression patterns, the V_{max}/K_M values will be more representative of the individual UGT. As for the overall physiological relevance of UGT's role on SAHA metabolism, it is known that SAHA-glucuronides have been found in patients in comparable ratio to the other metabolite (114, 246). These *in vivo* data support the significant role of glucuronidation in the metabolism of SAHA and our kinetic parameters suggest that UGT2B17, which is highly expressed in the liver (136) will significantly alter SAHA metabolism in liver.

Analysis using *in vivo* data could further support the current use of *in vitro* analysis systems. However, if these *in vitro* results are not reflected in the results of the *in vivo* analysis, this would not completely discredit the *in vitro* system. For example, the

present study has characterized the glucuronidation pathway of SAHA metabolism; however, an alternative pathway of SAHA metabolism has been identified, but has not been fully characterized. Hydrolysis and β -oxidation are common processes in the cell and many enzymes could potentially contribute to the formation of 4-anilino-4-oxobutanoic acid. Although the enzymes have not been identified, the levels of metabolite formation indicate that this pathway is also important in SAHA metabolism (114, 246). Discrepancies which may be observed between *in vitro* and *in vivo* SAHA glucuronidation could potentially be accounted for by contributions from this alternative pathway found *in vivo*; however, this remains to be examined. Furthermore, many tissues could be contributing to SAHA metabolism and therefore a complete understanding of tissue specific expression patterns of each UGT would be required to assess overall metabolism. Despite possible *in vivo* differences, the *in vitro* work presented in this study is necessary to completely characterize the individual UGTs responsible for SAHA glucuronidation, an important aspect that would not be possible to elucidate *in vivo*.

The work presented in this thesis also has implications beyond the relationship between UGTs and SAHA or other HDACi. Studies of other drugs or substrates which are glucuronidated can benefit from the methods used and information gained. For example, we show that UGT2B17 is a major glucuronidator of SAHA and that the UGT2B17*2/*2 genotype alters overall glucuronidation in HLMs. This implies that any drug or substrate that is predominantly glucuronidated by UGT2B17 may exhibit differences in response in the population. Similarly, this implication would also apply to gender differences based on the observations in HLMs. Together, the findings from this

research have laid a strong foundation for further investigation of the role of UGT genetic variants, the role of gender, and the importance of UGT2B17 in overall glucuronidation of drugs and other substrates as they relate to individual differences.

This dissertation has also highlighted the importance of regulation of UGT expression. Specifically, having either the UGT2B17*1/*1 or the UGT2B17*1/*2 genotype does not affect overall glucuronidation of SAHA in HLMs. This activity pattern was reflected in UGT2B17 mRNA expression patterns in HLM specimens having the same overall mRNA levels with either the UGT2B17*1/*1 or the UGT2B17*1/*2 genotype. These data suggest that mRNA levels of UGT2B17 are tightly regulated to achieve a set amount of UGT2B17. Also, a significant difference in UGT2B17 mRNA level in HLMs was observed when comparing specimens from men and women. Studies using the androgen receptor positive cell line LNCaP, showed that UGT2B17 mRNA and protein levels were down regulated in the presence of dihydrotestosterone [DHT; (297)] and have identified the androgen receptor and the subsequent signaling pathway to be required for UGT2B17 regulation (272). Initially, these data seem contradictory to the HLM data which showed that men exhibited higher mRNA levels of UGT2B17. These confounding differences led to further investigation of UGT2B17 in other tissues. This discrepancy is currently being examined by Nathan Jones of the Lazarus lab whose preliminary data suggests that endogenous UGT2B17 mRNA expression not only varies by gender but also by tissue type.

Together, these data suggest that UGT2B17 is regulated in a manner to achieve a set amount of UGT2B17, that androgens or other hormones are contributing to expression, and that there is tissue-specific regulation of UGT2B17. These three

observations, based on findings from this dissertation, may or may not be interrelated; however, they provide many avenues in which UGT2B17 regulation and expression may be examined. One method to better understand UGT2B17 regulation is by examining the factors which bind to the promoter. This has been done for the region including 596 bp upstream of the UGT2B17 ATG translational start site, and it was determined that HNF1 α can activate the promoter, but other unidentified factors are also contributing to UGT2B17 regulation (275). To further understand UGT2B17 regulation, studies are needed to examine more up-stream regions to identify other regions that are important for UGT2B17 mRNA expression (UGT2B17 driven induction of luciferase) and that could be binding sites for important factors (DNaseI footprint analysis). These studies should be conducted in cells from different tissue in order to identify the different factors which are contributing to the tissue specific expression of UGT2B17.

Identification of important regions and regulatory elements, should provide insight into why only one UGT2B17*1 allele is necessary for consistent mRNA levels. If these factors don't account for the observed regulation pattern of UGT2B17, this may suggest that epigenetic factors such as the methylation status of the promoter are responsible for UGT2B17 expression and studies should proceed in that direction. Furthermore, it would be possible to address hormonal regulation with the luciferase and DNaseI footprint systems. By incubating UGT2B17 controlled luciferase vectors of different sizes with hormones, one could identify what regions of the UGT2B17 promoter are important and which hormones cause induction. This information can then be used to conduct DNaseI footprinting of the crucial regions to help identify what transcription factors are binding to the location. Another method to address UGT2B17 regulation is to

examine tissues where UGT2B17 mRNA is expressed and then examine the mRNA expression of hormones and/or their associated regulatory elements in that tissue to see if there is a correlation with UGT2B17 levels. These are just some of the methods which could address the observed UGT2B17 mRNA levels. Such regulation and expression patterns could have important implications for clinical treatments that use drugs predominantly glucuronidated by UGT2B17, and further studies based on these observations are currently under way in the Lazarus laboratory.

Similar to UGT2B17, studies suggest that UGT1A10, one of the most active UGTs for SAHA, may also have hormone associated or inducible regulation factors. It has been suggested that UGT1A10 is regulated by Ahs (172, 277, 278), and that similar to UGT2B17 is regulated by hormones (176). Before examination of the specific mechanism inducing UGT1A10 expression, a screen for polymorphisms in the 2000 bp up stream of the ATG translational start site was conducted. This initial screen led to the identification of a novel 1664 bp deletion which was identified to have an allelic prevalence of 0.022 in whites and 0.056 in blacks. This UGT1A10 deletion promoter variant, along with a C>G SNP located -1271 bp upstream of the UGT1A10 ATG translational start site were included in the investigation of UGT1A10 induction.

Examination of UGT1A10 regulation and induction were tested using various regions of the UGT1A10 5' UTR inserted directly in front of the luciferase gene in the pGL3-Basic vector. These different size vectors exhibited altered expression in Caco-2 cells with 441 bp of wild-type UGT1A10 UTR exhibiting maximal luciferase activity relative to the wild-type 2204 bp construct. The deletion containing constructs exhibit significantly greater luciferase activity relative to the wild-type 2204 bp construct. These

data are consistent with similar studies of the UGT1A10 UTR (165) and support that a repressor element may reside within the deleted region of the UGT1A10 promoter. This suggests that individuals with the UGT1A10 promoter deletion may express UGT1A10 at higher levels. These individuals may glucuronidate drugs more rapidly and therefore may require a higher dose. Conversely, these individuals may glucuronidate carcinogens, such as NNAL or B[a]P, therefore more rapidly reducing the amount of exposure of tissue to carcinogens and ultimately reducing cancer susceptibility. This type of protective phenotype for a variant UGT has been observed for the UGT1A10*2 variant which is associated with reduced risk for orolaryngeal carcinoma, a cancer correlated with carcinogen exposure (203).

To further examine these initial observations, we tested lung cell lines to see if a similar pattern of luciferase induction was observed. Unlike the Caco-2 cells, there was no significant difference among the UGT1A10 wild-type or deletion containing constructs. This observation of cell line specific-expression regulated by UGT1A10 is consistent with endogenous UGT1A10 tissue specific expression (136).

Based on the observed difference between cell lines, we proposed that UGT1A10 may require induction by hormones or exogenous compounds to observe maximal expression. In the present study, no induction of the UGT1A10 wild-type or deletion containing luciferase vector was achieved when UGT1A10 luciferase construct containing cells (lung- and colon- derived) were treated with Ah's. UGT1A10 induction by Ahs was a novel attempt and therefore, we wanted to test our constructs overall ability to be induced. To test this, we used MCF7 cells that were shown to induce endogenous UGT1A10 via exposure to estradiol. The UGT1A10 luciferase constructs

did not induce UGT1A10 and luciferase activity in the presence of E₂ despite the positive control showing that E₂ induction of luciferase was occurring. This discrepancy could be interpreted in different ways. One possibility is that the constructs do not contain the regions required for regulation and that larger segments of the UTR are necessary. Another possibility is that regulation is occurring at different levels (DNA folding, methylation) and that a vector is not accurately representing these other factors necessary for expression. Studies examining larger regions of the UGT1A10 UTR or studies of endogenous UGT1A10 in cell lines may further the understanding of UGT1A10 regulation and induction.

Together, these data suggest that UGT1A10 is differentially expressed and that large regions of the DNA are utilized and/or complex regulatory mechanisms are necessary to regulate UGT1A10 and additional studies should be conducted to address these possibilities. Since UGT1A10 has been suggested to be regulated by E₂; it would be interesting to examine UGT1A10 expression at different points in the female menstrual cycle and in pre- versus post- menopausal women. Also, UGT1A10 is an important detoxifier and eliminator of drugs and carcinogens in the body and alterations in its expression can have profound effects on individuals. Further examination of this region may expand the role of the newly identified UGT1A10 promoter deletion and its effect on UGT1A10 expression.

In conclusion, this dissertation has characterized the glucuronidation pathway for the promising chemotherapeutic agent, SAHA. These data provide support for the examination of UGT genotype and consideration of the gender of a patient when planning treatment with SAHA and when monitoring response and toxicity to SAHA. In

addition to the clinical implications of this work, insight has been gained into the regulation of some of the UGTs that most actively metabolize SAHA. Furthermore, these findings may have potential relevance to other glucuronidated substrates (drugs or carcinogens) and have implications for individual differences in response to treatment or cancer susceptibility. Together, these data have enhanced the understanding of genetic differences that underlie altered glucuronidation which in turn contributes to the field of pharmacogenetics and aids in the development of personalized medicine.

APPENDIX A. Nucleotide Sugar Transporters

A.1 INTRODUCTION

Nucleotide sugar transporters (NSTs) are highly conserved transmembrane enzymes that transport nucleotide-sugars from the cytosol, where they are synthesized, to the lumen of the Golgi apparatus and the endoplasmic reticulum (298-300). The transfer of sugars is an essential step for the formation of glycoconjugates and the biosynthesis of polysaccharides (298). However, all studies to identify NSTs have been hampered by the need to use sugars that are radio-labeled and such compounds are limited (298). Individual NSTs transport multiple substrates and have substrate specificities that exhibit some overlap. Despite the redundancy from overlapping substrate specificities, some NST variants have been linked to human disease.

The first human NST to be linked to a disease phenotype was the GDP-fucose transporter (301). The original report identified a point mutation in the GDP-fucose transporter to be responsible for Leukocyte Adhesion Deficiency II (LAD II) which is characterized by impaired immune response and retarded growth, in addition to the lack of fucosylated glycoconjugates (301, 302). Earlier studies to try to understand the molecular basis of this disease examined the enzymes involved in the biosynthesis and transfer of fucose but found no direct link (303-305). However, cells from patients with LAD II had reduced GDP-fucose in the Golgi vesicles (305) which led to the hypothesis that an NST was linked to the decrease. Luhn et al. (2001) were the first to identify the human GDP-fucose transporter and the point mutation C439T, which results in the

amino acid change R147C, responsible for the LAD II phenotype (301). Similarly, another group identified a novel point mutation in the GDP-fucose transporter (C923G, resulting in the amino acid change T308R) in a LAD II patient (302). Interestingly, these distinct variants of the GDP-fucose transporter in patients resulted in differential response to treatment (304, 306, 307). In addition to the variant of the GDP-fucose transporter, a genetic variation located in the donor splice site of intron 6 (IVS6 + 1G>A) of the CMP-sialic acid transporter has also been linked to human disease (308). The association of these two NST variants with disease states supports the important role of the proper transportation of sugars in maintaining health.

Recently, four human NSTs, UGTrel1, UGTrel7, YEA4 and its splice variant YEA4S, have been identified to be responsible for the transport of UDPGA (309, 310). Transport of UDPGA, into the lumen of the endoplasmic reticulum, is necessary for glucuronidation because this is the site of the UGT catalytic domain (310, 311). Conjugation of UDPGA to substrates is an important process for detoxification and excretion of many endogenous and exogenous compounds (128, 312, 313). Variants of the enzymes responsible for glucuronidation, UGTs, have been linked to human disease, altered drug response, and risk for cancer (123, 129, 196, 199, 228, 256, 314, 315). Previous studies using urine analysis data have identified a wide range of glucuronidation abilities among individuals (283, 316). Therefore, it is possible that variants of the enzymes that transport the necessary co-substrate for the glucuronidation reaction are altering the ability to glucuronidate.

Four NSTs responsible for transfer of UDPGA have been identified and have been preliminarily characterized *in vitro*. UGTrel1, also known as SLC35B1 (solute

carrier family 35, member B1), is located on chromosome 17q21.33, contains 9 exons and transports UDP-Gal/GlcNAc/CMP-Sia/GlcA (298). UGTrel7, also known as SLC35D1, is located on 1p31, contains 11 exons, and transports UDP-GlcNAc/GlcA/Gal (317, 318). YEA4, also known as SLC35B4, is located on 7p31, contains 10 exons and transports UDP- Xyl/GlcA/GlcNAc (309). However, these enzymes are responsible for the transfer of multiple substrates and have not been fully characterized. For example, these NSTs all have the ability to transfer UDPGA, however, it is not known which NST is able to transfer the substrate most efficiently, whether or not these enzymes are differentially expressed in tissues, or whether variants exist that would alter the abilities to transport UDPGA into the lumen.

Since transportation of the co-substrate, UDPGA, precedes the glucuronidation of substrates, the ability to transfer UDPGA could be rate limiting and affect the efficacy of all UGTs to catalyze the glucuronidation of substrates. This important aspect of the glucuronidation pathway has yet to be fully characterized. Based on the important role that NSTs play upstream in the glucuronidation pathway, we hypothesize that alterations in the NSTs responsible for UDPGA transport may alter an individual's overall ability to glucuronidate compounds.

With the ultimate goal of identifying a genotype/phenotype correlation, a study was designed to identify NST variants to correlate with *in vivo* glucuronidation in humans. This study set out to determine if SNPs in the NSTs that transfer UDPGA alter the overall ability to glucuronidate substrates starting with the assessment of NNAL-glucuronide formation. NNAL is a byproduct of tobacco smoke, and urine samples

containing NNAL glucuronide were available along with matching genomic DNA. The preliminary results of this study are discussed below.

A.2 MATERIALS AND METHODS

A.2.1 Identification of SNPs

NSTs including: UGTrel7, also known as SLC35D1 (gi:14028875), UGTrel1, also known as SLC35B1 (gi: 5032213), and YEA3, also known as SLC35B4 (gi: 89161213) were analyzed for nonsynonymous SNPs using the HapMap data base. Haploview (Broad Institute, Boston) was used to analyze the haplotypes of each NST.

A.2.2 DNA samples

For optimization of the SNaPshot assay, genomic DNA from individuals who were participants in previous studies of genetic polymorphisms was used (281-283). As previously described, subjects were healthy adult smokers ranging in age from 21 – 50 years (283). They were recruited in Mount Vernon, New York, a community that had a population of 55% black and 40% white; a factor important to the original study of ethnic differences in carcinogen metabolism. DNA was isolated from patients' blood samples as previously described (281).

A.2.3 Multiplex PCR assay

Primers were designed to amplify 5 individual regions surrounding the SNPs of interest in a multiplex PCR reaction. Table A.1 lists the primer names, primer sequences, base pair changes, expected amplicon sizes and amino acid changes. These primers were tested for compatibility in the same PCR reaction using the web tool, FastPCR.

Multiplex PCR amplification was carried out using the Qiagen Multiplex PCR kit. Reactions (25 μ L) were performed in 0.5 mL tubes in a MyCycler (BioRad, Hercules, CA) with incubations performed at 95°C for 15 min; 40 cycles of 94°C for 30 sec, 60°C for 1min 30 s, 72°C for 1min; and a final extension of 72°C for 10 min . Reactions included Qiagen Multiplex PCR Mater Mix (1 X final concentration; Qiagen), 0.2 μ M of each primer, 0.5x Q-solution and 2 ng of DNA. PCR reaction products were separated on 1.5% agarose gels.

Name	Base pare	Amino acid	Primer (5' to 3')	Product size
rel728491020F	A>G (+1017)	Tyr329His	5' TGAAGCAATCCTCTGGTCAC 3'	251
rel728491020R			5' TGAATTTCCCCACTGTGAAAC3'	
rel710157422F	C>T (+276)	Ala82Thr	5' CTAGACTGGGCAATTTTGAGG 3'	305
rel710157422R			5' TGGCCAGGTTAGTTGGAATC 3'	
rel111552690F	A>C (+1023)	Asn312Lys	5' CAGTCCCATATTCCTATTAAGTCCA 3'	324
rel111552690R			5' ATCCTGGTGCCATTCTCTTG3'	
rel11135034F	G>A (+329)	Arg81His	5' TTCATGTGGCTTCAGCTTTG 3'	204
rel11135034R			5' AGACCATGGCACCCAGATAG 3'	
rel111552686F	C>T (+134)	Pro16Leu	5' CTCATGGCCTCTAGCAGCTC 3'	272
rel111552686R			5' TGGAATTCTGGGTAGGCTCA 3'	

Table A.1: Summary table of nonsynonymous NSTs. Table includes names of primers, locations of SNPs with base pair changes, the resulting amino acid changes, the sequences of the primers used to amplify regions around each SNP and the product sizes of amplified regions.

A.2.4 SNaPshot Assay for SNPs

Figure A.1 is an illustration of the overall procedure for the SNaPshot assay. Probes for the SNaPshot assay were designed to bind 1 nucleotide upstream or downstream of the SNP and are listed in Table A.2. Template DNA was prepared by multiplex PCR amplification, after which reactions were incubated with 5 units of SAP and 2 units of Exo I and incubated at 37°C for 1 h and then inactivated by incubation at 75°C for 15 min. Digested products (3 µL) were added to SNaPshot multiplex ready reaction mix (final concentration 1x; ABI), and 1 µL of pooled SNaPshot primers (0.2 µM each) in a total volume of 10 µL. Incubations were performed using rapid thermal ramp for 25 cycles of 96°C for 10 sec, 50°C for 5 s, 60°C for 30 s and then holding at 4°C until post-extension treatment. To this amplified reaction mix, 1 U of SAP was added and incubated at 37°C for 1 h followed by deactivation of the enzyme by incubating at 75°C for 15 min.

To prepare samples for analysis, 0.5 µL of SNaPshot product, described above, and 0.5 µL of GeneScan-120 LIZ size standard were added to 9 µL Hi-Di formamide. Samples were run by the Molecular Genetics/DNA Sequencing and SNPlex Core at the Penn State College of Medicine on the ABI Prism 3700 DNA analyzer. Data was analyzed using GeneScan analysis software version 3.1 with the GeneScan-120 LIZ size standard analysis parameter files (ABI).

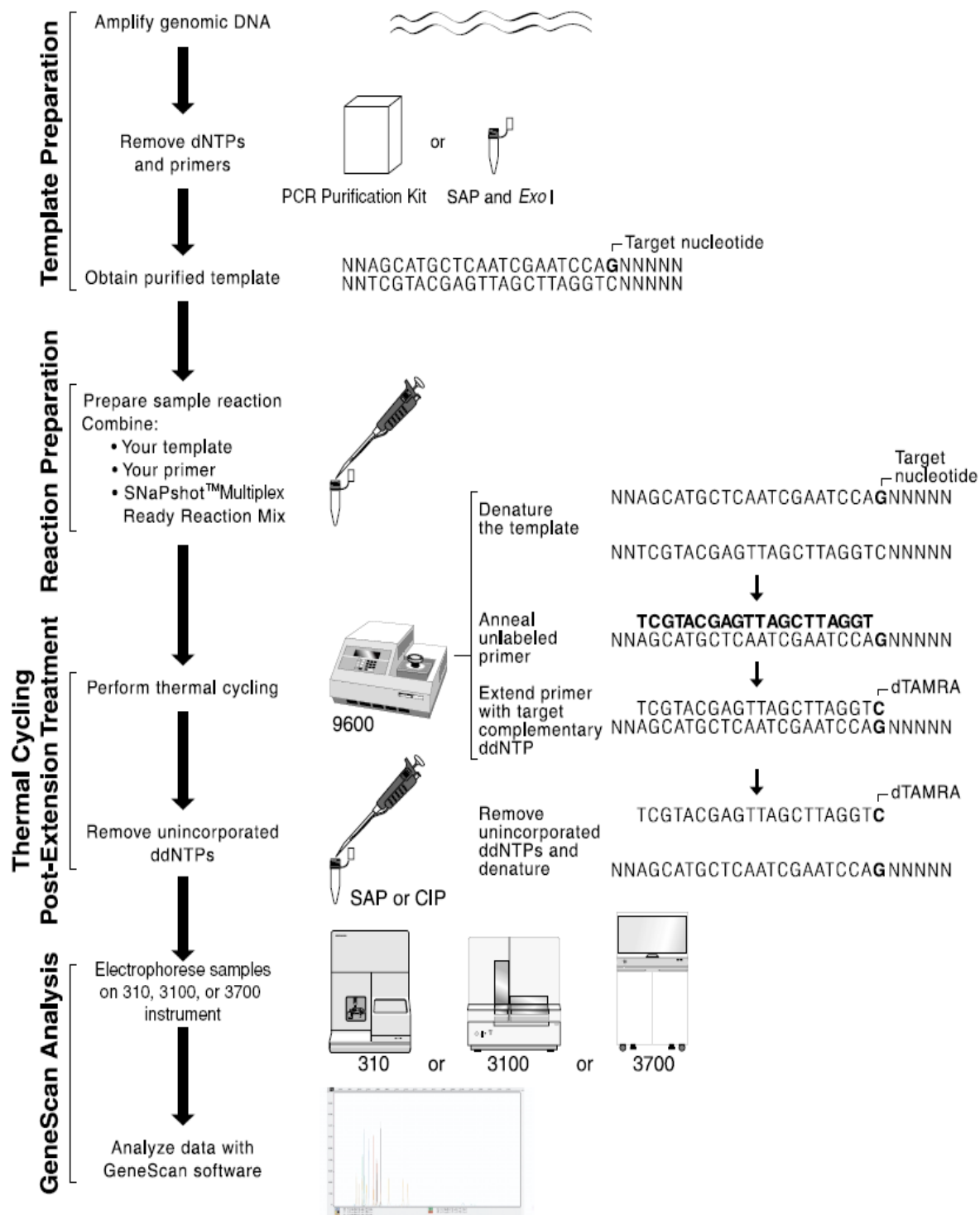


Figure A.1: Overview of SNaPshot procedure.
[Reference from AppliedBiosystems].

Name	Base pare	Amino acid	Probe (5' to 3')
UGTrel7rs28491020P	A>G (+1017)	Tyr 329His	AAAAACTGGGAGCCTGGTATATTCC
UGTrel7rs10157422P	C>T (+276)	Ala82Thr	TGTGTTCTCTTGTTTACAGATGGTG
UGTrel1rs11552690P	A>C (+1023)	Asn312Lys	GACTGACTGACTGACTGACTGTCTTCTTAGCTCCTTTCCCAA
UGTrel1rs1135034P	G>A (+329)	Arg81His	GACTGACTGACTGACTGACTGACTAGCCAGCTCCGGCTA
UGTrel1rs11552686P	C>T (+134)	Pro16Leu	AAAGACACCCAGGAAGCAG

Table A.2: Summary table of probes used for NST variant analysis. Table includes names of probes, locations of SNPs with base pair changes, the resulting amino acid changes, the sequences of the probes that bound one nucleotide upstream or downstream of the SNPs.

A.3 RESULTS

A.3.1 Identification of SNPs

The sequence of the coding region of each NST, along with 1000 kb upstream and downstream of the coding region, was identified in HapMap to examine known SNPs. The SNP data was exported to the Haploview program (Broad Institute) to determine tagging SNPs for haplotype analysis. Figure A.2 (A-C) shows the linkage disequilibrium plot for each NST; YEA4S is not illustrated because it is a splice variant of YEA4. In summary, UGTrel1 was composed of one haplotype block and had two tagging SNPs (rs2304917, rs2289601), UGTrel7 was composed of 2 haplotype blocks and had 9 tagging SNPs (rs2815359, rs10489633, rs2862728, rs12059957, rs1024228, rs10157422, rs2755259, rs12738583, rs2815359) and YEA4 was composed of one haplotype block and had 6 tagging SNPs (rs2504, rs1646694, rs12112626, rs13233589, rs12669902, rs722658).

As a result of the large number of SNPs necessary to analyze each gene, it was not feasible to conduct the haplotype analysis with our limited samples and therefore only the nonsynonymous SNPs were chosen for screening. Nonsynonymous SNPs include: UGTrel7 rs28491020 and rs10157422 and UGTrel1 rs11552690, rs1135034, and rs11552686; no nonsynonymous SNPs were identified for YEA4. A summary of the SNPs base pair changes along with the corresponding amino acid changes are found in Table A.2.

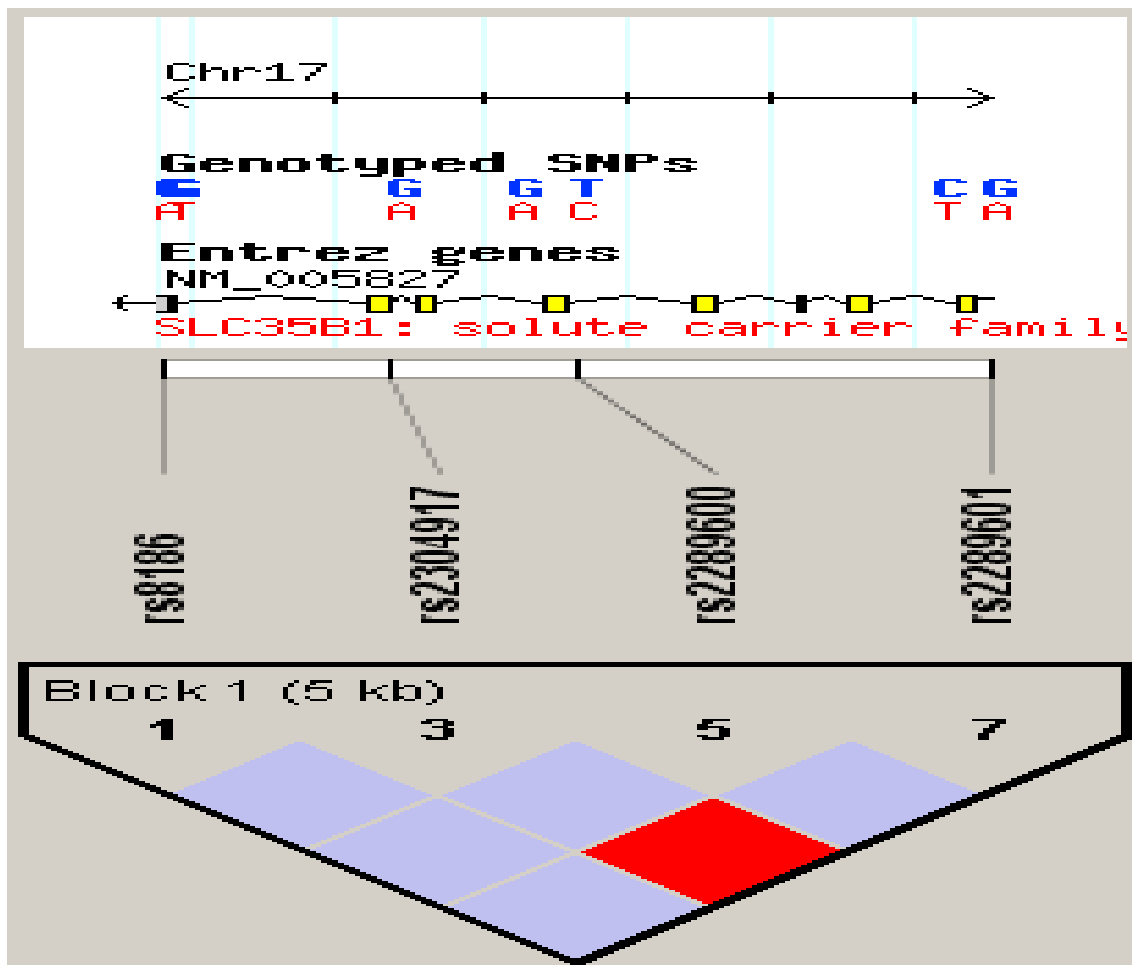


Figure A.2: Linkage Disequilibrium Plot of NSTs (A).

A. UGTrel 1 (SLC35B1)-two tagSNP one block



Figure A.2 Continued: Linkage Disequilibrium Plot of NSTs (B).
 B. UGTrel7 (SLC35D1) -9 or 11 (tagger) for 2 blocks

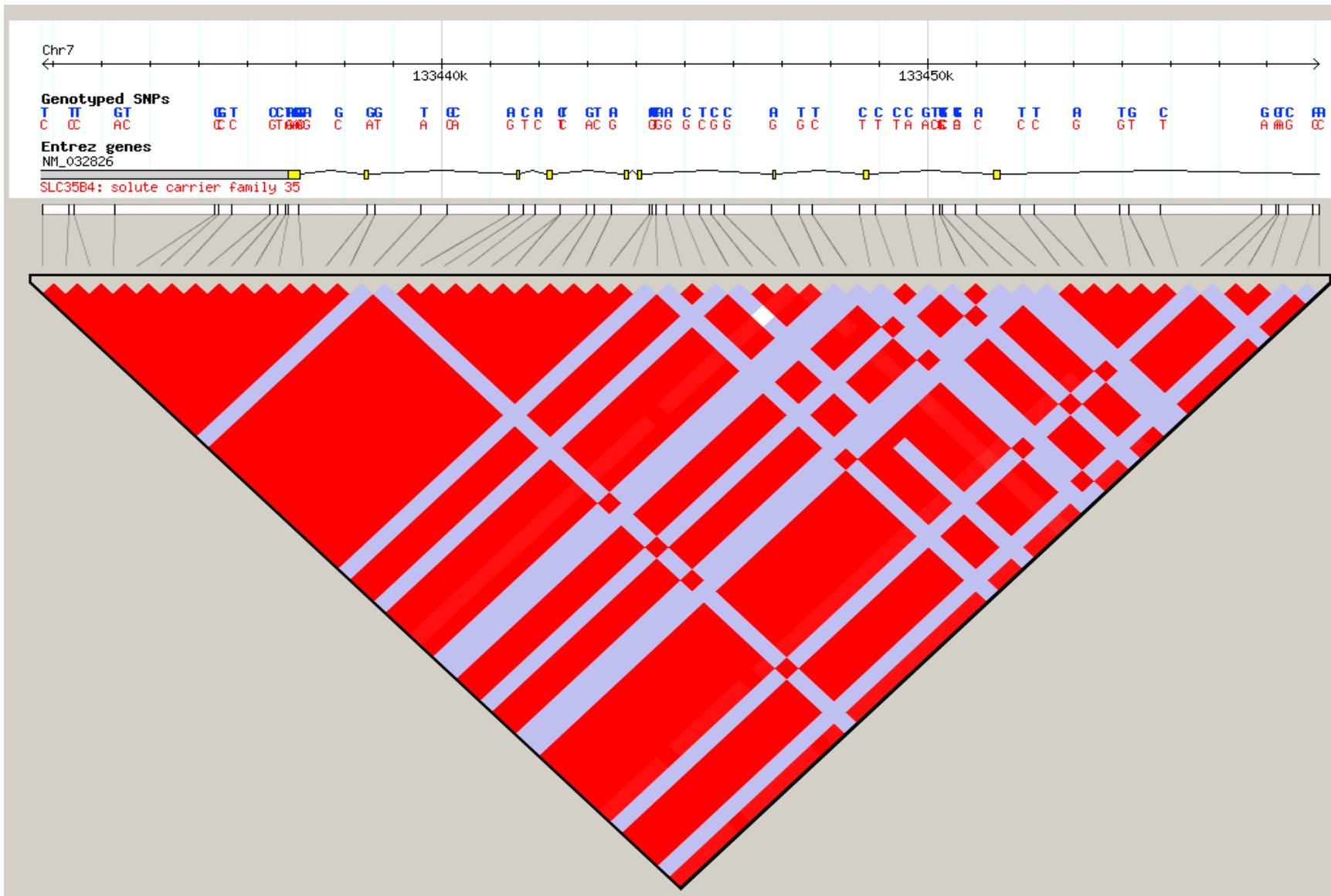


Figure A.2 Continued: Linkage Disequilibrium Plot of NSTs (C).
 C. YEA4 (SLC35B4; AJ315497) - One block 6 Tag SNPs (no coding)

A.3.2 Development of Multiplex PCR Assay to Analyze Nonsynonymous SNPs of the NSTs

A multiplex PCR assay was developed to minimize the amount of DNA necessary to analyze the nonsynonymous SNPs of all 5 NSTs. Five primer sets were designed to be used in combination to amplify all regions of interest in one PCR assay. Figure A.3 illustrates each primer set run separately and all sets run together; in addition, it shows the results from the use of various concentrations of DNA (2 ng to 10 ng) and the affect of an optional buffer (Q solution) on amplification. These data show that all primer sets amplify the DNA fragment of expected size, 2 ng of DNA was sufficient to yield detectable bands, and the addition of Q solution increases amplification efficiency. To further confirm correct amplification, bands were excised, purified, and sequenced. Each band was 100% homologous to the NST region of interest.

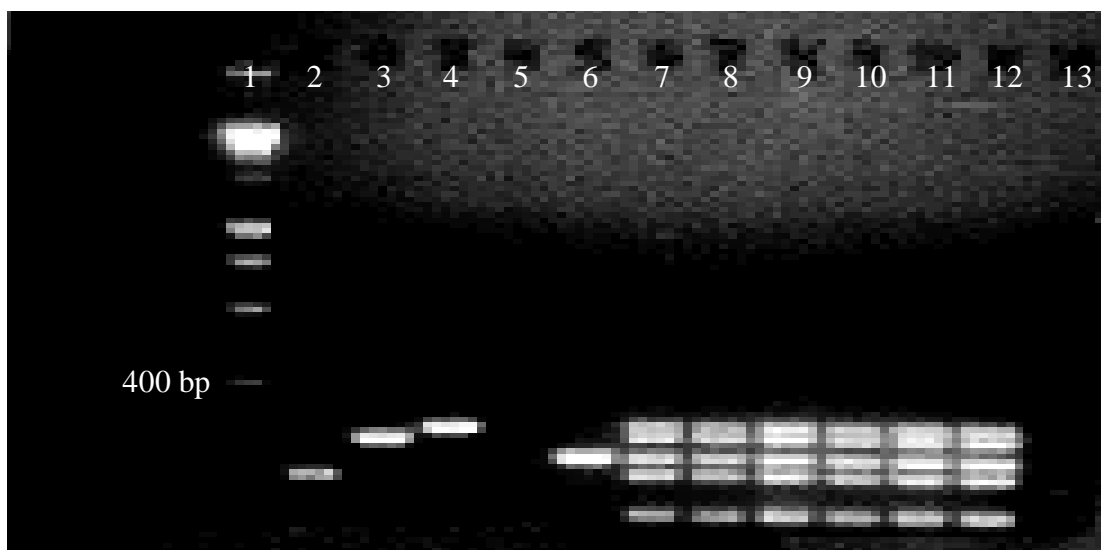


Figure A.3: Agarose gel of amplicons from PCR of NSTs. Lane1: DNA ladder; Lane2: UGTrel7rs28491020, 251 bp; Lane3: UGTrel7rs10157422, 305 bp; Lane4: UGTrel1rs11552690, 324 bp; Lane 5*: UGTrel1rs1135034, 204 bp; Lane 6: UGTrel1rs11552686, 272 bp. Lanes 7 and 8: 2 ng DNA, with solution Q and without solution Q, respectively; Lanes 9 and 10: 5 ng DNA, with solution Q and without solution Q, respectively; Lanes 11 and 12: 10 ng DNA, with solution Q and without solution Q, respectively; and Lane 13: water control. *Due to experimental error, the expected 204 bp band in lane 5 did not amplify; however, lanes 7-12 have amplification of the expected band (smallest fragment).

A.3.3 Optimization of SNaPshot Assay for SNPs

In order to assess multiple SNPs in different regions in the same assay, the SNaPshot system from ABI was used. This assay is designed to use genomic PCR amplicons that include SNPs of interest to which probes then bind to either one nucleotide upstream or downstream of the SNP. Detection of the SNP nucleotide is based on size of probe and the fluorescently labeled nucleotide which complements the SNP of interest. Therefore, primer size and the SNP nucleotide possibilities were considered when designing probes for this assay. The SNaPshot system can screen up

to 10 SNPs in one assay; however, the current study was optimized for 5 SNPs. Probes of varying lengths were designed (Table A.2). Probe UGTrel7rs28491020P, is 25 base pairs in length and is the reverse complement of the original sequence therefore detecting the T>C transition; in addition, probe UGTrel7rs10157422P is also 25 base pairs in length and is the reverse compliment of the original sequence; however, it detects the a G>A transition. Although these probes are similar in length, the different base pair composition and thus size will allow for identification of the correct SNP without confusion. The following probes were used to detect the UGTrel1 SNPs: UGTrel1rs11552690P, detecting an A>C transversion, is 43 base pairs in length; UGTrel1rs1135034P, (reverse complement) detecting a C>T transversion, is 39 base pairs in length; and UGTrel1rs11552686P, detecting a C>T transversion, is 19 base pairs in length. Figure A.4 illustrates chromatographs of each probe analyzed separately; panel A and D represent samples that are heterozygous for that SNP.

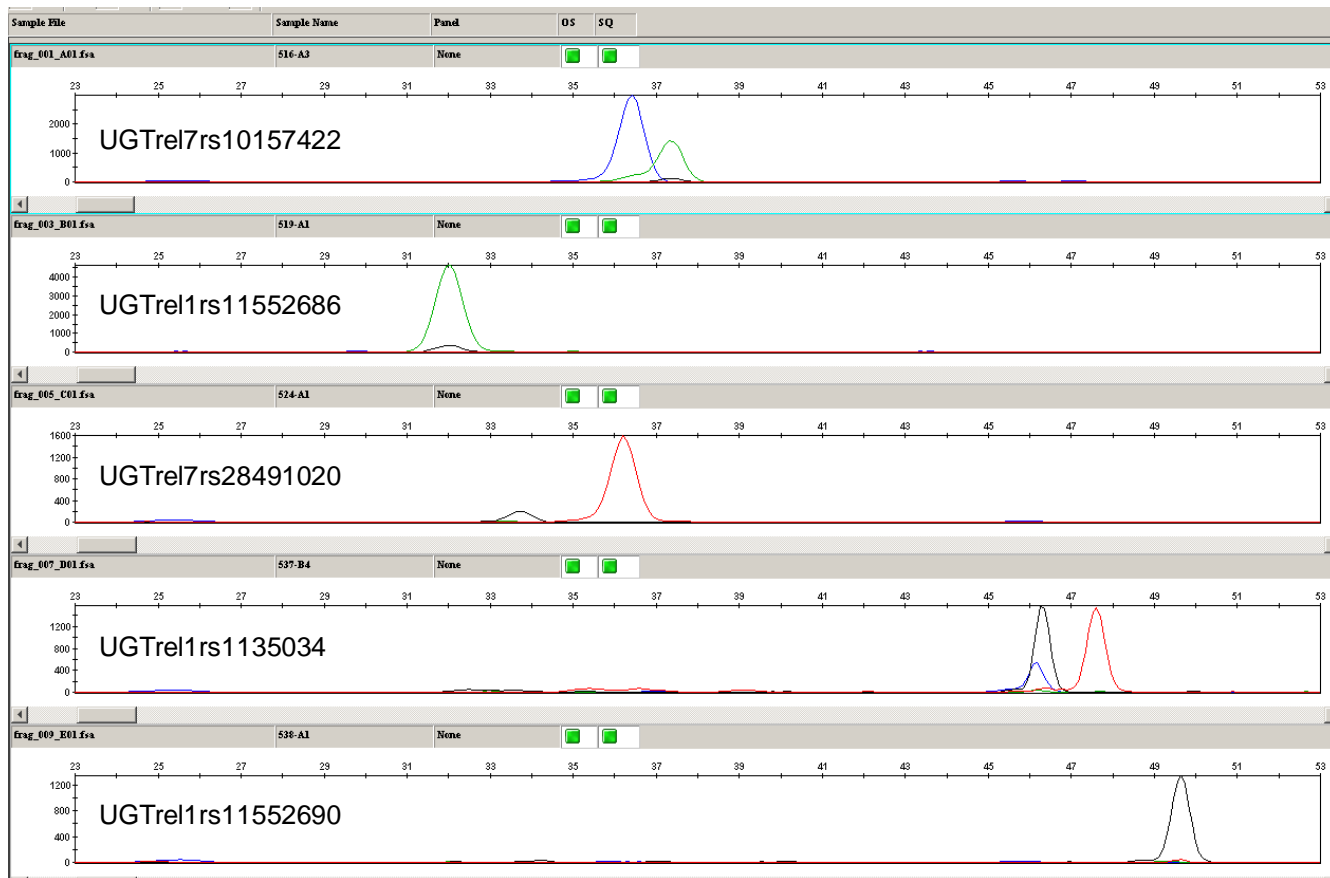


Figure A.4: SNaPshot chromatograms of individually run NST SNP analysis.

Each chromatogram is labeled with the NST name and SNP rs number. The Y axis is absorbance and the X axis is the base pair size (NOTE: Sizes on the scale are not representative of actual fragment size due to the column used). Each peak color represents a nucleotide (Red = Thymine; Green=Adenine; Blue=Guanine; Black=Cytosine)

After each probe was tested individually, the samples were analyzed using all of the probes. Figure A.5 (A-C) are representative of the chromatograms for 3 samples. In the samples we screened (n=30), SNPs UGTrel7rs10157422 and UGTrel1rs1135034 were identified to have the variant allele. No other SNP screened exhibited the variant allele. Once the probes and detection method were shown to work in the combined assay, it was then necessary to optimize the method for automated allele discrimination. This required the addition of the Genescan 120 LIZ size standard which is a five dye-labeled size standard that allows reproducible sizing of small fragments and automated data analysis. This optimization of the automatic allelic discrimination could not be completed due to constraints in sample amount.

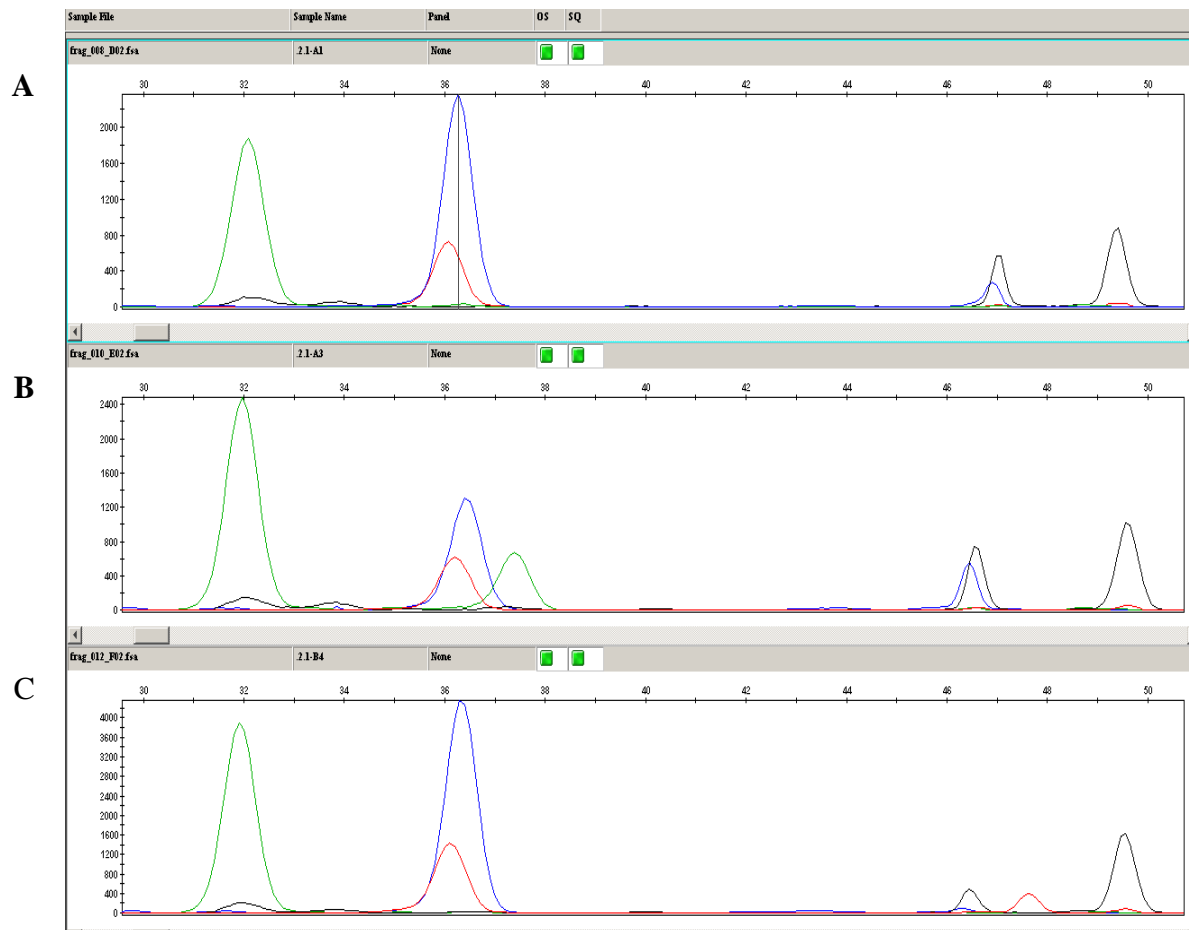


Figure A.5: Chromatograms of multiplex SNaPshot analysis. The Y axis is absorbance and the X axis is the base pair size (NOTE: Sizes on the scale are not representative of actual fragment size due to column used). Each peak color represents a nucleotide (Red = Thymine; Green=Adenine; Blue=Guanine; Back=Cytosine). The blue peak at position 46.5 is a background peak. A) Representing a sample homozygous wild-type for all alleles. B) Representing a sample that is heterozygous for UGTrel7rs10157422 (T/A) and wild-type for other alleles. C) Representing a sample that is heterozygous for UGTrel1rs1135034 (C/T) and wild-type for other alleles.

A.4 SUMMARY

The ultimate goal of this study was to determine if there is a genotype/phenotype correlation between genetic variants of NSTs that are responsible for UDPGA transport and glucuronide formation. To address this goal, two initial experiments were designed including the identification of genetic variants of the NSTs and the development and optimization of a method that would utilize minimal amounts of DNA to screen for genetic variations in the NSTs responsible for UDPGA transfer. The genetic analysis from this first set of experiments would have then been correlated with the amount of NNAL-glucuronide produced in urine from smokers. This preliminary study would have been the model for future studies to assess differences in overall glucuronidation that result from genetic variation of NSTs.

Genetic variations can be assessed by individual SNPs, whole gene variation, and whole genome variation. This study set out to determine if there were functional genetic variants of the NST genes that transfer UDPGA; therefore developing an assay which would detect the known amino acid changing variants was required to test our hypothesis. The haplotypes of each of the 4 NST genes were determined and tagging SNPs were identified. Analysis of the haplotypes of the 4 NSTs identified 17 tagging SNPs necessary for NST genotyping, which was more than our genotyping methods could feasibly assess.

We originally designed the experiment to look at gene-wide variation via haplotype analysis because this method characterizes the whole region including introns, exons, and SNPs that may not have been identified previously (319). Although

this method is optimal to initially assess the genes, it is limited because it cannot directly identify the SNP(s) responsible for the phenotype and therefore more characterization of the loci would be required (319, 320). An alternative and more traditional method for analyzing a genotype/phenotype correlation is to examine SNPs that result in alterations at the protein level. A total of 5 such nonsynonymous SNPs were identified for the NSTs of interest; a number more feasibly analyzed within our condition constraints.

Experimental constraints, including limited amounts of matched DNA/urine specimens and the number of SNPs that could be feasibly analyzed were factors in our project design. Although numerous genotyping methods are available, this study used SNaPshot multiplex system (ABI) to assess SNPs of interest. This is a primer extension-based method which has the advantage of screening up to 10 SNPs in one assay using minimal amounts of DNA. More traditional methods like RFLP or real-time PCR SNP assays would require PCR amplification of each SNP region. SNaPshot, on the other hand, allows for co-amplification of all regions and analysis of each SNP all in one assay, resulting in a reduction of the amount of DNA required, less preparation time, and greater cost effectiveness. Other methods like bead and microarray technologies are for larger scale analyses and would require more DNA and therefore were not optimal methods for this analysis.

Previous studies examining NSTs linked to human disease have used phenotypes of individuals to determine correlative genotypes (301, 308). Previous studies on *in vivo* glucuronidation have identified individuals with varying levels of glucuronidation (283, 316). Based on this information it was hypothesized that variants of NSTs may be responsible for varying levels of glucuronide formation *in vivo*. To test

this hypothesis, previously characterized data that identified individuals having variable abilities to glucuronidate NNAL was assessed (283, 316). The fact that this data was readily available made these samples ideal for our preliminary study on NST variants.

Our original hypothesis was to test a direct correlation between variant genotypes of NSTs and NNAL phenotype; however, there were limitations with the design of this study. First, the amount of DNA available for analysis was limited due to the high demand for these samples, making any large scale SNP screen impossible. This was the reason a haplotype analysis was not conducted for each gene and instead only nonsynonymous SNPs were examined. Secondly, there were only 150 DNA/urine matched specimens available which would make it difficult to assess low prevalence SNPs. Thirdly, data was only available for NNAL-glucuronide formation, which means that only smokers could be analyzed, which could possibly confound the data.

Minimal data exists on the characterization of the NSTs responsible for the transfer of UDPGA, with the only studies having been done in rats, mice, and yeast (309, 310, 317, 318, 321). This is an important area to address due to the vital role glucuronidation plays in humans (196, 198, 228). Although the direct goal of this project was to identify a genotype/phenotype with respect to NST function and glucuronidation, alternative methods could be used to characterize pathways upstream of the UGTs in the glucuronidation pathway. Human *in vitro* systems would aid in the understanding of links between NSTs and glucuronidation. For example, one could analyze each NST individually as well as in combination to determine rates of UDPGA transport using primary human cells. Also, variants of NSTs could be assessed in these *in vitro* systems to see if they alter the ability to transport UDPGA. To further understand the importance

of NST transport of UDPGA to the process of glucuronidation, it is necessary to determine in which human tissue each NST is expressed to see if expression coincides with known glucuronidation activity (i.e. liver, colon, breast). Individual NST expression data may also aid in understanding which tissues, with active glucuronidation, would be most affected by alterations of these genes.

This present study set out to identify a genotype/phenotype correlation to further knowledge of the NSTs involved in UDPGA transport. This study was able to optimize a genotype assay for detection of NST variants; however, the genotype correlation with phenotype was not able to be assessed and no conclusions can be made. Although a final conclusion could not be made, this study has provided a system to assess NST genotypes for future studies. Any studies that characterize NSTs will aid in the understanding of the glucuronidation pathway. Altered UDPGA transport could potentially have significant effects on phase II metabolism via glucuronidation. This could alter the overall ability to metabolize endogenous and exogenous compounds which could lead to increased cancer risk or altered drug response as seen with defects in glucuronidation due to UGT variants.

REFERENCES

1. Simon, R. Development and Validation of Biomarker Classifiers for Treatment Selection. *J Stat Plan Inference*, 138: 308-320, 2008.
2. Wang, S. J. Utility of adaptive strategy and adaptive design for biomarker-facilitated patient selection in pharmacogenomic or pharmacogenetic clinical development program. *J Formos Med Assoc*, 107: 19-27, 2008.
3. Stein, C. M. and Elston, R. C. Finding genes underlying human disease. *Clin Genet*, 75: 101-106, 2009.
4. Frazer, K. A., Ballinger, D. G., Cox, D. R., Hinds, D. A., Stuve, L. L., Gibbs, R. A., Belmont, J. W., Boudreau, A., Hardenbol, P., Leal, S. M., Pasternak, S., Wheeler, D. A., Willis, T. D., Yu, F., Yang, H., Zeng, C., Gao, Y., Hu, H., Hu, W., Li, C., Lin, W., Liu, S., Pan, H., Tang, X., Wang, J., Wang, W., Yu, J., Zhang, B., Zhang, Q., Zhao, H., Zhao, H., Zhou, J., Gabriel, S. B., Barry, R., Blumenstiel, B., Camargo, A., Defelice, M., Faggart, M., Goyette, M., Gupta, S., Moore, J., Nguyen, H., Onofrio, R. C., Parkin, M., Roy, J., Stahl, E., Winchester, E., Ziaugra, L., Altshuler, D., Shen, Y., Yao, Z., Huang, W., Chu, X., He, Y., Jin, L., Liu, Y., Shen, Y., Sun, W., Wang, H., Wang, Y., Wang, Y., Xiong, X., Xu, L., Wayne, M. M., Tsui, S. K., Xue, H., Wong, J. T., Galver, L. M., Fan, J. B., Gunderson, K., Murray, S. S., Oliphant, A. R., Chee, M. S., Montpetit, A., Chagnon, F., Ferretti, V., Leboeuf, M., Olivier, J. F., Phillips, M. S., Roumy, S., Sallee, C., Verner, A., Hudson, T. J., Kwok, P. Y., Cai, D., Koboldt, D. C., Miller, R. D., Pawlikowska, L., Taillon-Miller, P., Xiao, M., Tsui, L. C., Mak, W., Song, Y. Q., Tam, P. K., Nakamura, Y., Kawaguchi, T., Kitamoto, T., Morizono, T., Nagashima, A., Ohnishi, Y., Sekine, A., Tanaka, T., Tsunoda, T., Deloukas, P., Bird, C. P., Delgado, M., Dermitzakis, E. T., Gwilliam, R., Hunt, S., Morrison, J., Powell, D., Stranger, B. E., Whittaker, P., Bentley, D. R., Daly, M. J., de Bakker, P. I., Barrett, J., Chretien, Y. R., Maller, J., McCarroll, S., Patterson, N., Pe'er, I., Price, A., Purcell, S., Richter, D. J., Sabeti, P., Saxena, R., Schaffner, S. F., Sham, P. C., Varilly, P., Altshuler, D., Stein, L. D., Krishnan, L., Smith, A. V., Tello-Ruiz, M. K., Thorisson, G. A., Chakravarti, A., Chen, P. E., Cutler, D. J., Kashuk, C. S., Lin, S., Abecasis, G. R., Guan, W., Li, Y., Munro, H. M., Qin, Z. S., Thomas, D. J., McVean, G., Auton, A., Bottolo, L., Cardin, N., Eyheramendy, S., Freeman, C., Marchini, J., Myers, S., Spencer, C., Stephens, M., Donnelly, P., Cardon, L. R., Clarke, G., Evans, D. M., Morris, A. P., Weir, B. S., Tsunoda, T., Mullikin, J. C., Sherry, S. T., Feolo, M., Skol, A., Zhang, H., Zeng, C., Zhao, H., Matsuda, I., Fukushima, Y., Macer, D. R., Suda, E., Rotimi, C. N., Adebamowo, C. A., Ajayi, I., Aniagwu, T., Marshall, P. A., Nkwodimmah, C., Royal, C. D., Leppert, M. F., Dixon, M., Peiffer, A., Qiu, R., Kent, A., Kato, K., Niikawa, N., Adewole, I. F., Knoppers, B. M., Foster, M. W., Clayton, E. W., Watkin, J., Gibbs, R. A., Belmont, J. W., Muzny, D., Nazareth, L., Sodergren, E., Weinstock, G. M., Wheeler, D. A., Yakub, I., Gabriel, S. B., Onofrio, R. C., Richter, D. J., Ziaugra, L., Birren, B. W., Daly, M. J., Altshuler, D., Wilson, R. K., Fulton, L. L., Rogers, J., Burton, J., Carter, N. P., Clee, C. M., Griffiths, M., Jones, M. C., McLay, K., Plumb, R. W., Ross, M. T., Sims, S. K., Willey, D. L., Chen, Z., Han, H., Kang, L., Godbout, M., Wallenburg, J. C., L'Archeveque, P., Bellemare, G., Saeki, K., Wang, H., An, D., Fu, H., Li, Q., Wang, Z., Wang, R., Holden, A. L., Brooks, L. D., McEwen, J. E., Guyer, M. S., Wang, V. O., Peterson, J. L., Shi, M., Spiegel, J., Sung, L. M., Zacharia, L. F., Collins, F. S., Kennedy, K., Jamieson, R. and

- Stewart, J. A second generation human haplotype map of over 3.1 million SNPs. *Nature*, 449: 851-861, 2007.
5. Beecham, G. W., Martin, E. R., Li, Y. J., Slifer, M. A., Gilbert, J. R., Haines, J. L., and Pericak-Vance, M. A. Genome-wide association study implicates a chromosome 12 risk locus for late-onset Alzheimer disease. *Am J Hum Genet*, 84: 35-43, 2009.
 6. Sun, J., Zheng, S. L., Wiklund, F., Isaacs, S. D., Li, G., Wiley, K. E., Kim, S. T., Zhu, Y., Zhang, Z., Hsu, F. C., Turner, A. R., Stattin, P., Liu, W., Kim, J. W., Duggan, D., Carpten, J., Isaacs, W., Gronberg, H., Xu, J., and Chang, B. L. Sequence variants at 22q13 are associated with prostate cancer risk. *Cancer Res*, 69: 10-15, 2009.
 7. Pankratz, N., Wilk, J. B., Latourelle, J. C., DeStefano, A. L., Halter, C., Pugh, E. W., Doheny, K. F., Gusella, J. F., Nichols, W. C., Foroud, T., and Myers, R. H. Genomewide association study for susceptibility genes contributing to familial Parkinson disease. *Hum Genet*, 124: 593-605, 2009.
 8. Potkin, S. G., Turner, J. A., Guffanti, G., Lakatos, A., Fallon, J. H., Nguyen, D. D., Mathalon, D., Ford, J., Lauriello, J., and Macciardi, F. A genome-wide association study of schizophrenia using brain activation as a quantitative phenotype. *Schizophr Bull*, 35: 96-108, 2009.
 9. Ruchat, S. M., Elks, C. E., Loos, R. J., Vohl, M. C., Weisnagel, S. J., Rankinen, T., Bouchard, C., and Perusse, L. Association between insulin secretion, insulin sensitivity and type 2 diabetes susceptibility variants identified in genome-wide association studies. *Acta Diabetol*, 2008.
 10. Eeles, R. A., Kote-Jarai, Z., Giles, G. G., Olama, A. A., Guy, M., Jugurnauth, S. K., Mulholland, S., Leongamornlert, D. A., Edwards, S. M., Morrison, J., Field, H. I., Southey, M. C., Severi, G., Donovan, J. L., Hamdy, F. C., Dearnaley, D. P., Muir, K. R., Smith, C., Bagnato, M., Ardern-Jones, A. T., Hall, A. L., O'Brien, L. T., Gehr-Swain, B. N., Wilkinson, R. A., Cox, A., Lewis, S., Brown, P. M., Jhavar, S. G., Tymrakiewicz, M., Lophatananon, A., Bryant, S. L., Horwich, A., Huddart, R. A., Khoo, V. S., Parker, C. C., Woodhouse, C. J., Thompson, A., Christmas, T., Ogden, C., Fisher, C., Jamieson, C., Cooper, C. S., English, D. R., Hopper, J. L., Neal, D. E., and Easton, D. F. Multiple newly identified loci associated with prostate cancer susceptibility. *Nat Genet*, 40: 316-321, 2008.
 11. Gold, B., Kirchoff, T., Stefanov, S., Lautenberger, J., Viale, A., Garber, J., Friedman, E., Narod, S., Olshen, A. B., Gregersen, P., Kosarin, K., Olsh, A., Bergeron, J., Ellis, N. A., Klein, R. J., Clark, A. G., Norton, L., Dean, M., Boyd, J., and Offit, K. Genome-wide association study provides evidence for a breast cancer risk locus at 6q22.33. *Proc Natl Acad Sci U S A*, 105: 4340-4345, 2008.
 12. Hunter, D. J., Kraft, P., Jacobs, K. B., Cox, D. G., Yeager, M., Hankinson, S. E., Wacholder, S., Wang, Z., Welch, R., Hutchinson, A., Wang, J., Yu, K., Chatterjee, N., Orr, N., Willett, W. C., Colditz, G. A., Ziegler, R. G., Berg, C. D., Buys, S. S., McCarty, C. A., Feigelson, H. S., Calle, E. E., Thun, M. J., Hayes, R. B., Tucker, M., Gerhard, D. S., Fraumeni, J. F., Jr., Hoover, R. N., Thomas, G., and Chanock, S. J. A genome-wide association study identifies alleles in FGFR2 associated with risk of sporadic postmenopausal breast cancer. *Nat Genet*, 39: 870-874, 2007.
 13. Thomas, G., Jacobs, K. B., Yeager, M., Kraft, P., Wacholder, S., Orr, N., Yu, K., Chatterjee, N., Welch, R., Hutchinson, A., Crenshaw, A., Cancel-Tassin, G., Staats, B. J., Wang, Z., Gonzalez-Bosquet, J., Fang, J., Deng, X., Berndt, S. I., Calle, E. E., Feigelson,

- H. S., Thun, M. J., Rodriguez, C., Albanes, D., Virtamo, J., Weinstein, S., Schumacher, F. R., Giovannucci, E., Willett, W. C., Cussenot, O., Valeri, A., Andriole, G. L., Crawford, E. D., Tucker, M., Gerhard, D. S., Fraumeni, J. F., Jr., Hoover, R., Hayes, R. B., Hunter, D. J., and Chanock, S. J. Multiple loci identified in a genome-wide association study of prostate cancer. *Nat Genet*, 40: 310-315, 2008.
14. Hom, G., Graham, R. R., Modrek, B., Taylor, K. E., Ortmann, W., Garnier, S., Lee, A. T., Chung, S. A., Ferreira, R. C., Pant, P. V., Ballinger, D. G., Kosoy, R., Demirci, F. Y., Kamboh, M. I., Kao, A. H., Tian, C., Gunnarsson, I., Bengtsson, A. A., Rantapaa-Dahlqvist, S., Petri, M., Manzi, S., Seldin, M. F., Ronnblom, L., Syvanen, A. C., Criswell, L. A., Gregersen, P. K., and Behrens, T. W. Association of systemic lupus erythematosus with C8orf13-BLK and ITGAM-ITGAX. *N Engl J Med*, 358: 900-909, 2008.
 15. Chang, Y. K., Yang, W., Zhao, M., Mok, C. C., Chan, T. M., Wong, R. W., Lee, K. W., Mok, M. Y., Wong, S. N., Ng, I. O., Lee, T. L., Ho, M. H., Lee, P. P., Wong, W. H., Lau, C. S., Sham, P. C., and Lau, Y. L. Association of BANK1 and TNFSF4 with systemic lupus erythematosus in Hong Kong Chinese. *Genes Immun*, 2009.
 16. Kelly, J. A., Moser, K. L., and Harley, J. B. The genetics of systemic lupus erythematosus: putting the pieces together. *Genes Immun*, 3 *Suppl 1*: S71-85, 2002.
 17. Gray-McGuire, C., Moser, K. L., Gaffney, P. M., Kelly, J., Yu, H., Olson, J. M., Jedrey, C. M., Jacobs, K. B., Kimberly, R. P., Neas, B. R., Rich, S. S., Behrens, T. W., and Harley, J. B. Genome scan of human systemic lupus erythematosus by regression modeling: evidence of linkage and epistasis at 4p16-15.2. *Am J Hum Genet*, 67: 1460-1469, 2000.
 18. Grumet, F. C., Coukell, A., Bodmer, J. G., Bodmer, W. F., and McDevitt, H. O. Histocompatibility (HL-A) antigens associated with systemic lupus erythematosus. A possible genetic predisposition to disease. *N Engl J Med*, 285: 193-196, 1971.
 19. Karassa, F. B., Bijl, M., Davies, K. A., Kallenberg, C. G., Khamashta, M. A., Manger, K., Michel, M., Piette, J. C., Salmon, J. E., Song, Y. W., Tsuchiya, N., Yoo, D. H., and Ioannidis, J. P. Role of the Fcgamma receptor IIA polymorphism in the antiphospholipid syndrome: an international meta-analysis. *Arthritis Rheum*, 48: 1930-1938, 2003.
 20. Karassa, F. B., Trikalinos, T. A., and Ioannidis, J. P. The role of FcgammaRIIA and IIIA polymorphisms in autoimmune diseases. *Biomed Pharmacother*, 58: 286-291, 2004.
 21. Liu, C., Batliwalla, F., Li, W., Lee, A., Roubenoff, R., Beckman, E., Khalili, H., Damle, A., Kern, M., Furie, R., Dupuis, J., Plenge, R. M., Coenen, M. J., Behrens, T. W., Carulli, J. P., and Gregersen, P. K. Genome-wide association scan identifies candidate polymorphisms associated with differential response to anti-TNF treatment in rheumatoid arthritis. *Mol Med*, 14: 575-581, 2008.
 22. Takeuchi, F., McGinnis, R., Bourgeois, S., Barnes, C., Eriksson, N., Soranzo, N., Whittaker, P., Ranganath, V., Kumanduri, V., McLaren, W., Holm, L., Lindh, J., Rane, A., Wadelius, M., and Deloukas, P. A genome-wide association study confirms VKORC1, CYP2C9, and CYP4F2 as principal genetic determinants of warfarin dose. *PLoS Genet*, 5: e1000433, 2009.
 23. Turner, S. T., Bailey, K. R., Fridley, B. L., Chapman, A. B., Schwartz, G. L., Chai, H. S., Sicotte, H., Kocher, J. P., Rodin, A. S., and Boerwinkle, E. Genomic association analysis suggests chromosome 12 locus influencing antihypertensive response to thiazide diuretic. *Hypertension*, 52: 359-365, 2008.

24. Johnson, J. A., Boerwinkle, E., Zineh, I., Chapman, A. B., Bailey, K., Cooper-DeHoff, R. M., Gums, J., Curry, R. W., Gong, Y., Beitelshes, A. L., Schwartz, G., and Turner, S. T. Pharmacogenomics of antihypertensive drugs: rationale and design of the Pharmacogenomic Evaluation of Antihypertensive Responses (PEAR) study. *Am Heart J*, *157*: 442-449, 2009.
25. D'Andrea, G., D'Ambrosio, R. L., Di Perna, P., Chetta, M., Santacroce, R., Brancaccio, V., Grandone, E., and Margaglione, M. A polymorphism in the VKORC1 gene is associated with an interindividual variability in the dose-anticoagulant effect of warfarin. *Blood*, *105*: 645-649, 2005.
26. Lindh, J. D., Lundgren, S., Holm, L., Alfredsson, L., and Rane, A. Several-fold increase in risk of overanticoagulation by CYP2C9 mutations. *Clin Pharmacol Ther*, *78*: 540-550, 2005.
27. Wadelius, M., Chen, L. Y., Eriksson, N., Bumpstead, S., Ghorri, J., Wadelius, C., Bentley, D., McGinnis, R., and Deloukas, P. Association of warfarin dose with genes involved in its action and metabolism. *Hum Genet*, *121*: 23-34, 2007.
28. Wadelius, M., Chen, L. Y., Lindh, J. D., Eriksson, N., Ghorri, M. J., Bumpstead, S., Holm, L., McGinnis, R., Rane, A., and Deloukas, P. The largest prospective warfarin-treated cohort supports genetic forecasting. *Blood*, *113*: 784-792, 2009.
29. Kiyohara, C., Yoshimasu, K., Takayama, K., and Nakanishi, Y. NQO1, MPO, and the risk of lung cancer: a HuGE review. *Genet Med*, *7*: 463-478, 2005.
30. Hoffmann, D., Hoffmann, I., and El-Bayoumy, K. The less harmful cigarette: a controversial issue. a tribute to Ernst L. Wynder. *Chem Res Toxicol*, *14*: 767-790, 2001.
31. Spitz, M. R., Wei, Q., Dong, Q., Amos, C. I., and Wu, X. Genetic susceptibility to lung cancer: the role of DNA damage and repair. *Cancer Epidemiol Biomarkers Prev*, *12*: 689-698, 2003.
32. Lorenzo Bermejo, J. and Hemminki, K. Familial lung cancer and aggregation of smoking habits: a simulation of the effect of shared environmental factors on the familial risk of cancer. *Cancer Epidemiol Biomarkers Prev*, *14*: 1738-1740, 2005.
33. Czene, K., Lichtenstein, P., and Hemminki, K. Environmental and heritable causes of cancer among 9.6 million individuals in the Swedish Family-Cancer Database. *Int J Cancer*, *99*: 260-266, 2002.
34. Hemminki, K., Lonnstedt, I., Vaittinen, P., and Lichtenstein, P. Estimation of genetic and environmental components in colorectal and lung cancer and melanoma. *Genet Epidemiol*, *20*: 107-116, 2001.
35. Guo, Z., Peng, S., and Jiang, G. [A genetic epidemiological study on lung cancer]. *Zhonghua Yu Fang Yi Xue Za Zhi*, *30*: 154-156, 1996.
36. Prevalence and penetrance of BRCA1 and BRCA2 mutations in a population-based series of breast cancer cases. Anglian Breast Cancer Study Group. *Br J Cancer*, *83*: 1301-1308, 2000.
37. Wooster, R., Bignell, G., Lancaster, J., Swift, S., Seal, S., Mangion, J., Collins, N., Gregory, S., Gumbs, C., and Micklem, G. Identification of the breast cancer susceptibility gene BRCA2. *Nature*, *378*: 789-792, 1995.
38. Struwing, J. P., Hartge, P., Wacholder, S., Baker, S. M., Berlin, M., McAdams, M., Timmerman, M. M., Brody, L. C., and Tucker, M. A. The risk of cancer associated with specific mutations of BRCA1 and BRCA2 among Ashkenazi Jews. *N Engl J Med*, *336*: 1401-1408, 1997.

39. Tabori, U. and Malkin, D. Risk stratification in cancer predisposition syndromes: lessons learned from novel molecular developments in Li-Fraumeni syndrome. *Cancer Res*, *68*: 2053-2057, 2008.
40. Malkin, D., Li, F. P., Strong, L. C., Fraumeni, J. F., Jr., Nelson, C. E., Kim, D. H., Kassel, J., Gryka, M. A., Bischoff, F. Z., Tainsky, M. A., and et al. Germ line p53 mutations in a familial syndrome of breast cancer, sarcomas, and other neoplasms. *Science*, *250*: 1233-1238, 1990.
41. Klein, C. A. Parallel progression of primary tumours and metastases. *Nat Rev Cancer*, *9*: 302-312, 2009.
42. World Health Organization, W. Cancer, Fact sheet N297. July, 2008.
43. American Cancer Society, A. Cancer Facts & Figures, 2008. American Cancer Society, Atlanta, Georgia., 2008.
44. Marks, P., Rifkind, R. A., Richon, V. M., Breslow, R., Miller, T., and Kelly, W. K. Histone deacetylases and cancer: causes and therapies. *Nat Rev Cancer*, *1*: 194-202, 2001.
45. Phillips, D. M. The presence of acetyl groups of histones. *Biochem J*, *87*: 258-263, 1963.
46. Gregory, P. D., Wagner, K., and Horz, W. Histone acetylation and chromatin remodeling. *Exp Cell Res*, *265*: 195-202, 2001.
47. Deckert, J. and Struhl, K. Histone acetylation at promoters is differentially affected by specific activators and repressors. *Mol Cell Biol*, *21*: 2726-2735, 2001.
48. Kim, S. C., Sprung, R., Chen, Y., Xu, Y., Ball, H., Pei, J., Cheng, T., Kho, Y., Xiao, H., Xiao, L., Grishin, N. V., White, M., Yang, X. J., and Zhao, Y. Substrate and functional diversity of lysine acetylation revealed by a proteomics survey. *Mol Cell*, *23*: 607-618, 2006.
49. Xie, H., Bandhakavi, S., Roe, M. R., and Griffin, T. J. Preparative peptide isoelectric focusing as a tool for improving the identification of lysine-acetylated peptides from complex mixtures. *J Proteome Res*, *6*: 2019-2026, 2007.
50. Walkinshaw, D. R., Tahmasebi, S., Bertos, N. R., and Yang, X. J. Histone deacetylases as transducers and targets of nuclear signaling. *J Cell Biochem*, *104*: 1541-1552, 2008.
51. Yang, X. J. and Seto, E. HATs and HDACs: from structure, function and regulation to novel strategies for therapy and prevention. *Oncogene*, *26*: 5310-5318, 2007.
52. Lee, K. K. and Workman, J. L. Histone acetyltransferase complexes: one size doesn't fit all. *Nat Rev Mol Cell Biol*, *8*: 284-295, 2007.
53. Kimura, A., Matsubara, K., and Horikoshi, M. A decade of histone acetylation: marking eukaryotic chromosomes with specific codes. *J Biochem*, *138*: 647-662, 2005.
54. Yang, X. J. The diverse superfamily of lysine acetyltransferases and their roles in leukemia and other diseases. *Nucleic Acids Res*, *32*: 959-976, 2004.
55. Kelly, W. K., Richon, V. M., O'Connor, O., Curley, T., MacGregor-Curtelli, B., Tong, W., Klang, M., Schwartz, L., Richardson, S., Rosa, E., Drobnjak, M., Cordon-Cordo, C., Chiao, J. H., Rifkind, R., Marks, P. A., and Scher, H. Phase I clinical trial of histone deacetylase inhibitor: suberoylanilide hydroxamic acid administered intravenously. *Clin Cancer Res*, *9*: 3578-3588, 2003.
56. Bannister, A. J. and Kouzarides, T. The CBP co-activator is a histone acetyltransferase. *Nature*, *384*: 641-643, 1996.

57. Ogryzko, V. V., Schiltz, R. L., Russanova, V., Howard, B. H., and Nakatani, Y. The transcriptional coactivators p300 and CBP are histone acetyltransferases. *Cell*, 87: 953-959, 1996.
58. Rubinstein, J. H. Broad thumb-hallux (Rubinstein-Taybi) syndrome 1957-1988. *Am J Med Genet Suppl*, 6: 3-16, 1990.
59. Miller, R. W. and Rubinstein, J. H. Tumors in Rubinstein-Taybi syndrome. *Am J Med Genet*, 56: 112-115, 1995.
60. Borrow, J., Stanton, V. P., Jr., Andresen, J. M., Becher, R., Behm, F. G., Chaganti, R. S., Civin, C. I., Distèche, C., Dube, I., Frischauf, A. M., Horsman, D., Mitelman, F., Volinia, S., Watmore, A. E., and Housman, D. E. The translocation t(8;16)(p11;p13) of acute myeloid leukaemia fuses a putative acetyltransferase to the CREB-binding protein. *Nat Genet*, 14: 33-41, 1996.
61. Lai, J. L., Jouet, J. P., Bauters, F., and Deminatti, M. Chronic myelogenous leukemia with translocation (8;22): report of a new case. *Cancer Genet Cytogenet*, 17: 365-366, 1985.
62. Chaffanet, M., Gressin, L., Preudhomme, C., Soenen-Cornu, V., Birnbaum, D., and Pebusque, M. J. MOZ is fused to p300 in an acute monocytic leukemia with t(8;22). *Genes Chromosomes Cancer*, 28: 138-144, 2000.
63. de Ruijter, A. J., van Gennip, A. H., Caron, H. N., Kemp, S., and van Kuilenburg, A. B. Histone deacetylases (HDACs): characterization of the classical HDAC family. *Biochem J*, 370: 737-749, 2003.
64. Gregoret, I. V., Lee, Y. M., and Goodson, H. V. Molecular evolution of the histone deacetylase family: functional implications of phylogenetic analysis. *J Mol Biol*, 338: 17-31, 2004.
65. Marks, P. A. and Breslow, R. Dimethyl sulfoxide to vorinostat: development of this histone deacetylase inhibitor as an anticancer drug. *Nat Biotechnol*, 25: 84-90, 2007.
66. Halkidou, K., Gaughan, L., Cook, S., Leung, H. Y., Neal, D. E., and Robson, C. N. Upregulation and nuclear recruitment of HDAC1 in hormone refractory prostate cancer. *Prostate*, 59: 177-189, 2004.
67. Wilson, A. J., Byun, D. S., Popova, N., Murray, L. B., L'Italien, K., Sowa, Y., Arango, D., Velich, A., Augenlicht, L. H., and Mariadason, J. M. Histone deacetylase 3 (HDAC3) and other class I HDACs regulate colon cell maturation and p21 expression and are deregulated in human colon cancer. *J Biol Chem*, 281: 13548-13558, 2006.
68. Choi, J. H., Kwon, H. J., Yoon, B. I., Kim, J. H., Han, S. U., Joo, H. J., and Kim, D. Y. Expression profile of histone deacetylase 1 in gastric cancer tissues. *Jpn J Cancer Res*, 92: 1300-1304, 2001.
69. Zhang, Q., Wang, H. Y., Marzec, M., Raghunath, P. N., Nagasawa, T., and Wasik, M. A. STAT3- and DNA methyltransferase 1-mediated epigenetic silencing of SHP-1 tyrosine phosphatase tumor suppressor gene in malignant T lymphocytes. *Proc Natl Acad Sci U S A*, 102: 6948-6953, 2005.
70. Bolden, J. E., Peart, M. J., and Johnstone, R. W. Anticancer activities of histone deacetylase inhibitors. *Nat Rev Drug Discov*, 5: 769-784, 2006.
71. Zhu, P., Martin, E., Mengwasser, J., Schlag, P., Janssen, K. P., and Gottlicher, M. Induction of HDAC2 expression upon loss of APC in colorectal tumorigenesis. *Cancer Cell*, 5: 455-463, 2004.

72. Huang, B. H., Laban, M., Leung, C. H., Lee, L., Lee, C. K., Salto-Tellez, M., Raju, G. C., and Hooi, S. C. Inhibition of histone deacetylase 2 increases apoptosis and p21Cip1/WAF1 expression, independent of histone deacetylase 1. *Cell Death Differ*, *12*: 395-404, 2005.
73. Song, J., Noh, J. H., Lee, J. H., Eun, J. W., Ahn, Y. M., Kim, S. Y., Lee, S. H., Park, W. S., Yoo, N. J., Lee, J. Y., and Nam, S. W. Increased expression of histone deacetylase 2 is found in human gastric cancer. *Apmis*, *113*: 264-268, 2005.
74. Zhang, Z., Yamashita, H., Toyama, T., Sugiura, H., Omoto, Y., Ando, Y., Mita, K., Hamaguchi, M., Hayashi, S., and Iwase, H. HDAC6 expression is correlated with better survival in breast cancer. *Clin Cancer Res*, *10*: 6962-6968, 2004.
75. Minucci, S., Nervi, C., Lo Coco, F., and Pelicci, P. G. Histone deacetylases: a common molecular target for differentiation treatment of acute myeloid leukemias? *Oncogene*, *20*: 3110-3115, 2001.
76. Xu, L., Glass, C. K., and Rosenfeld, M. G. Coactivator and corepressor complexes in nuclear receptor function. *Curr Opin Genet Dev*, *9*: 140-147, 1999.
77. Fraga, M. F., Ballestar, E., Villar-Garea, A., Boix-Chornet, M., Espada, J., Schotta, G., Bonaldi, T., Haydon, C., Roperio, S., Petrie, K., Iyer, N. G., Perez-Rosado, A., Calvo, E., Lopez, J. A., Cano, A., Calasanz, M. J., Colomer, D., Piris, M. A., Ahn, N., Imhof, A., Caldas, C., Jenuwein, T., and Esteller, M. Loss of acetylation at Lys16 and trimethylation at Lys20 of histone H4 is a common hallmark of human cancer. *Nat Genet*, *37*: 391-400, 2005.
78. Dokmanovic, M., Clarke, C., and Marks, P. A. Histone deacetylase inhibitors: overview and perspectives. *Mol Cancer Res*, *5*: 981-989, 2007.
79. Xu, W. S., Parmigiani, R. B., and Marks, P. A. Histone deacetylase inhibitors: molecular mechanisms of action. *Oncogene*, *26*: 5541-5552, 2007.
80. Candido, E. P., Reeves, R., and Davie, J. R. Sodium butyrate inhibits histone deacetylation in cultured cells. *Cell*, *14*: 105-113, 1978.
81. Rasheed, W. K., Johnstone, R. W., and Prince, H. M. Histone deacetylase inhibitors in cancer therapy. *Expert Opin Investig Drugs*, *16*: 659-678, 2007.
82. Dokmanovic, M. and Marks, P. A. Prospects: histone deacetylase inhibitors. *J Cell Biochem*, *96*: 293-304, 2005.
83. Khan, N., Jeffers, M., Kumar, S., Hackett, C., Boldog, F., Khramtsov, N., Qian, X., Mills, E., Berghs, S. C., Carey, N., Finn, P. W., Collins, L. S., Tumber, A., Ritchie, J. W., Jensen, P. B., Lichenstein, H. S., and Sehested, M. Determination of the class and isoform selectivity of small-molecule histone deacetylase inhibitors. *Biochem J*, *409*: 581-589, 2008.
84. Breslow, R., Jursic, B., Yan, Z. F., Friedman, E., Leng, L., Ngo, L., Rifkind, R. A., and Marks, P. A. Potent cytodifferentiating agents related to hexamethylenebisacetamide. *Proc Natl Acad Sci U S A*, *88*: 5542-5546, 1991.
85. Richon, V. M., Webb, Y., Merger, R., Sheppard, T., Jursic, B., Ngo, L., Civoli, F., Breslow, R., Rifkind, R. A., and Marks, P. A. Second generation hybrid polar compounds are potent inducers of transformed cell differentiation. *Proc Natl Acad Sci U S A*, *93*: 5705-5708, 1996.
86. Reuben, R. C., Wife, R. L., Breslow, R., Rifkind, R. A., and Marks, P. A. A new group of potent inducers of differentiation in murine erythroleukemia cells. *Proc Natl Acad Sci U S A*, *73*: 862-866, 1976.

87. Marks, P. A., Breslow, R., Rifkind, R. A., Ngo, L., and Singh, R. Polar/apolar chemical inducers of differentiation of transformed cells: strategies to improve therapeutic potential. *Proc Natl Acad Sci U S A*, *86*: 6358-6362, 1989.
88. Andreeff, M., Stone, R., Michaeli, J., Young, C. W., Tong, W. P., Sogoloff, H., Ervin, T., Kufe, D., Rifkind, R. A., and Marks, P. A. Hexamethylene bisacetamide in myelodysplastic syndrome and acute myelogenous leukemia: a phase II clinical trial with a differentiation-inducing agent. *Blood*, *80*: 2604-2609, 1992.
89. Paris, M., Porcelloni, M., Binaschi, M., and Fattori, D. Histone deacetylase inhibitors: from bench to clinic. *J Med Chem*, *51*: 1505-1529, 2008.
90. Johnstone, R. W. Histone-deacetylase inhibitors: novel drugs for the treatment of cancer. *Nat Rev Drug Discov*, *1*: 287-299, 2002.
91. McLaughlin, F. and La Thangue, N. B. Histone deacetylase inhibitors open new doors in cancer therapy. *Biochem Pharmacol*, *68*: 1139-1144, 2004.
92. Minucci, S. and Pelicci, P. G. Histone deacetylase inhibitors and the promise of epigenetic (and more) treatments for cancer. *Nat Rev Cancer*, *6*: 38-51, 2006.
93. Gray, S. G., Qian, C. N., Furge, K., Guo, X., and Teh, B. T. Microarray profiling of the effects of histone deacetylase inhibitors on gene expression in cancer cell lines. *Int J Oncol*, *24*: 773-795, 2004.
94. Lee, J. H., Park, J. H., Jung, Y., Kim, J. H., Jong, H. S., Kim, T. Y., and Bang, Y. J. Histone deacetylase inhibitor enhances 5-fluorouracil cytotoxicity by down-regulating thymidylate synthase in human cancer cells. *Mol Cancer Ther*, *5*: 3085-3095, 2006.
95. Mitsiades, C. S., Mitsiades, N. S., McMullan, C. J., Poulaki, V., Shringarpure, R., Hideshima, T., Akiyama, M., Chauhan, D., Munshi, N., Gu, X., Bailey, C., Joseph, M., Libermann, T. A., Richon, V. M., Marks, P. A., and Anderson, K. C. Transcriptional signature of histone deacetylase inhibition in multiple myeloma: biological and clinical implications. *Proc Natl Acad Sci U S A*, *101*: 540-545, 2004.
96. Peart, M. J., Smyth, G. K., van Laar, R. K., Bowtell, D. D., Richon, V. M., Marks, P. A., Holloway, A. J., and Johnstone, R. W. Identification and functional significance of genes regulated by structurally different histone deacetylase inhibitors. *Proc Natl Acad Sci U S A*, *102*: 3697-3702, 2005.
97. Jung, M. Inhibitors of histone deacetylase as new anticancer agents. *Curr Med Chem*, *8*: 1505-1511, 2001.
98. Chen, G., Li, A., Zhao, M., Gao, Y., Zhou, T., Xu, Y., Du, Z., Zhang, X., and Yu, X. Proteomic analysis identifies protein targets responsible for depsipeptide sensitivity in tumor cells. *J Proteome Res*, *7*: 2733-2742, 2008.
99. Ungerstedt, J. S., Sowa, Y., Xu, W. S., Shao, Y., Dokmanovic, M., Perez, G., Ngo, L., Holmgren, A., Jiang, X., and Marks, P. A. Role of thioredoxin in the response of normal and transformed cells to histone deacetylase inhibitors. *Proc Natl Acad Sci U S A*, *102*: 673-678, 2005.
100. Mann, B. S., Johnson, J. R., Cohen, M. H., Justice, R., and Pazdur, R. FDA approval summary: vorinostat for treatment of advanced primary cutaneous T-cell lymphoma. *Oncologist*, *12*: 1247-1252, 2007.
101. Kim, S. A., Jin, Y. L., and Kim, H. S. Structure-activity relationship studies of novel oxygen-incorporated SAHA analogues. *Arch Pharm Res*, *32*: 15-21, 2009.

102. Codd, R., Braich, N., Liu, J., Soe, C. Z., and Pakchung, A. A. Zn(II)-dependent histone deacetylase inhibitors: suberoylanilide hydroxamic acid and trichostatin A. *Int J Biochem Cell Biol*, *41*: 736-739, 2009.
103. Codd, R. Traversing the coordination chemistry and chemical biology of hydroxamic acids. *Coordination Chemistry Reviews*, *252*: 1387-1408, 2008.
104. Richon, V. M., Emiliani, S., Verdin, E., Webb, Y., Breslow, R., Rifkind, R. A., and Marks, P. A. A class of hybrid polar inducers of transformed cell differentiation inhibits histone deacetylases. *Proc Natl Acad Sci U S A*, *95*: 3003-3007, 1998.
105. Finnin, M. S., Donigian, J. R., Cohen, A., Richon, V. M., Rifkind, R. A., Marks, P. A., Breslow, R., and Pavletich, N. P. Structures of a histone deacetylase homologue bound to the TSA and SAHA inhibitors. *Nature*, *401*: 188-193, 1999.
106. Vannini, A., Volpari, C., Filocamo, G., Casavola, E. C., Brunetti, M., Renzoni, D., Chakravarty, P., Paolini, C., De Francesco, R., Gallinari, P., Steinkuhler, C., and Di Marco, S. Crystal structure of a eukaryotic zinc-dependent histone deacetylase, human HDAC8, complexed with a hydroxamic acid inhibitor. *Proc Natl Acad Sci U S A*, *101*: 15064-15069, 2004.
107. Richon, V. M., Zhou, X., Rifkind, R. A., and Marks, P. A. Histone deacetylase inhibitors: development of suberoylanilide hydroxamic acid (SAHA) for the treatment of cancers. *Blood Cells Mol Dis*, *27*: 260-264, 2001.
108. Xu, W., Ngo, L., Perez, G., Dokmanovic, M., and Marks, P. A. Intrinsic apoptotic and thioredoxin pathways in human prostate cancer cell response to histone deacetylase inhibitor. *Proc Natl Acad Sci U S A*, *103*: 15540-15545, 2006.
109. Marks, P. A., Richon, V. M., and Rifkind, R. A. Histone deacetylase inhibitors: inducers of differentiation or apoptosis of transformed cells. *J Natl Cancer Inst*, *92*: 1210-1216, 2000.
110. Butler, L. M., Agus, D. B., Scher, H. I., Higgins, B., Rose, A., Cordon-Cardo, C., Thaler, H. T., Rifkind, R. A., Marks, P. A., and Richon, V. M. Suberoylanilide hydroxamic acid, an inhibitor of histone deacetylase, suppresses the growth of prostate cancer cells in vitro and in vivo. *Cancer Res*, *60*: 5165-5170, 2000.
111. Richon, V. M., Sandhoff, T. W., Rifkind, R. A., and Marks, P. A. Histone deacetylase inhibitor selectively induces p21WAF1 expression and gene-associated histone acetylation. *Proc Natl Acad Sci U S A*, *97*: 10014-10019, 2000.
112. Cohen, L. A., Amin, S., Marks, P. A., Rifkind, R. A., Desai, D., and Richon, V. M. Chemoprevention of carcinogen-induced mammary tumorigenesis by the hybrid polar cytodifferentiation agent, suberanilohydroxamic acid (SAHA). *Anticancer Res*, *19*: 4999-5005, 1999.
113. Desai, D., Arnold, M., Saha, S., Hinkle, G., Soble, D., Frye, J., DePalatis, L., Mantil, J., Satter, M., and Martin, E. Intraoperative Gamma Detection of FDG Distribution in Colorectal Cancer. *Clin Positron Imaging*, *2*: 325, 1999.
114. Kelly, W. K., O'Connor, O. A., Krug, L. M., Chiao, J. H., Heaney, M., Curley, T., MacGregore-Cortelli, B., Tong, W., Secrist, J. P., Schwartz, L., Richardson, S., Chu, E., Olgac, S., Marks, P. A., Scher, H., and Richon, V. M. Phase I study of an oral histone deacetylase inhibitor, suberoylanilide hydroxamic acid, in patients with advanced cancer. *J Clin Oncol*, *23*: 3923-3931, 2005.
115. Duvic, M., Talpur, R., Ni, X., Zhang, C., Hazarika, P., Kelly, C., Chiao, J. H., Reilly, J. F., Ricker, J. L., Richon, V. M., and Frankel, S. R. Phase 2 trial of oral vorinostat

- (suberoylanilide hydroxamic acid, SAHA) for refractory cutaneous T-cell lymphoma (CTCL). *Blood*, *109*: 31-39, 2007.
116. Piekarz, R. L., Robey, R., Sandor, V., Bakke, S., Wilson, W. H., Dahmouh, L., Kingma, D. M., Turner, M. L., Altemus, R., and Bates, S. E. Inhibitor of histone deacetylation, depsipeptide (FR901228), in the treatment of peripheral and cutaneous T-cell lymphoma: a case report. *Blood*, *98*: 2865-2868, 2001.
 117. Institute, N. C. 2007.
 118. O'Connor, O. A., Heaney, M. L., Schwartz, L., Richardson, S., Willim, R., MacGregor-Cortelli, B., Curly, T., Moskowitz, C., Portlock, C., Horwitz, S., Zelenetz, A. D., Frankel, S., Richon, V., Marks, P., and Kelly, W. K. Clinical experience with intravenous and oral formulations of the novel histone deacetylase inhibitor suberoylanilide hydroxamic acid in patients with advanced hematologic malignancies. *J Clin Oncol*, *24*: 166-173, 2006.
 119. Ramalingam, S. S., Parise, R. A., Ramanathan, R. K., Lagattuta, T. F., Musguire, L. A., Stoller, R. G., Potter, D. M., Argiris, A. E., Zwiebel, J. A., Egorin, M. J., and Belani, C. P. Phase I and pharmacokinetic study of vorinostat, a histone deacetylase inhibitor, in combination with carboplatin and paclitaxel for advanced solid malignancies. *Clin Cancer Res*, *13*: 3605-3610, 2007.
 120. Rubin, E. H., Agrawal, N. G., Friedman, E. J., Scott, P., Mazina, K. E., Sun, L., Du, L., Ricker, J. L., Frankel, S. R., Gottesdiener, K. M., Wagner, J. A., and Iwamoto, M. A study to determine the effects of food and multiple dosing on the pharmacokinetics of vorinostat given orally to patients with advanced cancer. *Clin Cancer Res*, *12*: 7039-7045, 2006.
 121. Blevins-Primeau A. S., S. D., Chen G., Sharma A. K., Gallagher C. J., Amin S. and Lazarus P. Functional significance of UDPglucuronosyltransferase (UGT) variants in the metabolism of active tamoxifen metabolites. *Cancer Res*, Accepted, 2008.
 122. Chen, Y., Kuehl, G. E., Bigler, J., Rimorin, C. F., Schwarz, Y., Shen, D. D., and Lampe, J. W. UGT1A6 polymorphism and salicylic acid glucuronidation following aspirin. *Pharmacogenet Genomics*, *17*: 571-579, 2007.
 123. Ando, Y., Saka, H., Ando, M., Sawa, T., Muro, K., Ueoka, H., Yokoyama, A., Saitoh, S., Shimokata, K., and Hasegawa, Y. Polymorphisms of UDP-glucuronosyltransferase gene and irinotecan toxicity: a pharmacogenetic analysis. *Cancer Res*, *60*: 6921-6926, 2000.
 124. Iolascon, A., Faienza, M. F., Centra, M., Storelli, S., Zelante, L., and Savoia, A. (TA)8 allele in the UGT1A1 gene promoter of a Caucasian with Gilbert's syndrome. *Haematologica*, *84*: 106-109, 1999.
 125. Iyer, L., Hall, D., Das, S., Mortell, M. A., Ramirez, J., Kim, S., Di Rienzo, A., and Ratain, M. J. Phenotype-genotype correlation of in vitro SN-38 (active metabolite of irinotecan) and bilirubin glucuronidation in human liver tissue with UGT1A1 promoter polymorphism. *Clin Pharmacol Ther*, *65*: 576-582, 1999.
 126. Hoskins, J. M., Goldberg, R. M., Qu, P., Ibrahim, J. G., and McLeod, H. L. UGT1A1*28 genotype and irinotecan-induced neutropenia: dose matters. *J Natl Cancer Inst*, *99*: 1290-1295, 2007.
 127. Owens, I. S. and Ritter, J. K. Gene structure at the human UGT1 locus creates diversity in isozyme structure, substrate specificity, and regulation. *Prog Nucleic Acid Res Mol Biol*, *51*: 305-338, 1995.

128. Ren, Q., Murphy, S. E., Zheng, Z., and Lazarus, P. O-Glucuronidation of the lung carcinogen 4-(methylnitrosamino)-1-(3-pyridyl)-1-butanol (NNAL) by human UDP-glucuronosyltransferases 2B7 and 1A9. *Drug Metab Dispos*, 28: 1352-1360, 2000.
129. Tukey, R. H. and Strassburg, C. P. Human UDP-glucuronosyltransferases: metabolism, expression, and disease. *Annu Rev Pharmacol Toxicol*, 40: 581-616, 2000.
130. Bock, K. W. Roles of UDP-glucuronosyltransferases in chemical carcinogenesis. *Crit Rev Biochem Mol Biol*, 26: 129-150, 1991.
131. Bock, K. W., Gschaidmeier, H., Heel, H., Lehmkoetter, T., Munzel, P. A., and Bock-Hennig, B. S. Functions and transcriptional regulation of PAH-inducible human UDP-glucuronosyltransferases. *Drug Metab Rev*, 31: 411-422, 1999.
132. Strassburg, C. P., Oldhafer, K., Manns, M. P., and Tukey, R. H. Differential expression of the UGT1A locus in human liver, biliary, and gastric tissue: identification of UGT1A7 and UGT1A10 transcripts in extrahepatic tissue. *Mol Pharmacol*, 52: 212-220, 1997.
133. Emi, Y., Ikushiro, S., and Iyanagi, T. Drug-responsive and tissue-specific alternative expression of multiple first exons in rat UDP-glucuronosyltransferase family 1 (UGT1) gene complex. *J Biochem*, 117: 392-399, 1995.
134. Mackenzie, P. I., Walter Bock, K., Burchell, B., Guillemette, C., Ikushiro, S., Iyanagi, T., Miners, J. O., Owens, I. S., and Nebert, D. W. Nomenclature update for the mammalian UDP glycosyltransferase (UGT) gene superfamily. *Pharmacogenet Genomics*, 15: 677-685, 2005.
135. Monaghan, G., Povey, S., Burchell, B., and Boxer, M. Localization of a bile acid UDP-glucuronosyltransferase gene (UGT2B) to chromosome 4 using the polymerase chain reaction. *Genomics*, 13: 908-909, 1992.
136. Ohno, S. and Nakajin, S. Determination of mRNA expression of human UGTs and application for localization in various human tissues by real time RT-PCR. *Drug Metab Dispos*, 2008.
137. Jedlitschky, G., Cassidy, A. J., Sales, M., Pratt, N., and Burchell, B. Cloning and characterization of a novel human olfactory UDP-glucuronosyltransferase. *Biochem J*, 340 (Pt 3): 837-843, 1999.
138. Nishimura, M. and Naito, S. Tissue-specific mRNA expression profiles of human phase I metabolizing enzymes except for cytochrome P450 and phase II metabolizing enzymes. *Drug Metab Pharmacokinet*, 21: 357-374, 2006.
139. Thum, T., Erpenbeck, V. J., Moeller, J., Hohlfeld, J. M., Krug, N., and Borlak, J. Expression of xenobiotic metabolizing enzymes in different lung compartments of smokers and nonsmokers. *Environ Health Perspect*, 114: 1655-1661, 2006.
140. Somers, G. I., Lindsay, N., Lowdon, B. M., Jones, A. E., Freathy, C., Ho, S., Woodrooffe, A. J., Bayliss, M. K., and Manchee, G. R. A comparison of the expression and metabolizing activities of phase I and II enzymes in freshly isolated human lung parenchymal cells and cryopreserved human hepatocytes. *Drug Metab Dispos*, 35: 1797-1805, 2007.
141. Court, M. H., Hazarika, S., Krishnaswamy, S., Finel, M., and Williams, J. A. Novel polymorphic human UDP-glucuronosyltransferase 2A3: cloning, functional characterization of enzyme variants, comparative tissue expression, and gene induction. *Mol Pharmacol*, 74: 744-754, 2008.
142. Itaaho, K., Mackenzie, P. I., Ikushiro, S., Miners, J. O., and Finel, M. The configuration of the 17-hydroxy group variably influences the glucuronidation of beta-estradiol and

- epiestradiol by human UDP-glucuronosyltransferases. *Drug Metab Dispos*, 36: 2307-2315, 2008.
143. Sten, T., Bichlmaier, I., Kuuranne, T., Leinonen, A., Yli-Kauhaluoma, J., and Finel, M. UDP-glucuronosyltransferases (UGTs) 2B7 and UGT2B17 display converse specificity in testosterone and epitestosterone glucuronidation, whereas UGT2A1 conjugates both androgens similarly. *Drug Metab Dispos*, 37: 417-423, 2009.
 144. Ritter, J. K., Chen, F., Sheen, Y. Y., Tran, H. M., Kimura, S., Yeatman, M. T., and Owens, I. S. A novel complex locus UGT1 encodes human bilirubin, phenol, and other UDP-glucuronosyltransferase isozymes with identical carboxyl termini. *J Biol Chem*, 267: 3257-3261, 1992.
 145. Tukey, R. H. and Strassburg, C. P. Genetic multiplicity of the human UDP-glucuronosyltransferases and regulation in the gastrointestinal tract. *Mol Pharmacol*, 59: 405-414, 2001.
 146. Nagar, S. and Remmel, R. P. Uridine diphosphoglucuronosyltransferase pharmacogenetics and cancer. *Oncogene*, 25: 1659-1672, 2006.
 147. Radomska-Pandya, A., Bratton, S., and Little, J. M. A historical overview of the heterologous expression of mammalian UDP-glucuronosyltransferase isoforms over the past twenty years. *Curr Drug Metab*, 6: 141-160, 2005.
 148. Hodges, D. and Bernstein, S. I. Genetic and biochemical analysis of alternative RNA splicing. *Adv Genet*, 31: 207-281, 1994.
 149. Riedy, M., Wang, J. Y., Miller, A. P., Buckler, A., Hall, J., and Guida, M. Genomic organization of the UGT2b gene cluster on human chromosome 4q13. *Pharmacogenetics*, 10: 251-260, 2000.
 150. Radomska-Pandya, A., Czernik, P. J., Little, J. M., Battaglia, E., and Mackenzie, P. I. Structural and functional studies of UDP-glucuronosyltransferases. *Drug Metab Rev*, 31: 817-899, 1999.
 151. Miles, K. K., Stern, S. T., Smith, P. C., Kessler, F. K., Ali, S., and Ritter, J. K. An investigation of human and rat liver microsomal mycophenolic acid glucuronidation: evidence for a principal role of UGT1A enzymes and species differences in UGT1A specificity. *Drug Metab Dispos*, 33: 1513-1520, 2005.
 152. Picard, N., Ratanasavanh, D., Premaud, A., Le Meur, Y., and Marquet, P. Identification of the UDP-glucuronosyltransferase isoforms involved in mycophenolic acid phase II metabolism. *Drug Metab Dispos*, 33: 139-146, 2005.
 153. Katoh, M., Matsui, T., Okumura, H., Nakajima, M., Nishimura, M., Naito, S., Tateno, C., Yoshizato, K., and Yokoi, T. Expression of human phase II enzymes in chimeric mice with humanized liver. *Drug Metab Dispos*, 33: 1333-1340, 2005.
 154. Senekeo-Effenberger, K., Chen, S., Brace-Sinnokrak, E., Bonzo, J. A., Yueh, M. F., Argikar, U., Kaeding, J., Trottier, J., Remmel, R. P., Ritter, J. K., Barbier, O., and Tukey, R. H. Expression of the human UGT1 locus in transgenic mice by 4-chloro-6-(2,3-xylylidino)-2-pyrimidinylthioacetic acid (WY-14643) and implications on drug metabolism through peroxisome proliferator-activated receptor alpha activation. *Drug Metab Dispos*, 35: 419-427, 2007.
 155. Sies, H., Packer, L., and ScienceDirect (Online service) Phase II conjugation enzymes and transport systems. San Diego, Calif.: Elsevier Academic Press, 2005.

156. Gregory, P. A., Lewinsky, R. H., Gardner-Stephen, D. A., and Mackenzie, P. I. Regulation of UDP glucuronosyltransferases in the gastrointestinal tract. *Toxicol Appl Pharmacol*, 199: 354-363, 2004.
157. Watkins, P. B. The barrier function of CYP3A4 and P-glycoprotein in the small bowel. *Adv Drug Deliv Rev*, 27: 161-170, 1997.
158. Mojarrabi, B. and Mackenzie, P. I. Characterization of two UDP glucuronosyltransferases that are predominantly expressed in human colon. *Biochem Biophys Res Commun*, 247: 704-709, 1998.
159. Grove, A. D., Kessler, F. K., Metz, R. P., and Ritter, J. K. Identification of a rat oltipraz-inducible UDP-glucuronosyltransferase (UGT1A7) with activity towards benzo(a)pyrene-7,8-dihydrodiol. *J Biol Chem*, 272: 1621-1627, 1997.
160. Basu, N. K., Kubota, S., Meselhy, M. R., Ciotti, M., Chowdhury, B., Hartori, M., and Owens, I. S. Gastrointestinally distributed UDP-glucuronosyltransferase 1A10, which metabolizes estrogens and nonsteroidal anti-inflammatory drugs, depends upon phosphorylation. *J Biol Chem*, 279: 28320-28329, 2004.
161. Zheng, Z., Fang, J. L., and Lazarus, P. Glucuronidation: an important mechanism for detoxification of benzo[a]pyrene metabolites in aerodigestive tract tissues. *Drug Metab Dispos*, 30: 397-403, 2002.
162. Starlard-Davenport, A., Lyn-Cook, B., and Radominska-Pandya, A. Identification of UDP-glucuronosyltransferase 1A10 in non-malignant and malignant human breast tissues. *Steroids*, 73: 611-620, 2008.
163. Gardner-Stephen, D. A. and Mackenzie, P. I. Isolation of the UDP-glucuronosyltransferase 1A3 and 1A4 proximal promoters and characterization of their dependence on the transcription factor hepatocyte nuclear factor 1alpha. *Drug Metab Dispos*, 35: 116-120, 2007.
164. Gardner-Stephen, D. A. and Mackenzie, P. I. Liver-enriched transcription factors and their role in regulating UDP glucuronosyltransferase gene expression. *Curr Drug Metab*, 9: 439-452, 2008.
165. Gregory, P. A., Lewinsky, R. H., Gardner-Stephen, D. A., and Mackenzie, P. I. Coordinate regulation of the human UDP-glucuronosyltransferase 1A8, 1A9, and 1A10 genes by hepatocyte nuclear factor 1alpha and the caudal-related homeodomain protein 2. *Mol Pharmacol*, 65: 953-963, 2004.
166. Sugatani, J., Mizushima, K., Osabe, M., Yamakawa, K., Kakizaki, S., Takagi, H., Mori, M., Ikari, A., and Miwa, M. Transcriptional regulation of human UGT1A1 gene expression through distal and proximal promoter motifs: implication of defects in the UGT1A1 gene promoter. *Naunyn Schmiedebergs Arch Pharmacol*, 377: 597-605, 2008.
167. Sugatani, J., Nishitani, S., Yamakawa, K., Yoshinari, K., Sueyoshi, T., Negishi, M., and Miwa, M. Transcriptional regulation of human UGT1A1 gene expression: activated glucocorticoid receptor enhances constitutive androstane receptor/pregnane X receptor-mediated UDP-glucuronosyltransferase 1A1 regulation with glucocorticoid receptor-interacting protein 1. *Mol Pharmacol*, 67: 845-855, 2005.
168. Basu, N. K., Kole, L., Basu, M., Chakraborty, K., Mitra, P. S., and Owens, I. S. The major chemical-detoxifying system of UDP-glucuronosyltransferases requires regulated phosphorylation supported by protein kinase C. *J Biol Chem*, 283: 23048-23061, 2008.

169. Basu, N. K., Kole, L., and Owens, I. S. Evidence for phosphorylation requirement for human bilirubin UDP-glucuronosyltransferase (UGT1A1) activity. *Biochem Biophys Res Commun*, *303*: 98-104, 2003.
170. Basu, N. K., Kovarova, M., Garza, A., Kubota, S., Saha, T., Mitra, P. S., Banerjee, R., Rivera, J., and Owens, I. S. Phosphorylation of a UDP-glucuronosyltransferase regulates substrate specificity. *Proc Natl Acad Sci U S A*, *102*: 6285-6290, 2005.
171. Strassburg, C. P., Kneip, S., Topp, J., Obermayer-Straub, P., Barut, A., Tukey, R. H., and Manns, M. P. Polymorphic gene regulation and interindividual variation of UDP-glucuronosyltransferase activity in human small intestine. *J Biol Chem*, *275*: 36164-36171, 2000.
172. Fujisawa-Sehara, A., Yamane, M., and Fujii-Kuriyama, Y. A DNA-binding factor specific for xenobiotic responsive elements of P-450c gene exists as a cryptic form in cytoplasm: its possible translocation to nucleus. *Proc Natl Acad Sci U S A*, *85*: 5859-5863, 1988.
173. Kitagawa, C., Ando, M., Ando, Y., Sekido, Y., Wakai, K., Imaizumi, K., Shimokata, K., and Hasegawa, Y. Genetic polymorphism in the phenobarbital-responsive enhancer module of the UDP-glucuronosyltransferase 1A1 gene and irinotecan toxicity. *Pharmacogenet Genomics*, *15*: 35-41, 2005.
174. Chouinard, S., Pelletier, G., Belanger, A., and Barbier, O. Isoform-specific regulation of uridine diphosphate-glucuronosyltransferase 2B enzymes in the human prostate: differential consequences for androgen and bioactive lipid inactivation. *Endocrinology*, *147*: 5431-5442, 2006.
175. Harrington, W. R., Sengupta, S., and Katzenellenbogen, B. S. Estrogen regulation of the glucuronidation enzyme UGT2B15 in estrogen receptor-positive breast cancer cells. *Endocrinology*, *147*: 3843-3850, 2006.
176. Starlard-Davenport, A., Lyn-Cook, B., and Radomska-Pandya, A. Novel identification of UDP-glucuronosyltransferase 1A10 as an estrogen-regulated target gene. *Steroids*, *73*: 139-147, 2008.
177. Girard, H., Levesque, E., Bellemare, J., Journault, K., Caillier, B., and Guillemette, C. Genetic diversity at the UGT1 locus is amplified by a novel 3' alternative splicing mechanism leading to nine additional UGT1A proteins that act as regulators of glucuronidation activity. *Pharmacogenet Genomics*, *17*: 1077-1089, 2007.
178. Levesque, E., Girard, H., Journault, K., Lepine, J., and Guillemette, C. Regulation of the UGT1A1 bilirubin-conjugating pathway: role of a new splicing event at the UGT1A locus. *Hepatology*, *45*: 128-138, 2007.
179. Oelberg, D. G., Chari, M. V., Little, J. M., Adcock, E. W., and Lester, R. Lithocholate glucuronide is a cholestatic agent. *J Clin Invest*, *73*: 1507-1514, 1984.
180. Strassburg, C. P., Kalthoff, S., and Ehmer, U. Variability and function of family 1 uridine-5'-diphosphate glucuronosyltransferases (UGT1A). *Crit Rev Clin Lab Sci*, *45*: 485-530, 2008.
181. Gantla, S., Bakker, C. T., Deocharan, B., Thummala, N. R., Zweiner, J., Sinaasappel, M., Roy Chowdhury, J., Bosma, P. J., and Roy Chowdhury, N. Splice-site mutations: a novel genetic mechanism of Crigler-Najjar syndrome type 1. *Am J Hum Genet*, *62*: 585-592, 1998.
182. Starlard-Davenport, A., Xiong, Y., Bratton, S., Gallus-Zawada, A., Finel, M., and Radomska-Pandya, A. Phenylalanine(90) and phenylalanine(93) are crucial amino

- acids within the estrogen binding site of the human UDP-glucuronosyltransferase 1A10. *Steroids*, *72*: 85-94, 2007.
183. Nakamura, A., Nakajima, M., Yamanaka, H., Fujiwara, R., and Yokoi, T. Expression of UGT1A and UGT2B mRNA in human normal tissues and various cell lines. *Drug Metab Dispos*, *36*: 1461-1464, 2008.
 184. Dellinger, R. W., Chen, G., Blevins-Primeau, A. S., Krzeminski, J., Amin, S., and Lazarus, P. Glucuronidation of PhIP and N-OH-PhIP by UDP-glucuronosyltransferase 1A10. *Carcinogenesis*, *28*: 2412-2418, 2007.
 185. Dellinger, R. W., Fang, J. L., Chen, G., Weinberg, R., and Lazarus, P. Importance of UDP-glucuronosyltransferase 1A10 (UGT1A10) in the detoxification of polycyclic aromatic hydrocarbons: decreased glucuronidative activity of the UGT1A10139Lys isoform. *Drug Metab Dispos*, *34*: 943-949, 2006.
 186. Wiener, D., Doerge, D. R., Fang, J. L., Upadhyaya, P., and Lazarus, P. Characterization of N-glucuronidation of the lung carcinogen 4-(methylnitrosamino)-1-(3-pyridyl)-1-butanol (NNAL) in human liver: importance of UDP-glucuronosyltransferase 1A4. *Drug Metab Dispos*, *32*: 72-79, 2004.
 187. Lazarus, P., Zheng, Y., Aaron Runkle, E., Muscat, J. E., and Wiener, D. Genotype-phenotype correlation between the polymorphic UGT2B17 gene deletion and NNAL glucuronidation activities in human liver microsomes. *Pharmacogenet Genomics*, *15*: 769-778, 2005.
 188. Wiener, D., Fang, J. L., Dossett, N., and Lazarus, P. Correlation between UDP-glucuronosyltransferase genotypes and 4-(methylnitrosamino)-1-(3-pyridyl)-1-butanone glucuronidation phenotype in human liver microsomes. *Cancer Res*, *64*: 1190-1196, 2004.
 189. Ren, Q., Murphy, S. E., Dannenberg, A. J., Park, J. Y., Tephly, T. R., and Lazarus, P. Glucuronidation of the lung carcinogen 4-(methylnitrosamino)-1-(3-pyridyl)-1-butanol (NNAL) by rat UDP-glucuronosyltransferase 2B1. *Drug Metab Dispos*, *27*: 1010-1016, 1999.
 190. Malfatti, M. A. and Felton, J. S. N-glucuronidation of 2-amino-1-methyl-6-phenylimidazo[4,5-b]pyridine (PhIP) and N-hydroxy-PhIP by specific human UDP-glucuronosyltransferases. *Carcinogenesis*, *22*: 1087-1093, 2001.
 191. Malfatti, M. A. and Felton, J. S. Human UDP-glucuronosyltransferase 1A1 is the primary enzyme responsible for the N-glucuronidation of N-hydroxy-PhIP in vitro. *Chem Res Toxicol*, *17*: 1137-1144, 2004.
 192. Liu, C. Y., Chen, P. M., Chiou, T. J., Liu, J. H., Lin, J. K., Lin, T. C., Chen, W. S., Jiang, J. K., Wang, H. S., and Wang, W. S. UGT1A1*28 polymorphism predicts irinotecan-induced severe toxicities without affecting treatment outcome and survival in patients with metastatic colorectal carcinoma. *Cancer*, *112*: 1932-1940, 2008.
 193. Paoluzzi, L., Singh, A. S., Price, D. K., Danesi, R., Mathijssen, R. H., Verweij, J., Figg, W. D., and Sparreboom, A. Influence of genetic variants in UGT1A1 and UGT1A9 on the in vivo glucuronidation of SN-38. *J Clin Pharmacol*, *44*: 854-860, 2004.
 194. Thomas, S. S., Li, S. S., Lampe, J. W., Potter, J. D., and Bigler, J. Genetic variability, haplotypes, and htSNPs for exons 1 at the human UGT1A locus. *Hum Mutat*, *27*: 717, 2006.

195. Maitland, M. L., Grimsley, C., Kuttub-Boulos, H., Witonsky, D., Kasza, K. E., Yang, L., Roe, B. A., and Di Rienzo, A. Comparative genomics analysis of human sequence variation in the UGT1A gene cluster. *Pharmacogenomics J*, 6: 52-62, 2006.
196. Ciotti, M., Obaray, R., Martin, M. G., and Owens, I. S. Genetic defects at the UGT1 locus associated with Crigler-Najjar type I disease, including a prenatal diagnosis. *Am J Med Genet*, 68: 173-178, 1997.
197. Levesque, E., Beaulieu, M., Green, M. D., Tephly, T. R., Belanger, A., and Hum, D. W. Isolation and characterization of UGT2B15(Y85): a UDP-glucuronosyltransferase encoded by a polymorphic gene. *Pharmacogenetics*, 7: 317-325, 1997.
198. Iyer, L., King, C. D., Whittington, P. F., Green, M. D., Roy, S. K., Tephly, T. R., Coffman, B. L., and Ratain, M. J. Genetic predisposition to the metabolism of irinotecan (CPT-11). Role of uridine diphosphate glucuronosyltransferase isoform 1A1 in the glucuronidation of its active metabolite (SN-38) in human liver microsomes. *J Clin Invest*, 101: 847-854, 1998.
199. Burchell, B. and Hume, R. Molecular genetic basis of Gilbert's syndrome. *J Gastroenterol Hepatol*, 14: 960-966, 1999.
200. Levesque, E., Beaulieu, M., Hum, D. W., and Belanger, A. Characterization and substrate specificity of UGT2B4 (E458): a UDP-glucuronosyltransferase encoded by a polymorphic gene. *Pharmacogenetics*, 9: 207-216, 1999.
201. Guillemette, C., Ritter, J. K., Auyeung, D. J., Kessler, F. K., and Housman, D. E. Structural heterogeneity at the UDP-glucuronosyltransferase 1 locus: functional consequences of three novel missense mutations in the human UGT1A7 gene. *Pharmacogenetics*, 10: 629-644, 2000.
202. Huang, Y. H., Galijatovic, A., Nguyen, N., Geske, D., Beaton, D., Green, J., Green, M., Peters, W. H., and Tukey, R. H. Identification and functional characterization of UDP-glucuronosyltransferases UGT1A8*1, UGT1A8*2 and UGT1A8*3. *Pharmacogenetics*, 12: 287-297, 2002.
203. Elahi, A., Bendaly, J., Zheng, Z., Muscat, J. E., Richie, J. P., Jr., Schantz, S. P., and Lazarus, P. Detection of UGT1A10 polymorphisms and their association with orolaryngeal carcinoma risk. *Cancer*, 98: 872-880, 2003.
204. Takahashi, H., Maruo, Y., Mori, A., Iwai, M., Sato, H., and Takeuchi, Y. Effect of D256N and Y483D on propofol glucuronidation by human uridine 5'-diphosphate glucuronosyltransferase (UGT1A9). *Basic Clin Pharmacol Toxicol*, 103: 131-136, 2008.
205. Wilson, W., 3rd, Pardo-Manuel de Villena, F., Lyn-Cook, B. D., Chatterjee, P. K., Bell, T. A., Detwiler, D. A., Gilmore, R. C., Valladeras, I. C., Wright, C. C., Threadgill, D. W., and Grant, D. J. Characterization of a common deletion polymorphism of the UGT2B17 gene linked to UGT2B15. *Genomics*, 84: 707-714, 2004.
206. Fang, J. L. and Lazarus, P. Correlation between the UDP-glucuronosyltransferase (UGT1A1) TATAA box polymorphism and carcinogen detoxification phenotype: significantly decreased glucuronidating activity against benzo(a)pyrene-7,8-dihydrodiol(-) in liver microsomes from subjects with the UGT1A1*28 variant. *Cancer Epidemiol Biomarkers Prev*, 13: 102-109, 2004.
207. Vogel, A., Kneip, S., Barut, A., Ehmer, U., Tukey, R. H., Manns, M. P., and Strassburg, C. P. Genetic link of hepatocellular carcinoma with polymorphisms of the UDP-glucuronosyltransferase UGT1A7 gene. *Gastroenterology*, 121: 1136-1144, 2001.

208. Zheng, Z., Park, J. Y., Guillemette, C., Schantz, S. P., and Lazarus, P. Tobacco carcinogen-detoxifying enzyme UGT1A7 and its association with orolaryngeal cancer risk. *J Natl Cancer Inst*, *93*: 1411-1418, 2001.
209. Murata, M., Warren, E. H., and Riddell, S. R. A human minor histocompatibility antigen resulting from differential expression due to a gene deletion. *J Exp Med*, *197*: 1279-1289, 2003.
210. Park, J., Chen, L., Ratnashinge, L., Sellers, T. A., Tanner, J. P., Lee, J. H., Dossett, N., Lang, N., Kadlubar, F. F., Ambrosone, C. B., Zachariah, B., Heysek, R. V., Patterson, S., and Pow-Sang, J. Deletion polymorphism of UDP-glucuronosyltransferase 2B17 and risk of prostate cancer in African American and Caucasian men. *Cancer Epidemiol Biomarkers Prev*, *15*: 1473-1478, 2006.
211. Karypidis, A. H., Olsson, M., Andersson, S. O., Rane, A., and Ekstrom, L. Deletion polymorphism of the UGT2B17 gene is associated with increased risk for prostate cancer and correlated to gene expression in the prostate. *Pharmacogenomics J*, *8*: 147-151, 2008.
212. Blevins-Primeau, A. S., Sun, D., Chen, G., Sharma, A. K., Gallagher, C. J., Amin, S., and Lazarus, P. Functional significance of UDP-glucuronosyltransferase variants in the metabolism of active tamoxifen metabolites. *Cancer Res*, *69*: 1892-1900, 2009.
213. Court, M. H., Krishnaswamy, S., Hao, Q., Duan, S. X., Patten, C. J., Von Moltke, L. L., and Greenblatt, D. J. Evaluation of 3'-azido-3'-deoxythymidine, morphine, and codeine as probe substrates for UDP-glucuronosyltransferase 2B7 (UGT2B7) in human liver microsomes: specificity and influence of the UGT2B7*2 polymorphism. *Drug Metab Dispos*, *31*: 1125-1133, 2003.
214. Ingelman-Sundberg, M., Sim, S. C., Gomez, A., and Rodriguez-Antona, C. Influence of cytochrome P450 polymorphisms on drug therapies: pharmacogenetic, pharmacoeconomic and clinical aspects. *Pharmacol Ther*, *116*: 496-526, 2007.
215. Green, H., Soderkvist, P., Rosenberg, P., Horvath, G., and Peterson, C. mdr-1 single nucleotide polymorphisms in ovarian cancer tissue: G2677T/A correlates with response to paclitaxel chemotherapy. *Clin Cancer Res*, *12*: 854-859, 2006.
216. Green, H., Soderkvist, P., Rosenberg, P., Mirghani, R. A., Rymark, P., Lundqvist, E. A., and Peterson, C. Pharmacogenetic Studies of Paclitaxel in the Treatment of Ovarian Cancer. *Basic Clin Pharmacol Toxicol*, 2008.
217. Meyer, U. A. Overview of enzymes of drug metabolism. *J Pharmacokinet Biopharm*, *24*: 449-459, 1996.
218. Zanger, U. M., Turpeinen, M., Klein, K., and Schwab, M. Functional pharmacogenetics/genomics of human cytochromes P450 involved in drug biotransformation. *Anal Bioanal Chem*, *392*: 1093-1108, 2008.
219. van Schaik, R. H. Cancer treatment and pharmacogenetics of cytochrome P450 enzymes. *Invest New Drugs*, *23*: 513-522, 2005.
220. Nowell, S., Sweeney, C., Winters, M., Stone, A., Lang, N. P., Hutchins, L. F., Kadlubar, F. F., and Ambrosone, C. B. Association between sulfotransferase 1A1 genotype and survival of breast cancer patients receiving tamoxifen therapy. *J Natl Cancer Inst*, *94*: 1635-1640, 2002.
221. Ekhardt, C., Rodenhuis, S., Smits, P. H., Beijnen, J. H., and Huitema, A. D. An overview of the relations between polymorphisms in drug metabolising enzymes and drug transporters and survival after cancer drug treatment. *Cancer Treat Rev*, *35*: 18-31, 2009.

222. Wegman, P., Vainikka, L., Stal, O., Nordenskjold, B., Skoog, L., Rutqvist, L. E., and Wingren, S. Genotype of metabolic enzymes and the benefit of tamoxifen in postmenopausal breast cancer patients. *Breast Cancer Res*, 7: R284-290, 2005.
223. Strange, R. C., Spiteri, M. A., Ramachandran, S., and Fryer, A. A. Glutathione-S-transferase family of enzymes. *Mutat Res*, 482: 21-26, 2001.
224. Davies, S. M., Robison, L. L., Buckley, J. D., Tjoa, T., Woods, W. G., Radloff, G. A., Ross, J. A., and Perentesis, J. P. Glutathione S-transferase polymorphisms and outcome of chemotherapy in childhood acute myeloid leukemia. *J Clin Oncol*, 19: 1279-1287, 2001.
225. Voso, M. T., D'Alo, F., Putzulu, R., Mele, L., Scardocci, A., Chiusolo, P., Latagliata, R., Lo-Coco, F., Rutella, S., Pagano, L., Hohaus, S., and Leone, G. Negative prognostic value of glutathione S-transferase (GSTM1 and GSTT1) deletions in adult acute myeloid leukemia. *Blood*, 100: 2703-2707, 2002.
226. Barragan, E., Collado, M., Cervera, J., Martin, G., Bolufer, P., Roman, J., and Sanz, M. A. The GST deletions and NQO1*2 polymorphism confers interindividual variability of response to treatment in patients with acute myeloid leukemia. *Leuk Res*, 31: 947-953, 2007.
227. Naoe, T., Tagawa, Y., Kiyoi, H., Kodera, Y., Miyawaki, S., Asou, N., Kuriyama, K., Kusumoto, S., Shimazaki, C., Saito, K., Akiyama, H., Motoji, T., Nishimura, M., Shinagawa, K., Ueda, R., Saito, H., and Ohno, R. Prognostic significance of the null genotype of glutathione S-transferase-T1 in patients with acute myeloid leukemia: increased early death after chemotherapy. *Leukemia*, 16: 203-208, 2002.
228. Bosma, P. J., Chowdhury, J. R., Bakker, C., Gantla, S., de Boer, A., Oostra, B. A., Lindhout, D., Tytgat, G. N., Jansen, P. L., Oude Elferink, R. P., and et al. The genetic basis of the reduced expression of bilirubin UDP-glucuronosyltransferase 1 in Gilbert's syndrome. *N Engl J Med*, 333: 1171-1175, 1995.
229. Haaz, M. C., Rivory, L., Jantet, S., Ratanasavanh, D., and Robert, J. Glucuronidation of SN-38, the active metabolite of irinotecan, by human hepatic microsomes. *Pharmacol Toxicol*, 80: 91-96, 1997.
230. Ramchandani, R. P., Wang, Y., Booth, B. P., Ibrahim, A., Johnson, J. R., Rahman, A., Mehta, M., Innocenti, F., Ratain, M. J., and Gobburu, J. V. The role of SN-38 exposure, UGT1A1*28 polymorphism, and baseline bilirubin level in predicting severe irinotecan toxicity. *J Clin Pharmacol*, 47: 78-86, 2007.
231. Darbari, D. S., van Schaik, R. H., Capparelli, E. V., Rana, S., McCarter, R., and van den Anker, J. UGT2B7 promoter variant -840G>A contributes to the variability in hepatic clearance of morphine in patients with sickle cell disease. *Am J Hematol*, 83: 200-202, 2008.
232. Holthe, M., Klepstad, P., Zahlsten, K., Borchgrevink, P. C., Hagen, L., Dale, O., Kaasa, S., Krokan, H. E., and Skorpen, F. Morphine glucuronide-to-morphine plasma ratios are unaffected by the UGT2B7 H268Y and UGT1A1*28 polymorphisms in cancer patients on chronic morphine therapy. *Eur J Clin Pharmacol*, 58: 353-356, 2002.
233. Simons, P. J., Cockshott, I. D., Douglas, E. J., Gordon, E. A., Hopkins, K., and Rowland, M. Disposition in male volunteers of a subanaesthetic intravenous dose of an oil in water emulsion of 14C-propofol. *Xenobiotica*, 18: 429-440, 1988.
234. Court, M. H. Isoform-selective probe substrates for in vitro studies of human UDP-glucuronosyltransferases. *Methods Enzymol*, 400: 104-116, 2005.

235. Sun, D., Chen, G., Dellinger, R. W., Duncan, K., Fang, J. L., and Lazarus, P. Characterization of tamoxifen and 4-hydroxytamoxifen glucuronidation by human UGT1A4 variants. *Breast Cancer Res*, 8: R50, 2006.
236. Allegaert, K., van den Anker, J. N., Naulaers, G., and de Hoon, J. Determinants of drug metabolism in early neonatal life. *Curr Clin Pharmacol*, 2: 23-29, 2007.
237. Ulrich, C. M., Robien, K., and McLeod, H. L. Cancer pharmacogenetics: polymorphisms, pathways and beyond. *Nat Rev Cancer*, 3: 912-920, 2003.
238. Relling, M. V. and Dervieux, T. Pharmacogenetics and cancer therapy. *Nat Rev Cancer*, 1: 99-108, 2001.
239. Rasheed, W., Bishton, M., Johnstone, R. W., and Prince, H. M. Histone deacetylase inhibitors in lymphoma and solid malignancies. *Expert Rev Anticancer Ther*, 8: 413-432, 2008.
240. Vansteenkiste, J., Van Cutsem, E., Dumez, H., Chen, C., Ricker, J. L., Randolph, S. S., and Schoffski, P. Early phase II trial of oral vorinostat in relapsed or refractory breast, colorectal, or non-small cell lung cancer. *Invest New Drugs*, 2008.
241. Barbier, O., Albert, C., Martineau, I., Vallee, M., High, K., Labrie, F., Hum, D. W., Labrie, C., and Belanger, A. Glucuronidation of the nonsteroidal antiestrogen EM-652 (SCH 57068), by human and monkey steroid conjugating UDP-glucuronosyltransferase enzymes. *Mol Pharmacol*, 59: 636-645, 2001.
242. Graham, F. L., Smiley, J., Russell, W. C., and Nairn, R. Characteristics of a human cell line transformed by DNA from human adenovirus type 5. *J Gen Virol*, 36: 59-74, 1977.
243. Fang, J. L., Beland, F. A., Doerge, D. R., Wiener, D., Guillemette, C., Marques, M. M., and Lazarus, P. Characterization of benzo(a)pyrene-trans-7,8-dihydrodiol glucuronidation by human tissue microsomes and overexpressed UDP-glucuronosyltransferase enzymes. *Cancer Res*, 62: 1978-1986, 2002.
244. Upadhyaya, P., Kenney, P. M., Hochalter, J. B., Wang, M., and Hecht, S. S. Tumorigenicity and metabolism of 4-(methylnitrosamino)-1-(3-pyridyl)-1-butanol enantiomers and metabolites in the A/J mouse. *Carcinogenesis*, 20: 1577-1582, 1999.
245. Sun, D., Sharma, A. K., Dellinger, R. W., Blevins-Primeau, A. S., Balliet, R. M., Chen, G., Boyiri, T., Amin, S., and Lazarus, P. Glucuronidation of active tamoxifen metabolites by the human UDP glucuronosyltransferases. *Drug Metab Dispos*, 35: 2006-2014, 2007.
246. Du, L., Musson, D. G., and Wang, A. Q. High turbulence liquid chromatography online extraction and tandem mass spectrometry for the simultaneous determination of suberoylanilide hydroxamic acid and its two metabolites in human serum. *Rapid Commun Mass Spectrom*, 19: 1779-1787, 2005.
247. Parise, R. A., Holleran, J. L., Beumer, J. H., Ramalingam, S., and Egorin, M. J. A liquid chromatography-electrospray ionization tandem mass spectrometric assay for quantitation of the histone deacetylase inhibitor, vorinostat (suberoylanilide hydroxamic acid, SAHA), and its metabolites in human serum. *J Chromatogr B Analyt Technol Biomed Life Sci*, 840: 108-115, 2006.
248. Strassburg, C. P., Strassburg, A., Nguyen, N., Li, Q., Manns, M. P., and Tukey, R. H. Regulation and function of family 1 and family 2 UDP-glucuronosyltransferase genes (UGT1A, UGT2B) in human oesophagus. *Biochem J*, 338 (Pt 2): 489-498, 1999.
249. Perou, C. M., Sorlie, T., Eisen, M. B., van de Rijn, M., Jeffrey, S. S., Rees, C. A., Pollack, J. R., Ross, D. T., Johnsen, H., Akslén, L. A., Fluge, O., Pergamenschikov, A.,

- Williams, C., Zhu, S. X., Lonning, P. E., Borresen-Dale, A. L., Brown, P. O., and Botstein, D. Molecular portraits of human breast tumours. *Nature*, *406*: 747-752, 2000.
250. Sorlie, T., Perou, C. M., Tibshirani, R., Aas, T., Geisler, S., Johnsen, H., Hastie, T., Eisen, M. B., van de Rijn, M., Jeffrey, S. S., Thorsen, T., Quist, H., Matese, J. C., Brown, P. O., Botstein, D., Eystein Lonning, P., and Borresen-Dale, A. L. Gene expression patterns of breast carcinomas distinguish tumor subclasses with clinical implications. *Proc Natl Acad Sci U S A*, *98*: 10869-10874, 2001.
251. Sorlie, T., Tibshirani, R., Parker, J., Hastie, T., Marron, J. S., Nobel, A., Deng, S., Johnsen, H., Pesich, R., Geisler, S., Demeter, J., Perou, C. M., Lonning, P. E., Brown, P. O., Borresen-Dale, A. L., and Botstein, D. Repeated observation of breast tumor subtypes in independent gene expression data sets. *Proc Natl Acad Sci U S A*, *100*: 8418-8423, 2003.
252. Evans, W. E. and Relling, M. V. Pharmacogenomics: translating functional genomics into rational therapeutics. *Science*, *286*: 487-491, 1999.
253. Wang, L. and Weinshilboum, R. M. Pharmacogenomics: candidate gene identification, functional validation and mechanisms. *Hum Mol Genet*, *17*: R174-179, 2008.
254. Fantin, V. R. and Richon, V. M. Mechanisms of resistance to histone deacetylase inhibitors and their therapeutic implications. *Clin Cancer Res*, *13*: 7237-7242, 2007.
255. Olsson, M., Lindstrom, S., Haggkvist, B., Adami, H. O., Balter, K., Stattin, P., Ask, B., Rane, A., Ekstrom, L., and Gronberg, H. The UGT2B17 gene deletion is not associated with prostate cancer risk. *Prostate*, *68*: 571-575, 2008.
256. Gallagher, C. J., Kadlubar, F. F., Muscat, J. E., Ambrosone, C. B., Lang, N. P., and Lazarus, P. The UGT2B17 gene deletion polymorphism and risk of prostate cancer. A case-control study in Caucasians. *Cancer Detect Prev*, *31*: 310-315, 2007.
257. Kesarwani, P. and Mittal, R. D. Selection of inappropriate controls in lieu of paper published by Gallagher et al. [*Cancer Detect Prev* 2007;31 (4): 310-315]. *Cancer Detect Prev*, *32*: 185; author reply 186-187, 2008.
258. Operana, T. N. and Tukey, R. H. Oligomerization of the UDP-glucuronosyltransferase 1A proteins: homo- and heterodimerization analysis by fluorescence resonance energy transfer and co-immunoprecipitation. *J Biol Chem*, *282*: 4821-4829, 2007.
259. Jounaidi, Y. Cytochrome P450-based gene therapy for cancer treatment: from concept to the clinic. *Curr Drug Metab*, *3*: 609-622, 2002.
260. Pond, S. M. and Tozer, T. N. First-pass elimination. Basic concepts and clinical consequences. *Clin Pharmacokinet*, *9*: 1-25, 1984.
261. Kostrubsky, V. E., Lewis, L. D., Strom, S. C., Wood, S. G., Schuetz, E. G., Schuetz, J. D., Sinclair, P. R., Wrighton, S. A., and Sinclair, J. F. Induction of cytochrome P4503A by taxol in primary cultures of human hepatocytes. *Arch Biochem Biophys*, *355*: 131-136, 1998.
262. Hariparsad, N., Sane, R. S., Strom, S. C., and Desai, P. B. In vitro methods in human drug biotransformation research: implications for cancer chemotherapy. *Toxicol In Vitro*, *20*: 135-153, 2006.
263. van de Kerkhof, E. G., de Graaf, I. A., and Groothuis, G. M. In vitro methods to study intestinal drug metabolism. *Curr Drug Metab*, *8*: 658-675, 2007.
264. Tucker, G. T., Houston, J. B., and Huang, S. M. Optimizing drug development: strategies to assess drug metabolism/transporter interaction potential--toward a consensus. *Pharm Res*, *18*: 1071-1080, 2001.

265. Jia, L. and Liu, X. The conduct of drug metabolism studies considered good practice (II): in vitro experiments. *Curr Drug Metab*, 8: 822-829, 2007.
266. Pelkonen, O., Kaltiala, E. H., Larmi, T. K., and Karki, N. T. Cytochrome P-450-linked monooxygenase system and drug-induced spectral interactions in human liver microsomes. *Chem Biol Interact*, 9: 205-216, 1974.
267. Coughtrie, M. W., Burchell, B., and Bend, J. R. A general assay for UDPglucuronosyltransferase activity using polar amino-cyano stationary phase HPLC and UDP[U-14C]glucuronic acid. *Anal Biochem*, 159: 198-205, 1986.
268. Redon, R., Ishikawa, S., Fitch, K. R., Feuk, L., Perry, G. H., Andrews, T. D., Fiegler, H., Shapero, M. H., Carson, A. R., Chen, W., Cho, E. K., Dallaire, S., Freeman, J. L., Gonzalez, J. R., Gratacos, M., Huang, J., Kalaitzopoulos, D., Komura, D., MacDonald, J. R., Marshall, C. R., Mei, R., Montgomery, L., Nishimura, K., Okamura, K., Shen, F., Somerville, M. J., Tchinda, J., Valsesia, A., Woodwark, C., Yang, F., Zhang, J., Zerjal, T., Zhang, J., Armengol, L., Conrad, D. F., Estivill, X., Tyler-Smith, C., Carter, N. P., Aburatani, H., Lee, C., Jones, K. W., Scherer, S. W., and Hurles, M. E. Global variation in copy number in the human genome. *Nature*, 444: 444-454, 2006.
269. Bodin, L., Beaune, P. H., and Lorient, M. A. Determination of cytochrome P450 2D6 (CYP2D6) gene copy number by real-time quantitative PCR. *J Biomed Biotechnol*, 2005: 248-253, 2005.
270. Khaja, R., Zhang, J., MacDonald, J. R., He, Y., Joseph-George, A. M., Wei, J., Rafiq, M. A., Qian, C., Shago, M., Pantano, L., Aburatani, H., Jones, K., Redon, R., Hurles, M., Armengol, L., Estivill, X., Mural, R. J., Lee, C., Scherer, S. W., and Feuk, L. Genome assembly comparison identifies structural variants in the human genome. *Nat Genet*, 38: 1413-1418, 2006.
271. Xue, Y., Sun, D., Daly, A., Yang, F., Zhou, X., Zhao, M., Huang, N., Zerjal, T., Lee, C., Carter, N. P., Hurles, M. E., and Tyler-Smith, C. Adaptive evolution of UGT2B17 copy-number variation. *Am J Hum Genet*, 83: 337-346, 2008.
272. Bao, B. Y., Chuang, B. F., Wang, Q., Sartor, O., Balk, S. P., Brown, M., Kantoff, P. W., and Lee, G. S. Androgen receptor mediates the expression of UDP-glucuronosyltransferase 2 B15 and B17 genes. *Prostate*, 68: 839-848, 2008.
273. Chouinard, S., Pelletier, G., Belanger, A., and Barbier, O. Cellular specific expression of the androgen-conjugating enzymes UGT2B15 and UGT2B17 in the human prostate epithelium. *Endocr Res*, 30: 717-725, 2004.
274. Yang, T. L., Chen, X. D., Guo, Y., Lei, S. F., Wang, J. T., Zhou, Q., Pan, F., Chen, Y., Zhang, Z. X., Dong, S. S., Xu, X. H., Yan, H., Liu, X., Qiu, C., Zhu, X. Z., Chen, T., Li, M., Zhang, H., Zhang, L., Drees, B. M., Hamilton, J. J., Papasian, C. J., Recker, R. R., Song, X. P., Cheng, J., and Deng, H. W. Genome-wide copy-number-variation study identified a susceptibility gene, UGT2B17, for osteoporosis. *Am J Hum Genet*, 83: 663-674, 2008.
275. Gregory, P. A., Hansen, A. J., and Mackenzie, P. I. Tissue specific differences in the regulation of the UDP glucuronosyltransferase 2B17 gene promoter. *Pharmacogenetics*, 10: 809-820, 2000.
276. Mackenzie, P. I., Gregory, P. A., Gardner-Stephen, D. A., Lewinsky, R. H., Jorgensen, B. R., Nishiyama, T., Xie, W., and Radominska-Pandya, A. Regulation of UDP glucuronosyltransferase genes. *Curr Drug Metab*, 4: 249-257, 2003.

277. Munzel, P. A., Schmohl, S., Buckler, F., Jaehrling, J., Raschko, F. T., Kohle, C., and Bock, K. W. Contribution of the Ah receptor to the phenolic antioxidant-mediated expression of human and rat UDP-glucuronosyltransferase UGT1A6 in Caco-2 and rat hepatoma 5L cells. *Biochem Pharmacol*, 66: 841-847, 2003.
278. Yueh, M. F., Huang, Y. H., Hiller, A., Chen, S., Nguyen, N., and Tukey, R. H. Involvement of the xenobiotic response element (XRE) in Ah receptor-mediated induction of human UDP-glucuronosyltransferase 1A1. *J Biol Chem*, 278: 15001-15006, 2003.
279. Sies, H. and Packer, L. Phase II conjugation enzymes and transport systems, p. xxxix, 695, [628] p. Amsterdam ; Boston: Elsevier Academic Press, 2005.
280. Lepine, J., Bernard, O., Plante, M., Tetu, B., Pelletier, G., Labrie, F., Belanger, A., and Guillemette, C. Specificity and regioselectivity of the conjugation of estradiol, estrone, and their catecholestrogen and methoxyestrogen metabolites by human uridine diphospho-glucuronosyltransferases expressed in endometrium. *J Clin Endocrinol Metab*, 89: 5222-5232, 2004.
281. Elahi, A., Zheng, Z., Park, J., Eyring, K., McCaffrey, T., and Lazarus, P. The human OGG1 DNA repair enzyme and its association with orolaryngeal cancer risk. *Carcinogenesis*, 23: 1229-1234, 2002.
282. Park, J. Y., Schantz, S. P., Stern, J. C., Kaur, T., and Lazarus, P. Association between glutathione S-transferase pi genetic polymorphisms and oral cancer risk. *Pharmacogenetics*, 9: 497-504, 1999.
283. Richie, J. P., Jr., Carmella, S. G., Muscat, J. E., Scott, D. G., Akerkar, S. A., and Hecht, S. S. Differences in the urinary metabolites of the tobacco-specific lung carcinogen 4-(methylnitrosamino)-1-(3-pyridyl)-1-butanone in black and white smokers. *Cancer Epidemiol Biomarkers Prev*, 6: 783-790, 1997.
284. Hinds, D. A., Kloek, A. P., Jen, M., Chen, X., and Frazer, K. A. Common deletions and SNPs are in linkage disequilibrium in the human genome. *Nat Genet*, 38: 82-85, 2006.
285. McCarroll, S. A., Hadnott, T. N., Perry, G. H., Sabeti, P. C., Zody, M. C., Barrett, J. C., Dallaire, S., Gabriel, S. B., Lee, C., Daly, M. J., and Altshuler, D. M. Common deletion polymorphisms in the human genome. *Nat Genet*, 38: 86-92, 2006.
286. Cutaneous Lymphoma Foundation, C. CTCL-MF Fast Facts. Vol. 2009. Cutaneous Lymphoma Foundation, 2009, Accessed
287. American Cancer Society, A. Cancer Facts and Figures, 2009. American Cancer Society, Atlanta, Georgia., 2009.
288. Chung, J. Y., Cho, J. Y., Yu, K. S., Kim, J. R., Lim, K. S., Sohn, D. R., Shin, S. G., and Jang, I. J. Pharmacokinetic and pharmacodynamic interaction of lorazepam and valproic acid in relation to UGT2B7 genetic polymorphism in healthy subjects. *Clin Pharmacol Ther*, 83: 595-600, 2008.
289. Ethell, B. T., Anderson, G. D., and Burchell, B. The effect of valproic acid on drug and steroid glucuronidation by expressed human UDP-glucuronosyltransferases. *Biochem Pharmacol*, 65: 1441-1449, 2003.
290. Chen, G., Blevins-Primeau, A. S., Dellinger, R. W., Muscat, J. E., and Lazarus, P. Glucuronidation of nicotine and cotinine by UGT2B10: loss of function by the UGT2B10 Codon 67 (Asp>Tyr) polymorphism. *Cancer Res*, 67: 9024-9029, 2007.
291. Engtrakul, J. J., Foti, R. S., Strelevitz, T. J., and Fisher, M. B. Altered AZT (3'-azido-3'-deoxythymidine) glucuronidation kinetics in liver microsomes as an explanation for

- underprediction of in vivo clearance: comparison to hepatocytes and effect of incubation environment. *Drug Metab Dispos*, 33: 1621-1627, 2005.
292. Miners, J. O., Knights, K. M., Houston, J. B., and Mackenzie, P. I. In vitro-in vivo correlation for drugs and other compounds eliminated by glucuronidation in humans: pitfalls and promises. *Biochem Pharmacol*, 71: 1531-1539, 2006.
293. Mistry, M. and Houston, J. B. Glucuronidation in vitro and in vivo. Comparison of intestinal and hepatic conjugation of morphine, naloxone, and buprenorphine. *Drug Metab Dispos*, 15: 710-717, 1987.
294. Soars, M. G., Burchell, B., and Riley, R. J. In vitro analysis of human drug glucuronidation and prediction of in vivo metabolic clearance. *J Pharmacol Exp Ther*, 301: 382-390, 2002.
295. Boase, S. and Miners, J. O. In vitro-in vivo correlations for drugs eliminated by glucuronidation: investigations with the model substrate zidovudine. *Br J Clin Pharmacol*, 54: 493-503, 2002.
296. Fisher, M. B., Campanale, K., Ackermann, B. L., VandenBranden, M., and Wrighton, S. A. In vitro glucuronidation using human liver microsomes and the pore-forming peptide alamethicin. *Drug Metab Dispos*, 28: 560-566, 2000.
297. Guillemette, C., Levesque, E., Beaulieu, M., Turgeon, D., Hum, D. W., and Belanger, A. Differential regulation of two uridine diphospho-glucuronosyltransferases, UGT2B15 and UGT2B17, in human prostate LNCaP cells. *Endocrinology*, 138: 2998-3005, 1997.
298. Handford, M., Rodriguez-Furlan, C., and Orellana, A. Nucleotide-sugar transporters: structure, function and roles in vivo. *Braz J Med Biol Res*, 39: 1149-1158, 2006.
299. Caffaro, C. E. and Hirschberg, C. B. Nucleotide sugar transporters of the Golgi apparatus: from basic science to diseases. *Acc Chem Res*, 39: 805-812, 2006.
300. Endou, H., Reuter, E., and Weber, H. J. Inhibition of gluconeogenesis in rat renal cortex slices by metabolites of L-tryptophan in vitro. *Naunyn Schmiedebergs Arch Pharmacol*, 287: 297-308, 1975.
301. Luhn, K., Wild, M. K., Eckhardt, M., Gerardy-Schahn, R., and Vestweber, D. The gene defective in leukocyte adhesion deficiency II encodes a putative GDP-fucose transporter. *Nat Genet*, 28: 69-72, 2001.
302. Lubke, T., Marquardt, T., Etzioni, A., Hartmann, E., von Figura, K., and Korner, C. Complementation cloning identifies CDG-IIc, a new type of congenital disorders of glycosylation, as a GDP-fucose transporter deficiency. *Nat Genet*, 28: 73-76, 2001.
303. Becker, D. J. and Lowe, J. B. Leukocyte adhesion deficiency type II. *Biochim Biophys Acta*, 1455: 193-204, 1999.
304. Marquardt, T., Luhn, K., Srikrishna, G., Freeze, H. H., Harms, E., and Vestweber, D. Correction of leukocyte adhesion deficiency type II with oral fucose. *Blood*, 94: 3976-3985, 1999.
305. Lubke, T., Marquardt, T., von Figura, K., and Korner, C. A new type of carbohydrate-deficient glycoprotein syndrome due to a decreased import of GDP-fucose into the golgi. *J Biol Chem*, 274: 25986-25989, 1999.
306. Etzioni, A. and Tonetti, M. Fucose supplementation in leukocyte adhesion deficiency type II. *Blood*, 95: 3641-3643, 2000.
307. Sturla, L., Puglielli, L., Tonetti, M., Berninsone, P., Hirschberg, C. B., De Flora, A., and Etzioni, A. Impairment of the Golgi GDP-L-fucose transport and unresponsiveness to fucose replacement therapy in LAD II patients. *Pediatr Res*, 49: 537-542, 2001.

308. Martinez-Duncker, I., Dupre, T., Piller, V., Piller, F., Candelier, J. J., Trichet, C., Tchernia, G., Oriol, R., and Mollicone, R. Genetic complementation reveals a novel human congenital disorder of glycosylation of type II, due to inactivation of the Golgi CMP-sialic acid transporter. *Blood*, *105*: 2671-2676, 2005.
309. Ashikov, A., Routier, F., Fuhlrott, J., Helmus, Y., Wild, M., Gerardy-Schahn, R., and Bakker, H. The human solute carrier gene SLC35B4 encodes a bifunctional nucleotide sugar transporter with specificity for UDP-xylose and UDP-N-acetylglucosamine. *J Biol Chem*, *280*: 27230-27235, 2005.
310. Kobayashi, T., Sleeman, J. E., Coughtrie, M. W., and Burchell, B. Molecular and functional characterization of microsomal UDP-glucuronic acid uptake by members of the nucleotide sugar transporter (NST) family. *Biochem J*, *400*: 281-289, 2006.
311. Dutton, G. J. a. B., B. Newer aspects of glucuronidation. *Prog. Drug Metab.* *2*, 1-70., 1977.
312. Gueraud, F. and Paris, A. Glucuronidation: a dual control. *Gen Pharmacol*, *31*: 683-688, 1998.
313. Tephly, T. R. and Burchell, B. UDP-glucuronosyltransferases: a family of detoxifying enzymes. *Trends Pharmacol Sci*, *11*: 276-279, 1990.
314. Araki, J., Kobayashi, Y., Iwasa, M., Urawa, N., Gabazza, E. C., Taguchi, O., Kaito, M., and Adachi, Y. Polymorphism of UDP-glucuronosyltransferase 1A7 gene: a possible new risk factor for lung cancer. *Eur J Cancer*, *41*: 2360-2365, 2005.
315. Blevins-Primeau A. S., S. D., Chen G., Sharma A. K., Gallagher C. J., Amin S. and Lazarus P. Functional significance of UDPglucuronosyltransferase (UGT) variants in the metabolism of active tamoxifen metabolites. *Cancer Res*, *In press*.
316. Muscat, J. E., Djordjevic, M. V., Colosimo, S., Stellman, S. D., and Richie, J. P., Jr. Racial differences in exposure and glucuronidation of the tobacco-specific carcinogen 4-(methylnitrosamino)-1-(3-pyridyl)-1-butanone (NNK). *Cancer*, *103*: 1420-1426, 2005.
317. Muraoka, M., Kawakita, M., and Ishida, N. Molecular characterization of human UDP-glucuronic acid/UDP-N-acetylgalactosamine transporter, a novel nucleotide sugar transporter with dual substrate specificity. *FEBS Lett*, *495*: 87-93, 2001.
318. Hiraoka, S., Furuichi, T., Nishimura, G., Shibata, S., Yanagishita, M., Rimoïn, D. L., Superti-Furga, A., Nikkels, P. G., Ogawa, M., Katsuyama, K., Toyoda, H., Kinoshita-Toyoda, A., Ishida, N., Isono, K., Sanai, Y., Cohn, D. H., Koseki, H., and Ikegawa, S. Nucleotide-sugar transporter SLC35D1 is critical to chondroitin sulfate synthesis in cartilage and skeletal development in mouse and human. *Nat Med*, *13*: 1363-1367, 2007.
319. Altshuler, D., Daly, M. J., and Lander, E. S. Genetic mapping in human disease. *Science*, *322*: 881-888, 2008.
320. Chen, G., Dellinger, R. W., Gallagher, C. J., Sun, D., and Lazarus, P. Identification of a prevalent functional missense polymorphism in the UGT2B10 gene and its association with UGT2B10 inactivation against tobacco-specific nitrosamines. *Pharmacogenet Genomics*, *18*: 181-191, 2008.
321. Ishida, N., Miura, N., Yoshioka, S., and Kawakita, M. Molecular cloning and characterization of a novel isoform of the human UDP-galactose transporter, and of related complementary DNAs belonging to the nucleotide-sugar transporter gene family. *J Biochem*, *120*: 1074-1078, 1996.

Curriculum Vitae

Renee Marie Balliet

EDUCATION

Penn State University, College of Medicine

Ph.D. Genetics

The Pennsylvania State University

MBA, Master of Business Administration

Moravian College

B.S. Biology

Hershey, PA

August 2004 - August 2009

Harrisburg, PA

February 2007 - December 2008

Bethlehem, PA

Aug 2000-May 2004 *Magna Cum Laude*

PROFESSIONAL EXPERIENCE

The Pennsylvania State University

Adjunct Professor

Fox Chase Cancer Center

Summer Research Assistant

Johns Hopkins, Center for Talented Youth

Teaching Assistant

Moravian College

Resident Director/Advisor

Whitehall-Coplay Press

Newspaper Columnist

Harrisburg, PA

March 2009 – May 2009

Philadelphia, PA

May 2003 – August 2003

Bethlehem, PA

May 2003 – August 2003

Bethlehem, PA

August 2002 – August 2004

Whitehall, PA

September 1999 – May 2000

HONORS

U.S. Department of State Critical Language Scholarship, 2009

Class of 1982 Endowed Scholarship, 2008

Graduate Alumni Endowment Scholarship, 2007

Graduated with Honors in Biology, 2004

Graduated Magna cum Laude, 2004

Bristol Myers Squibb Fellowship, 2003

PUBLICATIONS

Sun D, Sharma A, Blevins-Primeau AS, **Balliet RM**, Amin S, and Lazarus P. Glucuronidation of *cis* isomers of active Tamoxifen metabolites – potential role of UDP-glucuronosyltransferases (UGTs) variants in tamoxifen metabolism. *In preparation*.

Balliet RM, Chen G, Lazarus P, and Gallagher CJ. Gender differences in expression and glucuronidation of UGTs . *In preparation*.

Balliet RM, Dellinger RW, Chen G, and Lazarus P. UGT1A10: Activity against the tobacco-specific nitrosamine, NNAL, and a potential role for a novel UGT1A10 promoter deletion polymorphism in cancer susceptibility. *Submitted to Pharmacogenetics and Genomics*.

Balliet RM, Chen G, Dellinger RW, Sun D, and Lazarus P. Identification and Characterization of UGTs responsible for suberoylanilide hydroxamic acid (SAHA) glucuronidation . *Cancer Research* (April, 2009).

Sun D, Sharma A, Dellinger RW, Blevins-Primeau AS, **Balliet RM**, Chen G, Boyiri T, Amin S, and Lazarus P. Glucuronidation of active tamoxifen metabolites by the human UDP-glucuronosyltransferases (UGTs). *Drug Metab Dispos*. 2007 Nov; 35(11):2006-14. Epub 2007 Jul 30.